MONASH University

ENGINEERING CELLULOSE FIBRE COMPOSITES FOR LIQUID FILTRATION

Thesis in the fulfilment of the requirement for the degree of Doctor of Philosophy in Chemical Engineering

by

Aysu Onur

B. Eng. (Chem.)

Department of Chemical Engineering

Faculty of Engineering

MONASH UNIVERSITY

FEBRUARY 2019

THIS PAGE HAS BEEN INTENTIONALLY LEFT BLANK

Dedicated to my beloved family

Canim annem ve babama. . .

THIS PAGE HAS BEEN INTENTIONALLY LEFT BLANK

COPYRIGHT NOTICE

© Aysu Onur, 2019. Except as provided in the Copyright Act 1968, this thesis may not be reproduced in any form without written permission of the author.

I certify that I have made all reasonable efforts to secure copyright permissions for third-party content included in this thesis and have not knowingly added copyright content to my work without the owner's permission.

……

Aysu Onur

GENERAL DECLARATION

This thesis contains no material which has been accepted for the award of any other degree or diploma at any university or equivalent institution and that, to the best of my knowledge and belief, this thesis contains no material previously published or written by another person, except where due reference is made in the text of the thesis.

Signature:

Print Name: **Aysu Onur**

Date: **21/05/2019**

TABLE OF CONTENTS

Monash University

Thesis including published works declaration

I hereby declare that this thesis contains no material which has been accepted for the award of any other degree or diploma at any university or equivalent institution and that, to the best of my knowledge and belief, this thesis contains no material previously published or written by another person, except where due reference is made in the text of the thesis.

This thesis includes 3 original papers published in peer reviewed journals (Chapter 2, 3 and 5) and 1 submitted publication (Chapter 4). The core theme of the thesis is engineering cellulose fibre composites for liquid filtration. The ideas, development and writing up of all the papers in the thesis were the principal responsibility of myself, the student, working within the Department of Chemical Engineering, Monash University under the supervision of Associate Professor Warren Batchelor and Professor Gil Garnier.

(The inclusion of co-authors reflects the fact that the work came from active collaboration between researchers and acknowledges input into team-based research.)

In the case of Chapter 2, 3 and 5 my contribution to the work involved the following:

Thesis Chapter	Publication Title	Status	Nature and % of student contribution	Co-author name(s) Nature and % of Co-author's contribution*	Co-author(s), Monash student Y/N*
2	Engineering cellulose fibre inorganic composites for depth filtration and adsorption	Published	60%. Key ideas, experimental works, analysis or results, writing up.	1) Aaron Ng, input into manuscript 10% 2) Gil Garnier, supervision, input into manuscript 15% 3) Warren Batchelor, supervision, input into manuscript 15%	1) No 2) No 3) No
3	Multi-Layer filters: Adsorption and filtration mechanisms for improved separation	Published	60%. Key ideas, experimental works, analysis or results, writing up.	1) Aaron Ng, input into manuscript 10% 2) Gil Garnier, supervision, input into manuscript 15% 3) Warren Batchelor, supervision, input into manuscript 15%	1) No 2) No 3) No
5	The use of nanofibrillated cellulose to reduce the wet strength polymer quantity for	Published	60%. Key ideas, experimental works, analysis or results,	1) Aaron Ng, input into manuscript 10% 2) Gil Garnier, supervision, input into manuscript 15%	1) No 2) No 3) No

	development of cleaner filters		writing up.	3) Warren Batchelor, supervision, input into manuscript 15%	

I have renumbered sections of submitted or published papers in order to generate a consistent presentation within the thesis.

Student signature: **Date:** 21/05/2019

The undersigned hereby certify that the above declaration correctly reflects the nature and extent of the student's and co-authors' contributions to this work. In instances where I am not the responsible author I have consulted with the responsible author to agree on the respective contributions of the authors.

Main Supervisor signature: **Date:** 21/05/2019

Monash University

Traditional thesis declaration

I hereby declare that this thesis contains no material which has been accepted for the award of any other degree or diploma at any university or equivalent institution and that, to the best of my knowledge and belief, this thesis contains no material previously published or written by another person, except where due reference is made in the text of the thesis.

This thesis includes 3 original papers published in peer reviewed journals (Chapter 2, 3 and 5) and 1 submitted publication (Chapter 4). The core theme of the thesis is engineering cellulose fibre composites for liquid filtration. The ideas, development and writing up of all the papers in the thesis were the principal responsibility of myself, the student, working within the Department of Chemical Engineering, Monash University under the supervision of Associate Professor Warren Batchelor and Professor Gil Garnier.

(The inclusion of co-authors reflects the fact that the work came from active collaboration between researchers and acknowledges input into team-based research.)

In the case of Chapter 4 my contribution to the work involved the following:

Thesis Chapter	Publication Title	Status	Nature and % of student contribution	Co-author name(s) Nature and % of Co-author's contribution*	Co-author(s), Monash student Y/N*
4	Cellulose Fibre-perlite depth filters with nanofibrillated cellulose top coating for improved filtration	Under final review	60%. Key ideas, experimental works, analysis or results, writing up.	1) Aaron Ng, input into manuscript, 10% 2) Gil Garnier, supervision, input into manuscript 10% 3) Warren Batchelor, supervision, input into manuscript 10% 4) Kirubanandan Shanmugam, help with experimental work, input into manuscript 10%	1) No 2) No 3) No 4) Yes

I have renumbered sections of submitted or published papers in order to generate a consistent presentation within the thesis.

Student signature: **Date:** 21/05/2019

The undersigned hereby certify that the above declaration correctly reflects the nature and extent of the student's and co-authors' contributions to this work. In instances where I am not the responsible author I have consulted with the responsible author to agree on the respective contributions of the authors.

Main Supervisor signature: **Date:** 21/05/2019

ACKNOWLEDGEMENTS

First of all, I would like to express my sincere gratitude to my supervisors Associate Professor Warren Batchelor and Professor Gil Garnier for their guidance, expertise and constant support during almost three and a half year time at Monash University. I would not have been able to complete my study with all these successful outcomes without their valuable input and supervision. Thank you so much for being there whenever I needed help and showing me the right thing and supporting my professional development constantly.

Next, I would like to give my sincere gratitude to 3M ANZ people. Many thanks to my industry supervisor Dr Aaron Ng for the supervision, constant support and guidance during my PhD. He has always been helpful with a kind and humble attitude whenever I needed. I would like to thank to Dr Erwin Ona for supervising me and giving me hands-on experiences during my internship at 3M. Thank you for being only one call away for any help related to my project. Thanks to Vivienne Austria for sharing her knowledge and being so nice to me. They really became the best colleagues to me during my time in Sydney and helped me to settle very quickly from my very first day.

I would like to acknowledge the technical and administrative staff at BioPRIA and Department of Chemical Engineering. Janette Anthony thanks for helping out with any problems and particularly thanks for all the social events you organised in BioPRIA. BioPRIA would not be the same without your positive energy. Also, many thanks to Scot Sharman for any helps related to trainings and OHS in a very patient attitude. Thanks to the other staff Dr Vikram Raghuwanshi, Dr Joanne Tanner, Heather McLiesh, Dr Rosi Eka, Dr Christine Browne, Dr Clare Manderson, Kim Phu, Ross Ellingham, Harry Bouwmeester. I also would like to thank Professor Antonio Patti and Dr Gary Annat for their constant helps with any problems I faced during my PhD.

I acknowledge the financial support given by 3M ANZ and Victorian Government through the Chemicals and Plastics Manufacturing Innovation Network and Training Program. I am grateful for the FEIPRS and ERLA scholarships given by the Faculty of Engineering and Monash University.

Thanks so much to my dear BioPRIAn friends for sharing this long time all together with lunches, coffee breaks, games nights, cake clubs, parties, dinners, conferences and many more. You all truly left a mark in my heart and will be missed so much. I would like to thank Llyza Mendoza for being

my coffee and PhD buddy from the very beginning. Thanks to Dr Praveena Veronica Raj, Dr Whui Lyn, Dr Natasha Yeow, Dr Uthpala Garusinghe and Dr Windy Huang as my senior PhD colleagues for the memorable times we had during their times at BioRPIA. Thank you to Maisha Maliha, Thilina Gunawardhana, Laila Hossein, Shaun Ang, Janine Lodewyke, Saveen Giri, Diana Alves, Rodrigo Curvello, Michael Hertaeg, Marek Bialkower, David Mendoza, Melany Barajasledesma, Kirubanandan Shanmugam. This PhD was too enjoyable and meaningful with all of you!

I also would like to thank my friends from Turkey who are miles away but always in my heart. Ezgi Ozdemir, thanks a lot for being only one text or voice message away at anytime anywhere. Even though we are miles away, we never had the feeling of being apart. I rather feel like I see you every day since our high school days. Thanks for being in my life for so long. Your support means a lot to me. Another thank you to Canan Yagmur Boynukara and Gonca Taşci. Life has always been in different directions for each of us after the first year of University but we have always managed to find a way to keep in touch for 10 years. Catching up only once a year never changes anything. We keep texting each other girls! Many thanks to Selin Bilek Kurt for the support, especially for my professional life. Your help during my interview stages really helped me to relieve my stress. I appreciate the help and like your presence in my life.

Next, I will thank my soulmate, Dr Baris Demir. You have always been supportive and encouraging to me with your endless optimism and love. This is the characteristic that only very few people could be given in life and I am so much thankful that I have you in my life as my other half. You truly helped me more than you did to yourself in every phase of difficulty we had. You are always changing my life towards a better direction. Thanks for being in my life, being patient to my grumpy moods and making my life so magically beautiful with your presence.

Now it is time to write my very final words for my dear parents. Thank you for everything you have given me. Having such supporting and selfless parents like you two is my best luck in life and I feel blessed. You always respected my decisions and wanted the best for me even though it was hard for all of us to be apart. Thank you so much for having the full trust in me and never hesitating to do anything for my benefit. I would have never been able to succeed without your constant support and understanding. I owe you so many things that are certainly impossible to be paid off.

ABSTRACT

A depth filter is a porous filtration medium that is used for clarification of suspensions including food and beverage process streams as well as pharmaceuticals streams. Depth filters are typically composed of cellulose fibre, a type of filter aid and a charged polymer, and they receive significant attention in industrial applications thanks to their advantages over membrane filtration. Depth filters are capable of retaining contaminants throughout the thickness which avoids rapid surface fouling. Furthermore, the filtration process is governed by two crucial mechanisms, size-based and adsorption-based separation. This functionality makes filters even more efficient by producing a high contaminant holding capacity. Although depth filters are used in many industrial purification processes, the use of depth filters is not fully explored and adapted to different applications. Particularly, the extent of performance improvement that could be obtained from depth filters is not investigated. Therefore, the focus of this doctoral thesis is to expand the range of functionalities that could be imparted to depth filters. The initial focus of this thesis is understanding the concept of depth filtration with each of the individual components involved. This is followed by adding impact and innovation to depth filters by engineering new state-of-the-art structures. In the last section of the thesis, new materials as filter components are explored for creating a sustainable and more environmentally-friendly depth filter concept.

Understanding the contribution of each component to depth filtration is a crucial step to improve the performance further. Filters were prepared by embedding perlite particles into the cellulose fibre matrix with a commonly used, charged, wet strength polymer polyamideamine-epichlorohydrin (PAE) to investigate the role of each component. Perlite was selected as the inorganic filler since perlite is one of the widely used filter aids for depth filters. Following fabrication, filters were tested with a dead-end filtration unit for separation performances. The role of increased fibrillation in nanofibrillated cellulose (NFC) along with other individual components were examined. The outcome is that the structural properties, such as pore size distribution, can be altered by increased NFC content and addition of perlite particles. Increased NFC fibrillation doubled the removal of a cationic contaminant; it however decreased the removal of an anionic contaminant by 75%. PAE addition decreased the adsorption of the cationic contaminant, while also significantly

increasing the adsorption of the anionic contaminant. This study demonstrates that each component is important and has a role to tailor the filter structure and properties.

Furthermore, the lack of new developments in filter structures is limiting the use of depth filters. The range of achievable properties could be improved by creating innovative structures. Therefore, multi-layered filter structure and top barrier layer coating of the filters were investigated separately. Filters were prepared by multi-layers and single layer with the same overall basis weight and compared for separation performance. Adsorption capacity increased up to 118% by increasing the number of layers, while holding the basis weight constant. Additionally, barrier layers made from NFC were coated onto filters at a range of different grammages. The size of contaminants that could be separated by the filters expanded with a barrier layer and rejection of 600 and 5,000 kDa polyethylene glycol molecules reached up to 84% with 30 gsm coating. These two studies indicate that the depth filter performance can be significantly improved by engineering new structures in the filters.

Reducing the impact of filters on environment was investigated in the last part of this thesis. NFC as an emerging material was explored further for substitution of toxic component, PAE, in the filters. Filters with different NFC composition were prepared while gradually decreasing the quantity of PAE. The results showed that PAE could be reduced by 95% using NFC substitution without changing wet strength properties. Retention of cationic contaminants was further improved by the reduced use of PAE; however; a small quantity of non-toxic, positively charged polyelectrolyte addition was required to retain the overall positive charge of the filter, to allow the retention of negatively charged contaminants. The highlight of this study is that we could replace the toxic wet strength chemical, PAE, with a biodegradable and renewable material, NFC, without sacrificing any of the filter properties.

All of the works mentioned above show that depth filters can be successfully engineered to improve the separation performance. This can be done by fine-tuning the quantity of different components and introducing new structures that could add a wide range of new functionalities. Moreover, nanoscale biopolymers like nanofibrillated cellulose can be used for wet strength development as a substitute for the toxic components contained in depth filters.

LIST OF PUBLICATIONS

Peer Reviewed Journal Papers

The following published and submitted papers are included in the body of this thesis as individual chapters. The sections of these published papers have been renumbered in order to generate a consistent presentation within the thesis. Papers in the published format are included as Appendix II.

1. **Aysu Onur,** Aaron Ng, Gil Garnier, Warren Batchelor. Engineering cellulose fibre inorganic composites for depth filtration and adsorption, *Sep. Purif. Technol.* 203, 2018, 209-216.
2. **Aysu Onur**, Aaron Ng, Warren Batchelor, Gil Garnier. Multi-Layer filters: Adsorption and filtration mechanisms for improved separation, *Front. Chem.* 6, 2018, 417.
3. **Aysu Onur**, Aaron Ng, Gil Garnier, Warren Batchelor. The use of cellulose nanofibres to reduce the wet strength polymer quantity for development of cleaner filters, *JOCP*, 215, 2019, 226-231.
4. **Aysu Onur**, Kirubanandan Shanmugam, Aaron Ng, Gil Garnier, Warren Batchelor. Cellulose fibre-perlite depth filters with cellulose nanofibre top coating for improved filtration (Manuscript is under final review with Cellulose)

LIST OF FIGURES

Chapter 1

Chapter 4

Chapter 5

LIST OF TABLES

Chapter 1

LIST OF ABBREVIATIONS

AFM	Atomic force microscopy
Ag	Silver
Al	Aluminum
Al_2O_3	Aluminum oxide
AlO_4	Aluminum tetrahedra
AOX	Adsorbable organic halogens
A-PAM	Anionic polyacrylamide
Ar	Argon
ATR	Attenuated total reflectance
BC	Bacterial cellulose
CA	Cellulose acetate
CaO	Calcium oxide
CN	Crowding number theory

CNC	Cellulose nanocrystals
CNF	Cellulose nanofibres
CPAM	Cationic polyacrylamide
CSF	Canadian standard freeness
CP-MAS NMR	Cross polarisation magic angle spinning nuclear magnetic resonance
DE	Diatomaceous earth
DLS	Dynamic light scattering
E. coli	Escherichia coli
EDS	X-ray energy dispersive spectroscopy
EDL	Electrical double layer
EDX	Energy dispersive X-ray
EM	Electron microscopy
EMT	Effective medium theory
ESR	Electron spin resonance
FE-SEM	Field-emission SEM
Fe_2O_3	Iron oxide
FTIR	Fourier transform infrared spectroscopy
K_2O	Potassium oxide
MB	Methylene blue

MD	Membrane distillation
MFC	Microfibrillated cellulose
MgO	Magnesium oxide
MY	Metanil yellow
MWCO	Molecular weight cut-off
N_2	Nitrogen
Na_2O	Sodium oxide
NBSK	Northern bleached softwood kraft
NC	Nanocellulose
NF	Nanofiltration
NFC	Nanofibrillated cellulose
NMR	Nucleic magnetic resonance
NP	Nanoparticle
PA	Polyamide
PAE	Polyamideamine-epichlorohydrin
PEG	Polyethylene glycol
PEI	Polyethylenimine
PES	Polyethersulfone
PET	Polyethylene terephthalate

PDADMAC	Polydiallyldimethylammonium chloride
PP	Polypropylene
PS	Polysulfone
PVDF	Polyvinylidene fluoride
RO	Reverse osmosis
SANS	Small-angle neutron scattering
SAXS	Small-angle X-ray scattering
SEM	Scanning electron microscopy
Si	Silicon
SiO_2	Silicon dioxide
SiO_4	Silicate
SMMs	Surface modifying macromolecules
TEM	Transmission electron microscopy
TEMPO	2,2,6,6,-tetra-methylpiperidine-1-oxyl
TFC	Thin film composite
TFNC	Thin-film nanofibrous composite
TOC	Total Organic Carbon
UF	Ultrafiltration
UO_2	Uranium dioxide

UV-Vis	Ultraviolet Visible
VOCs	Volatile organic compounds
WAXS	Wide-angle X-ray scattering
XPS	X-ray photon spectroscopy

LIST OF NOMENCLATURE

gsm	grams per square metre
Mw	average molecular weights
mm	millimetre
µm	micrometer
nm	manometre
%	percentage
wt%	weight percentage
w/v%	weight by volume concentration
φ_c	connectivity threshold
°C	celsius degree
°	degree
m^2/g	square metre per gram
g/cm^3	grams per cubic centimetre
meq/g	milliequivalent units per gram

mg/g	milligram per gram
ms	millisecond
s	second
min	minute
h	hour
mV	millivolt
Da	dalton
kDa	kilo dalton
kPa	kilopascal
psia	pounds per square inch absolute
mL	millilitre
L	litre
mg	milligram
g	gram
kV	kilovolt
m^2	square metre
ppm	parts per million
LMH	litre per square meter per hour
C/C_o	normalised concentration

$\dot{Q}$	volumetric flow rate
µm/Pa.s	micrometres per pascal per second
ζ	zeta potential

CHAPTER 1

INTRODUCTION & LITERATURE REVIEW

THIS PAGE HAS BEEN INTENTIONALLY LEFT BLANK

CHAPTER 1 INTRODUCTION AND LITERATURE REVIEW

1.1. INTRODUCTION

Liquid filtration is a very commonly used technique for the removal of suspended particles and solute molecules from a fluid. The purpose of filtration could be for the recovery of any valuable components from the effluent as well as purification of the main product streams in industry. The majority of liquid filtration processes are performed by membranes which usually do the separation by surface filtration. However, surface filtration results in membranes being very prone to fouling which restricts the efficiency of the process. Additionally, the production of conventional membrane products mainly relies on petroleum-based materials with cost-intensive methods that does not really match with the sustainable and cost-effective production concepts. Therefore, these inadequacies and challenges in membrane technology have led to the development of depth filters. Depth filters are fabricated in a relatively easy and inexpensive way and separation of contaminants is commonly performed throughout the thickness of the filter rather than with surface filtration. Separation is controlled by two main mechanisms: adsorption by surface interactions and mechanical entrapment.

Depth filters are commonly made of cellulose fibres and an inorganic adsorbent. Additional polymers are also added to modify the charge characteristics of the filter media to further improve the contaminant removal by physical interactions. Depth filters contribute to more environmentally-friendly, eco-friendly and sustainable product development with biodegradable and renewable cellulose fibres obtained from naturally occurring biomass. These industrial cellulose-based depth filters are used in a variety of food and beverage applications. 3M Company is currently manufacturing depth filter products Zeta Plus™ SP Series filter cartridges that are composed of high surface area adsorbents embedded in a cellulose fibre matrix. Even though these filters are commercially available, there is still need to improve these existing filter products. Therefore, the aim of this doctoral thesis is to address the limiting issues of depth filters to enhance the performance of the filters.

Depth filters are studied in the literature; however, there are still information about depth filters that are not covered. Firstly, understanding each components' contributions to structural changes as well as separation performance is a crucial step. Therefore, our first objective is to develop filters

with cellulose, perlite and wet strength polymer similar to commercial depth filters and investigate the effect of each component on filtration performance. Furthermore, potential benefits that could be received from nanofibrillated cellulose in depth filters have not been researched. Nanofibrillated cellulose could provide improvement in filter performance by its outstanding properties of increased surface area and wet strength and reduced pore size, compared to conventional cellulose fibres. Therefore, nanofibrillated cellulose is a crucial material to investigate.

Structure-property relationship is another area that needs to be explored in depth filters. Engineering new structures will enable us to understand how the properties change and will allow us to expand the range of properties available with these filters. This is currently a challenge in membrane technology and there are plenty of studies in literature to address this challenge and initiate new developments in membrane structures. However, none of these improvements have been adapted to depth filters. Therefore, introducing new and innovative structures to our depth filters and characterising their separation performance is the second objective. With the aid of new state-of-the-art structures, such as multi-layered depth filters and coating a barrier layer on top of depth filters, other functionalities will be imparted to filters.

The current filter products inevitably contain some positively charged polymers to achieve the required wet strength and overall charge. However, the most widely used of these polymers has some toxic by-products and their use is restricted by regulation to a very limited concentration. After developing a deep understanding about depth filter preparation and the extent of improvements could be introduced to the filters with new structures, the third objective is to replace the wet strength polymer with nanofibrillated cellulose for a reduced impact on the environment. This would also contribute to the food grade filter production for food and beverage applications.

Chapter 1 presents a critical review of cellulose fibre depth composites to identify the current gaps in literature. This information leads us directly to the specific research objectives of this doctoral thesis. This chapter has four main parts: Literature Review, Gaps in Knowledge, Research Objectives and Thesis Outline, which are given in sections 1.2, 1.3, 1.4 and 1.5, respectively. In the Literature Review (Section 1.2), principles of liquid filtration, types of materials used in filters and depth filters are reviewed in Subsection 1.2.1. Cellulose, different sources of cellulose, nanofibrillated cellulose;

production methods, characterization methods and applications are reviewed in Section 1.2.2. Filter aids and their role, properties and applications in filter products are reviewed in Section 1.2.3.

Polyelectrolytes, their properties and applications in filters are reviewed in Section 1.2.4. These sections are followed by cellulose fibre composite preparation methods in Section 1.2.5 and characterisation techniques for the composites in Section 1.2.6. The final Subsection (Section 1.2.7.) gives the perspective and conclusion about cellulose fibre composites as depth filters that has been gained from the literature. The next section (Section 1.3) identifies the significant gaps in knowledge which helps determining the specific research objectives in Section 1.4. Finally, the last section provides the organization of this thesis (Section 1.5).

1.2. LITERATURE REVIEW

This review focuses on development of novel structured cellulose fibre-inorganic composites as a depth type filter product in liquid filtration applications. The project was conducted under 3M industry partnership and it was based on 3M's Zeta Plus depth type filters. The objective of this review then is to examine cellulose fibre-inorganic composites as a depth type filter medium for liquid filtration in order to identify the latest developments as well as gaps in knowledge and opportunities. The review begins with a general discussion of liquid filtration, then reviews depth filters as a sub-class of filters and then focuses on the materials used for fabrication of filter products. Then, it continues with the commercially available depth filter products from 3M.

Currently, depth filters are made with conventional cellulose pulp fibres, inorganic adsorbents and polymeric additives for wet strength and charge control. The work of this thesis has focussed on understanding the effect of each component on filter performance, structural modification of filters for improved performance and substituting toxic wet strength polymer with nanofibrillated celullose to reduce the impact on environment. The review of the cellulose fibres starts with the definition of cellulose, sources of cellulose pulp fibres and the properties of refined and unrefined cellulose pulp fibres. One of the focuses of the thesis has been to use nanofibrillated cellulose to enhance the functionality of depth filters. Therefore, the review also covers nanofibrillated cellulose production, characterisation and applications of nanofibrillated cellulose. Furthermore, polymeric additives are discussed in the next section. Industrial type filter aids and absorbents are briefly

mentioned, although it should be noted that this has not been a major focus of the thesis. The following section covers the preparation and characterisation methods of cellulose fibre-inorganic particle composites. Finally, the last section includes future perspective and conclusions reached by critically analysing the use of composites as depth filters in liquid filtration applications.

1.2.1. Liquid filtration

Liquid filtration is a separation process of removing suspended solid particles and dissolved solute molecules from fluids by depositing them on or within a filter medium [1]. The filter medium is required to be permeable only to the fluid phase of the mixture whereas particles and any dissolved molecules in the liquid phase are trapped either at the surface of the filter medium and/or within its depth. Liquid filtration is usually employed for two main applications. The first use is to recover any valuable suspended solids in the fluid in a concentrated form for further use [2]. The other use for filtration is to clarify the fluid by separating solid particles from the filtrate [3]. Although, achieving both purposes is usually desirable.

Filtration is a key process for product recovery in industry because it is more economic to remove particles by size-based separation or adsorption mechanisms rather than any thermally driven processes such as evaporation. These two mechanisms of mechanical entrapment and adsorption are the most commonly used principles in filtration and membrane processes. Detailed information about the principles of filtration is given in the next section (Section 1.2.1.1). Filtration process can be divided into the two main groups of depth filtration and surface filtration. Depth filtration uses a porous filtration medium to retain particles throughout the medium combining both adsorption and mechanical entrapment, whereas surface filtration retains molecules or particles on the surface of the filter medium by using mainly mechanical capture [4]. This doctoral thesis has studied depth filtration and this has been discussed in detail in section 1.2.1.2.

1.2.1.1. Principles of filtration

Separation processes can be classified based on the physical and chemical properties of the components to be separated. Separation of any substance can be accomplished by differences in molecule size, vapour pressure, freezing point, affinity, charge, density and chemical nature of the

components [5]. All those differences in physical/chemical properties correlate with the selection of separation process. Microfiltration and ultrafiltration processes are generally used in size-based separation while extraction, adsorption and absorption rely upon the affinity between substances. In our project, separation was performed by both mechanical entrapment (size-exclusion based separation) and adsorption (surface interactions-based separation) on a porous material. Both principles are explained thoroughly below.

1.2.1.1.1. Pressure driven size-based filtration process

When a liquid on one side of a porous material is exposed to pressure, it will begin flowing through the porous medium as the opposite side has a lower pressure. The pressure is the driving force for the filtration. The initial solution that is fed to filter media is often called the feed solution and the liquid which passes through the media is commonly referred to as filtrate or permeate. Figure 1 shows the general principle of feed and filtrate/permeate through a porous material.

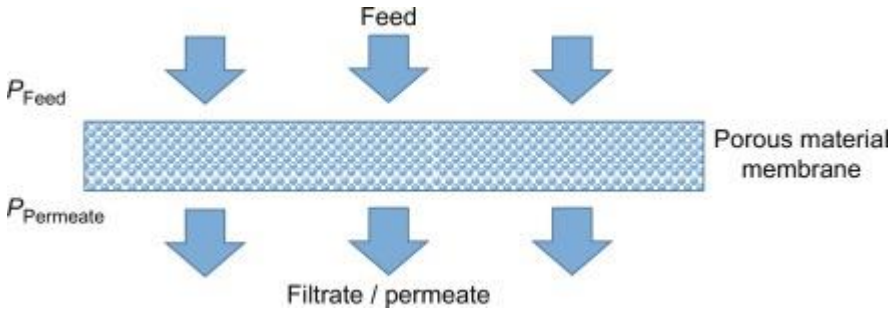

Figure 1: **General principles on flow through a porous material. When $P_{feed} > P_{permeate}$, flow will occur through the porous material (Reprinted from Biopharmaceutical Processing, 1st edition, Jakob Liderfelt, Jonathan Royce, Filtration Principles, 279-293, Copyright © 2018, with permission from Elsevier [6]).**

There are two modes of operation that can be used in filtration: normal flow filtration, also called dead-end filtration, and cross-flow filtration that is also called tangential flow filtration. In ***dead-end filtration*** (Figure 2), all flow is passed directly through the filter and filtrate is accumulated on the membrane surface or within the membrane thickness. In ***cross-flow*** filtration (Figure 2), the flow is passing across, or tangential to the membrane. The flow that is permeating through the membrane

is called the permeate flow. Cross-flow filtration prevents the build-up contaminants on the membrane surface by the sweeping action of the cross-flow and can be advantageous thanks to this feature. In this thesis, dead-end filtration is used as operation mode as it is more suitable for laboratory scale experiments. The schematic illustration of both modes is shown in Figure 2.

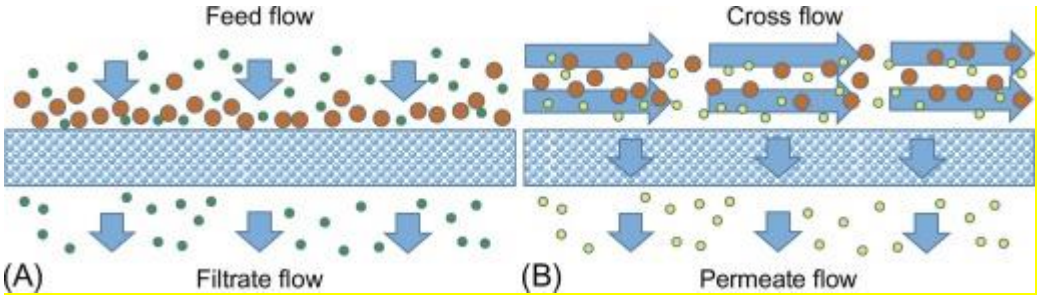

Figure 2: **The two most common filtration modes: (A) dead-end filtration and (B) cross-flow filtration (Reprinted from Biopharmaceutical Processing, 1st edition, Jakob Liderfelt, Jonathan Royce, Filtration Principles, 279-293, Copyright © 2018, with permission from Elsevier [6]).**

Filtration processes can be operated either under constant flux or constant pressure conditions. In ***constant flux operations***, flux will be constant while pressure drop across the membrane will be increasing as the materials build up on surface or within the pore structure. In ***constant pressure mode***, pressure will be constant while the permeate flux will be decreasing in time. In either case, the non-constant parameter is being monitored, and the recorded changes are used to assess the filter performance. The constant pressure condition is mainly used for the work in this thesis. However, constant flux condition is also employed and the effect on separation performance is described. More information about evaluation of filtration performance can be found in section 1.2.6.

1.2.1.1.1.1. Application of pressure-driven membrane processes

Pressure-driven membrane processes can serve a variety of applications. Membrane types can be categorised depending on their pore size distribution and intended application. Figure 3 below shows the various application areas according to different membrane types.

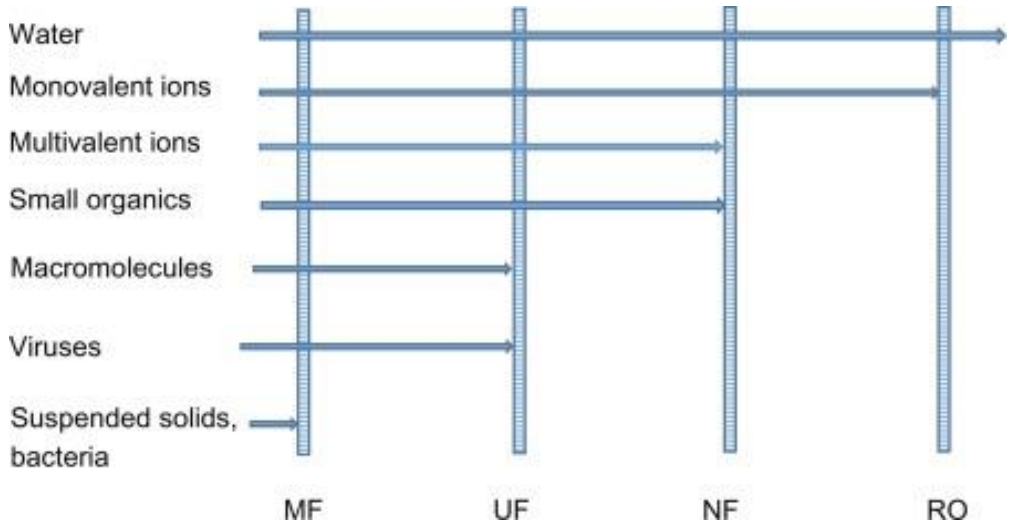

Figure 3: Application scope of pressure-driven membrane processes: microfiltration (MF), ultrafiltration (UF), nanofiltration (NF) and reverse osmosis (RO) (Reprinted from Fundamental Modelling of Membrane Systems, 1st edition, Bart Van der Bruggen, Microfiltration, ultrafiltration, nanofiltration, reverse osmosis, and forward osmosis, 25-70, Copyright © 2018 with permission from Elsevier [7]).

These membranes can be classified into polymeric (organic) membranes and ceramic (inorganic) membranes. The typical polymers used are cellulose acetate (CA), polyamide (PA), polysulfone (PS), polyethersulfone (PES), polyvinylidene fluoride (PVDF), and polypropylene (PP) [8]. From microfiltration to reverse osmosis the pore size of the membranes is reducing significantly, and this requires increasing operating pressures. Permeate flux of each membrane type is a function of operating conditions as well as function of feed and membrane properties. Numerous different models are used to predict the permeate flux [8].

Microfiltration (MF) is applied to remove any of non-dissolved matters with a pore size rating of 0.1 to 5 µm [8]. This includes suspended solids, blood cells, large macromolecules and large bacteria. Microfiltration is commonly used as a pre-treatment to significantly reduce the quantity of particulate material with a resulting permeate, free of turbidity, for subsequent operations. The purpose is to improve the efficiency of downstream processes by removing contaminants which could produce fouling. Microfiltration has intensively been used in food processing for clarification of fruit juices and beverages [9-12]. Microfiltration is also used in oil-water separation [13, 14] and

membrane bioreactors [15, 16]. The operation pressure for microfiltration is typically around 1 bar [7].

Ultrafiltration (UF) is a cost effective and efficient method of removing suspended solids and bacteria [17]. Considering the disinfection effect which is generally an important consideration for some applications such as water treatment, ultrafiltration seems to be superior to microfiltration. This is particularly the case when the water reuse is targeted; ultrafiltration is preferred since viruses can also be efficiently removed with ultrafiltration as well as bacteria. Ultrafiltration membrane pore sizes range between 10 to 100 nm and this reduced pore size requires increased pressures in the range of 1 to 10 bar to operate [8]. Other applications of ultrafiltration are the separation of macromolecules [18], the colour removal [19], the pre-concentration of milk [20], the recovery of vaccines from fermentation [21], and the concentration of fruit juices [22].

Nanofiltration (NF) and ***Reverse Osmosis (RO)*** processes can be considered almost the same process as they have the same principle. They are used to separate low molecular weight solutes, such as inorganic salts or small organic compounds, from the solvent. However, nanofiltration membranes tend to perform this separation to a lower extent than reverse osmosis membranes. They have pore size rating between 0.5 to 10 nm and operating pressure is between 10 to 30 bar [8]. Nanofiltration membranes are made in the same way as reverse osmosis membranes, which is by the addition of an interfacially polymerized thin polyamide layer on top of an asymmetric phase inversion membrane [7]. Nanofiltration membranes are used in applications where a complete rejection of salts (specifically monovalent salts) is not necessary or expected. Desalination of seawater is not a target application. However, it can be used for modifying the concentration of multivalent ions and organic compounds for producing other water sources, such as drinking water. The combination of natural organic matter and hardness removal from water is one of the key applications [23]. RO is intensively being used in desalination applications [24] as well as for the production of ultrapure water [25]. Moreover, it can also be employed for water recycling directly from wastewater [26, 27]. The pore size of RO membranes are less than 0.5 nm and the required pressure to operate RO membranes is between 35 and 100 bar [8].

1.2.1.1.2. Adsorption-based separation

Adsorption process includes the separation of a substance from one phase accompanied by its accumulation or concentration on or within the surface of another [28]. The material adsorbed at the surface is the adsorbate, whereas the adsorbing material is referred as adsorbent. Adsorption occurs as a result of binding forces between the individual atoms, ions, or molecules of an adsorbate and the surface of an adsorbent [28]. Adsorption might occur by electrostatic attachment of the ionic species to sites of opposite charge at the surface of an adsorbent or by physical adsorption which is caused by van der Waals forces [28]. Furthermore, chemical adsorption is likely to happen when a reaction between adsorbent and adsorbate results in a change in the chemical form of the adsorbate [28]. There is a wide range of porous adsorbents used in adsorption processes such as activated carbon, clay, zeolite, silica gel, activated alumina and perlite. Adsorbents can be selected for specific component separation based on their functionality. The types of adsorption-based filter aids that are used in this doctoral thesis are discussed comprehensively in the following sections of this review.

1.2.1.2. Depth filtration

Depth filtration involves the separation of suspended particles and solute molecules throughout the thickness of filter medium. Depth filters usually have a graduated pore size that becomes smaller through the thickness in the direction of the fluid flow. The decreasing pore size give the filters their high dirt-holding capacity. The coarser layers will act as pre-filter that traps the larger particles, while the smaller particles will be retained in the finer layers [29].

There are two types of depth filter: the deep bed (or sand) filter and the thick filter medium. Deep bed filters involve vertical filtration through a packed bed of granular or fibrous material and the height can be significantly larger than even the thickest filter media [30, 31]. The other form of depth filters is the filter cartridges that are made of thick porous material [32, 33]. They are usually in the form of cylindrical cartridges fitted into a cylindrical filter housing.

Depth filter sheet thicknesses range from 3 to 4 mm and they are usually composed of cellulose fibres and a number of filter aids, commonly diatomaceous earth or perlite [34]. These filter media

can be further modified to possess a cationic charge to enable electrokinetic adsorption. Therefore, two separation principles can be combined into one medium.

Thick media filters are used in many different industrial applications such as treatment of ventilation air, for engine air intakes, and increasingly for vehicle cabin air filtration. They are also used to maintain the integrity of hydraulic and pneumatic systems, and for cleaning machine tool coolant. The most common application is to remove contaminants in food and beverage [35], and in fine chemicals production [36].

1.2.1.3. Types of materials used in filter production

A filter media is made of any material that is permeable to one or more components of a mixture, solution or suspension, and is impermeable to the remaining components under the operating conditions of the filtration process. The filter medium's performance and whether the particles and solute molecules are being captured on the surface or within the thickness of a filter is determined by the structure and properties of the materials used in the filter.

The polymer choice for the membrane-based filters affects the surface properties, such as hydrophilicity or adsorptive abilities, as well as strength and chemical stability. Very often, it is desirable to have an inert polymer material that has no interaction with the material being filtered. Production of membrane-based filters is commonly performed by phase inversion method as this method gives relatively homogenous pore structures [37, 38].

On the other hand, nonmembrane-based filters are typically employed for coarse separation and usually solids content is high where pre-filtration or recovery is targeted. These filters are produced based on woven media, such as glass fibre, polypropylene (PP) or cellulose fibres. Using a charged-depth filter in food & beverage and biopharmaceutical applications is an example of nonmembrane-based filtration.

Table 1 shows the summary of the types of materials that are used for filtration purposes in biopharmaceuticals. Both membrane-based and nonmembrane-based filters are shown together with the properties of the filters. Different filter characteristics, such as pore size and porosity, mechanical strength or chemical stability, can be achieved by material selection. For instance, pH tolerance is very limited when cellulose acetate is used in membrane-based filters, whereas

polymers like polysulphone (PS), polyether sulphone (PES) and PP give a broad range of pH tolerance. This would expand the tolerance of filters to different process conditions. Furthermore, membrane-based filters will provide a sharper size cut-off whereas nonmembrane-based filters mainly perform prefiltration and clarification with a much broader cut-off range. Similarly, nonmembrane-based filter sheets, which are produced by wet laying technique, are also employed to clarify beverages such as beer, whisky and wine. These filter sheets resemble thick filter paper and are made of cellulose fibres and diatomaceous earth [39].

Table I: **Typical polymer materials used in liquid filtration for biopharmaceuticals and their properties (Reprinted from Biopharmaceutical Processing, 1st edition, Jakob Liderfelt, Jonathan Royce, Filtration Principles, 279-293, Copyright © 2018, with permission from Elsevier [6]).**

	Name	Hydro-phobic	Thermal Tolerance	Solvent Resistance	Protein Adsorption	pH Tolerance	Application
Non-membrane based							
Non-woven	Polypropylene	+	+++	+++	+	+++	Prefiltration
	Glass fiber	+	+++	++	+	++	Prefiltration
Depth	Cellulose-diatomaceous earth	+	++	+	++	++	Recovery
Membrane-based							
Cellulose	Cellulose acetate	–	–	+	+++	4–8	MF/UF
	Regenerated cellulose	–	+	+	+++	1–13	MF/UF
Synthetic	Nylon	+/–	+	++	++	3.5–10	MF/RO
	Polysulphone (PS)	+	++	+	++	1–14	MF/UF
	Polyether sulphone (PES)	+	++	+	++	1–14	MF/UF
	Polypropylene (PP)	++	++	+	+	1–14	MF
	Polyvinylfluorodyne (PVDF)	+/–	++	++	+++	1–12	MF/UF
	PTFE (Teflon)	+++	+++	+++	+++	1–14	MF-gas

As can be seen in Table 1, a cellulose fibre-diatomaceous earth composite is classified under nonmembrane-based depth filtration. Depth filters are being produced by a variety of manufacturers. Although 3M is well known as a producer of depth filter products, Millipore and Pall Corporation are the other major manufacturers of depth filter products.

Millipore Corporation is offering Millistak+® depth filter media [40] for a variety of primary and secondary clarification applications, including cell cultures, yeast and Escherichia coli (E. coli) lysates post centrifuge, E. coli refolds, media, vaccines, plasma proteins and sera. It is in a scalable, disposable format. These filters are available in three different series of media grades to meet the different application needs. Pall Corporation is offering Stax™ disposable depth filter systems [41] for prefiltration and clarification in biopharmaceutical applications. Furthermore, SUPRApak™ depth filter modules [42] are also manufactured by Pall Corporation for food and beverage filtration.

This PhD thesis has focused on a 3M depth filter product and therefore the next section gives an overview of 3M's depth filter products.

1.2.1.4. 3M's Zeta Plus™ filter cartridges

3M offers a broad range of stackable filter elements. Zeta Plus™ series filter medium is a rigid depth type filter which is positively charged [34]. Added positive charges enhance the filters' ability to trap oppositely charged materials that cannot be held by size exclusion through the filter medium. Zeta Plus™ S series depth filters are comprised of cellulose fibres, perlite and diatomaceous earth. 3M also has Zeta Plus™ Activated Carbon cartridges that consists of activated carbon in addition to cellulose fibres and a positively charged resin. Zeta Plus™ series filters can be used for pharmaceuticals, chemicals, cosmetics and food and beverage products for the removal of trace organic contaminants as well as decolourisation. 3M Zeta Plus™ S series and Zeta Plus™ Activated Carbon cartridges are shown in Figure 4.

Figure 4: **Zeta Plus™ S series (the two on the right) and Zeta Plus™ Activated Carbon cartridges (on the left) (Reprinted from Handbook of Nonwoven Filter Media, 2nd edition, Irwin M. Hutten, Liquid Filter Applications, 409-450, Copyright © 2016 with permission from Elsevier [34]).**

Additionally, the Zeta Plus™ Encapsulated system [43] is a single-use depth filtration system for cell culture clarification applications for biopharmaceutical customers. They are designed to make a fast, easy and clean cell clarification by depth filtration. They are available in a variety of formats for research and development activities, process development and commercial large-scale production. The Zeta Plus™ encapsulated series is shown in Figure 5.

Figure 5: **Zeta Plus Encapsulated Holders (Reprinted from Filtration & Separation, 50/6, Anthony Bennett, Pharmaceuticals and fine chemicals: Filtration and separation in the diverse fine chemical sectors, 30-33, Copyright © 2013, with permission from Elsevier [36]).**

With the knowledge obtained until this section regarding depth filters and 3M's depth filter products, we now know that the main components of depth filter products are cellulose fibres, an inorganic filler and a charged polymer. Now, the next section will give a brief review about the properties and role of each component used to make these depth filters. The review starts with cellulose fibres, after which charged polymers and filter aids are discussed.

1.2.2. Cellulose

Cellulose is the most abundant polymer on Earth. It is biodegradable, natural, renewable, non-toxic and the major component of paper [44], wood [45], cotton [46], bamboo [47, 48], agricultural residues such as straw [49]. The empirical formula of cellulose is $[C_6H_{10}O_5]_n$ [50]. It is a linear polysaccharide which is derived from long linear chains of β-linked anhydro-glucopyranose units [50]. The basic chemical structure of repeating unit of cellulose is given in Figure 6 and Figure 7 shows the hierarchical structure of a tree with a breakdown through cellulose microfibril and cellulose molecule.

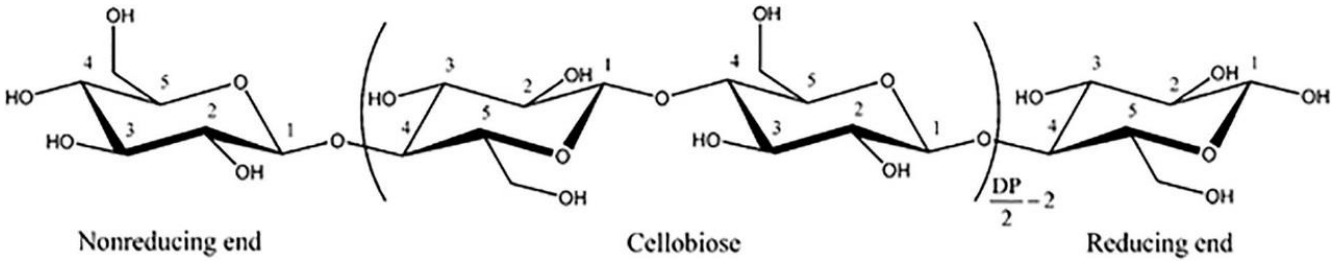

Figure 6: **Molecular structure of cellulose (Reprinted from Nanocellulose as a natural source for groundbreaking applications in materials science: Today's state, 21/7, Dieter Klemm, Emily D. Cranston, Dagmar Fischer, Miguel Gama, Stephanie A. Kedzior, Dana Kralisch, Friederike Kramer, Tetsuo Kondo, Tom Lindström, Sandor Nietzsche, Katrin Petzold-Welcke, Falk Rauchfuß, 720-748., Copyright © 2018, with permission from Elsevier [51]).**

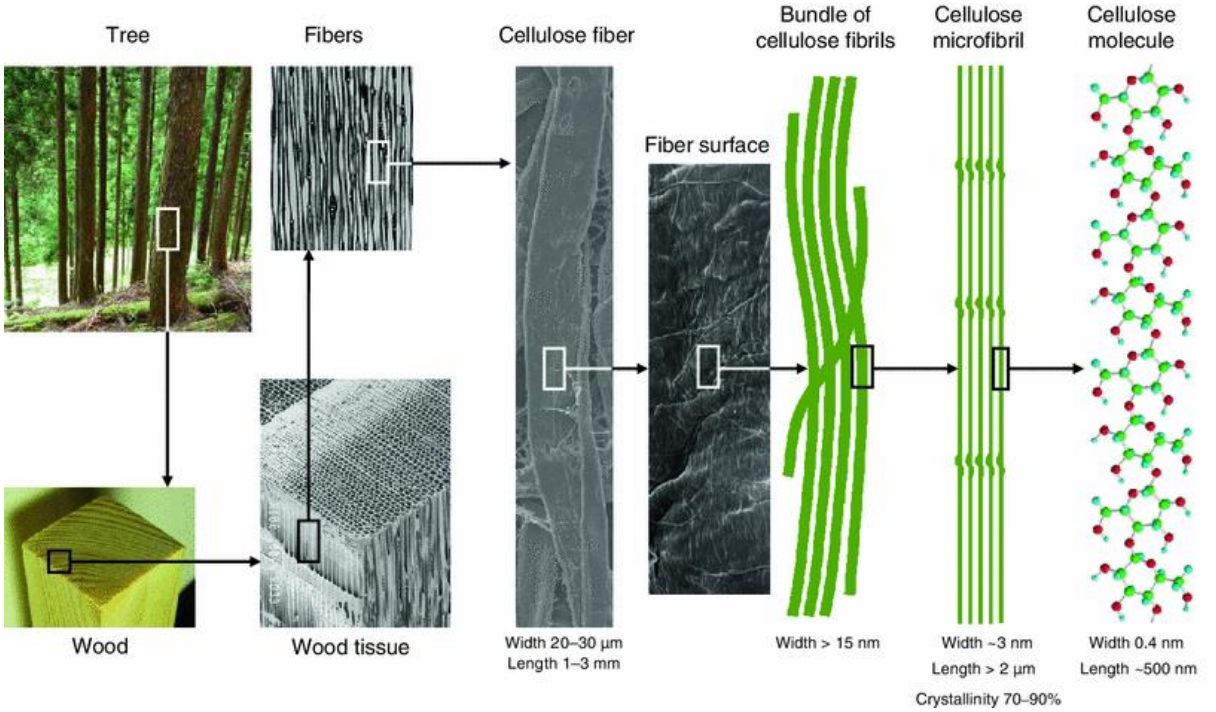

Figure 7: Hierarchical breakdown of the tree to cellulose molecule (Reprinted from TEMPO oxidized cellulose nanofibers, 3/1, Akira Isogai, Tsuguyuki Saito and Hayaka Fukuzumia, 71-85., Copyright © 2011, with permission from Royal Society of Chemistry [52]).

The most important function that is ascribed to wood and other lignocellulosic materials are their impressive mechanical properties. These materials provide high mechanical strength and high strength to weight ratio, as well as providing flexibility against changes due to shrinking and swelling [53]. Tensile strength of cellulose fibres obtained from wood is ascribed to its ability to form both amorphous and crystalline regions and its uniformity. Cellulose molecules, which are held together very rigidly in crystalline region, show stiffness and elasticity, while the molecules in amorphous region contribute to the flexibility and plasticity of the material. By controlling the ratio between crystalline and amorphous regions, some improvements on mechanical properties would be achievable [54]. Cellulose is abundant, renewable, biodegradable, eco-friendly and has been developed for many applications, particularly in the last 150 years [55].

In this thesis, different aspects of cellulose fibres is researched to improve depth filter performance and properties. First, cellulose fibres help development of dry strength by hydrogen bond formation. However, wet strength still remains very poor as the hydrogen bonds can be easily disrupted by

water. For materials requiring wet strength, such as depth filters, a wet strength agent is added to crosslink the fibres and protect the bonds. However, the toxic nature of wet strength agents means that new methods for wet strength development are required. Cellulose nanofibres (the nanometre diameter bundles of cellulose fibrils shown in Figure 7) with increased surface area and bonding could help achieving the required wet strength for filters without resins. Therefore, nanofibrillated cellulose is one of the research focuses of this thesis. However, changing surface area, fibre dimension and surface charge of cellulose fibres could change the filter performance completely. Wood pulp fibre diameter ranges from 10-50 μm thus pore sizes between fibres will also be in this range [56]. As discussed previously in section 1.2.1.1.1.1, this size range will only allow for very coarse contaminants to be removed by filtration. However, controlling fibre dimension of cellulose fibres and in turn the pore size of filters could reduce the size of contaminants that can be filtered. Furthermore, increased surface area of cellulose fibres could change the charge and selective adsorption of particular contaminants. Cellulose fibres from wood have relatively low surface area and charge is negative due to positive charges dissolving from surface [57]. This sharply limits adsorption of negatively charged particles. The poor adsorption capacity on negatively charged contaminants is a distinct drawback that needs to be tackled. To sum up, the application of nanofibrillated cellulose in depth filters has been little explored; therefore, it is one of the significant areas of investigation of this thesis.

1.2.2.1. Sources of cellulose

Although cellulose can be extracted from a variety of resources, wood pulp remains the primary raw material for cellulose and most of the cellulose extracted from wood is used for the production of paper and paperboard; more than 50% of the average global paper furnish uses virgin wood-based pulp [58].

Cellulose can be synthesized in a rather pure form, for example in the seed hairs of the cotton plant [59]. However, it is mostly combined with lignin and other polysaccharides (e.g. hemicelluloses) in the cell wall of woody plants [60]. Although wood is the primary resource of cellulose, it can be obtained from other sources as well, such as agricultural residues [61], grasses [62], and other plant substances [63, 64]. These resources also contain hemicelluloses, lignin, and small quantities of

extractives [65]. The extensive use of wood-based materials in many industries (the building, furniture, pulp and paper industries, etc.) creates a demand for other sources of cellulose. Therefore, the interest in other sources of cellulose has been increasing. Particularly, agricultural crops and their by-products offer lower energy consumption during the processing of cellulose compared to wood-based materials [66]. Cellulose micro fibrils from agricultural fibres are easier to separate from the primary wall [67], therefore the fibrillation of this pulp demands less energy.

Cellulose can be also produced by several bacteria. *Acetobacter, Agrobacterium, Sarcina, Rhizobium* are some of the important bacteria for cellulose production [68]. Bacterial cellulose (BC) generally does not contain any other components, such as lignin and hemicelluloses. They have a highly crystalline structure with a high degree of polymerization.

As stated above, fibres from wood are the most abundantly used cellulose fibres in paper [69] and natural fibre composite materials [70]. This is due to excellent mechanical properties of wood fibres, particularly the high strength to weight ratio [56]. In this thesis, softwood fibre is used and mechanically treated by refining process to make the fibres flexible and start to break down the fibres to microfibrils. Refining process, which also refers to beating, is one of the widely used stock preparation stage in papermaking and is used to fibrillate the cellulose fibres. It describes the mechanical treatment of pulps by using special equipment, refiners, to develop optimum fibre properties for the end-use of fibres, such as papermaking or filter manufacturing. In the refining process, fibres are exposed to various forces, including compression and shear forces, which improves the quality of fibres by affecting their structure [71]. The first effect of refining is partially delaminating the cell wall, which introduces water into the cell wall, which makes fibres much more flexible. The second effect is fibrillation of fibres that increases the surface area of fibres, thereby improving fibre–fibre bonding in the final sheet. The third effect is delamination of the cell wall, such as between the primary and secondary layers, and delamination increases the fibre flexibility [72]. Thus, refining overall increases the sheet density and the bonding as the fibres pack together better. It also increases the sheet surface area by fibrillating fibres, reducing the pore between the fibres with the fibrils while increasing the bonded area. The decrease in pore size will reduce the size cut-off in filtering and the increased bonding helps both dry and wet strength development. However, refining process makes individual fibres shorter due to cutting action which is an

undesired effect in most cases [72]. Consequently, refining is generally a trade-off between improving fibre-to-fibre bonding and decreasing the strength of individual fibres. However, most strength properties of paper increase with pulp refining since they mainly rely on fibre-to-fibre bonding. In this thesis, refining of cellulose fibres is a fundamental step to prepare the fibres for depth filter development and also employed as the initial treatment before producing nanofibrillated cellulose with high aspect ratio.

1.2.2.2. Nanofibrillated cellulose

Nanocellulose (NC) is a generic term that refers to any material obtained from cellulose which has at least one of its dimensions in nanometre range. There are different terms used in literature for nanocellulose: including micro fibrillated cellulose (MFC) and nanofibrillated cellulose (NFC). MFC and NFC are typically referring to fibres which have diameters between 20-50 nm and are several micrometres in length [73]. NFC or MFC is formed by bundle of elementary fibrils (microfibrils) of which diameter is around 5 nm [73]. In this thesis, we have used the term “nanofibrillated cellulose (NFC)” for a nanocellulose fibre network containing microfibrils and bundle of cellulose microfibrils. In addition to that, the cellulose nanofibre (CNF) term was used in literature review for fibres that are completely separated into individual microfibrils or nanofibres.

NFC has many advantages which are favouring its usage, such as high aspect ratio, high surface area and a web-like entangled structure [74]. In addition, its largely crystalline nature and the ability to form dense percolating network of NFC will result in low permeability [53]. There are many reasons for the increasing usage of NFC. The recent advances in nanotechnology field has drawn attention towards nanomaterials and nanofibres obtained from cellulose is a promising raw material as it can be produced from the renewable and abundant ligno-cellulosic biomass. NFC has a great potential to be used as a new bio-based nanomaterial. The table 2 below shows the differences between NFC and unrefined softwood pulp properties. Dimensions and Young’s modulus of unrefined and nanofibrillated wood pulp are presented in the table.

Table II: Properties of unrefined and nanofibrillated wood pulp.

Fibre material	Surface area (m^2/g)	Diameter	Length	Young's modulus (GPa)
Unrefined softwood [56]	0.97	20-40 μm	2-6 mm	18-40
NFC	100-200 [73]	20-60 nm [73]	Several micrometres [73]	100 [53]

1.2.2.2.1. Production methods of nanofibrillated cellulose

Applying mechanical shearing to cellulose fibres lead to the formation of individual microfibrils. Before formation of microfibrils, there are some pre-treatment processes involved subjecting cellulose fibres through various treatment to remove the primary cell wall, exposing the secondary cell wall for further processing. These are disintegration in waring blenders, beating and refining in either a PFI mill or a disk refiner [75].

Even though pulp refining is a fundamental step as explained in previous section 1.2.2.1, excessive refining has some changes in the fibre structure that are not desirable, such as fibre shortening. Excessive fibre shortening is not desirable as we would like to have as high aspect ratio NFC as possible in further applications to be able to benefit from highly entangled and web-like structure of fibres. In this thesis, we used refined pulp supplied from 3M Australia and further homogenised the pulp in homogeniser that would mainly fibrillate the fibres to produce high aspect ratio NFC.

After pre-treatment, different mechanical treatments are being applied to obtain NFC. Homogenization [76], grinding [77] and cryocrushing [67] are amongst the methods used, with homogenization and grinding being the widely used methods. However, each method is energy intensive. The consumption required for homogenization is as high as 70,000 kWh/t [78]. Also,

Zimmermann et al. estimated the energy consumption of 8.5 kWh for processing 10 L cellulose pulp (1–2 wt%) with 4 passes in microfluidizer [79].

To decrease the energy consumption during these mechanical treatments, some chemical, physical and enzymatic pre-treatments are proposed to reduce the fibre stiffness and cohesiveness prior to mechanical treatment. In that way, the energy required for fibrillation will be reduced. Enzymatic pre-treatment [80], TEMPO mediated oxidation [81] and carboxymethylation and acetylation [82] are some of the pre-treatments, where TEMPO oxidation might be considered as the most commonly used method.

The basic principle of TEMPO oxidation pre-treatment is subjecting fibres to oxidative treatments in aqueous cellulose fibre suspensions with 2,2,6,6,-tetramethylpiperidine-1-oxyl (TEMPO) catalyst. The C6 primary hydroxyl groups of cellulose are selectively being converted to sodium carboxylate groups via the C6 aldehyde groups [83]. As a result, the nanofibrils within the fibres have lower cohesive forces among the ionized carboxylate groups, reducing the energy required to separate the fibrils [84].

Enzymatic pre-treatment combines the disintegration of cellulosic wood fibre pulp by increasing its swelling in water, which makes fibrillation process easier. The other chemical pre-treatment is carboxymethylation. This pre-treatment facilitates the increase in the quantity of anionic charges in the formation of carboxyl groups on the surface of the fibres.

Even though mechanical treatments require high energy consumption, these are major methods used for NFC production and still worth considering as there are significant research efforts to reduce the energy consumption during NFC production. Recently, Cavitron® developed by the Papiertechnische Stiftung (PTS) in Germany as part of the project SUNPAP (2009) and the GEA Niro Soavi ARIETE NS3075H, which was used for CNF sample preparation by Centre Technique du Papier (CTP) in France, developed as part of the same project SUNPAP (2009) are commercially available processes for CNF production with reduced energy [73]. However, there is still need for more research to increase the efficiency of these processes and all these efforts should allow the production of CNF with much lower energy consumption in the coming years.

1.2.2.2.2. Characterisation of nanofibrillated cellulose

The efficiency of fibre fibrillation process and the dimensions and structure of the produced NFC can be characterised by a set of different techniques. SEM, TEM, field-emission SEM (FE-SEM), atomic force microscopy (AFM) [85, 86], small-angle neutron scattering (SANS), small-angle X-ray scattering (SAXS), and dynamic light scattering (DLS) techniques [87] provide a useful platform for the determination of width distribution of NFC. Even though these image analysis techniques can provide a useful information regarding the width of the fibrils, it is difficult to determine the length due to the entanglement and difficulties of observing both ends of the individual fibres [53]. Recently, sedimentation technique is used in literature to estimate an average fibre aspect ratio and an average fibre length from the width measurements [88-90]. Sedimentation measurements can be used to obtain the gel point, which is the lowest solids content at which a fibre suspension forms a continuously connected network. The gel point is also known as the connectivity threshold, φ_c, which is defined as the boundary between the dilute and semi-dilute region of a fibre suspension. The gel point obtained by sedimentation is used to calculate aspect ratio with either the effective medium theory (EMT) or the crowding number theory (CN) [91].

Other characterization techniques for further characterisation on other properties of NFC include solid state ^{13}C cross polarisation magic angle spinning nuclear magnetic resonance (CP-MAS NMR) [92] and wide-angle X-ray scattering (WAXS) [93] that are used to measure width and crystallinity.

Turbidity measurements have also been used by researchers for the evaluation of NFC quality. It is an easy and fast measurement tool as opposed to complex and demanding imaging techniques explained above. Japanese researchers has shown that thickness of the fibres can be calculated from turbidity measurements according to the theory of light scattering of thin and long particles [94]. They have also shown the consistency between fibre diameters obtained by turbidity and AFM measurement for a wide range of NFC [94].

Another relatively easy and fast method is centrifugation. Several research groups have used centrifugation to estimate the fraction of nanomaterial content in NFC suspensions [95-97]. Furthermore, characterisation on surface area and electrokinetic properties of NFC can be easily linked to performance of final filter products. For example, zeta potential of NFC suspension could

give an approximate idea about adsorption of oppositely charged compounds onto NFC and NFC composites. The specific surface area of NFC would also affect both available surface area for adsorption and increase negative charges on the surface of NFC. Surface area of NFC can be analysed by mercury porosimetry [98] and gas adsorption techniques [99]. Additionally, charge characteristics of NFC can be determined by zeta potential measurements [100]. Zeta potential gives the potential at the slip plane in the electric double layer [101] and this technique is further explained in section 1.2.6.

All these characterisation techniques provide valuable information about NFC quality that is closely related to the final product performance. A particular property of final product could be achieved by fine tuning the NFC quality. For example, zeta potential measurements of NFC or NFC composite suspensions would make it possible to estimate the adsorption characteristics of filter products. In NFC composites, other charged additives can be added to achieve the aimed charge and adsorption properties.

1.2.2.2.3. Application of nanofibrillated cellulose

NFC has been recently used to engineer new materials as it combines important cellulose properties with the features of nanomaterials. Shatkin et al. has recently reviewed comprehensively the variety of applications where NFC is currently or potentially employed [102]. The largest potential volume of cellulose nanomaterial applications is in paper and paper packaging, textiles, cement, and automobile parts. Other promising technical applications include gels/foams and thickeners/stabilizers in pharmaceuticals [103, 104]. Other possible applications are in the areas of cosmetic products [105], wound dressings [106], drug carriers [107], medical implants [108], tissue engineering [109], food [110] and composites [111].

NFC has also been considerably researched in the fields of energy harvesting and electronic applications. In the energy field [112], the research effort is on energy storage devices such as lithium ion batteries, supercapacitors, and solar cells [113, 114]. Such features as low surface roughness, transparency, low thermal expansion, and strong mechanical properties are desirable properties in NFC films that enhance suitability of NFC for various electronic smart materials, sensors, and various electronic devices in printed electronics [115]. Additionally, the suitability of

orientation and alignment to form ordered structures of NFC materials allows them to be used in sensors and optical devices [116].

The interest in NFC application as an additive in papermaking has also recently emerged. Even though it is quite recent, the use of NFC is expected to increase in the near future as a sustainable reinforcement material [117, 118]. One interest in papermaking applications is using NFC as a coating material to improve barrier properties of the paper and packaging materials. [119, 120]. The environmental problems possessed by non-biodegradable and petro-chemical based food packaging materials have attracted attention towards the use of renewable and biodegradable bio-based materials. NFC has emerged as a promising material for packaging [121, 122]. The aim with NFC is to produce transparent and biodegradable packaging films with high barrier properties against water vapour and oxygen, which prevents or delays the decaying of food. However, the most likely initial application is using NFC as a wet-end additive as dry and wet strength agent for improved mechanical properties [123, 124]. The NFC boosts the load-bearing capacity of the materials as it acts as an adhesion enhancer by increasing the fibre to fibre bonding with highly increased surface area. Kose et al. showed that addition of NFC by 10% increased dry tensile index of paper products by 40% without any other additives [125].

NFC has been investigated for its potential in various water treatment technologies thanks to its high specific surface area, high strength, ease of functionalization, environmental-friendliness, stability in a range of pH and resistance to contaminants. It has been used as contaminant adsorbents for metal ions, as well as in membrane technologies for water filtration [126-128]. Additionally, it has been explored as a potential material in the manufacture of thin-film nanofibrous composite (TFNC) membranes [129]. Ma et. al [130, 131] showed the use of ultra-fine cellulose nanofibres as a top layer to achieve high-flux membranes with high retention and high durability. The conventional polymers used for the top barrier layer are very limited and have some disadvantages such as their hydrophobic nature which causes a decrease in water permeability during filtration. When ultra-fine cellulose nanofibres were used as barrier layer, they yielded two to ten times higher permeation flux in comparison with commercial membranes for ultrafiltration of oil and water emulsions, at a similar separation efficiency [130]. Ma et al. studied CNF top layer and achieved a very high rejection ratio of the microsphere with 0.10 ± 0.01 μm diameter (>99.9%)

with 5 times higher permeate flux than that of commercial UF membranes (e.g., PAN10) produced with the same polymer components but without cellulose nanofibre barrier layer [131]. Another concept was to develop a thin-film composite (TFC) membrane with directed water-channels in the barrier layer, which shows significantly higher water permeability than those of conventional TFC while providing the same rejection capability for nanofiltration and desalination applications [132].

Even though NFC has been investigated for water treatment, the use of NFC in depth filters is very limited. A study was recently published [33] and is presenting nanoparticle capture by tortuous depth filter structure that is created by NFC. However, there are other potential benefits of using NFC in depth filters. One possibility could be adding NFC as a barrier layer on top of the depth filter layer. Although barrier layers have been researched in TFNC membranes, it is not used in depth filters. Another potential application could be using NFC as a wet strength agent in depth filters. Currently, depth filters contain a well-known wet strength resin, PAE. As discussed in section 1.2.2, this resin produces toxic by-products. Therefore, an additive that is chemically-inert and environmentally-friendly is of interest for depth filters. However, it is not known how NFC will work in depth filters in terms of filtration performance. In this thesis, the use of NFC in depth filters is explored both by substituting for wet strength agent and forming a barrier layer on top of filters.

1.2.3. Adsorbents

Filter aid is the term that is used in depth filters for the adsorbent phase. A filter aid is a finely divided solid material, consisting of strong hard and incompressible particles. They are used to improve the filtration processes and the most common filter aids include diatomaceous earth (DE) [133, 134], perlite [135], cellulose [136] and activated carbon [137].

In depth filters, filter aids can also act as an adsorbing agent to retain contaminants by electrostatic interactions [138, 139]. This is usually performed in depth filters where the contaminants are smaller than the pore size of filters and not really available to be retained by size exclusion. Adsorption is an effective process for the removal of trace quantities of some contaminants. In principle, any solid material with a microporous structure can be used as an adsorbent. All the filter aids mentioned above can be used as adsorbents. Additionally, bone char [140], clays [141], iron oxides [142], synthetic zeolites [143] and natural zeolites [144] have also been used as adsorbents. The most

important property of any adsorbent is the internal and external surface area and structure, as well as the chemical nature and polarity, which determines, together with the adsorbate, the interaction force between the adsorbent and adsorbate [145].

In this thesis, only expanded perlite has been used as the absorbent to fabricate the depth filters and is comprehensively discussed. However, the following section briefly reviews diatomaceous earth and zeolites as well which are also widely used in depth filters and composites, respectively. Zeolite is a recognized adsorbent, while diatomaceous earth is a very commonly used food grade filter aid in beverage purification.

1.2.3.1. Perlite and expanded perlite

Perlite is a hydrated volcanic glass mainly composed of amorphous silica (65–75% SiO_2), with 10-18% aluminum oxide (Al_2O_3), lesser amounts of the potassium and sodium oxide (6–9% $K_2O + Na_2O$) and minor amounts of iron oxide (1-5% Fe_2O_3), magnesium and calcium oxide (2-6% MgO +CaO) [146, 147]. It is the water content of 2-5% that makes it a commercially valuable material. Unlike other volcanic glasses, perlite will expand to 5 to 20 times its original volume when quickly exposed to a temperature of 900°C to 1200°C [148]. Exposure to heat results in simultaneous softening of the glass matrix and volatilization of the water content, which expands perlite grains by forming small bubbles within glass matrix and decreasing bulk density by up to 90% [146]. Parameters such as size and quality of perlite feed and the design and operation of the furnace can be used to control and maximize the desired product specifications. After expansion, any unexpanded particles and fines are removed by air classification. The particles are hollow and porous with many shapes [148] and Figure 8 shows the irregular shapes of expanded perlite particles in scanning electron microscopy image at 1000 x magnification.

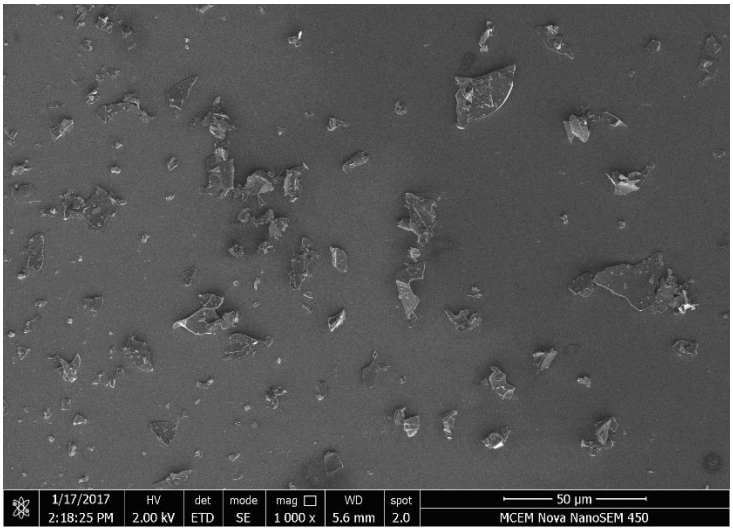

Figure 8: Scanning electron microscopy image of expanded perlite.

The resultant low-density particles with cellular interiors are used for their acoustical and thermal insulating properties, chemical inertness, physical resilience, fire resistance, water retention ability and low bulk density [146].

Perlite products are usually categorised according to whether it is expanded or unexpanded. Most of the commercially used perlite is in expanded form. The specific surface area of expanded perlite is around 1-3 m^2/g [149-153] with a pore size distribution reported as having a maximum peak at 3 nm [151]. Interestingly, this is sharply different from the pore size distribution of the expanded perlite used in this thesis, which was measured as a BJH Adsorption average pore diameter of around 14 nm. As discussed before in section 1.2.2.2, gas adsorption is used for surface area and porosity measurements. Besides NFC, gas adsorption techniques are also widely used for adsorbent materials and these methods are discussed more in detail in section 1.2.6. The size of perlite used in this thesis is largely between 5 to 10 μm; however, it is also possible to find other size distributions of perlite in literature [154].

The surface chemistry of perlite is the main contributor to the adsorption capacity. In the surface hydroxyl groups, the silicon atoms at the surface tend to maintain their tetrahedral coordination with oxygen. They complete their coordination at room temperature by attachment to monovalent hydroxyl groups, forming silanol groups [138]. The different types of silanol groups (a) and the hydrous oxide surface groups in alumina (b) are shown in Figure 9 and these are the ones that give perlite its adsorption capacity [138, 155].

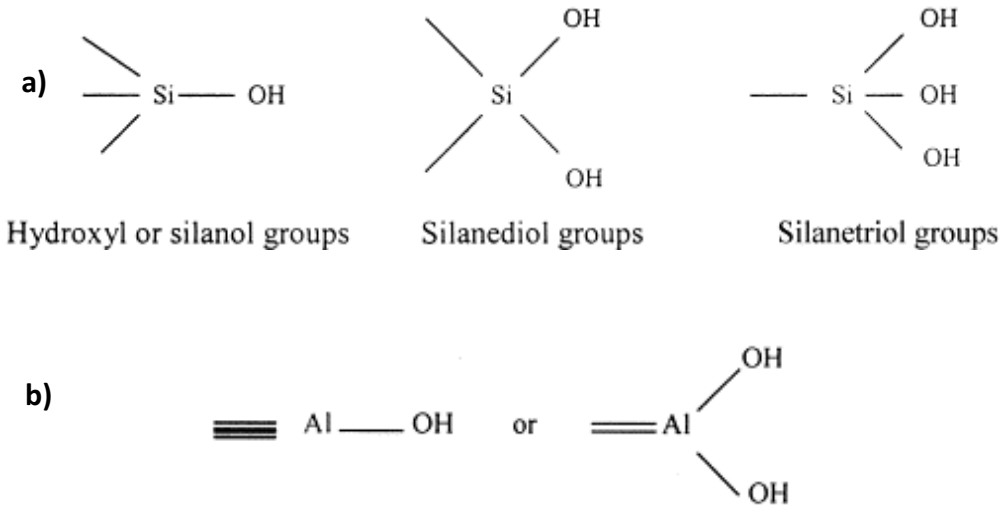

Figure 9: Surface chemistry of expanded perlite with a) different types of silanol groups b) hydrous oxide surface groups in alumina (Reprinted by permission from Springer Nature, Water, Air and Soil Pollution, Adsorption of Methylene Blue from Aqueous Solution onto Perlite, Mehmet Doğan, Mahir Alkan, Yavuz Onganer, Copyright © 2000 [138]).

Adsorption onto perlite is governed by electrostatic interactions and perlite can be used as an adsorbent for heavy metals [156], dyes [138] and oil spills [157]. Positively charged contaminants are adsorbed onto negatively charged sites of perlite given in the Figure 9. However, opposite charge adsorption is also possible by altering the surface charge of perlite. For example, positively charged polymers in a suspension can adsorb onto the perlite surface and promote negatively charged contaminant adsorption onto perlite. Even though perlite has been studied widely as an adsorbent, its surface area is very limited as stated above. In this thesis, the function of perlite is also forming a porous structure by preserving open channels through the filter media besides its contribution to adsorption.

Expanded perlite is used in a variety of applications. The most important market is for formed insulation products [158], followed by filter aid [159], horticultural products [160] and filler applications [161]. Expanded perlite as a filter aid is widely used in the processing of food and beverage products [162] as well as of chemical products and industrial effluents.

1.2.3.2. Diatomaceous earth

Diatomite ($SiO_2 \cdot nH_2O$), or diatomaceous earth (DE), which has amorphous SiO_2 as the primary content, is a siliceous, soft and lightweight rock available in large deposits around the world [163]. It contains up to 80–90% voids [163] and the density is around 1.9–2.3 g/cm^3 [164]. Diatoms have high porosity, good hydrophilicity, and high chemical stability [163] and are negatively charged in water in the pH range 2-12 [164, 165]. Diatomite is composed of the fossilised remains of diatoms, a class of unicellular algae found in both fresh and sea water [146]. These skeletons can be in a variety of sizes and shapes such as spheres, disks, wheels, needles, ladders and they all possess a porous, lace-like structure [166]. Diatomite is particularly used for depth filters in beverage purification. Beverage products such as beer and wine mainly rely on agricultural raw materials which can show significant variation. Therefore, besides many other important properties, diatomite is also found to be highly adaptable to varying conditions with its variety of size and shape for depth filters in food and pharmaceutical applications. The size of individual skeletons (called frustules) can typically range from 10 to 150 µm [146]. Scanning electron microscopy image of diatomaceous earth is shown in Figure 10.

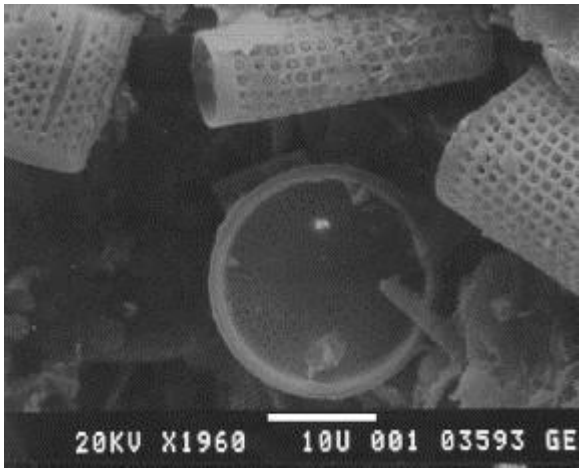

Figure 10: Scanning electron microscopy image of diatomite (magnification is 1960×) (Reprinted from Remediation of wastewater containing heavy metals using raw and modified diatomite, 99/2, Majeda A.M. Khraisheh, Yahya S. Al-degs, Wendy A.M. Mcminn, Copyright © 2004, with permission from Elsevier [163]).

Diatomite can be categorised by their size and the further processing applied. They can be in natural, calcined and flux calcined states [146]. Due to their low cost, environmentally friendly nature,

chemical inertness as well as high surface area and porosity, diatomite has been widely used as filter aid [167], adsorbent [168, 169] and catalytic support [170]. It is used in various industrial applications such as filtration media for different beverages and inorganic and organic chemicals, and as an adsorbent for pet litter and oil spills [171].

1.2.3.3. Zeolites

Zeolites are crystalline, hydrated aluminosilicates of alkali elements such as sodium, potassium, magnesium, calcium, strontium and barium [172]. Due to the channels and pores in the structure, they have a high internal surface area which makes them heavily used in adsorption processes [173]. Tetrahedra of silicon and aluminium (SiO_4 and AlO_4) are the primary structural unit of zeolites and these structures assemble and construct secondary polyhedral building units [174]. Structurally, the final framework is based on an assemblage of the secondary building units in a three-dimensional crystalline framework. The framework also has interconnected voids and channels which are occupied by cations and water molecules. Those voids and channels enable any molecules inside to move around. Figure 11 shows the structure of zeolite with three dimensional channels and cages.

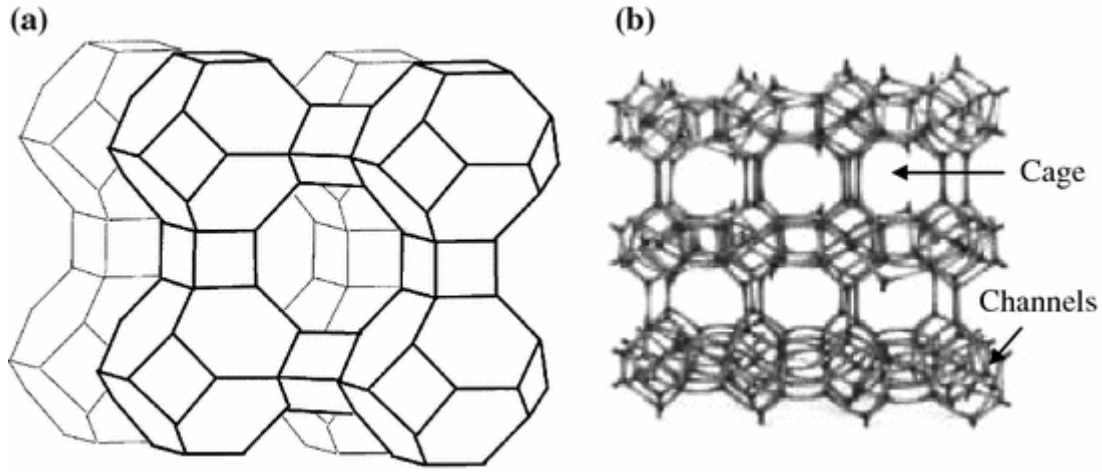

Figure 11: **(a) The schematic view of the crystal structure of zeolite 4A and (b) typical zeolite structure showing three dimensional cages and channels. (Reprinted by permission from Springer Nature, Fly Ash Zeolites, Basics of Zeolite, Bhagwanjee Jha, Devendra Narain Singh, COPYRIGHT © 2016 [174]).**

The main feature of zeolites that distinguishes them from other porous material is their great variety of pore sizes and shapes [173]. Furthermore, high internal and external surface areas [175], and chemical and mechanical stability [176] are also the other important characteristics of zeolites that make them recognized as an excellent adsorbent material.

Zeolites are mainly classified by framework structures which define the connectivity (topology) of tetrahedrally coordinated atoms in the highest possible symmetry. There are more than 135 different structures [177]. The framework type describes the structure family that a zeolite belongs to. Each type has an assigned three letter code such as Linde type A (LTA) and Faujasite (FAU). Zeolites, which have the same framework type, can also vary with chemical composition (Silicon Aluminium ratio (Si/Al)), type of extra framework cations and distribution, possible Si-Al ordering in tetrahedral sites and different guest species [174]. Si/Al ratio is a relatively important parameter to describe the composition of a zeolite. Different properties such as hydrophilicity and acidity will change with the difference in Si/Al ratio [172]. Zeolite A, Y and X are some of the zeolites which have industrial importance. Moreover, zeolites are more importantly categorised into inexpensive naturally occurring zeolites [178] and more expensive synthetic ones [179].

1.2.4. Polyelectrolytes

Polyelectrolytes are charged polymers that are carrying either positively or negatively charged ionizable groups [180, 181]. These ionizable groups can dissociate into a highly charged polymeric molecule in polar solvents, such as water, and leave their charges on the polymer chain while releasing the counter ions into solution [182]. Polyelectrolyte morphologies can be divided into linear and branched/cross-linked and they can further be classified into anionic and cationic polyelectrolytes according to the nature of ionic groups they possess. Polyelectrolytes can either be natural or synthetic [183] and synthetic commercial types are usually produced by polycondensation and polyaddition processes [184]. Further information about types of polyelectrolytes is given in the review done by Meka et al. [185]. The functionality of polyelectrolytes is determined by the polymer backbone structure as well as the functional groups attached to the backbone. Predominant polyelectrolytes are polyacrylamide copolymers of acrylamide and acrylate, or monomers containing ammonium groups [186].

Polyelectrolytes are characterised firstly by polydispersity index, which is the ratio of the weight average and number average molar masses. Most of the synthetic polyelectrolytes have a polydispersity index larger than 1, which refers to a broader molar mass distribution [187]. The second important variable is the charge density of polyelectrolytes, which measures the total charge of the polyelectrolyte. It is measured by titration with an oppositely charged polyelectrolyte until the zero electrokinetic potential is achieved and usually given in meg/g.

Polyelectrolytes in an uncharged state act like normal macromolecules, however their properties can significantly change with even a small dissociation of the ionic groups. Electrostatic interactions could arise due to the partial or complete dissociation of ionic groups, and this could lead to deviations of polymer behaviour [185]. When a polyelectrolyte interacts with an oppositely charged surface, it is adsorbed onto surface by various sites, usually not covering the whole surface. The process of polyelectrolyte adsorption onto a surface includes the following steps: transport of the polyelectrolytes in solution to the surface, attachment of polyelectrolytes on the surface and reconformation of the polyelectrolytes on the surface [188]. The adsorption of linear polymers onto a surface can also produce tails and loops, which can protrude from the surfaces. The equilibrium conformation of an adsorbed linear polymer is shown in Figure 12.

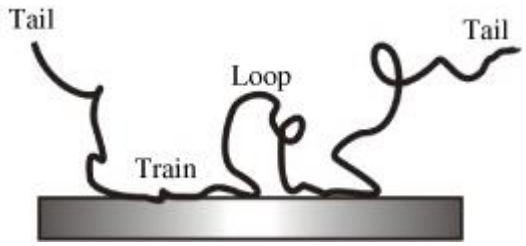

Figure 12: **Train, loop and tail segments of a polymer chain adsorbed onto a surface (Reproduced from Direct measurements of polymer-induced forces, Dzina Kleshchanok, Remco Tuinier and Peter R Lang, 20/7, Copyright © 2008, with permission from IOP Publishing [189]).**

There are three different segments in the typical configuration of an adsorbed polymer at a surface. The parts that are interacting with the surface are referred to as trains, the connection between the trains are loops which have no contact with the surface; non-adsorbed chain ends that do not touch

the surface are called as tails. The adsorbed polymer conformation model was proposed by Jenkel and Rumbach in 1951 [190].

Polyelectrolytes are used in various fields such as pharmaceutical industry [191], medicine [192], water plantation [193], cosmetics [194], food [195] and paper industries [196, 197]. Cationic polyelectrolytes have been commonly used in papermaking industry as retention aids, as well as dry and wet strength agents to control the structure of paper, pore size and porosity, and to improve papermaking process.

Cellulose-polyelectrolyte interactions have been extensively studied [198-203]. In this thesis, polyelectrolytes are employed to provide dry and wet strength to the filters as well as to engineer the adsorption performance through charge modification. Polyamideamine-epichlorohydrin is the predominantly used polymer for both wet strength and charge modification. Cationic polyacrylamide and polyethylenimine are further investigated for both purposes. The types of polyelectrolytes used are explained in the following section.

1.2.4.1. Polyamideamine-epichlorohydrin

Polyamideamine-epichlorohydrin (PAE) is one of the most common additives to manufacture wet strengthened papers [204-207]. It is synthesized by the reaction of polyamideamine chains with epichlorohydrin and the resulting polymer has an amideamine repeating unit together with partial cross-linking between polyamideamine chains through 2-hydroxypropane bridges originating from the attached epichlorohydrin [208]. Therefore, the commercial PAE/water solutions are cross-linked and highly dense polymers. Average weight and number molecular mass values of these polymer could be around 1,140,000 and 27,000, respectively, with polydispersity index of 42 [209].

Wet strength is developed through a water-soluble three-dimensional network. This network is formed by the crosslinking of cationic azetidinium groups present in the polymer structure with carboxyl groups of cellulose when heated. The reinforcement and protection mechanisms generated by PAE [210] are shown in Figure 13.

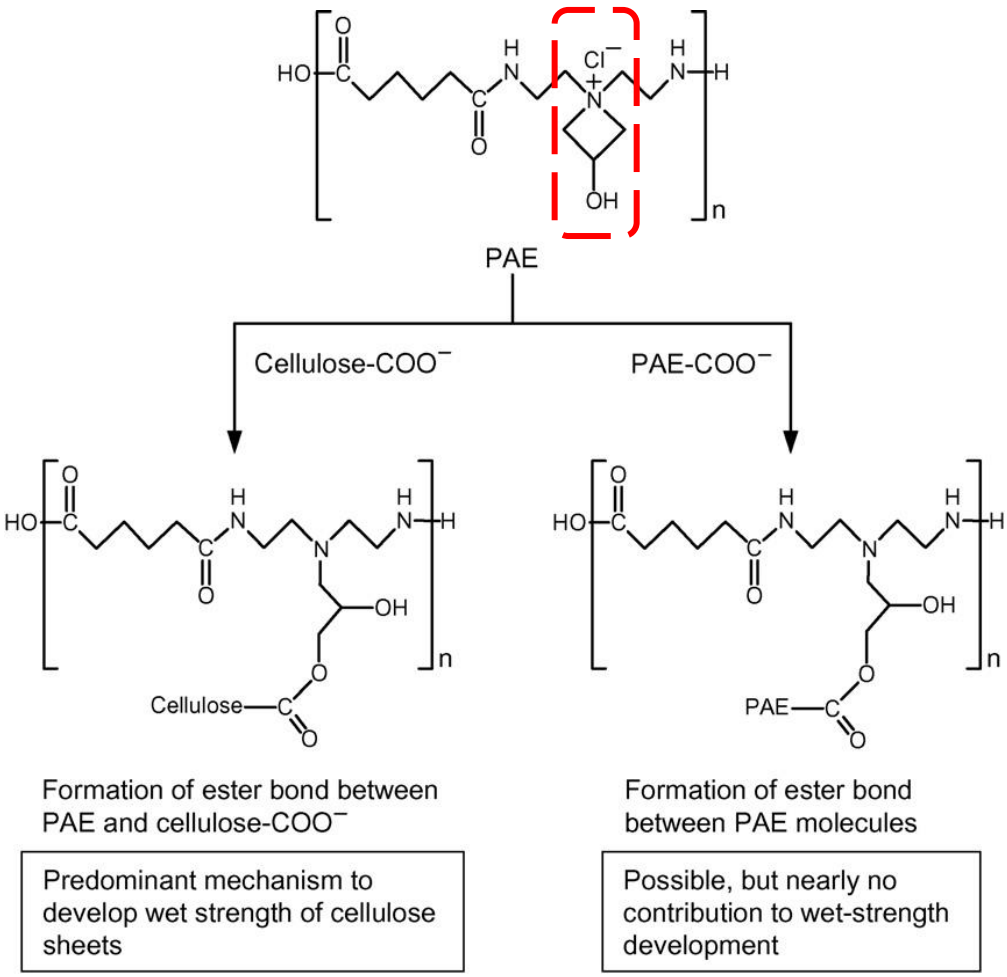

Figure 13: **Ester bond formations between azetidinium groups (highlighted) of PAE and either carboxyl groups of cellulose fibres or carboxylate groups of PAE molecules (Reprinted from The mechanism of wet-strength development of cellulose sheets prepared with polyamideamine-epichlorohydrin (PAE) resin, 302/1-3, Takao Obokata, Akira Isogai, 525-531., Copyright © 2007, with permission from Elsevier [211]).**

The reaction between azetidinium groups of PAE and carboxyl groups of cellulose fibres is the predominant mechanism that contributes to wet strength. The protection mechanism is the reaction of azetidinium groups through the amine groups of resin molecules to create a homo-crosslinked network. These reactions generate a partial water-proof barrier around the fibre-to-fibre contact point, which restrict water from hydrolysing hydrogen bonds and ionic bonds of cellulose sheets when they are re-wetted. PAE also provides positive charges to the filter medium

through the positively charged site of azetidinium group highlighted in Figure 13. When PAE added into a filter suspension, it is adsorbed onto negatively charged surfaces and creates available positively charged surfaces for adsorption of negatively charged species. In this work, PAE is employed as a wet strength agent as well as for charge modification of the filter medium. However, this polymer has some major problems as a material in depth filters. Firstly, PAE contributes to AOX (adsorbable organic halogen) content of waste streams by generating some toxic by-products [204]. This is usually a problem during PAE manufacturing step. However, PAE in paper and paperboard products as an indirect food additive is also limited by food regulations since any uncrosslinked PAE can be toxic for food products. Secondly, PAE has a short shelf life as it can homo-crosslink with itself [204]. Thus, making depth filters with the same properties while minimising the use of toxic PAE remains as the main issue. As discussed previously in section 1.2.2, nanofibrillated cellulose can be a promising substitute for wet strength resin as a sustainable reinforcement material. However, substituting PAE for NFC results in a complete change in the charge characteristics of filters and it would no longer be possible to adsorb negatively charged contaminants. Accordingly, addition of non-toxic cationic polymers would be essential. Therefore, the branched polymer polyethylenimine and the linear polymer cationic polyacrylamide are considered for charge modification of filters. Their contribution to wet strength is also investigated. The next two sections are dedicated for discussion of these two polymers.

1.2.4.2. Cationic polyacrylamide

Polyacrylamide is the basis of many commercial flocculants [212] and it can be easily synthesized up to very high molecular weights. Cationic polyacrylamide (CPAM) is a synthetic macromolecule made from copolymers of acrylamide and various cationic derivatives of acrylic acid. CPAM is available in branched and linear forms however linear CPAM is the type that is commonly used in the paper making industry. Cationic polyacrylamide can be prepared by co-polymerization of acrylamide with a cationic monomer, such as DDMAC [213] or by modifying the initial polyacrylamide chain. The chemical structure of CPAM is given in Figure 14.

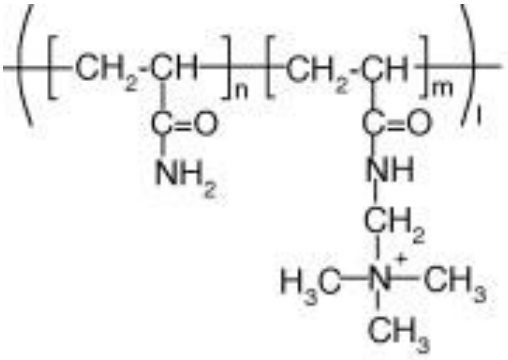

Figure 14: The chemical structure of CPAM (Reprinted from The role of cationic polyacrylamide in the reverse flotation of diasporic bauxite, 20/13, Guangyi Liu,Hong Zhong,Yuehua Hu,Shenggui Zhao,Liuyin Xia, 1191-1199, Copyright © 2007, with permission from Elsevier [214]).

CPAM has been used as a dry strength agent [215] and a retention aid [216] in the papermaking industry. CPAM is available in a range of molecular weights up to 13 MDa [217] and charge density up to 80% [218]. The efficiency of CPAM in some applications (e.g. flocculant) is usually dependent on the molecular weight, charge density and molecular conformation [219, 220]. In this thesis, we will investigate incorporating positively charged CPAM into filters for removal of charged contaminants as well as investigating its contribution to wet strength development.

1.2.4.3. Polyethylenimine

Polyethylenimine (PEI) is a cationic polyelectrolyte which is typically used in a highly branched form, which can be modelled as a rigid particle [221]. PEI has long been employed to improve drainage and retention [222, 223]. This polymer is produced from cationic polymerisation of aziridine (ethylenimine) in an aqueous or alcoholic solution in the presence of an acid catalyst [224, 225]. The weight average molecular weights (M_w) achieved with this synthesis are typically in the range 20,000–50,000 g/mol [226]. The effectiveness of the polymer increases with the increasing molar mass. However, there would be a risk of forming an insoluble gel if the molar mass of the branched form is too high, due to the branched characteristics of polyethylenimine chains [225]. The structure of branched and linear PEI is shown in Figure 15.

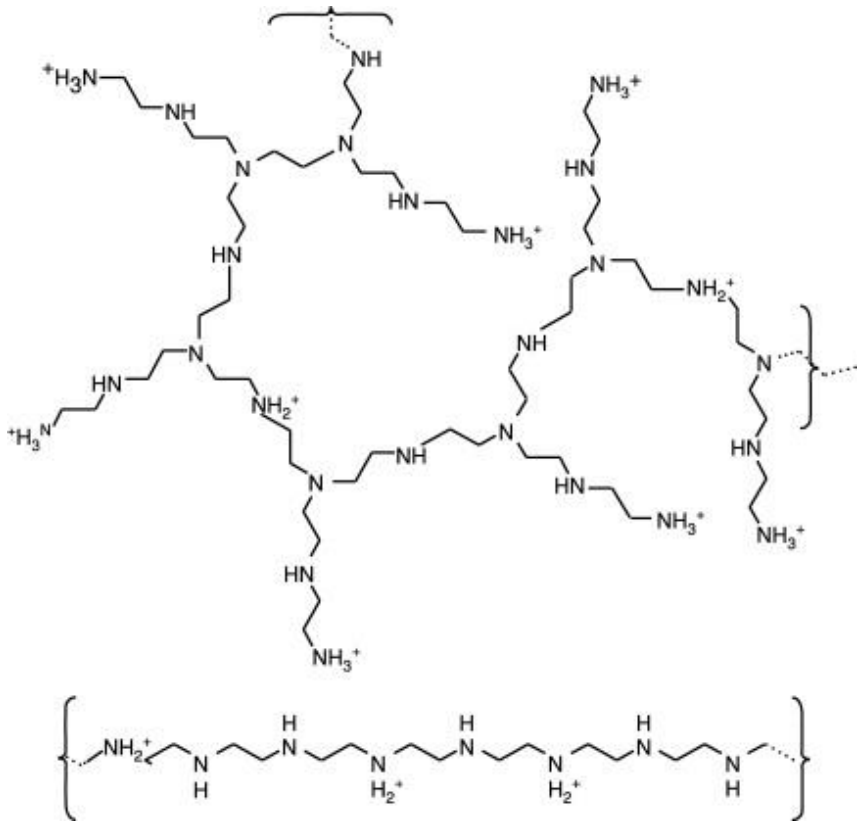

Figure 15: The chemical structure of branched (upper) and linear (lower) PEI (Reprinted from Advances in Genetics, 53, Barbara Demeneix,Jean-Paul Behr, Polyethylenimine (PEI), 215-230, Copyright © 2005, with permission from Elsevier [227]).

The adsorption conformation of PEI is different than CPAM. PEI is adsorbed onto oppositely charged surfaces as large rigid bridges, maintaining its shape without any reconformation and flattening [228]. Unlike PEI, CPAM is adsorbed onto surfaces with a tails and loops conformation as shown in Figure 12. PEI is a strong polyelectrolyte, with 20 to 40% of its amino groups protonated [229]. These protonated amino groups associate with the oppositely charged surfaces [230].

In this thesis, PEI is investigated as a charge modifying agent in our filter media. Additionally, the effect of PEI on wet strength contribution is studied as there are some studies indicating that it improves wet strength [231, 232]. PEI particularly helps us understanding the effect of polymer morphologies on the properties mentioned above.

One of the questions here is to investigate whether the adsorption of these cationic polyelectrolytes onto fibres and adsorbents affects the adsorption capacity of the filters by blocking the pores.

1.2.5. Cellulose based membrane/filter preparation techniques

This section briefly reviews preparation methods of cellulose fibre-based membranes and filters. Phase inversion is the most widely used technique for polymeric membrane fabrication. However, this method is not suited for making depth filters. Papermaking technique serves as a simple and quick technique compared to traditional membrane fabrication techniques and is widely used for depth filter production. There are also other techniques used for cellulose based membrane preparation, even though they are not being used on a larger scale, such as electrospinning [233-235], layer-by-layer deposition [236], solvent casting [237], spray deposition [238] and the sol-gel process [239]. Phase inversion and standard papermaking techniques are explained in detail below.

1.2.5.1. Phase inversion

Majority of commercially available membranes are prepared by phase inversion method. This is a process by which a polymer is transformed from a liquid or soluble state to a solid state [240]. Phase inversion can be done by a number of techniques: solvent evaporation, precipitation from vapour phase, thermal precipitation and immersion precipitation or dry–wet phase inversion [241-249]. The majority of phase inversion membranes are prepared by immersion precipitation [250-253]. Even though phase inversion has almost entirely been used for membranes prepared from fossil-based polymers, increasing environmental restrictions have led to a demand for membrane production from more environmentally sustainable polymers. Cellulose is one of the strong alternatives as a bio-based membrane material [254].

Bio-based membranes are commonly produced in a similar way to the traditional fossil-based membranes. Phase inversion technique still remains as the most widespread process for the preparation of bio-based membranes [254]. Cellulose acetate (CA) membranes derived from the acetyl substitution of the cellulose, have been widely used in industrial applications to reduce the microorganism content in raw water as well as RO and UF processes [255-258]. A variety of raw materials such as cotton, recycled paper or wood cellulose have also been used to produce cellulose ester biopolymers [259].

However, the performance of both petroleum and bio-derived polymer-based membranes still needs to be improved further. Composite membrane materials formed by blending nanosized inorganic and organic materials are attractive for the purpose of creating new materials with new or enhanced properties such as high permselectivity, good hydrophilicity and excellent fouling resistance compared with single organic or inorganic membranes [260]. Incorporating nanosized organic/inorganic materials into polymer matrix has been widely studied in petroleum-derived polymeric membrane fabrication [261-265].

The same blending approach has been studied in cellulose based membranes as well. Goetz et al. [266] coated CA membrane surface with chitin nanocrystals. 5% self-assembled chitin nanocrystals coating increased the strength of membrane by 131% and stiffness by 340%. The resulting environmentally friendly membrane mixture has high hydrophilicity that significantly reduced membrane fouling. Kanagaraj et al. [267] investigated the effect of incorporating hydrophilic surface modifying macromolecules (SMMs) into CA matrix on the membrane flux, selectivity and antifouling properties. Surface modified ultrafiltration (UF) membranes were prepared by phase inversion and tested for protein and humic acid removal. The study showed that addition of SMMs to CA membrane could reduce fouling from 40.6% to 25.6% showing that novel SMM modified filters play an important role in water treatment by UF.

The phase inversion method requires the use of hazardous solvents during fabrication which can pose some environmental problems. Therefore, other synthesis methods with lower impact are sought. Furthermore, phase inversion cannot be used for depth filter preparation as the fabricated layer by phase inversion is typically continuous with uniform pore size throughout the entire thickness. However, depth filters are targeted to have a density gradient through the thickness with a large variety of pore size, i.e., the upper layers remove the large particle from the fluid where the fine particles are removed through the thickness. Such a structure cannot be obtained by a phase inversion technique. Another drawback of the phase inversion method is that blending nanosized materials with polymeric solution is also a challenge [268]. Adding high loading of nanomaterials can cause particle aggregation, and in turn produce macrovoids [268].

1.2.5.2. Papermaking

Paper media is a special sub-category of non-woven filer media and this paper-based filter media is commonly made by wet laying of cellulose fibres onto a woven wire band [39]. In an industrial papermaking process, the major sections of a paper machine consist of the forming section, press section, and dryer section [269, 270]. The water in the suspension filters through the wire or forming fabric driven by gravity or vacuum, which allows fibres to settle to produce a continuous sheet on the forming section of a paper machine [270]. Commonly, the pulp slurry is made of cellulose fibres and other additional components (inorganic fillers and polymers), if used, evenly fed onto the woven fabric. The fibres settle randomly to form the sheet. In the press section, further dewatering of sheets is performed by mechanical pressure applied through press or rotating rolls [269]. The next step is drying section where the remaining water is evaporated. In this section, the web contacts a series of internally steam-heated cylinders. These dryers are hollow, revolving and steam-filled drums, applying heat to the web by contact [269]. This describes how a large-scale paper media production is conducted. Applications of papermaking for filters can be found in various types of laboratory filter papers, industrial filter papers, coffee filter and depth filters [271]. However, standard papermaking is not used for membrane preparation as the random settlement of fibres does not provide an absolute cut-off value. There will almost certainly always be larger pore sizes than the nominal rating and random larger particles may pass through the filter. This limits the suitability of paper elements for ultrafine filtering. However, they can be made of nominal cut-offs in the range of 10-20 μm or larger [39].

Standard papermaking method has been employed for decades as a rapid preparation method for paper-based filter medium. Additionally, this method can be practised easily in laboratories as well. In a laboratory scale filter preparation, sheet mixture is prepared in a slurry form and sheets are formed on a small mesh by draining water. The time requires for water drainage and paper forming can be greatly reduced by applying variable vacuum [90]. Once the sheets are formed, they are dried by using different methods such as oven drying [272], hot pressing [273], air drying [274] and drying under vacuum followed by a sheet dryer [275]. Filter sheet preparation by this method followed by drying has been extensively studied in literature [44, 275, 276].

Ichiura et al. reported a series of works [277-282] which address the preparation of cellulose-zeolite filter sheets via papermaking technique. They tested adsorption performance of composite sheets on gaseous compounds. In one of their study [281], they reported the use of a dual polymer system to achieve high retention of the stock components. Their process involved mixing pulp slurry and cationic polymer (polydiallyldimethylammonium chloride) (PDADMAC), followed by the addition of inorganic suspension (Zeolite Y, kaolin and glass fibre) and anionic polymer (anionic polyacrylamide) (A-PAM) respectively. The sheets were prepared in a hand sheet making machine according to TAPPI method-205. The wet sheets were pressed under 350 kPa for 5 minutes and then dried in the oven for 30 minutes at 105˚C. They showed that these composite papers can be used as adsorbents for the removal of gaseous compounds, such as volatile organic compounds (VOCs).

However, there are some drawbacks involved in papermaking process. Firstly, papermaking is a one-sided filtration process. This leads to non-uniformities and agglomeration of fibres and inorganic adsorbents in the sheet. The effect of this defect on depth filtration performance is unknown. Also, depth filters have very high loading of inorganic adsorbents and the sheet structure with high levels of inorganic adsorbents is another gap in knowledge. Retention of inorganic particles in cellulose fibre matrix is a major issue in papermaking techniques, therefore, retention aids are often used to bridge the particles to the fibre network. Retention can also be controlled by size of both fillers and fibres. Higher aspect ratio fibres can entangle more and act as a mesh to retain the particles.

There are a few studies addressing the preparation of nanofibrillated cellulose membranes by this technique [111, 283-286]. Varanasi et al. [111] prepared biodegradable and recyclable ultrafiltration (UF) membranes from NFC, silica nanoparticles and polyamideamine-epichlorohydrin (PAE). Membranes were made using a standard British hand sheet maker, which is reported as a simple and rapid technique [287]. Silica nanoparticles were used to control the pore size of the NFC fibre network by filling the largest pores. Silica nanoparticles have been employed as fillers in many different applications because they can promote adhesion between materials. Additionally, they are favourable due to their high mechanical strength and high thermal stability. However, one of the challenges regarding nanoparticle addition to NFC fibre network is retention of those nanoparticles. Therefore, PAE was added to increase the retention of negatively-charged nanoparticles in the fibre network and also to improve the wet strength of the membrane. Pure NFC membranes were also

fabricated as control samples. These membranes showed high flux but low rejection due to large pore size of the membranes. In contrast, composite membranes showed greatly improved rejection of 300 kDa PEG at the same thickness membrane, thanks to the controlled pore size provided by the silica nanoparticles. These results demonstrate the potential of NFC composite membranes in ultrafiltration. The produced membranes can also be recycled with a conventional paper recycling process. While there have been several studies addressing membranes from nanofibrillated cellulose, it is not clear how depth filters will perform when NFC is added as part of a papermaking process. There are some studies on adding NFC to conventional pulp fibres to make paper [78, 288-290]. However, application of NFC in depth filter manufacture, as mentioned in section 1.2.2, is a significant gap in knowledge.

In this thesis, papermaking technique is used to form the cellulose fibre composite filters. A mixture of cellulose fibre, perlite particles and PAE is prepared as a slurry before papermaking. Perlite particles are easier to retain than nanoparticles as they are in micrometre range. However, PAE also helps to retain the perlite particles. Following the preparation, sheets were characterised in terms of both structural characteristics and filtration properties. The next section reviews the different characterisation techniques to analyse the performance of filters.

1.2.6. Characterization techniques for cellulose based filters/ membranes

Characterisation of the filters with different techniques is the most crucial part after the fabrication process. As the overall goal of this thesis is to improve the current filter products, structural and performance-based characterisation is essential to have a deep understanding about them. There are three important aspects that need to be characterised. Firstly, the filter structure must be measured by imaging and porosimetry techniques. Secondly, the surface chemistry must be characterised. Thirdly, the separation performance must be quantified as this is the main purpose of the filter production. The next sections cover the different techniques that are used to characterise the filters in this thesis.

1.2.6.1. Imaging techniques

Imaging techniques are one of the primary tools to observe the structure of the membranes and filters. Optical microscopy is mainly used for biological samples [291]. However, it can also do surface and cross-sectional imaging in paper like materials down to 1 μm resolution. It only provides two-dimensional characterisation; imaging in the z-dimension is not possible. Due to the wavelength of visible light which limits the magnification, the use of optical microscope is limited in the characterisation of nanomaterials and composites. The limitations in optical microscopy have led to use of advanced microscopic techniques to produce highly magnified images of nanomaterial surfaces.

Electron microscopy (EM) techniques such as transmission electron microscopy (TEM) and scanning electron microscopy (SEM) are widely used as advanced imaging techniques. Both SEM and TEM can image morphological characterization (shape, size, roughness, etc.) and can also have an analytical mode for chemical information (elemental analysis by X-ray energy dispersive spectroscopy, EDS) [292]. SEM is most commonly used to understand sample morphology. It gives only a two-dimensional (x- and y-) image of the sample, while the z-dimension cannot be observed directly [293]. In SEM, electron beams are traversed over each point of a specimen surface. Then, the reflected electrons from each point on the specimen, resulting from the interaction between electrons and sample, are collected by a detector and converted into images [294]. The resolution of SEM is limited to 5 nm, which can only be achieved under vacuum [293]. However, SEM is limited to a very small area and it is a continual question as to whether images are representative of the whole sample. Also, it is not possible to estimate the pore size distribution and porosity throughout the sample only with surface visualisation by SEM.

TEM is used to visualise atomic structures in samples. This is achieved by an interaction between a high-energy beam of electrons and the sample [293]. The basic principle of TEM is based on transmitted electrons through the specimen to form the sample image. This is different from SEM where backscattered and secondary electrons emitted from specimen surface are used for image construction. TEM can be used to structurally and chemically characterise particles at high spatial resolution close to 0.1 nm [295]. For example, TEM images can be used to show the distribution and dispersion of nanoparticles in polymer matrices of nanocomposite materials [293]. It is capable of

imaging at a significantly higher resolution and producing high-quality images. However, it requires a special sample preparation to obtain a good contrast. Furthermore, the specimen thickness in TEM is generally limited to a few hundred nanometres to be able to have a proper image formation [296].

X-ray computed 3D tomography is another tool which is used to assess the three-dimensional structure of the composites. It is a non-destructive method that uses X-rays to produce cross-sectional images, or virtual slices of specimens, allowing users to see inside the object without cutting [297]. The basic principle is based on a set of images of beam transmitted through the sample while the sample is rotated to different positions in small increments for each image taken [298]. The 3D structure is then reconstructed from these images. X-ray microtomography allows 3D imaging of most paper grades at a high resolution of approximately 1 µm [298]. This resolution is sufficient for observing most features of the fibre network and having a structural assessment. However, it is not sufficient to detect all fine fibres and inorganic particles. Although, it is not sufficient to observe everything, we can still obtain both a quantitative and a qualitative analysis on the internal structure of composites showing how the fibre network can build up to form the composite. It is possible to quantify length, diameter and orientation distributions of fibres as well as void ratio of the composites from the reconstructed 3D images [299]. No specific sample preparation is required for this technique and the sample dimension used for the analysis is usually in mm range. However, the small dimensions might not be representative for the entire sample.

In this thesis, the composite depth filters are characterised using SEM and 3D X-ray tomography techniques. SEM is used to image the surface and cross section of the composites, as well as measure fibre diameter and particle size distribution, while X-ray tomography is used to observe the void formation in the composites.

1.2.6.2. Pore size distribution and porosity

Pore size and porosimetry are also important to characterise. They are particularly significant to identify the extent of size exclusion that can be performed by a filter. The overall porosity, together with pore size, would also have an effect on the flux of the filters. Pore size and porosity can be estimated by mercury porosimetry for cellulose fibre composites [300] and other porous samples

[301, 302]. A small specimen is first dried to empty the pores from any existing fluids or contaminants and then tested by applying increasing pressure to the sample immersed in mercury. The size of the pore that the mercury can enter decreases, as the pressure increases. Mercury porosimetry can be used to measure pore sizes between 3.5 nm to 500 µm [111, 303-305]. However, this technique has some limitations. One of them is that it usually estimates the largest entrance of the pores, not the actual inner pore size. Any closed pore would remain unanalysed [303]. Also, this calculated pore size assumes a cylindrical pore geometry, which might not be the case for each pore [303]. However, mercury porosimetry is still an extremely useful technique that provides important information about porosity of samples [303].

Gas adsorption is a technique that can performed with gases such as nitrogen (N_2), Krypton (Kr) and Argon (Ar), for surface area and pore size characterisation of porous materials. Gas adsorption allows assessment of a wide range of pore sizes (from 0.35 nm up to > 100 nm) [306]. This range includes the complete range of micropores (less than 2 nm) and mesopores (2-50 nm) and even some macropores (greater than 50 nm) [306]. Additionally, gas adsorption techniques are convenient to use, non-destructive and are not as costly as mercury porosimetry. Therefore, this technique is very useful to analyse the pore size characteristics of mesoporous industrial adsorbents such as zeolite and perlite [151, 307, 308].

In this thesis, mercury porosimetry is used to estimate the pore size distribution and porosity of the final composites as the composites' pore size is in the range of applicability of mercury porosimetry. Also, N_2 adsorption is used to analyse the surface area and porosity of the inorganic filler, perlite, used in the filter preparation.

Table 3 below presents a summary of particular size-based features of filters along with the imaging and porosimetry techniques that are used to measure them. The features are given based on perlite particles and refined cellulose fibres. Features on the final filter products are given based on a widely prepared reference filter sample that can be found in the following chapters.

Table III: Particular features of filter and filter components with the characterisation techniques used.

Feature	Method	Approximate value
Filter pore size distribution	Mercury porosimetry	Pore size: 1-3 μm
Expanded perlite surface area and porosity	Gas adsorption (3Flex)	BET surface area: 3.3372 m^2/g BHJ adsorption average pore diameter: 14 nm
Perlite particle and nanofibrillated cellulose size distribution	SEM	Perlite particle size distribution: 5-10 μm Nanofibre size distribution: 50-55 nm
Cross section imaging and porosity of the filter	3D X-ray tomography	Void Fraction: 14%

1.2.6.3. Surface chemistry

Surface chemistry is an important parameter which can impact the membrane and filter performance. Surface chemistry in filters and membranes can be described as the physical and chemical phenomena that occur between filter medium and the surrounding medium. These interactions are important as they may affect membrane flux, rejection and fouling. So, characterisation of membrane surface properties is essential, and it can be performed via spectroscopic techniques, microscopic techniques and characterisation of surface charge [309]. Surface modification is a very widely used method to increase interactions between membrane/filter surfaces with the surrounding molecules that will increase the retention of contaminants. First, these chemical modifications can be investigated through Fourier Transform Infrared (FTIR) spectroscopy that uses electromagnetic radiation. The FTIR uses a beam of IR light that is passed through the sample and the transmitted energy is detected and used to produce the resultant spectrum [309]. FTIR is one of the most commonly used spectroscopy techniques. When used in Attenuated Total Reflectance (ATR) mode, FTIR can be used to assess the functional groups present in membrane surfaces [310-312].

Raman spectroscopy is a complementary method to IR spectroscopy. It is possible to obtain both qualitative and quantitative information on polymer functional groups and structure and also their conformation and orientation [313, 314]. It uses a beam of monochromatic laser light, with a frequency range varying from the visible to near UV, passing through a sample. This technique is sensitive to molecular vibrations, rotations and other low frequency modes and in turn, can provide useful information on the crystalline structure of polymers and other macromolecules [315, 316]. Membrane fouling can also be investigated by Raman spectroscopy [317].

Other spectroscopic techniques that are used for membranes can be listed as follows. Nuclear Magnetic Resonance (NMR) can be used to investigate polymer blend miscibility in membrane fabrication [318, 319]. Electron spin resonance (ESR) gives absorption spectra of a particular material which can provide information about the chemical and structural properties of a material [320]. X-ray photon spectroscopy (XPS) is a quantitative surface analytical technique and provides information on the surface elemental composition [321, 322]. Small angle scattering spectroscopic techniques using neutron (SANS) and X-rays (SAXS) are used for the characterisation of membrane structures at length scales typically in nanometre range [323].

Additionally, SEM and TEM can provide information about the elemental composition of membrane/filter surfaces by using a technique called energy dispersive X-ray (EDX) spectroscopy [324, 325].

Contact angle measurements are conducted to understand surface wetting which controls interaction between fluids and solid surfaces. The degree of wetting is controlled by surface morphology, surface energy and charge, liquid pH and temperature [326]. The wettability or hydrophilicity is measured by contact angle formed by a droplet of a fluid, commonly water, on the surface of a material [309]. Wettability is important as it affects water flux, solute rejection as well as fouling behaviour [309] and there are numerous studies that measure wettability by contact angle [312, 327, 328].

Lastly, surface charge measurement is of great importance to membrane characterisation. Membrane surface charge mediates the separation properties of the membrane, the extent of fouling as well as concentration polarisation [329]. As the actual membrane surface charge is very difficult to quantify, zeta potential estimation is more extensively used as a representative for

electrical potential of the membrane surface. The interactions between charged species and the membrane surface lead to an arrangement of charged species on the membrane surface called the electrical double layer (EDL) [330]. Charge in the EDL is highest close to the membrane surface and steadily decreases with increasing distance from the membrane surface [329, 331]. Counterion concentration is higher near the membrane surface than in the bulk solution to neutralize the charge of membrane surface. Figure 16 below shows the distribution of ionic species in the EDL as a function of distance from the surface.

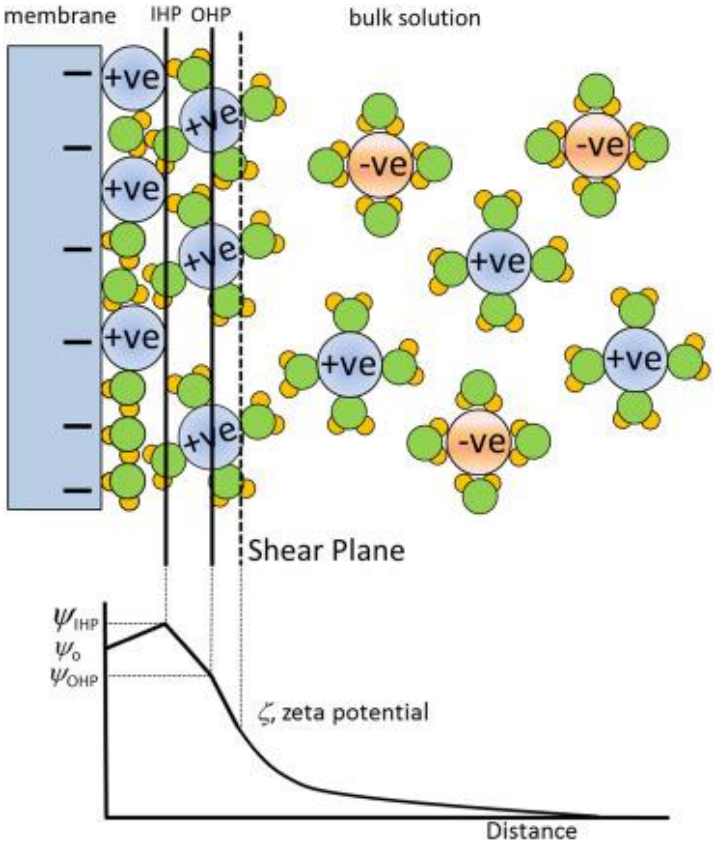

Figure 16: A schematic representation of the electrical double layer and potential (ψ) distribution at the membrane surface. (Reprinted from Membrane Characterization, D.L. Oatley-Radcliffe,N. Aljohani,P.M. Williams,N. Hilal, Chapter 18 - Electrokinetic Phenomena for Membrane Charge, 405-422, Copyright © 2017, with permission from Elsevier [329]).

The layer where ions are close to the membrane surface is the Stern layer. Beyond the Stern layer, where ions are free to move by thermally driven motion, is the shear plane. Zeta potential (ζ) is

defined at the shear plane. Zeta potential measurement has been used in many studies to characterise the surface charge [332-336].

1.2.6.4. Filtration performance

Filtration performance of composites is the primary characteristic of the filters that needs to be investigated. Filtration performance is measured from the molecular weight cut-off (MWCO) and particle size cut-off that give retention rates of contaminants by a filter. These performance measures are important for all types of membranes and filters. For depth-type adsorption filters, the breakthrough curve is also important. These curves show how the concentration of a contaminant increases with time as the adsorbent becomes saturated. Flux and pressure drop are the other key performance parameters for all types of membranes and filters. These parameters are all linked to each other while filtration is performed. For example, for constant pressure operations, increased pressure will result in a quicker filter fouling and a decrease in flux. Also, adsorption capacity will decrease due to the decreased contact time of feed solution with the filter material. All these parameters are explained in detail below.

Commonly, a dead-end stirred cell filtration unit is used to assess the performance of filters and membranes [284, 285, 337]. A dead-end stirred cell filtration unit has detachable parts which consist of a top part with a lid connected to pressurised gas, a middle cylindrical cell body with a constant volume and a lower grooved base where the filters are placed [338]. Various device sizes are available with different volumes. The flow is usually generated by gas pressure while the feed solution is inside the cell. However, there is also a different type of setup which involves small filter housings where the feed solution is pumped through the housings by a peristaltic pump [339]. The stirred cell unit is working with constant pressure mode, while the filter housings with peristaltic pump are working with constant flow rate. Both filtration processes are characterised by monitoring the non-constant variable across the membrane. The difference between these two operating modes is explained in section 1.2.1.1.1.

Even though dead-end stirred cell filtration unit is the most commonly used device for characterisation of filters and membranes at the laboratory scale, most industrial applications use cross flow filtration [340, 341]. Cross flow filtration is used to enhance the filter performance and

service life. This type of filtration is used industrially in depth filters as well as RO, NF and MF applications as it allows continuous feed while reducing clogging [341, 342]. The difference between dead-end and cross flow filtration is explained previously. (Section 1.2.1.1.1.)

At the end of each filtration process, permeate solution is analysed further to calculate the rejection rates of species involved. Particle rejection can be simply calculated by measuring the concentration of particles in feed and permeate. Membranes can also be characterised by their molecular weight cut-off (MWCO). MWCO is the smallest molecular weight of solute species, of which the membrane could achieve more than 90% rejection [8]. The separation mechanism is mainly the size exclusion and nominal ratings of membranes are correlated with the pore size of a membrane.

Adsorption-based separation involves the surface and electrostatic interactions between solutes and membranes, which are highly depended on the surface and physiochemical properties of solute molecules and membranes. Breakthrough curves are very commonly used to assess adsorption performance [343-345]. These curves show the concentration of an adsorbate in the filtrate as a function of time. Therefore, it allows us to identify the time that adsorbent reaches saturation point and replacement is required. Furthermore, adsorption capacity can be easily calculated from the curves.

Permeate flux is another important parameter to measure. Flux is defined as the volume that is flowing through the membrane per unit area per time. It is usually expressed in Litres per square Meter per Hour (LMH) at a given pressure. Flux is also an indication of the pore size of a membrane. Furthermore, monitoring the change in flux can provide a good indication of fouling. Decreasing flux indicates the increased fouling in membrane in time.

In this thesis, we perform separation by two mechanisms: rejection of particulate materials and adsorption of solute molecules. Therefore, a setup which can assess both aspects is required. We used a dead-end stirred cell filtration unit with a gas cylinder under constant pressure mode. In our case, an additional micro flow cell is connected between the cell body and UV-Vis (Ultraviolet Visible) spectrometer. This is done to obtain a continuous flow of permeate through UV-Vis spectrometer to continuously measure particular contaminants in the permeate. Therefore, we could obtain dynamic breakthrough curves for the evaluation of adsorption performance, while

particle rejection is calculated by measuring the concentration of species in permeate by either UV-Vis spectrometer or by a total carbon analyser (TOC).

1.2.7. Perspective and conclusion

Depth filters made of cellulose fibre composites are mainly of interest for industrial applications. Depth filtration uses a combination of size exclusion and adsorption-based separation. This concept brings some advantages to the filtration process, such as larger surface area for separation in the core of the filters, which makes it attractive for industrial use. The use of depth filters is mainly in food and beverage and pharmaceutical industries. In literature, Sehaqui et al. [33] reported the nanoparticle (NP) capture by depth filters prepared only from NFC fibres by water-based cationisation and freeze-drying. Separation of NPs were performed by surface interaction and tortuous structure that is built by the NFC network. They concluded that the NFC depth filters offer an alternative to the current membrane technology by allowing the retention of NPs in its interior area. Retention of NPs was analysed both in terms of adsorption with surface interactions and size-exclusion. In another study, commercial depth filters were tested for use in DNA retention [339] and found to be very effective. Even though there are studies about depth filters in literature [346-349], there are only limited studies of cellulose fibre-based depth filters. Therefore, more research efforts are required to engineer and improve the performance of depth filters by new concepts with reduced impact on the environment. The potential areas to explore in depth filters are defined throughout this review, and now they are summarised as gaps in knowledge in the next section.

1.3. GAPS IN KNOWLEDGE

This critical review has highlighted the principles of liquid filtration, depth filters, preparation of cellulose fibre composites as depth filter products including the detailed review of each component and followed by the emerging use of cellulose based materials in the filters and membranes field. The review has shown us that depth filter provides more efficient contaminant capture as compared to surface type membranes. However, this review has also identified a number of significant gaps in the literature.

There are studies on depth filters in literature; however, these are mainly covering conventional depth filters. There are not many studies which have researched new concepts in depth filters to improve the performance. Firstly, the impact that can be added to filters by nanofibrillated cellulose addition to improve filter functionality remains unknown. Secondly, the role of inorganic fillers and charged polymers is not fully explored. Depth filters are composites combining cellulose with an inorganic filler and a charged polymer. Therefore, the role of each component must be investigated and identified properly in terms of both structural changes and separation performance.

The need for new developments in membrane technology is already a well-known fact and there is intensive research in this field. However, there is much less research on depth filters, even though they are commonly used in industrial applications. The extent of performance improvement that can be provided by structural changes has not been investigated. Therefore, new state-of-the-art structures are required for depth filters to produce high filtration performances.

Lastly, current depth filter products still use PAE to produce the required wet strength, which generates some toxic by-products. Filters must be produced with more environmentally benign components to be sustainable. Therefore, the other gap that clearly appears here is the need for cleaner production with environmentally-friendly filter components.

The critical issues identified as significant gaps in knowledge are:

1) The effect of perlite particles, charged polymer as well as increased fibrillation of cellulose fibres on the depth filter structure and depth filtration performance
    - What is the effect of perlite loading and charged polymer concentration on the structure of filters and their separation performance?
    - What is the effect of increased mechanical treatment of the fibres on the structural properties of the final filter product?
    - Does the changing fibre morphology and filter structure have an impact on the adsorption and size exclusion characteristics of the filters?
2) Engineering new innovative structures for depth filters with improved functionalities
    - What impact does single layer versus multi-layer formation have on the adsorption and size exclusion performance?

- What effect does single versus multi-layered structure have on flux?
- How does coating nanofibrillated cellulose top barrier layer onto depth filters affect the adsorption and size exclusion performance?

3) Development of cleaner filter products
    - Would it be possible to fully or partially replace the toxic wet strength resin (charged polymer) with nanofibrillated cellulose without changing the properties?
    - How does eliminating wet strength resin affect the charge characteristics of the filters?
    - What is the overall effect of reducing the charged polymer component on the adsorption properties of the filters?

These gaps in knowledge have then been addressed by the research objectives of this thesis, which are discussed next.

1.4. RESEARCH OBJECTIVES

This doctoral thesis has three crucial research objectives. The first objective is to understand the effect of each filter component, as well as increasing fibrillation of cellulose fibres, on structural characteristics and filtration performance. This is done to have a better understanding about structure-property relationship of these cellulose-fibre composites as filter products. The second objective is engineering new filter structures and subsequently characterising their separation performance to develop an innovative approach in the filter production. The production of cleaner filter products to have a reduced impact on the environment is the third objective. Our research aims are as listed below.

The specific research aims are:

1. Quantify the effect of each component in filters and increased mechanical treatment on cellulose fibres on structural changes as well as adsorption and particle filtration characteristics of the filters.

2. Quantify the effect of introducing multi-layers and multi-interfaces within and between the filters on adsorption and size and molecular weight cut-off characteristics.

3. Quantify the effect of coating nanofibrillated cellulose top barrier layer on top of the filters to improve overall filtration performance.
4. Develop cleaner filters by using nanofibrillated cellulose as a substitute for the toxic wet strength agent, PAE, and adjust the filter charge with other cationic polymers.

1.5. THESIS OUTLINE

This thesis consists of four experimental chapters of which three of them are already published and one is under final review. All published papers are reformatted for a consistent presentation whilst the content remains unchanged. The original publications are provided in Appendix II.
A chapter-by-chapter outline based on the research aims, the conducted research studies and the successful outcomes are presented.

- **Chapter 1 - Introduction and Literature Review**

This chapter reviews the preparation of cellulose fibre composites as depth filters along with a detailed review of each component of the filters. The preparation and use of composites in filtration processes are reviewed further and the current understanding and gaps in knowledge are identified from literature review. The research objectives are defined in order to address the gaps identified.

- **Chapter 2 - Engineering Cellulose Fibre Inorganic Composites for Depth Filtration and Adsorption**

Aysu Onur, Aaron Ng, Gil Garnier, Warren Batchelor. Engineering cellulose fibre inorganic composites for depth filtration and adsorption, Sep. Purif. Technol. 203, 2018, 209-216.

Impact factor: 3.927

Depth type composite filters are porous materials heavily loaded with adsorbents and can remove contaminants from liquids by combining mechanical entrapment and adsorption. There is still a need for developing high performance filters by controlling the internal structure at micro and nano level. In this study, highly fibrillated cellulose fibres with increased surface area was used as partial substitute for the fibre matrix to tailor the filter structure as well as the adsorption and filtration performance. Polyamideamine-epichlorohydrin (PAE) was added both to adjust the charge of

medium and provide wet strength. Filters were fabricated by embedding perlite particles into the cellulose fibre matrix by papermaking technique. The structure of composites was characterised for pore size distribution and surface morphology. Adsorption and filtration characteristics were quantified using two model dyes and silicon dioxide particles. Adsorption was found to be electrostatically controlled and dependent on the charge of the dye molecules and the filter medium. The addition of NFC doubled the removal of a cationic dye by increasing the surface area and the available negative charges; it however decreased the removal of an anionic dye by 75%. PAE addition decreased the adsorption of the cationic methylene blue dye, while increasing the adsorption of the anionic metanil yellow dye. Rejection by filtration of 1 µm particles was over 90% for all filters. This study demonstrates that highly fibrillated cellulose fibres combined with a cationic wet strength polyelectrolyte can be used to tailor the filter structure and properties.

- **Chapter 3 - Multi-Layer Filters: Adsorption and Filtration Mechanisms for Improved Separation**

Aysu Onur, Aaron Ng, Warren Batchelor, Gil Garnier. Multi-Layer Filters: Adsorption and filtration mechanisms for improved separation, Front. Chem. 6, 2018, 417.

Impact factor: 4.115

The aim of this chapter is to quantify the effect of different filter configurations on filtration and adsorption properties. Even though there are many studies regarding improvement of membrane processes, the literature is still lacking in how depth filter structure and in turn the performance can be engineered. In our study, we investigated the effect of introducing multi-interfaces on structure of filters as well as liquid filtration performance.

Filters made of cellulose fibre and perlite particles were prepared using a wet laying papermaking technique. Polyamideamine-epichlorohydrin (PAE) was added to provide wet strength. Filters were prepared at two different total basis weights of 200 and 400 grams per square metre (gsm). Single and multi-layered filters were structured for each total basis weights. The effect of total basis weights and multi-layered structure on methylene blue adsorption and silicon dioxide (SiO_2) particle filtration was investigated. Methylene blue adsorption was performed either under constant pressure or constant flow rate. In both operational modes, the adsorption capacity of multi-layered

filters was 16 to 100% higher than for single-layer filters at the same overall weight. The effect of layer separation was also characterised using polypropylene separators and tested under constant flow rate operation. Separators provided more effective methylene blue adsorption by generating a well distributed flow. Filtration performance was quantified with 0.5 µm silicon dioxide particles under constant pressure conditions, in order to mimic bacteria rejection. Filtration capability of SiO2 particles was reduced slightly (12%) with decreasing individual filter layer thickness regardless of the multi-layered structure. Filtering polyethylene glycol (PEG) molecules with two different molecular weights was performed; however, no rejection was recorded. The filter internal pore structure was visualised by 3D-X ray computed tomography and the void fraction was quantified. 400 gsm single layer presented areas of low fibre density forming pores, while the pore volume decreased for thinner filter layers.

- **Chapter 4 - Cellulose Fibre-Perlite Depth Filters with Nanofibrillated Cellulose Top Coating for Improved Filtration**

Aysu Onur, Kirubanandan Shanmugam, Aaron Ng, Gil Garnier, Warren Batchelor. Cellulose Fibre-Perlite Depth Filters with Cellulose Nanofibre Top Coating for Improved Filtration (Manuscript is under final review with Cellulose)

Impact factor: 3.809

Depth type composite filters are used to remove contaminants from liquids by combining mechanical entrapment and adsorption. Commonly, adsorption of one type of charged contaminants and micro particle filtration are successfully performed with depth filtration. However, it is not fully possible to obtain multiple functionalities in one type of depth filter, such as adsorption of oppositely charged contaminants as well as ultrafiltration. Therefore, there is still a need of new techniques to improve the existing filter performances with small modifications made on filters. In this study, we investigate the effect of adding a top barrier layer on imparting additional functionalities to the filters. The original depth filters remain unchanged in terms of composition and preparation and the nanofibrillated cellulose fibre layer that is coated on top of the filters becomes the primary area to explore. Depth filters were prepared with cellulose, perlite and PAE via papermaking technique with a set composition and used as base sheet. Nanofibrillated cellulose

fibre barrier layers were coated onto base sheets by spray coating technique. Different thicknesses were investigated in terms of water flux, adsorption of a positively charged contaminant and rejection of two different molecular weights of a polymer. Additionally, barrier properties were analysed according to air permeability.

In summary, NFC barrier layers added functionalities in filters that were not previously available. NFC top coating enabled us performing rejection up to more than 80% of two different molecular weights of PEG, 600 and 5000 kDa. Furthermore, removal of positively charged contaminants increased significantly after adding NFC layer. The coating of the layers was done by a technique that is as simple as a spray coating. This technique is also robust in terms of getting an adequate internal strength at the interface of base sheet and top layer. However, the major drawback was the reduced flux caused by NFC layers. Our study shows that the concept of top barrier coating is a promising and easy method to improve the filter performance and increase the depth filter functionality.

- **Chapter 5 - The Use of Nanofibrillated Cellulose to Reduce the Wet strength Polymer Quantity for Development of Cleaner Filters**

Aysu Onur, Aaron Ng, Gil Garnier, Warren Batchelor. *The use of cellulose nanofibres to reduce the wet strength polymer quantity for development of cleaner filters, JOCP, 215, 2019, 226-231.*

Impact factor: 5.651

Polyamideamine-epichlorohydrin resin (PAE) is one of the most commonly used wet strength agents in the papermaking industry. However, adsorbable organic halogens (AOX) are known to be a toxic side product of the PAE manufacturing process; therefore, the use of PAE is restricted by regulations for food and medical applications. In this study, we investigated partially replacing the indirect food additive, PAE, with a renewable, biodegradable material, nanofibrillated cellulose (NFC), in order to drastically reduce the amount of PAE used while maintaining the same wet tensile strength properties. The concept is to replace covalent bonds by hydrogen bonds and to drastically increase bonding area. Depth-type filters were prepared with cellulose (30%), perlite (70%) and lesser amounts of PAE via papermaking technique. A small fraction of cellulose fibre composition was substituted with NFC while the PAE amount was gradually decreased. The substitution of positively

charged PAE for negatively charged nanofibrillated cellulose switched the overall charge of the system from cationic to anionic. Therefore, two cationic polyelectrolytes, CPAM or PEI, were investigated to control the overall charge and adsorption performance of the filter system.

The substitution of NFC enabled PAE dosage to be reduced by over 95% while retaining the wet strength properties of the filters. The wet strength obtained from the small quantity of wet strength polymer could be further maximised by increasing the curing temperature to 150^{o}C with a much shorter curing period. The filters with reduced PAE dosage have also improved adsorption of positively charged contaminants. However, for negatively charged contaminants a very minor amount (around 25 mg) of cationic polymer addition would be required to maintain the performance. Our study shows that partial replacement of fibre composition with nanofibrillated cellulose allows us to reduce the quantity of wet strength polymer remarkably and achieve a sustainable and environmentally-friendly concept for filter manufacturing or for any paper-products requiring wet strength.

- **Chapter 6 – Conclusion and Perspective**

1.6. REFERENCES

[1] R. G. Holdich, *Fundamentals of Particle Technology*: Midland Information Technology and Publishing, 2002.

[2] J. Royce, J. Liderfelt, and C. Robinson, "Chapter 15 - Filtration Methods for Use in Recovery Processes," in *Biopharmaceutical Processing*, G. Jagschies, E. Lindskog, K. Łącki, and P. Galliher, Eds., ed: Elsevier, 2018, pp. 295-315.

[3] Y. E. Rayess, Y. Manon, N. Jitariouk, C. Albasi, M. M. Peuchot, A. Devatine*, et al.*, "Wine clarification with Rotating and Vibrating Filtration (RVF): Investigation of the impact of membrane material, wine composition and operating conditions," *Journal of Membrane Science,* vol. 513, pp. 47-57, 2016/09/01/ 2016.

[4] N. P. Cheremisinoff, "1 - An Introduction to Liquid Filtration," in *Liquid Filtration (Second Edition)*, ed Woburn: Butterworth-Heinemann, 1998, pp. 1-18.

[5] J. Mulder, *Basic Principles of Membrane Technology*, 2 ed.: Springer Netherlands, 1996.

[6] J. Liderfelt and J. Royce, "Chapter 14 - Filtration Principles," in *Biopharmaceutical Processing*, ed: Elsevier, 2018, pp. 279-293.

[7] B. Van der Bruggen, "Chapter 2 - Microfiltration, ultrafiltration, nanofiltration, reverse osmosis, and forward osmosis," in *Fundamental Modelling of Membrane Systems*, P. Luis, Ed., ed: Elsevier, 2018, pp. 25-70.

[8] Z. F. Cui, Y. Jiang, and R. W. Field, "Chapter 1 - Fundamentals of Pressure-Driven Membrane Separation Processes," in *Membrane Technology*, Z. F. Cui and H. S. Muralidhara, Eds., ed Oxford: Butterworth-Heinemann, 2010, pp. 1-18.

[9] R. C. de Oliveira, R. C. Docê, and S. T. D. de Barros, "Clarification of passion fruit juice by microfiltration: Analyses of operating parameters, study of membrane fouling and juice quality," *Journal of Food Engineering,* vol. 111, pp. 432-439, 2012/07/01/ 2012.

[10] C. D. dos Santos, R. K. Scherer, A. S. Cassini, L. D. F. Marczak, and I. C. Tessaro, "Clarification of red beet stalks extract by microfiltration combined with ultrafiltration," *Journal of Food Engineering,* vol. 185, pp. 35-41, 2016/09/01/ 2016.

[11] F. de Santana Magalhães, V. L. Cardoso, and M. H. M. Reis, "Sequential process with bioadsorbents and microfiltration for clarification of pequi (Caryocar brasiliense Camb.) fruit extract," *Food and Bioproducts Processing,* vol. 108, pp. 105-116, 2018/03/01/ 2018.

[12] B. Girard and L. R. Fukumoto, "Membrane Processing of Fruit Juices and Beverages: A Review," *Critical Reviews in Food Science and Nutrition,* vol. 40, pp. 91-157, 2000/03/01 2000.

[13] Y. Yang, A. Raza, F. Banat, and K. Wang, "The separation of oil in water (O/W) emulsions using polyether sulfone & nitrocellulose microfiltration membranes," *Journal of Water Process Engineering,* vol. 25, pp. 113-117, 2018/10/01/ 2018.

[14] R. Liu, A. K. Y. Raman, I. Shaik, C. Aichele, and S.-J. Kim, "Inorganic microfiltration membranes incorporated with hydrophilic silica nanoparticles for oil-in-water emulsion separation," *Journal of Water Process Engineering,* vol. 26, pp. 124-130, 2018/12/01/ 2018.

[15] N. Pathak, S. Li, Y. Kim, L. Chekli, S. Phuntsho, A. Jang*, et al.*, "Assessing the removal of organic micropollutants by a novel baffled osmotic membrane bioreactor-microfiltration hybrid system," *Bioresource Technology,* vol. 262, pp. 98-106, 2018/08/01/ 2018.

[16] X. Wang, Y. Zhao, X. Li, and Y. Ren, "Performance evaluation of a microfiltration-osmotic membrane bioreactor (MF-OMBR) during removing silver nanoparticles from simulated wastewater," *Chemical Engineering Journal,* vol. 313, pp. 171-178, 2017/04/01/ 2017.

[17] S. Jamaly, N. N. Darwish, I. Ahmed, and S. W. Hasan, "A short review on reverse osmosis pretreatment technologies," *Desalination,* vol. 354, pp. 30-38, 2014/12/01/ 2014.

[18] C. M. Galanakis, "Separation of functional macromolecules and micromolecules: From ultrafiltration to the border of nanofiltration," *Trends in Food Science & Technology,* vol. 42, pp. 44-63, 2015/03/01/ 2015.

[19] M. Bernal, M. O. Ruiz, R. M. Geanta, J. M. Benito, and I. Escudero, "Colour removal from beet molasses by ultrafiltration with activated charcoal," *Chemical Engineering Journal,* vol. 283, pp. 313-322, 2016/01/01/ 2016.

[20] N. Rajagopalan and M. Cheryan, "Total Protein Isolate from Milk by Ultrafiltration: Factors Affecting Product Composition," *Journal of Dairy Science,* vol. 74, pp. 2435-2439, 1991/08/01/ 1991.

[21] V. M. Gonçalves, M. Takagi, T. S. Carmo, R. B. Lima, S. M. F. Albani, J. V. Pinto*, et al.*, "Simple and efficient method of bacterial polysaccharides purification for vaccines production using hydrolytic enzymes and tangential flow ultrafiltration," *Communicating Current Research and Educational Topics and Trends in Applied Microbiology,* vol. 1, pp. 450-457, 2007.

[22] C. Bhattacharjee, V. K. Saxena, and S. Dutta, "Fruit juice processing using membrane technology: A review," *Innovative Food Science & Emerging Technologies,* vol. 43, pp. 136-153, 2017/10/01/ 2017.

[23] B. Van der Bruggen and C. Vandecasteele, "Removal of pollutants from surface water and groundwater by nanofiltration: overview of possible applications in the drinking water industry," *Environmental Pollution,* vol. 122, pp. 435-445, 2003/04/01/ 2003.

[24] M. Sarai Atab, A. J. Smallbone, and A. P. Roskilly, "A hybrid reverse osmosis/adsorption desalination plant for irrigation and drinking water," *Desalination,* vol. 444, pp. 44-52, 2018/10/15/ 2018.

[25] H. Lee, Y. Jin, and S. Hong, "Recent transitions in ultrapure water (UPW) technology: Rising role of reverse osmosis (RO)," *Desalination,* vol. 399, pp. 185-197, 2016/12/01/ 2016.

[26] S. K. Nataraj, K. M. Hosamani, and T. M. Aminabhavi, "Distillery wastewater treatment by the membrane-based nanofiltration and reverse osmosis processes," *Water Research,* vol. 40, pp. 2349-2356, 2006.

[27] M.-L. Lameloise, M. Gavach, M. Bouix, and C. Fargues, "Combining reverse osmosis and ion-exchange allows beet distillery condensates to be recycled as fermentable dilution water," *Desalination,* vol. 363, pp. 75-81, 2015/05/01/ 2015.

[28] R. G. Carbonell, "Adsorption technology: A step-by-step approach to process evaluation and application (chemical industries series, vol. 19). Edited by Frank L. Slejko, Marcel Dekker, inc., 1985, 240 pp., $55.00 (U.S. and Canada); $66.00 (all other countries)," *AIChE Journal,* vol. 32, 1986.

[29] A. Mukhopadhyay, "8 - Composite nonwovens in filters: applications," in *Composite Non-Woven Materials*, D. Das and B. Pourdeyhimi, Eds., ed: Woodhead Publishing, 2014, pp. 164-210.

[30] E. Knapik and J. Stopa, "Fibrous deep-bed filtration for oil/water separation using sunflower pith as filter media," *Ecological Engineering,* vol. 121, pp. 44-52, 2018/10/01/ 2018.

[31] K. Nakamura, J. Nakamura, and K. Matsumoto, "Filtration and backwashing behaviors of the deep bed filtration using long length poly-propylene fiber filter media," *Journal of the Taiwan Institute of Chemical Engineers,* 2018/02/09/ 2018.

[32] N. Hasolli, Y. O. Park, and Y. W. Rhee, "Filtration performance evaluation of depth filter media cartridges as function of layer structure and pleat count," *Powder Technology,* vol. 237, pp. 24-31, 2013/03/01/ 2013.

[33] H. Sehaqui, P. Spera, A. Huch, and T. Zimmermann, "Nanoparticles capture on cellulose nanofiber depth filters," *Carbohydrate Polymers,* vol. 201, pp. 482-489, 2018/12/01/ 2018.

[34] I. M. Hutten, "Chapter 7 - Liquid Filter Applications," in *Handbook of Nonwoven Filter Media (Second Edition)*, ed Oxford: Butterworth-Heinemann, 2016, pp. 409-450.

[35] "Filter cartridges reduce spoilage micro-organisms," *Filtration + Separation,* vol. 54, p. 13, 2017/11/01/ 2017.

[36] A. Bennett, "Pharmaceuticals and fine chemicals: Filtration and separation in the diverse fine chemical sectors," *Filtration + Separation,* vol. 50, pp. 30-33, 2013/11/01/ 2013.

[37] E. N. Durmaz and P. Zeynep Çulfaz-Emecen, "Cellulose-based membranes via phase inversion using [EMIM]OAc-DMSO mixtures as solvent," *Chemical Engineering Science,* vol. 178, pp. 93-103, 2018/03/16/ 2018.

[38] Z. Zhu, J. Xiao, W. He, T. Wang, Z. Wei, and Y. Dong, "A phase-inversion casting process for preparation of tubular porous alumina ceramic membranes," *Journal of the European Ceramic Society,* vol. 35, pp. 3187-3194, 2015/10/01/ 2015.

[39] T. Sparks and G. Chase, "Section 2 - Filter Media," in *Filters and Filtration Handbook (Sixth Edition)*, T. Sparks and G. Chase, Eds., ed Oxford: Butterworth-Heinemann, 2016, pp. 55-115.

[40] (2018). *Millistak+® Pod Disposable Depth Filter Systems*. Available: http://www.merckmillipore.com/AU/en/product/Millistak+-Pod-Disposable-Depth-Filter-Systems,MM_NF-C9485

[41] (2018). *Stax™ Disposable Depth Filter Systems*. Available: https://shop.pall.com/us/en/biotech/depth-filtration/depth-filter-housings/stax-disposable-depth-filter-systems-zidgri78m6c?_ga=2.53943595.2030430694.1544137175-1812937177.1544137175

[42] *SUPRApak™ Depth Filter Modules*. Available: https://shop.pall.com/us/en/food-beverage/juice/polishing-filtration/suprapak-depth-filter-modules-zidgri78lum

[43] M. K. M. Wang, R. Sale, M. Entezarian. (2012) Single-Use Depth-Filtration System. *GEN Genetic Engineering and Biotechnology News*. Available: https://www.genengnews.com/magazine/179/single-use-depth-filtration-system/4058/

[44] M. Nogi, S. Iwamoto, A. N. Nakagaito, and H. Yano, "Optically Transparent Nanofiber Paper," *Advanced Materials,* vol. 21, pp. 1595-1598, 2009.

[45] K. Abe, S. Iwamoto, and H. Yano, "Obtaining Cellulose Nanofibers with a Uniform Width of 15 nm from Wood," *Biomacromolecules,* vol. 8, pp. 3276-3278, 2007/10/01 2007.

[46] W. Chen, K. Abe, K. Uetani, H. Yu, Y. Liu, and H. Yano, "Individual cotton cellulose nanofibers: pretreatment and fibrillation technique," *Cellulose,* vol. 21, pp. 1517-1528, 2014.

[47] K. Abe and H. Yano, "Comparison of the characteristics of cellulose microfibril aggregates isolated from fiber and parenchyma cells of Moso bamboo (Phyllostachys pubescens)," *Cellulose,* vol. 17, pp. 271-277, 2009.

[48] W. Chen, H. Yu, and Y. Liu, "Preparation of millimeter-long cellulose I nanofibers with diameters of 30–80 nm from bamboo fibers," *Carbohydrate Polymers,* vol. 86, pp. 453-461, 8/15/ 2011.

[49] K. Abe and H. Yano, "Comparison of the characteristics of cellulose microfibril aggregates of wood, rice straw and potato tuber," *Cellulose,* vol. 16, pp. 1017-1023, 2009.

[50] *Handbook of pulp and paper technology*

[51] D. Klemm, E. D. Cranston, D. Fischer, M. Gama, S. A. Kedzior, D. Kralisch*, et al.*, "Nanocellulose as a natural source for groundbreaking applications in materials science: Today's state," *Materials Today,* vol. 21, pp. 720-748, 2018/09/01/ 2018.

[52] A. Isogai, T. Saito, and H. Fukuzumi, "TEMPO-oxidized cellulose nanofibers," *Nanoscale,* vol. 3, pp. 71-85, 2011.

[53] A. Dufresne, "Nanocellulose: a new ageless bionanomaterial," *Materials Today,* vol. 16, pp. 220-227, 6// 2013.

[54] M. M. Khattab, N. A. Abdel-Hady, and Y. Dahman, "21 - Cellulose nanocomposites: Opportunities, challenges, and applications," in *Cellulose-Reinforced Nanofibre Composites*, M. Jawaid, S. Boufi, and A. K. H.P.S, Eds., ed: Woodhead Publishing, 2017, pp. 483-516.

[55] D. Klemm, B. Heublein, H. P. Fink, and A. Bohn, "Cellulose: Fascinating Biopolymer and Sustainable Raw Material," *Angewandte Chemie International Edition,* vol. 44, pp. 3358-3393, 2005.

[56] D. Dai and M. Fan, "1 - Wood fibres as reinforcements in natural fibre composites: structure, properties, processing and applications," in *Natural Fibre Composites*, A. Hodzic and R. Shanks, Eds., ed: Woodhead Publishing, 2014, pp. 3-65.

[57] Y. Sood, R. Tyagi, S. Tyagi, P. Pande, and R. Tondon, "Surface charge of different paper making raw materials and its influence on paper properties," 2010.

[58] J. R. Dillen, S. Dillén, and M. F. Hamza, "Pulp and Paper: Wood Sources," in *Reference Module in Materials Science and Materials Engineering*, ed: Elsevier, 2016.

[59] X. Miao, J. Lin, F. Tian, X. Li, F. Bian, and J. Wang, "Cellulose nanofibrils extracted from the byproduct of cotton plant," *Carbohydrate Polymers,* vol. 136, pp. 841-850, 2016/01/20/ 2016.

[60] R. W. Lenz, "Cellulose, structure, accessibility and reactivity, by H. A. Krässig, Gordon and Breach Publishers, 5301 Tacony Street, Philadelphia, PA, 1993; xvi + 376 pp. Price: $260.00," *Journal of Polymer Science Part A: Polymer Chemistry,* vol. 32, pp. 2401-2401, 1994.

[61] A. M. Adel, A. A. El-Gendy, M. A. Diab, R. E. Abou-Zeid, W. K. El-Zawawy, and A. Dufresne, "Microfibrillated cellulose from agricultural residues. Part I: Papermaking application," *Industrial Crops and Products,* vol. 93, pp. 161-174, 2016/12/25/ 2016.

[62] S. A. Nascimento and C. A. Rezende, "Combined approaches to obtain cellulose nanocrystals, nanofibrils and fermentable sugars from elephant grass," *Carbohydrate Polymers,* vol. 180, pp. 38-45, 2018/01/15/ 2018.

[63] G. Bali, R. Khunsupat, H. Akinosho, R. S. Payyavula, R. Samuel, G. A. Tuskan*, et al.*, "Characterization of cellulose structure of Populus plants modified in candidate cellulose biosynthesis genes," *Biomass and Bioenergy,* vol. 94, pp. 146-154, 2016/11/01/ 2016.

[64] I. Kouadri and H. Satha, "Extraction and characterization of cellulose and cellulose nanofibers from Citrullus colocynthis seeds," *Industrial Crops and Products,* vol. 124, pp. 787-796, 2018/11/15/ 2018.

[65] D. S. E. Hon, *Chemical Modification of Lignocellulosic Materials*: New York: Routledge., 1996.

[66] A. Alemdar and M. Sain, "Isolation and characterization of nanofibers from agricultural residues – Wheat straw and soy hulls," *Bioresource Technology,* vol. 99, pp. 1664-1671, 2008/04/01/ 2008.

[67] A. Dufresne, J.-Y. Cavaillé, and M. R. Vignon, "Mechanical behavior of sheets prepared from sugar beet cellulose microfibrils," *Journal of Applied Polymer Science,* vol. 64, pp. 1185-1194, 1997.

[68] R. Jonas and L. F. Farah, "Production and application of microbial cellulose," *Polymer Degradation and Stability,* vol. 59, pp. 101-106, 1998/01/03/ 1998.

[69] M. Åkerholm and L. Salmén, "Interactions between wood polymers studied by dynamic FT-IR spectroscopy," *Polymer,* vol. 42, pp. 963-969, 2001/02/01/ 2001.

[70] J. J. Robin and Y. Breton, "Reinforcement of recycled polyethylene with wood fibers heat treated," *Journal of Reinforced Plastics and Composites,* vol. 20, pp. 1253-1262, 2001.

[71] S. Gharehkhani, E. Sadeghinezhad, S. N. Kazi, H. Yarmand, A. Badarudin, M. R. Safaei*, et al.*, "Basic effects of pulp refining on fiber properties—A review," *Carbohydrate Polymers,* vol. 115, pp. 785-803, 1/22/ 2015.

[72] P. Bajpai, "Chapter 1 - Refining and Pulp Characterization," in *Biermann's Handbook of Pulp and Paper (Third Edition)*, P. Bajpai, Ed., ed: Elsevier, 2018, pp. 1-34.

[73] N. Lavoine, I. Desloges, A. Dufresne, and J. Bras, "Microfibrillated cellulose – Its barrier properties and applications in cellulosic materials: A review," *Carbohydrate Polymers,* vol. 90, pp. 735-764, 10/1/ 2012.

[74] Q. Li, W. Chen, Y. Li, X. Guo, S. Song, Q. Wang*, et al.*, "Comparative study of the structure, mechanical and thermomechanical properties of cellulose nanopapers with different thickness," *Cellulose,* vol. 23, pp. 1375-1382, 2016.

[75] I. Siró and D. Plackett, "Microfibrillated cellulose and new nanocomposite materials: a review," *Cellulose,* vol. 17, pp. 459-494, June 01 2010.

[76] A. F. Turbak, F. W. Snyder, and K. R. Sandberg, *Microfibrillated cellulose, a new cellulose product: properties, uses, and commercial potential*, 1983.

[77] S. Iwamoto, A. N. Nakagaito, and H. Yano, "Nano-fibrillation of pulp fibers for the processing of transparent nanocomposites," *Applied Physics A,* vol. 89, pp. 461-466, 2007.

[78] Ø. Eriksen, K. Syverud, and Ø. Gregersen, "The use of microfibrillated cellulose produced from kraft pulp as strength enhancer in TMP paper," in *Nordic Pulp & Paper Research Journal* vol. 23, ed, 2008, p. 299.

[79] T. Zimmermann, N. Bordeanu, and E. Strub, "Properties of nanofibrillated cellulose from different raw materials and its reinforcement potential," *Carbohydrate Polymers,* vol. 79, pp. 1086-1093, 2010.

[80] M. Pääkkö, M. Ankerfors, H. Kosonen, A. Nykänen, S. Ahola, M. Österberg*, et al.*, "Enzymatic Hydrolysis Combined with Mechanical Shearing and High-Pressure

Homogenization for Nanoscale Cellulose Fibrils and Strong Gels," *Biomacromolecules,* vol. 8, pp. 1934-1941, 2007/06/01 2007.

[81] E. V. Gert, V. I. Torgashov, O. V. Zubets, and F. N. Kaputskii, "Preparation and Properties of Enterosorbents Based on Carboxylated Microcrystalline Cellulose," *Cellulose,* vol. 12, pp. 517-526.

[82] C. Aulin, S. Ahola, P. Josefsson, T. Nishino, Y. Hirose, M. Österberg*, et al.*, "Nanoscale Cellulose Films with Different Crystallinities and Mesostructures—Their Surface Properties and Interaction with Water," *Langmuir,* vol. 25, pp. 7675-7685, 2009/07/07 2009.

[83] T. Saito and A. Isogai, "Introduction of aldehyde groups on surfaces of native cellulose fibers by TEMPO-mediated oxidation," *Colloids and Surfaces A: Physicochemical and Engineering Aspects,* vol. 289, pp. 219-225, 2006/10/15/ 2006.

[84] S. J. Eichhorn, A. Dufresne, M. Aranguren, N. E. Marcovich, J. R. Capadona, S. J. Rowan*, et al.*, "Review: current international research into cellulose nanofibres and nanocomposites," *Journal of Materials Science,* vol. 45, p. 1, September 24 2009.

[85] R. R. Lahiji, X. Xu, R. Reifenberger, A. Raman, A. Rudie, and R. J. Moon, "Atomic Force Microscopy Characterization of Cellulose Nanocrystals," *Langmuir,* vol. 26, pp. 4480-4488, 2010/03/16 2010.

[86] V. A. Barbash, O. V. Yaschenko, and O. M. Shniruk, "Preparation and Properties of Nanocellulose from Organosolv Straw Pulp," *Nanoscale Research Letters,* vol. 12, p. 241, March 31 2017.

[87] Y. Mao, K. Liu, C. Zhan, L. Geng, B. Chu, and B. S. Hsiao, "Characterization of Nanocellulose Using Small-Angle Neutron, X-ray, and Dynamic Light Scattering Techniques," *The Journal of Physical Chemistry B,* vol. 121, pp. 1340-1351, 2017/02/16 2017.

[88] S. Varanasi, R. He, and W. Batchelor, "Estimation of cellulose nanofibre aspect ratio from measurements of fibre suspension gel point," *Cellulose,* vol. 20, pp. 1885-1896, August 01 2013.

[89] P. Raj, A. Mayahi, P. Lahtinen, S. Varanasi, G. Garnier, D. Martin*, et al.*, "Gel point as a measure of cellulose nanofibre quality and feedstock development with mechanical energy," *Cellulose,* vol. 23, pp. 3051-3064, October 01 2016.

[90] L. Zhang, W. Batchelor, S. Varanasi, T. Tsuzuki, and X. Wang, "Effect of cellulose nanofiber dimensions on sheet forming through filtration," *Cellulose,* vol. 19, pp. 561-574, April 01 2012.

[91] A. Celzard, V. Fierro, and A. Pizzi, "Flocculation of cellulose fibre suspensions: the contribution of percolation and effective-medium theories," *Cellulose,* vol. 15, p. 803, May 28 2008.

[92] A. Idström, S. Schantz, J. Sundberg, B. F. Chmelka, P. Gatenholm, and L. Nordstierna, "13C NMR assignments of regenerated cellulose from solid-state 2D NMR spectroscopy," *Carbohydrate Polymers,* vol. 151, pp. 480-487, 2016/10/20/ 2016.

[93] E. E. Ureña-Benavides and C. L. Kitchens, "Wide-Angle X-ray Diffraction of Cellulose Nanocrystal−Alginate Nanocomposite Fibers," *Macromolecules,* vol. 44, pp. 3478-3484, 2011/05/10 2011.

[94] M. Shimizu, T. Saito, Y. Nishiyama, S. Iwamoto, H. Yano, A. Isogai*, et al.*, "Fast and Robust Nanocellulose Width Estimation Using Turbidimetry," *Macromolecular Rapid Communications,* vol. 37, pp. 1581-1586, 2016.

[95] S. Iwamoto, W. Kai, T. Isogai, T. Saito, A. Isogai, and T. Iwata, "Comparison study of TEMPO-analogous compounds on oxidation efficiency of wood cellulose for preparation of cellulose nanofibrils," *Polymer Degradation and Stability,* vol. 95, pp. 1394-1398, 2010/08/01/ 2010.

[96] A. B. Fall, S. B. Lindström, O. Sundman, L. Ödberg, and L. Wågberg, "Colloidal Stability of Aqueous Nanofibrillated Cellulose Dispersions," *Langmuir,* vol. 27, pp. 11332-11338, 2011/09/20 2011.

[97] A. Naderi, T. Lindström, and J. Sundström, "Repeated homogenization, a route for decreasing the energy consumption in the manufacturing process of carboxymethylated nanofibrillated cellulose?," *Cellulose,* vol. 22, pp. 1147-1157, April 01 2015.

[98] L. Mendoza, L. Hossain, E. Downey, C. Scales, W. Batchelor, and G. Garnier, "Carboxylated nanocellulose foams as superabsorbents," *Journal of Colloid and Interface Science,* vol. 538, pp. 433-439, 2019/03/07/ 2019.

[99] J. Guo and J. M. Catchmark, "Surface area and porosity of acid hydrolyzed cellulose nanowhiskers and cellulose produced by Gluconacetobacter xylinus," *Carbohydrate Polymers,* vol. 87, pp. 1026-1037, 2012/01/15/ 2012.

[100] G. H. D. Tonoli, E. M. Teixeira, A. C. Corrêa, J. M. Marconcini, L. A. Caixeta, M. A. Pereira-da-Silva*, et al.*, "Cellulose micro/nanofibres from Eucalyptus kraft pulp: Preparation and properties," *Carbohydrate Polymers,* vol. 89, pp. 80-88, 2012/06/05/ 2012.

[101] A. V. Delgado, F. González-Caballero, R. J. Hunter, L. K. Koopal, and J. Lyklema, "Measurement and interpretation of electrokinetic phenomena," *Journal of Colloid and Interface Science,* vol. 309, pp. 194-224, 2007.

[102] J. A. W. Shatkin, Theodore H.; Bilek, E.M. (Ted); Cowie, John, "Market projections of cellulose nanomaterial-enabled products- Part 1: Applications. ," *TAPPI JOURNAL,* vol. 13, pp. pp. 9-16, 2014.

[103] R. J. Crawford, K. J. Edler, S. Lindhoud, J. L. Scott, and G. Unali, "Formation of shear thinning gels from partially oxidised cellulose nanofibrils," *Green Chemistry,* vol. 14, pp. 300-303, 2012.

[104] D. Celebi, R. H. Guy, K. J. Edler, and J. L. Scott, "Ibuprofen delivery into and through the skin from novel oxidized cellulose-based gels and conventional topical formulations," *International Journal of Pharmaceutics,* vol. 514, pp. 238-243, 2016/11/30/ 2016.

[105] D. Mishra, P. Khare, D. K. Singh, S. Luqman, P. V. Ajaya Kumar, A. Yadav*, et al.*, "Retention of antibacterial and antioxidant properties of lemongrass oil loaded on cellulose nanofibre-poly ethylene glycol composite," *Industrial Crops and Products,* vol. 114, pp. 68-80, 2018/04/01/ 2018.

[106] S. P. Miguel, D. R. Figueira, D. Simões, M. P. Ribeiro, P. Coutinho, P. Ferreira*, et al.*, "Electrospun polymeric nanofibres as wound dressings: A review," *Colloids and Surfaces B: Biointerfaces,* vol. 169, pp. 60-71, 2018/09/01/ 2018.

[107] K. Löbmann and A. J. Svagan, "Cellulose nanofibers as excipient for the delivery of poorly soluble drugs," *International Journal of Pharmaceutics,* vol. 533, pp. 285-297, 2017/11/25/ 2017.

[108] B. M. Cherian, A. L. Leão, S. F. de Souza, L. M. M. Costa, G. M. de Olyveira, M. Kottaisamy*, et al.*, "Cellulose nanocomposites with nanofibres isolated from pineapple leaf fibers for medical applications," *Carbohydrate Polymers,* vol. 86, pp. 1790-1798, 2011/10/15/ 2011.

[109] A. H. Bhat, I. Khan, M. A. Usmani, R. Umapathi, and S. M. Z. Al-Kindy, "Cellulose an ageless renewable green nanomaterial for medical applications: An overview of ionic liquids in extraction, separation and dissolution of cellulose," *International Journal of Biological Macromolecules,* 2018/12/26/ 2018.

[110] B. Bideau, E. Loranger, and C. Daneault, "Nanocellulose-polypyrrole-coated paperboard for food packaging application," *Progress in Organic Coatings,* vol. 123, pp. 128-133, 2018/10/01/ 2018.

[111] S. Varanasi, Z.-X. Low, and W. Batchelor, "Cellulose nanofibre composite membranes – Biodegradable and recyclable UF membranes," *Chemical Engineering Journal,* vol. 265, pp. 138-146, 2015/04/01/ 2015.

[112] R. Sabo, A. Yermakov, C. T. Law, and R. Elhajjar, "Nanocellulose-Enabled Electronics, Energy Harvesting Devices, Smart Materials and Sensors: A Review," *Journal of Renewable Materials,* vol. 4, pp. 297-312, // 2016.

[113] X. Du, Z. Zhang, W. Liu, and Y. Deng, "Nanocellulose-based conductive materials and their emerging applications in energy devices - A review," *Nano Energy,* vol. 35, pp. 299-320, 2017/05/01/ 2017.

[114] Y. Li, H. Zhu, F. Shen, J. Wan, S. Lacey, Z. Fang*, et al.*, "Nanocellulose as green dispersant for two-dimensional energy materials," *Nano Energy,* vol. 13, pp. 346-354, 2015/04/01/ 2015.

[115] F. Hoeng, A. Denneulin, and J. Bras, "Use of nanocellulose in printed electronics: a review," *Nanoscale,* vol. 8, pp. 13131-13154, 2016.

[116] N. Lin and A. Dufresne, "Nanocellulose in biomedicine: Current status and future prospect," *European Polymer Journal,* vol. 59, pp. 302-325, 2014/10/01/ 2014.

[117] S. Boufi, I. González, M. Delgado-Aguilar, Q. Tarrès, M. À. Pèlach, and P. Mutjé, "Nanofibrillated cellulose as an additive in papermaking process: A review," *Carbohydrate Polymers,* vol. 154, pp. 151-166, 2016/12/10/ 2016.

[118] B. Venugopal and J. Gopalakrishnan, "Reinforcement of natural rubber using cellulose nanofibres isolated from Coconut spathe," *Materials Today: Proceedings,* vol. 5, pp. 16724-16731, 2018/01/01/ 2018.

[119] M. A. Herrera, J. A. Sirviö, A. P. Mathew, and K. Oksman, "Environmental friendly and sustainable gas barrier on porous materials: Nanocellulose coatings prepared using spin- and dip-coating," *Materials & Design,* vol. 93, pp. 19-25, 3/5/ 2016.

[120] A. Mandal and D. Chakrabarty, "Studies on the mechanical, thermal, morphological and barrier properties of nanocomposites based on poly(vinyl alcohol) and nanocellulose from sugarcane bagasse," *Journal of Industrial and Engineering Chemistry,* vol. 20, pp. 462-473, 3/25/ 2014.

[121] C. Aulin and G. Ström, "Multilayered Alkyd Resin/Nanocellulose Coatings for Use in Renewable Packaging Solutions with a High Level of Moisture Resistance," *Industrial & Engineering Chemistry Research,* vol. 52, pp. 2582-2589, 2013/02/20 2013.

[122] N. Lavoine, J. Bras, and I. Desloges, "Mechanical and barrier properties of cardboard and 3D packaging coated with microfibrillated cellulose," *Journal of Applied Polymer Science,* vol. 131, 2014.

[123] S. H. Osong, S. Norgren, and P. Engstrand, "Processing of wood-based microfibrillated cellulose and nanofibrillated cellulose, and applications relating to papermaking: a review," *Cellulose,* vol. 23, pp. 93-123, February 01 2016.

[124] F. W. Brodin, Ø. W. Gregersen, and K. Syverud, "Cellulose nanofibrils: Challenges and possibilities as a paper additive or coating material û€“ A review," *Nordic Pulp & Paper Research Journal,* vol. 29, pp. 156-166, 03/30 2014.

[125] R. Kose, K. Yamaguchi, and T. Okayama, "Influence of addition of fine cellulose fibers on physical properties and structure of paper," *Journal of Fiber Science and Technology,* vol. 71, pp. 85-90, 2015.

[126] A. W. Carpenter, C.-F. de Lannoy, and M. R. Wiesner, "Cellulose Nanomaterials in Water Treatment Technologies," *Environmental Science & Technology,* vol. 49, pp. 5277-5287, 2015/05/05 2015.

[127] V. K. Thakur and S. I. Voicu, "Recent advances in cellulose and chitosan based membranes for water purification: A concise review," *Carbohydrate Polymers,* vol. 146, pp. 148-165, 2016/08/01/ 2016.

[128] H. Voisin, L. Bergström, P. Liu, and A. Mathew, "Nanocellulose-Based Materials for Water Purification," *Nanomaterials,* vol. 7, p. 57, 2017.

[129] H. Ma, C. Burger, B. S. Hsiao, and B. Chu, "Ultrafine Polysaccharide Nanofibrous Membranes for Water Purification," *Biomacromolecules,* vol. 12, pp. 970-976, 2011/04/11 2011.

[130] H. Ma, C. Burger, B. S. Hsiao, and B. Chu, "Ultra-fine cellulose nanofibers: new nano-scale materials for water purification," *Journal of Materials Chemistry,* vol. 21, pp. 7507-7510, 2011.

[131] H. Ma, C. Burger, B. S. Hsiao, and B. Chu, "Fabrication and characterization of cellulose nanofiber based thin-film nanofibrous composite membranes," *Journal of Membrane Science,* vol. 454, pp. 272-282, 2014/03/15/ 2014.

[132] H. Ma, C. Burger, B. S. Hsiao, and B. Chu, "Highly Permeable Polymer Membranes Containing Directed Channels for Water Purification," *ACS Macro Letters,* vol. 1, pp. 723-726, 2012/06/19 2012.

[133] M. F. Islam, M. H. Rizvi, T. A. Khan, and M. Hasanuzzaman, "Development of Ceramic Candle Filters by Slip Casting Process," *Key Engineering Materials,* vol. 608, pp. 85-90, 2014.

[134] L. Du, X. Chen, W. Li, and Q. Zhu, "A Study on Enhancement of Filtration Process with Filter Aids Diatomaceous Earth and Wood Pulp Cellulose," *Chinese Journal of Chemical Engineering,* vol. 19, pp. 792-798, 2011/10/01/ 2011.

[135] J. Missau, J. d. G. d. Rocha, G. L. Dotto, D. A. Bertuol, L. P. Ceron, and E. H. Tanabe, "Purification of crude wax using a filter medium modified with a nanofiber coating," *Chemical Engineering Research and Design,* vol. 136, pp. 734-743, 2018/08/01/ 2018.

[136] J. Lozano-Sánchez, A. Segura-Carretero, and A. Fernández-Gutiérrez, "Characterisation of the phenolic compounds retained in different organic and inorganic filter aids used for filtration of extra virgin olive oil," *Food Chemistry,* vol. 124, pp. 1146-1150, 2011/02/01/ 2011.

[137] C. Himcinschi, C. Biermann, E. Storti, B. Dietrich, G. Wolf, J. Kortus*, et al.*, "Innovative carbon-bonded filters based on a new environmental-friendly binder system for steel melt filtration," *Journal of the European Ceramic Society,* vol. 38, pp. 5580-5589, 2018/12/01/ 2018.

[138] M. Doğan, M. Alkan, and Y. Onganer, "Adsorption of Methylene Blue from Aqueous Solution onto Perlite," *Water, Air, and Soil Pollution,* vol. 120, pp. 229-248, June 01 2000.

[139] Z. Talip, M. Eral, and Ü. Hiçsönmez, "Adsorption of thorium from aqueous solutions by perlite," *Journal of Environmental Radioactivity,* vol. 100, pp. 139-143, 2009/02/01/ 2009.

[140] N. M. Zúñiga-Muro, A. Bonilla-Petriciolet, D. I. Mendoza-Castillo, H. E. Reynel-Ávila, and J. C. Tapia-Picazo, "Fluoride adsorption properties of cerium-containing bone char," *Journal of Fluorine Chemistry,* vol. 197, pp. 63-73, 2017/05/01/ 2017.

[141] A. Kausar, M. Iqbal, A. Javed, K. Aftab, Z.-i.-H. Nazli, H. N. Bhatti*, et al.*, "Dyes adsorption using clay and modified clay: A review," *Journal of Molecular Liquids,* vol. 256, pp. 395-407, 2018/04/15/ 2018.

[142] Z. Ajmal, A. Muhmood, M. Usman, S. Kizito, J. Lu, R. Dong*, et al.*, "Phosphate removal from aqueous solution using iron oxides: Adsorption, desorption and regeneration characteristics," *Journal of Colloid and Interface Science,* vol. 528, pp. 145-155, 2018/10/15/ 2018.

[143] S. Zhang, M. Cui, J. Chen, Z. Ding, X. Wang, Y. Mu*, et al.*, "Modification of synthetic zeolite X by thiourea and its adsorption for Cd (II)," *Materials Letters,* 2018/10/16/ 2018.

[144] R. I. Yousef, B. El-Eswed, and A. a. H. Al-Muhtaseb, "Adsorption characteristics of natural zeolites as solid adsorbents for phenol removal from aqueous solutions: Kinetics, mechanism, and thermodynamics studies," *Chemical Engineering Journal,* vol. 171, pp. 1143-1149, 7/15/ 2011.

[145] N. B. Singh, G. Nagpal, S. Agrawal, and Rachna, "Water purification by using Adsorbents: A Review," *Environmental Technology & Innovation,* vol. 11, pp. 187-240, 2018/08/01/ 2018.

[146] P. A. Ciullo, "2. The Industrial Minerals," in *Industrial Minerals and Their Uses - A Handbook and Formulary*, ed: William Andrew Publishing/Noyes.

[147] A. Krzyzak, W. Kucharczyk, J. Gaska, and R. Szczepaniak, "Ablative test of composites with epoxy resin and expanded perlite," *Composite Structures,* vol. 202, pp. 978-987, 2018/10/15/ 2018.

[148] A. M. Rashad, "A synopsis about perlite as building material – A best practice guide for Civil Engineer," *Construction and Building Materials,* vol. 121, pp. 338-353, 2016/09/15/ 2016.

[149] H. Ghassabzadeh, A. Mohadespour, M. Torab-Mostaedi, P. Zaheri, M. G. Maragheh, and H. Taheri, "Adsorption of Ag, Cu and Hg from aqueous solutions using expanded perlite," *Journal of Hazardous Materials,* vol. 177, pp. 950-955, 2010/05/15/ 2010.

[150] M. Alkan and M. Do ğ, "Surface Titrations of Perlite Suspensions," *Journal of Colloid and Interface Science,* vol. 207, pp. 90-96, 1998/11/01/ 1998.

[151] W. Wheelwright, R. P. Cooney, S. Ray, Z. Zujovic, and K. de Silva, "Ultra-high surface area nano-porous silica from expanded perlite: Formation and characterization," *Ceramics International,* vol. 43, pp. 11495-11504, 2017/10/01/ 2017.

[152] G. Deganello, L. Liotta, A. Longo, A. Martorana, Y. Yanev, and N. Zotov, "Structure of natural water-containing glasses from Lipari (Italy) and Eastern Rhodopes (Bulgaria): SAXS, WAXS and IR studies," *Journal of Non-Crystalline Solids,* vol. 232-234, pp. 547-553, 1998/07/11/ 1998.

[153] W. J. Luo, Q. Gao, X. L. Wu, and C. G. Zhou, "Removal of Cationic Dye (Methylene Blue) from Aqueous Solution by Humic Acid-Modified Expanded Perlite: Experiment and Theory," *Separation Science and Technology (Philadelphia),* vol. 49, pp. 2400-2411, 2014.

[154] M. Taherishargh, M. A. Sulong, I. V. Belova, G. E. Murch, and T. Fiedler, "On the particle size effect in expanded perlite aluminium syntactic foam," *Materials & Design (1980-2015),* vol. 66, pp. 294-303, 2015/02/05/ 2015.

[155] T. Mathialagan and T. Viraraghavan, "Adsorption of cadmium from aqueous solutions by perlite," *Journal of Hazardous Materials,* vol. 94, pp. 291-303, 2002/10/14/ 2002.

[156] M. Irani, M. Amjadi, and M. A. Mousavian, "Comparative study of lead sorption onto natural perlite, dolomite and diatomite," *Chemical Engineering Journal,* vol. 178, pp. 317-323, 2011/12/15/ 2011.

[157] D. Bastani, A. A. Safekordi, A. Alihosseini, and V. Taghikhani, "Study of oil sorption by expanded perlite at 298.15K," *Separation and Purification Technology,* vol. 52, pp. 295-300, 2006/12/01/ 2006.

[158] J. Zhang and Y. Xue, "Hydrophobic Expanded Perlite Used in External Insulation of the Building Engineering," *Applied Mechanics and Materials,* vol. 584-586, pp. 1835-1838, 2014.

[159] A. Sarı, M. Tuzen, D. Cıtak, and M. Soylak, "Adsorption characteristics of Cu(II) and Pb(II) onto expanded perlite from aqueous solution," *Journal of Hazardous Materials,* vol. 148, pp. 387-394, 2007/09/05/ 2007.

[160] A. Silber, B. Bar-Yosef, I. Levkovitch, and S. Soryano, "pH-Dependent surface properties of perlite: Effects of plant growth," *Geoderma,* vol. 158, pp. 275-281, 2010/09/15/ 2010.

[161] L. Wang, P. Liu, Q. Jing, Y. Liu, W. Wang, Y. Zhang*, et al.*, "Strength properties and thermal conductivity of concrete with the addition of expanded perlite filled with aerogel," *Construction and Building Materials,* vol. 188, pp. 747-757, 2018/11/10/ 2018.

[162] G. J. Freeman, "11 - Reducing microbial spoilage of beer using filtration," in *Brewing Microbiology*, A. E. Hill, Ed., ed Oxford: Woodhead Publishing, 2015, pp. 241-251.

[163] M. A. M. Khraisheh, Y. S. Al-degs, and W. A. M. McMinn, "Remediation of wastewater containing heavy metals using raw and modified diatomite," *Chemical Engineering Journal,* vol. 99, pp. 177-184, 2004/06/15/ 2004.

[164] C.-D. Wu, X.-J. Xu, J.-L. Liang, Q. Wang, Q. Dong, and W.-L. Liang, "Enhanced coagulation for treating slightly polluted algae-containing surface water combining polyaluminum chloride (PAC) with diatomite," *Desalination,* vol. 279, pp. 140-145, 2011/09/15/ 2011.

[165] G. Sheng, S. Wang, J. Hu, Y. Lu, J. Li, Y. Dong*, et al.*, "Adsorption of Pb(II) on diatomite as affected via aqueous solution chemistry and temperature," *Colloids and Surfaces A: Physicochemical and Engineering Aspects,* vol. 339, pp. 159-166, 2009/05/01/ 2009.

[166] N. Kröger, "Prescribing diatom morphology: toward genetic engineering of biological nanomaterials," *Current Opinion in Chemical Biology,* vol. 11, pp. 662-669, 2007/12/01/ 2007.

[167] B. Michen, A. Diatta, J. Fritsch, C. Aneziris, and T. Graule, "Removal of colloidal particles in ceramic depth filters based on diatomaceous earth," *Separation and Purification Technology,* vol. 81, pp. 77-87, 2011/09/05/ 2011.

[168] S. S. Salih and T. K. Ghosh, "Adsorption of Zn(II) ions by chitosan coated diatomaceous earth," *International Journal of Biological Macromolecules,* vol. 106, pp. 602-610, 2018/01/01/ 2018.

[169] B. S. Stromer, B. Woodbury, and C. F. Williams, "Tylosin sorption to diatomaceous earth described by Langmuir isotherm and Freundlich isotherm models," *Chemosphere,* vol. 193, pp. 912-920, 2018/02/01/ 2018.

[170] E. Alvarez, J. Blanco, P. Avila, and C. Knapp, "Activation of monolithic catalysts based on diatomaceous earth for sulfur dioxide oxidation," *Catalysis Today,* vol. 53, pp. 557-563, 1999/11/12/ 1999.

[171] J. F. Lemonas, "Diatomite," *Am. Ceram. Soc. Bull.,* vol. 76, pp. 92-95, 1997.

[172] D. W. Breck, *Zeolite molecular sieves: structure, chemistry, and use*: Wiley, 1973.

[173] P. Kresimir and H. Mirko, "Medical Applications of Zeolites," in *Handbook of Zeolite Science and Technology*, ed: CRC Press, 2003.

[174] B. Jha and D. N. Singh, "Basics of Zeolites," in *Fly Ash Zeolites: Innovations, Applications, and Directions*, ed Singapore: Springer Singapore, 2016, pp. 5-31.

[175] M. Jiang and F. T. T. Ng, "Adsorption of benzothiophene on Y zeolites investigated by infrared spectroscopy and flow calorimetry," *Catalysis Today,* vol. 116, pp. 530-536, 2006/09/15/ 2006.

[176] V. M. Radak, I. J. Gal, R. Radulović-Hercigonja, and D. Seidel, "Some physical and chemical properties of Fe(II)X, Fe(II)Y and Fe(III)Y zeolites," *Journal of Inorganic and Nuclear Chemistry,* vol. 40, pp. 75-77, 1978/01/01/ 1978.

[177] F. L. Raúl, "Introduction to the Structural Chemistry of Zeolites," in *Handbook of Zeolite Science and Technology*, ed: CRC Press, 2003.

[178] G. D. Gatta and P. Lotti, "Chapter 1 - Systematics, crystal structures, and occurrences of zeolites," in *Modified Clay and Zeolite Nanocomposite Materials*, M. Mercurio, B. Sarkar, and A. Langella, Eds., ed: Elsevier, 2019, pp. 1-25.

[179] J. Liu and J. Yu, "Chapter 1 - Toward Greener and Designed Synthesis of Zeolite Materials," in *Zeolites and Zeolite-Like Materials*, B. F. Sels and L. M. Kustov, Eds., ed Amsterdam: Elsevier, 2016, pp. 1-32.

[180] S. Förster and M. Schmidt, "Polyelectrolytes in solution," in *Physical Properties of Polymers*, ed Berlin, Heidelberg: Springer Berlin Heidelberg, 1995, pp. 51-133.

[181] J. L. Barrat and J. F. Joanny, "Theory of polyelectrolyte solutions," in *Advances in Chemical Physics* vol. 94, ed, 1996, pp. 1-66.

[182] A. V. Dobrynin and M. Rubinstein, "Theory of polyelectrolytes in solutions and at surfaces," *Progress in Polymer Science,* vol. 30, pp. 1049-1118, 2005/11/01/ 2005.

[183] W. Jaeger, J. Bohrisch, and A. Laschewsky, "Synthetic polymers with quaternary nitrogen atoms—Synthesis and structure of the most used type of cationic polyelectrolytes," *Progress in Polymer Science,* vol. 35, pp. 511-577, 2010/05/01/ 2010.

[184] G. G. Cameron, "Polyelectrolytes: formation, characterization and application. H. Dautzenberg, W. Jaeger, J. Kötz, B. Philipp, Ch. Seidel and D. Stscherbina. Carl Hanser Verlag, Munich, 1994. pp. xiv + 343, price DM168.00. ISBN 1-56990-127-9. ISBN 3-446-17127-4," *Polymer International,* vol. 38, pp. 106-106, 1995.

[185] V. S. Meka, M. K. G. Sing, M. R. Pichika, S. R. Nali, V. R. M. Kolapalli, and P. Kesharwani, "A comprehensive review on polyelectrolyte complexes," *Drug Discovery Today,* vol. 22, pp. 1697-1706, 2017/11/01/ 2017.

[186] B. M. Baraniak and E. Waleriańczyk, "FLOCCULATION," in *Encyclopedia of Food Sciences and Nutrition (Second Edition)*, B. Caballero, Ed., ed Oxford: Academic Press, 2003, pp. 2531-2535.

[187] M. Rubinstein and R. H. Colby, "Polymer Physics. 2003," ed: Oxford University Press.

[188] L. Wågberg and R. Hägglund, "Kinetics of Polyelectrolyte Adsorption on Cellulosic Fibers," *Langmuir,* vol. 17, pp. 1096-1103, 2001/02/01 2001.

[189] R. T. a. P. R. L. Dzina Kleshchanok, "Direct measurements of polymer-induced forces," *Journal of Physics: Condensed Matter,* vol. 20, 2008.

[190] J. E. a. R. B, *Elektrochem.,* vol. 55, p. 612, 1951.

[191] A. Matsuda, M. Mimura, T. Maruyama, T. Kurinomaru, M. Shiuhei, and K. Shiraki, "Liquid Droplet of Protein-Polyelectrolyte Complex for High-Concentration Formulations," *Journal of Pharmaceutical Sciences,* vol. 107, pp. 2713-2719, 2018/10/01/ 2018.

[192] M. G. Kim, S. D. Jo, J. H. Jeong, and S. H. Kim, "Nanoscale polyelectrolyte complexes encapsulating mRNA and long-chained siRNA for combinatorial cancer gene therapy," *Journal of Industrial and Engineering Chemistry,* vol. 64, pp. 430-437, 2018/08/25/ 2018.

[193] M. I. Aguilar, J. Sáez, M. Lloréns, A. Soler, J. F. Ortuño, V. Meseguer*, et al.*, "Improvement of coagulation–flocculation process using anionic polyacrylamide as coagulant aid," *Chemosphere,* vol. 58, pp. 47-56, 2005/01/01/ 2005.

[194] S. Llamas, E. Guzmán, F. Ortega, N. Baghdadli, C. Cazeneuve, R. G. Rubio*, et al.*, "Adsorption of polyelectrolytes and polyelectrolytes-surfactant mixtures at surfaces: a physico-chemical approach to a cosmetic challenge," *Advances in Colloid and Interface Science,* vol. 222, pp. 461-487, 2015/08/01/ 2015.

[195] F. Şen, İ. Uzunsoy, E. Baştürk, and M. V. Kahraman, "Antimicrobial agent-free hybrid cationic starch/sodium alginate polyelectrolyte films for food packaging materials," *Carbohydrate Polymers,* vol. 170, pp. 264-270, 2017/08/15/ 2017.

[196] P. Bajpai, "Chapter 4 - Additives for Papermaking," in *Biermann's Handbook of Pulp and Paper (Third Edition)*, P. Bajpai, Ed., ed: Elsevier, 2018, pp. 77-94.

[197] M. S. Nasser, F. A. Twaiq, and S. A. Onaizi, "Effect of polyelectrolytes on the degree of flocculation of papermaking suspensions," *Separation and Purification Technology,* vol. 103, pp. 43-52, 2013/01/15/ 2013.

[198] P. Raj, W. Batchelor, A. Blanco, E. de la Fuente, C. Negro, and G. Garnier, "Effect of polyelectrolyte morphology and adsorption on the mechanism of nanocellulose flocculation," *Journal of Colloid and Interface Science,* vol. 481, pp. 158-167, 2016/11/01/ 2016.

[199] P. Raj, A. Blanco, E. de la Fuente, W. Batchelor, C. Negro, and G. Garnier, "Microfibrilated cellulose as a model for soft colloid flocculation with polyelectrolytes," *Colloids and Surfaces A: Physicochemical and Engineering Aspects,* vol. 516, pp. 325-335, 2017/03/05/ 2017.

[200] V. S. Raghuwanshi, U. M. Garusinghe, J. Ilavsky, W. J. Batchelor, and G. Garnier, "Effect of nanoparticles size and polyelectrolyte on nanoparticles aggregation in a cellulose fibrous matrix," *Journal of Colloid and Interface Science,* vol. 510, pp. 190-198, 2018/01/15/ 2018.

[201] E. Larsson, C. C. Sanchez, C. Porsch, E. Karabulut, L. Wågberg, and A. Carlmark, "Thermo-responsive nanofibrillated cellulose by polyelectrolyte adsorption," *European Polymer Journal,* vol. 49, pp. 2689-2696, 2013/09/01/ 2013.

[202] D. Solberg and L. Wågberg, "Adsorption and flocculation behavior of cationic polyacrylamide and colloidal silica," *Colloids and Surfaces A: Physicochemical and Engineering Aspects,* vol. 219, pp. 161-172, 2003/06/19/ 2003.

[203] A. Lu, Y. Song, and Y. Boluk, "Electrolyte effect on gelation behavior of oppositely charged nanocrystalline cellulose and polyelectrolyte," *Carbohydrate Polymers,* vol. 114, pp. 57-64, 2014/12/19/ 2014.

[204] F. Linhart, "The practical application of wet-strength resins," in *Applications of Wet-End Paper Chemistry*, C. O. Au and I. Thorn, Eds., ed Dordrecht: Springer Netherlands, 1995, pp. 102-119.

[205] J. C. Roberts, *Paper Chemistry*: Springer Netherlands, 1996.

[206] N. A. Bates, *Tappi Journal,* vol. 52, p. 1162, 1969.

[207] H. H. Espy, *Tappi Journal,* vol. 70, p. 129, 1987.

[208] T. Obokata and A. Isogai, "1H- and 13C-NMR analyses of aqueous polyamideamine–epichlorohydrin resin solutions," *Journal of Applied Polymer Science,* vol. 92, pp. 1847-1854, 2004.

[209] T. Obokata, M. Yanagisawa, and A. Isogai, "Characterization of polyamideamine-epichlorohydrin (PAE) resin: Roles of azetidinium groups and molecular mass of PAE in wet strength development of paper prepared with PAE," *Journal of Applied Polymer Science,* vol. 97, pp. 2249-2255, 2005.

[210] H. H. Espy, *Tappi Journal,* vol. 78, p. 90, 1995.

[211] T. Obokata and A. Isogai, "The mechanism of wet-strength development of cellulose sheets prepared with polyamideamine-epichlorohydrin (PAE) resin," *Colloids and Surfaces A: Physicochemical and Engineering Aspects,* vol. 302, pp. 525-531, 7/20/ 2007.

[212] A. Rabiee, "Acrylamide-based anionic polyelectrolytes and their applications: A survey," *Journal of Vinyl and Additive Technology,* vol. 16, pp. 111-119, 2010.

[213] C. Wandrey and W. Jaeger, "Copolymerization of dimethyl diallyl ammonium chloride and acryl amide," *Acta Polymerica,* vol. 36, pp. 100-102, 1985.

[214] G. Liu, H. Zhong, Y. Hu, S. Zhao, and L. Xia, "The role of cationic polyacrylamide in the reverse flotation of diasporic bauxite," *Minerals Engineering,* vol. 20, pp. 1191-1199, 2007/11/01/ 2007.

[215] N. M. Main, R. A. Talib, R. A. Rahman, A. Z. Mohamed, R. Ibrahim, and S. Adnan, "Effect of Amphoteric and Cationic Polyacrylamide on the Structural and Strength Properties of Coir Paper," *Procedia Manufacturing,* vol. 2, pp. 28-34, 2015/01/01/ 2015.

[216] S. R. Djafari Petroudy, K. Syverud, G. Chinga-Carrasco, A. Ghasemain, and H. Resalati, "Effects of bagasse microfibrillated cellulose and cationic polyacrylamide on key properties of bagasse paper," *Carbohydrate Polymers,* vol. 99, pp. 311-318, 2014/01/02/ 2014.

[217] V. S. Raghuwanshi, U. M. Garusinghe, P. Raj, N. Kirby, A. Hoell, W. Batchelor*, et al.*, "Cationic polyacrylamide induced nanoparticles assembly in a cellulose nanofiber network," *Journal of Colloid and Interface Science,* vol. 529, pp. 180-186, 2018/11/01/ 2018.

[218] W. K. J. Mosse, D. V. Boger, G. P. Simon, and G. Garnier, "Effect of cationic polyacrylamides on the interactions between cellulose fibers," *Langmuir,* vol. 28, pp. 3641-3649, 2012.

[219] E. Antunes, F. A. P. Garcia, P. Ferreira, A. Blanco, C. Negro, and M. G. Rasteiro, "Use of new branched cationic polyacrylamides to improve retention and drainage in papermaking," *Industrial and Engineering Chemistry Research,* vol. 47, pp. 9370-9375, 2008.

[220] B. K. Song, M. S. Cho, K. J. Yoon, and D. C. Lee, "Dispersion polymerization of acrylamide with quaternary ammonium cationic comonomer in aqueous solution," *Journal of Applied Polymer Science,* vol. 87, pp. 1101-1108, 2002.

[221] T. G. M. Van De Ven, "Kinetic aspects of polymer and polyelectrolyte adsorption on surfaces," *Advances in Colloid and Interface Science,* vol. 48, pp. 121-140, 1994/04/15/ 1994.

[222] F. S. Chen, H. F. Xu, X. Y. Jiang, and S. L. Wang, "Effects of PEI as ATC on the Retention and Drainage of APMP," *Advanced Materials Research,* vol. 233-235, pp. 1587-1591, 2011.

[223] C. J. Wang, C. Chen, H. Ren, Y. Yang, and H. Q. Dai, "Polyethyleneimine Addition for Control of Dissolved and Colloidal Substances: Effects on Wet-End Chemistry," *BioResources,* vol. 11, pp. 9756-9770, 2016.

[224] A. von Harpe, H. Petersen, Y. Li, and T. Kissel, "Characterization of commercially available and synthesized polyethylenimines for gene delivery," *Journal of Controlled Release,* vol. 69, pp. 309-322, 2000/11/03/ 2000.

[225] J. C. Roberts, *Paper chemistry : Retention Aids*, 2nd ed. ed. London: London : Blackie Academic & Professional, 1996.

[226] C. R. Dick and G. E. Ham, "Characterization of Polyethylenimine," *Journal of Macromolecular Science: Part A - Chemistry,* vol. 4, pp. 1301-1314, 1970/10/01 1970.

[227] B. Demeneix and J. P. Behr, "Polyethylenimine (PEI)," in *Advances in Genetics*. vol. 53, ed: Academic Press, 2005, pp. 215-230.

[228] Á. Blanco, E. Fuente, M. C. Monte, N. Cortés, and C. Negro, "Polymeric Branched Flocculant Effect on the Flocculation Process of Pulp Suspensions in the Papermaking Industry," *Industrial & Engineering Chemistry Research,* vol. 48, pp. 4826-4836, 2009/05/20 2009.

[229] A. S. Santos, L. F. S. Oliveira, A. M. T. Marques, D. C. A. Silva, and C. R. E. Mansur, "Evaluation of the efficiency of polyethylenimine as flocculants in the removal of oil present in produced water," *Colloids and Surfaces A: Physicochemical and Engineering Aspects,* vol. 558, pp. 200-210, 2018/12/05/ 2018.

[230] K. P. Sharma, C. K. Choudhury, S. Srivastava, H. Davis, P. R. Rajamohanan, S. Roy*, et al.*, "Assembly of Polyethyleneimine in the Hexagonal Mesophase of Nonionic Surfactant: Effect of pH and Temperature," *The Journal of Physical Chemistry B,* vol. 115, pp. 9059-9069, 2011/07/28 2011.

[231] P. E. Trout, *The mechanism of the improvement of the wet strength of paper by polyethylenimine* vol. 34, 1951.

[232] K. Sarkanen, "Wet strength in paper and paperboard," *Tappi Monograph Series,* vol. 29, pp. 38-49, 1965.

[233] S. S. Nair and A. P. Mathew, "Porous composite membranes based on cellulose acetate and cellulose nanocrystals via electrospinning and electrospraying," *Carbohydrate Polymers,* vol. 175, pp. 149-157, 2017/11/01/ 2017.

[234] M. M. Castillo-Ortega, J. Romero-García, F. Rodríguez, A. Nájera-Luna, and P. J. Herrera-Franco, "Fibrous membranes of cellulose acetate and poly(vinyl pyrrolidone) by electrospinning method: Preparation and characterization," *Journal of Applied Polymer Science,* vol. 116, pp. 1873-1878, 2010.

[235] K. Zhang, Z. Li, W. Kang, N. Deng, J. Yan, J. Ju*, et al.*, "Preparation and characterization of tree-like cellulose nanofiber membranes via the electrospinning method," *Carbohydrate Polymers,* vol. 183, pp. 62-69, 2018/03/01/ 2018.

[236] L. Peng, H. Li, and Y. Meng, "Layer-by-layer structured polysaccharides-based multilayers on cellulose acetate membrane: Towards better hemocompatibility, antibacterial and antioxidant activities," *Applied Surface Science,* vol. 401, pp. 25-39, 2017/04/15/ 2017.

[237] R. Sabarish and G. Unnikrishnan, "Polyvinyl alcohol/carboxymethyl cellulose/ZSM-5 zeolite biocomposite membranes for dye adsorption applications," *Carbohydrate Polymers,* vol. 199, pp. 129-140, 2018/11/01/ 2018.

[238] J. Huang, S. Wang, S. Lyu, and F. Fu, "Preparation of a robust cellulose nanocrystal superhydrophobic coating for self-cleaning and oil-water separation only by spraying," *Industrial Crops and Products,* vol. 122, pp. 438-447, 2018/10/15/ 2018.

[239] P. Wojciechowska, Z. Foltynowicz, and M. Nowicki, "Synthesis and Characterization of Modified Cellulose Acetate Propionate Nanocomposites via Sol-Gel Process," *Journal of Spectroscopy,* vol. 2013, p. 8, 2013.

[240] M. Mulder, "MEMBRANE PREPARATION | Phase Inversion Membranes," in *Encyclopedia of Separation Science*, I. D. Wilson, Ed., ed Oxford: Academic Press, 2000, pp. 3331-3346.

[241] S. Hermans, H. Mariën, C. Van Goethem, and I. F. J. Vankelecom, "Recent developments in thin film (nano)composite membranes for solvent resistant nanofiltration," *Current Opinion in Chemical Engineering,* vol. 8, pp. 45-54, 2015/05/01/ 2015.

[242] R.-C. Ruaan, T. Chang, and D.-M. Wang, "Selection criteria for solvent and coagulation medium in view of macrovoid formation in the wet phase inversion process," *Journal of Polymer Science Part B: Polymer Physics,* vol. 37, pp. 1495-1502, 1999.

[243] S. Perez, E. Merlen, E. Robert, J. P. C. Addad, and A. Viallat, "Characterization of the surface layer of integrally skinned polyimide membranes: Relationship with their mechanism of formation," *Journal of Applied Polymer Science,* vol. 47, pp. 1621-1631, 1993.

[244] G. R. Guillen, Y. Pan, M. Li, and E. M. V. Hoek, "Preparation and Characterization of Membranes Formed by Nonsolvent Induced Phase Separation: A Review," *Industrial & Engineering Chemistry Research,* vol. 50, pp. 3798-3817, 2011/04/06 2011.

[245] A. K. Hołda and I. F. J. Vankelecom, "Understanding and guiding the phase inversion process for synthesis of solvent resistant nanofiltration membranes," *Journal of Applied Polymer Science,* vol. 132, 2015.

[246] N. Han, J. Xiong, S. Chen, X. Zhang, Y. Li, and L. Tan, "Structure and properties of poly(acrylonitrile-co-methyl acrylate) membranes prepared via thermally induced phase separation," *Journal of Applied Polymer Science,* vol. 133, 2016.

[247] Z. Qiu, X. Ji, and C. He, "Fabrication of a loose nanofiltration candidate from Polyacrylonitrile/Graphene oxide hybrid membrane via thermally induced phase separation," *Journal of Hazardous Materials,* vol. 360, pp. 122-131, 2018/10/15/ 2018.

[248] E. J. Vriezekolk, K. Nijmeijer, and W. M. de Vos, "Dry–wet phase inversion block copolymer membranes with a minimum evaporation step from NMP/THF mixtures," *Journal of Membrane Science,* vol. 504, pp. 230-239, 2016/04/15/ 2016.

[249] L. Gao, B. Tang, and P. Wu, "An experimental investigation of evaporation time and the relative humidity on a novel positively charged ultrafiltration membrane via dry–wet phase inversion," *Journal of Membrane Science,* vol. 326, pp. 168-177, 2009/01/05/ 2009.

[250] H. D. Chaudhari, R. Illathvalappil, S. Kurungot, and U. K. Kharul, "Preparation and investigations of ABPBI membrane for HT-PEMFC by immersion precipitation method," *Journal of Membrane Science,* vol. 564, pp. 211-217, 2018/10/15/ 2018.

[251] A. Aulova, A. Cvenkel, S. Žakelj, O. Planinšek, A. Kristl, and I. Emri, "Mechanical properties and drug permeability of the PA6 membranes prepared by immersion precipitation from PA6 – formic acid – water system," *Journal of Membrane Science,* vol. 562, pp. 67-75, 2018/09/15/ 2018.

[252] S. K. Karode and A. Kumar, "Formation of polymeric membranes by immersion precipitation: an improved algorithm for mass transfer calculations," *Journal of Membrane Science,* vol. 187, pp. 287-296, 2001/06/15/ 2001.

[253] D.-J. Lin, C.-L. Chang, T.-C. Chen, and L.-P. Cheng, "Microporous PVDF membrane formation by immersion precipitation from water/TEP/PVDF system," *Desalination,* vol. 145, pp. 25-29, 2002/09/10/ 2002.

[254] F. Galiano, K. Briceño, T. Marino, A. Molino, K. V. Christensen, and A. Figoli, "Advances in biopolymer-based membrane preparation and applications," *Journal of Membrane Science,* vol. 564, pp. 562-586, 2018/10/15/ 2018.

[255] J.-J. Qin, Y. Li, L.-S. Lee, and H. Lee, "Cellulose acetate hollow fiber ultrafiltration membranes made from CA/PVP 360 K/NMP/water," *Journal of Membrane Science,* vol. 218, pp. 173-183, 2003/07/01/ 2003.

[256] J. Su, Q. Yang, J. F. Teo, and T.-S. Chung, "Cellulose acetate nanofiltration hollow fiber membranes for forward osmosis processes," *Journal of Membrane Science,* vol. 355, pp. 36-44, 2010/06/15/ 2010.

[257] R. Haddada, E. Ferjani, M. S. Roudesli, and A. Deratani, "Properties of cellulose acetate nanofiltration membranes. Application to brackish water desalination," *Desalination,* vol. 167, pp. 403-409, 2004/08/15/ 2004.

[258] E. Ferjani, E. Ellouze, and R. Ben Amar, "Treatment of seafood processing wastewaters by ultrafiltration-nanofiltration cellulose acetate membranes," *Desalination,* vol. 177, pp. 43-49, 2005/06/20/ 2005.

[259] A. K. Mohanty, A. Wibowo, M. Misra, and L. T. Drzal, "Development of renewable resource–based cellulose acetate bioplastic: Effect of process engineering on the performance of cellulosic plastics," *Polymer Engineering & Science,* vol. 43, pp. 1151-1161, 2003.

[260] Y. Yang, H. Zhang, P. Wang, Q. Zheng, and J. Li, "The influence of nano-sized TiO2 fillers on the morphologies and properties of PSF UF membrane," *Journal of Membrane Science,* vol. 288, pp. 231-238, 2/1/ 2007.

[261] A. Bottino, G. Capannelli, V. D'Asti, and P. Piaggio, "Preparation and properties of novel organic–inorganic porous membranes," *Separation and Purification Technology,* vol. 22-23, pp. 269-275, 2001/03/01/ 2001.

[262] P.-C. Chiang and W.-T. Whang, "The synthesis and morphology characteristic study of BAO-ODPA polyimide/TiO2 nano hybrid films," *Polymer,* vol. 44, pp. 2249-2254, 2003/04/01/ 2003.

[263] M. Moaddeb and W. J. Koros, "Gas transport properties of thin polymeric membranes in the presence of silicon dioxide particles," *Journal of Membrane Science,* vol. 125, pp. 143-163, 1997/03/05/ 1997.

[264] K. G. Neoh, K. K. Tan, P. L. Goh, S. W. Huang, E. T. Kang, and K. L. Tan, "Electroactive polymer–SiO2 nanocomposites for metal uptake," *Polymer,* vol. 40, pp. 887-893, 1999/02/01/ 1999.

[265] I. F. J. Vankelecom, S. De Beukelaer, and J. B. Uytterhoeven, "Sorption and Pervaporation of Aroma Compounds Using Zeolite-Filled PDMS Membranes," *The Journal of Physical Chemistry B,* vol. 101, pp. 5186-5190, 1997/06/01 1997.

[266] L. A. Goetz, B. Jalvo, R. Rosal, and A. P. Mathew, "Superhydrophilic anti-fouling electrospun cellulose acetate membranes coated with chitin nanocrystals for water filtration," *Journal of Membrane Science,* vol. 510, pp. 238-248, 2016/07/15/ 2016.

[267] P. Kanagaraj, A. Nagendran, D. Rana, and T. Matsuura, "Separation of macromolecular proteins and removal of humic acid by cellulose acetate modified UF membranes," *International Journal of Biological Macromolecules,* vol. 89, pp. 81-88, 2016/08/01/ 2016.

[268] J. García-Ivars, M.-J. Corbatón-Báguena, and M.-I. Iborra-Clar, "Chapter 6 - Development of Mixed Matrix Membranes: Incorporation of Metal Nanoparticles in Polymeric Membranes," in *Nanoscale Materials in Water Purification*, S. Thomas, D. Pasquini, S.-Y. Leu, and D. A. Gopakumar, Eds., ed: Elsevier, 2019, pp. 153-178.

[269] P. Bajpai, "Chapter 6 - Paper Manufacture—Dry End Operation," in *Biermann's Handbook of Pulp and Paper (Third Edition)*, P. Bajpai, Ed., ed: Elsevier, 2018, pp. 137-158.

[270] P. Bajpai, "Chapter 5 - Paper Manufacture—Wet End Operation," in *Biermann's Handbook of Pulp and Paper (Third Edition)*, P. Bajpai, Ed., ed: Elsevier, 2018, pp. 95-135.

[271] I. M. Hutten, "Chapter 3 - Properties of Nonwoven Filter Media," in *Handbook of Nonwoven Filter Media (Second Edition)*, I. M. Hutten, Ed., ed Oxford: Butterworth-Heinemann, 2016, pp. 108-157.

[272] M. Henriksson, L. A. Berglund, P. Isaksson, T. Lindström, and T. Nishino, "Cellulose Nanopaper Structures of High Toughness," *Biomacromolecules,* vol. 9, pp. 1579-1585, 2008/06/01 2008.

[273] A. N. Nakagaito and H. Yano, "The effect of morphological changes from pulp fiber towards nano-scale fibrillated cellulose on the mechanical properties of high-strength plant fiber based composites," *Applied Physics A,* vol. 78, pp. 547-552, March 01 2004.

[274] T. Taniguchi and K. Okamura, "New films produced from microfibrillated natural fibres," *Polymer International,* vol. 47, pp. 291-294, 1998.

[275] H. Sehaqui, A. Liu, Q. Zhou, and L. A. Berglund, "Fast Preparation Procedure for Large, Flat Cellulose and Cellulose/Inorganic Nanopaper Structures," *Biomacromolecules,* vol. 11, pp. 2195-2198, 2010/09/13 2010.

[276] K. Syverud and P. Stenius, "Strength and barrier properties of MFC films," *Cellulose,* vol. 16, p. 75, August 19 2008.

[277] H. Ichiura, N. Okamura, T. Kitaoka, and H. Tanaka, "Preparation of zeolite sheet using a papermaking technique Part II The strength of zeolite sheet and its hygroscopic characteristics," *Journal of Materials Science,* vol. 36, pp. 4921-4926.

[278] H. Ichiura, M. Nozaki, T. Kitaoka, and H. Tanaka, "Influence of uniformity of zeolite sheets prepared using a papermaking technique on VOC adsorptivity," *Advances in Environmental Research,* vol. 7, pp. 975-979, 6// 2003.

[279] H. Ichiura, T. Kitaoka, and H. Tanaka, "Preparation of composite TiO2-zeolite sheets using a papermaking technique and their application to environmental improvement Part I Removal of acetaldehyde with and without UV irradiation," *Journal of Materials Science,* vol. 37, pp. 2937-2941.

[280] H. Ichiura, T. Kitaoka, and H. Tanaka, "Preparation of composite TiO2-zeolite sheets using a papermaking technique and their application to environmental improvement Part II Effect of zeolite coexisting in the composite sheet on NO x removal," *Journal of Materials Science,* vol. 38, pp. 1611-1615, 2003/04/01 2003.

[281] H. Ichiura, Y. Kubota, Z. Wu, and H. Tanaka, "Preparation of zeolite sheets using a papermaking technique Part I Dual polymer system for high retention of stock components," *Journal of Materials Science,* vol. 36, pp. 913-917.

[282] H. Ichiura, T. Kitaoka, and H. Tanaka, "Removal of indoor pollutants under UV irradiation by a composite TiO2–zeolite sheet prepared using a papermaking technique," *Chemosphere,* vol. 50, pp. 79-83, 1// 2003.

[283] M. Visanko, H. Liimatainen, J. A. Sirviö, A. Haapala, R. Sliz, J. Niinimäki*, et al.*, "Porous thin film barrier layers from 2,3-dicarboxylic acid cellulose nanofibrils for membrane structures," *Carbohydrate Polymers,* vol. 102, pp. 584-589, 2014.

[284] A. Mautner, K.-Y. Lee, T. Tammelin, A. P. Mathew, A. J. Nedoma, K. Li*, et al.*, "Cellulose nanopapers as tight aqueous ultra-filtration membranes," *Reactive and Functional Polymers,* vol. 86, pp. 209-214, 1// 2015.

[285] A. Mautner, K. Y. Lee, P. Lahtinen, M. Hakalahti, T. Tammelin, K. Li*, et al.*, "Nanopapers for organic solvent nanofiltration," *Chemical Communications,* vol. 50, pp. 5778-5781, 2014.

[286] H. Sehaqui, B. Michen, E. Marty, L. Schaufelberger, and T. Zimmermann, "Functional Cellulose Nanofiber Filters with Enhanced Flux for the Removal of Humic Acid by Adsorption," *ACS Sustainable Chemistry & Engineering,* vol. 4, pp. 4582-4590, 2016/09/06 2016.

[287] S. Varanasi and W. J. Batchelor, "Rapid preparation of cellulose nanofibre sheet," *Cellulose,* vol. 20, pp. 211-215, February 01 2013.

[288] A. Mtibe, L. Z. Linganiso, A. P. Mathew, K. Oksman, M. J. John, and R. D. Anandjiwala, "A comparative study on properties of micro and nanopapers produced from cellulose and cellulose nanofibres," *Carbohydrate Polymers,* vol. 118, pp. 1-8, 2015/03/15/ 2015.

[289] J. Su, W. K. J. Mosse, S. Sharman, W. J. Batchelor, and G. Garnier, "Effect of tethered and free microfibrillated cellulose (MFC) on the properties of paper composites," *Cellulose,* vol. 20, pp. 1925-1935, 2013.

[290] K. Mörseburg and G. Chinga-Carrasco, "Assessing the combined benefits of clay and nanofibrillated cellulose in layered TMP-based sheets," *Cellulose,* vol. 16, pp. 795-806, 2009.

[291] Y. Wu, M. R. K. Ali, K. Chen, N. Fang, and M. A. El-Sayed, "Gold nanoparticles in biological optical imaging," *Nano Today,* 2019/01/05/ 2019.

[292] P. Krishnamachari, R. Hashaikeh, and M. Tiner, "Modified cellulose morphologies and its composites; SEM and TEM analysis," *Micron,* vol. 42, pp. 751-761, 2011/12/01/ 2011.

[293] A. T. Kola-Mustapha, "Chapter 10 - Microscopy of Nanomaterial for Drug Delivery," in *Characterization and Biology of Nanomaterials for Drug Delivery*, S. S. Mohapatra, S. Ranjan, N. Dasgupta, R. K. Mishra, and S. Thomas, Eds., ed: Elsevier, 2019, pp. 265-280.

[294] M. de Assumpção Pereira-da-Silva and F. A. Ferri, "1 - Scanning Electron Microscopy," in *Nanocharacterization Techniques*, A. L. Da Róz, M. Ferreira, F. de Lima Leite, and O. N. Oliveira, Eds., ed: William Andrew Publishing, 2017, pp. 1-35.

[295] S. Charurvedi and P. N. Dave, "Microscopy in Nanotechnology," 2012.

[296] V. Klang, C. Valenta, and N. B. Matsko, "Electron microscopy of pharmaceutical systems," *Micron,* vol. 44, pp. 45-74, 2013/01/01/ 2013.

[297] S. Wang, P. Yang, and Z. Yang, "Characterization of freeze–thaw effects within clay by 3D X-ray Computed Tomography," *Cold Regions Science and Technology,* vol. 148, pp. 13-21, 2018/04/01/ 2018.

[298] R. Holmstad, "Methods for Paper Structure Characterisation by Means of Image Analysis," Doctorate, Norges teknisk-naturvitenskapelige universitet 2004.

[299] T. Joffre, A. Miettinen, F. Berthold, and E. K. Gamstedt, "X-ray micro-computed tomography investigation of fibre length degradation during the processing steps of short-fibre composites," *Composites Science and Technology,* vol. 105, pp. 127-133, 2014/12/10/ 2014.

[300] J. Rantanen and T. C. Maloney, "Consolidation and dewatering of a microfibrillated cellulose fiber composite paper in wet pressing," *European Polymer Journal,* vol. 68, pp. 585-591, 2015/07/01/ 2015.

[301] D. Julve, J. Ramos, J. Pérez, and M. Menéndez, "Analysis of mercury porosimetry curves of precipitated silica, as an example of compressible porous solids," *Journal of Non-Crystalline Solids,* vol. 357, pp. 1319-1327, 2011/02/15/ 2011.

[302] K. L. Stefanopoulos, T. A. Steriotis, A. C. Mitropoulos, N. K. Kanellopoulos, and W. Treimer, "Characterisation of porous materials by combining mercury porosimetry and scattering techniques," *Physica B: Condensed Matter,* vol. 350, pp. E525-E527, 2004/07/15/ 2004.

[303] H. Giesche, "Mercury Porosimetry: A General (Practical) Overview," *Particle & Particle Systems Characterization,* vol. 23, pp. 9-19, 2006.

[304] H. P. Karki, L. Kafle, D. P. Ojha, J. H. Song, and H. J. Kim, "Cellulose/polyacrylonitrile electrospun composite fiber for effective separation of the surfactant-free oil-in-water mixture under a versatile condition," *Separation and Purification Technology,* vol. 210, pp. 913-919, 2019/02/08/ 2019.

[305] U. M. Garusinghe, S. Varanasi, G. Garnier, and W. Batchelor, "Strong cellulose nanofibre-nanosilica composites with controllable pore structure," *Cellulose,* vol. 24, pp. 2511-2521, Jun 2017.

[306] S. Lowell, *Characterization of porous solids and powders : surface area, pore size and density, 2004*.

[307] M. Pérez-Page, J. Makel, K. Guan, S. Zhang, J. Tringe, R. H. R. Castro*, et al.*, "Gas adsorption properties of ZSM-5 zeolites heated to extreme temperatures," *Ceramics International,* vol. 42, pp. 15423-15431, 2016/11/01/ 2016.

[308] Y.-S. Bae, A. Ö. Yazaydın, and R. Q. Snurr, "Evaluation of the BET Method for Determining Surface Areas of MOFs and Zeolites that Contain Ultra-Micropores," *Langmuir,* vol. 26, pp. 5475-5483, 2010/04/20 2010.

[309] D. J. Johnson, D. L. Oatley-Radcliffe, and N. Hilal, "State of the art review on membrane surface characterisation: Visualisation, verification and quantification of membrane properties," *Desalination,* vol. 434, pp. 12-36, 2018/05/15/ 2018.

[310] H. Abdul Mannan, H. Mukhtar, M. Shima Shaharun, M. Roslee Othman, and T. Murugesan, "Polysulfone/poly(ether sulfone) blended membranes for CO2 separation," *Journal of Applied Polymer Science,* vol. 133, 2016.

[311] B. Bae, B. H. Chun, and D. Kim, "Surface characterization of microporous polypropylene membranes modified by plasma treatment," *Polymer,* vol. 42, pp. 7879-7885, 2001/08/01/ 2001.

[312] D. S. Wavhal and E. R. Fisher, "Hydrophilic modification of polyethersulfone membranes by low temperature plasma-induced graft polymerization," *Journal of Membrane Science,* vol. 209, pp. 255-269, 2002/11/01/ 2002.

[313] T. Boccaccio, A. Bottino, G. Capannelli, and P. Piaggio, "Characterization of PVDF membranes by vibrational spectroscopy," *Journal of Membrane Science,* vol. 210, pp. 315-329, 2002.

[314] K. C. Khulbe, S. Gagné, A. Tabe Mohammadi, T. Matsuura, and A. M. Lamarche, "Investigation of polymer morphology of integral-asymmetric membranes by ESR and Raman spectroscopy and its comparison with homogeneous films," *Journal of Membrane Science,* vol. 98, pp. 201-208, 1995.

[315] K. C. Khulbe, T. Matsuura, S. Singh, G. Lamarche, and S. H. Noh, "Study on fouling of ultrafiltration membrane by electron spin resonance," *Journal of Membrane Science,* vol. 167, pp. 263-273, 2000.

[316] E. Dufour, S. Gassara, E. Petit, C. Pochat-Bohatier, and A. Deratani, "Quantitative PVP mapping in PVDF hollow fiber membranes by using Raman spectroscopy coupled with spectral chemiometrics analysis," *European Physical Journal: Special Topics,* vol. 224, pp. 1911-1919, 2015.

[317] R. Lamsal, S. G. Harroun, C. L. Brosseau, and G. A. Gagnon, "Use of surface enhanced Raman spectroscopy for studying fouling on nanofiltration membrane," *Separation and Purification Technology,* vol. 96, pp. 7-11, 2012.

[318] D. Rana, T. Matsuura, K. C. Khulbe, and C. Feng, "Study on the spin probe added polymeric dense membranes by13C solid-state nuclear magnetic resonance spectroscopy," *Journal of Applied Polymer Science,* vol. 99, pp. 3062-3069, 2006.

[319] A. C. Nechifor, V. Panait, L. Naftanaila, D. Batalu, and S. I. Voicu, "Symmetrically polysulfone membranes obtained by solvent evaporation using carbon nanotubes as additives. Synthesis, characterization and applications," *Digest Journal of Nanomaterials and Biostructures,* vol. 8, pp. 875-884, 2013.

[320] K. C. Khulbe, G. Chowdhury, T. Matsuura, and G. Lamarche, "Characterization of PPO [poly(phenylene oxide)] powder and membranes from it by ESR technique," *Journal of Membrane Science,* vol. 123, pp. 9-15, 1997.

[321] M. J. Ariza, J. Benavente, E. Rodríguez-Castellón, and L. Palacio, "Effect of hydration of polyamide membranes on the surface electrokinetic parameters: Surface characterization

by X-ray photoelectronic spectroscopy and atomic force microscopy," *Journal of Colloid and Interface Science,* vol. 247, pp. 149-158, 2002.

[322] X. Wei, B. Zhao, X. M. Li, Z. Wang, B. Q. He, T. He*, et al.*, "CF 4 plasma surface modification of asymmetric hydrophilic polyethersulfone membranes for direct contact membrane distillation," *Journal of Membrane Science,* vol. 407-408, pp. 164-175, 2012.

[323] P. S. Singh and V. K. Aswal, "Compacted nanoscale blocks to build skin layers of reverse osmosis and nanofiltration membranes: A revelation from small-angle neutron scattering," *Journal of Physical Chemistry C,* vol. 111, pp. 16219-16226, 2007.

[324] M. G. Buonomenna, E. Drioli, R. Bertoncello, L. Milanese, L. J. Prins, P. Scrimin*, et al.*, "Ti(IV)/trialkanolamine catalytic polymeric membranes: Preparation, characterization, and use in oxygen transfer reactions," *Journal of Catalysis,* vol. 238, pp. 221-231, 2006.

[325] B. H. Jeong, E. M. V. Hoek, Y. Yan, A. Subramani, X. Huang, G. Hurwitz*, et al.*, "Interfacial polymerization of thin film nanocomposites: A new concept for reverse osmosis membranes," *Journal of Membrane Science,* vol. 294, pp. 1-7, 2007.

[326] M. J. Rosa and M. N. De Pinho, "Membrane surface characterisation by contact angle measurements using the immersed method," *Journal of Membrane Science,* vol. 131, pp. 167-180, 1997.

[327] M. C. García-Payo, M. A. Izquierdo-Gil, and C. Fernández-Pineda, "Wetting study of hydrophobic membranes via liquid entry pressure measurements with aqueous alcohol solutions," *Journal of Colloid and Interface Science,* vol. 230, pp. 420-431, 2000.

[328] X. Chen, J. Luo, B. Qi, W. Cao, and Y. Wan, "NOM fouling behavior during ultrafiltration: Effect of membrane hydrophilicity," *Journal of Water Process Engineering,* vol. 7, pp. 1-10, 2015.

[329] D. Oatley-Radcliffe, N. Aljohani, P. Williams, and N. Hilal, "Electrokinetic Phenomena for Membrane Charge," in *Membrane Characterization*, ed: Elsevier, 2017, pp. 405-422.

[330] R. Hunter, "Zeta Potential in Colloid Science (Academic, New York, 1981)," *Google Scholar,* p. 69.

[331] D. Möckel, E. Staude, M. Dal-Cin, K. Darcovich, and M. Guiver, "Tangential flow streaming potential measurements: Hydrodynamic cell characterization and zeta potentials of

carboxylated polysulfone membranes," *Journal of Membrane Science,* vol. 145, pp. 211-222, 1998.

[332] T. E. Thomas, S. A. Aani, D. L. Oatley-Radcliffe, P. M. Williams, and N. Hilal, "Laser Doppler Electrophoresis and electro-osmotic flow mapping: A novel methodology for the determination of membrane surface zeta potential," *Journal of Membrane Science,* vol. 523, pp. 524-532, 2017.

[333] C. Bellona and J. E. Drewes, "The role of membrane surface charge and solute physico-chemical properties in the rejection of organic acids by NF membranes," *Journal of Membrane Science,* vol. 249, pp. 227-234, 2005.

[334] M. Elimelech, W. H. Chen, and J. J. Waypa, "Measuring the zeta (electrokinetic) potential of reverse osmosis membranes by a streaming potential analyzer," *Desalination,* vol. 95, pp. 269-286, 1994.

[335] A. Szymczyk, P. Fievet, M. Mullet, J. C. Reggiani, and J. Pagetti, "Study of electrokinetic properties of plate ceramic membranes by electroosmosis and streaming potential," *Desalination,* vol. 119, pp. 309-313, 1998/09/20/ 1998.

[336] P. Narong and A. E. James, "Sodium chloride rejection by a UF ceramic membrane in relation to its surface electrical properties," *Separation and Purification Technology,* vol. 49, pp. 122-129, 2006.

[337] Z. Karim, A. P. Mathew, V. Kokol, J. Wei, and M. Grahn, "High-flux affinity membranes based on cellulose nanocomposites for removal of heavy metal ions from industrial effluents," *RSC Advances,* vol. 6, pp. 20644-20653, 2016.

[338] S. Banerjee, S. Mondal, and S. De, "Gel controlling dead-end membrane filtration: Theory revisited," *Separation and Purification Technology,* vol. 99, pp. 77-85, 2012/10/08/ 2012.

[339] O. Khanal, X. Xu, N. Singh, S. J. Traylor, C. Huang, S. Ghose*, et al.*, "DNA retention on depth filters," *Journal of Membrane Science,* vol. 570-571, pp. 464-471, 2019/01/15/ 2019.

[340] K. Araus and F. Temelli, "Separation of major and minor lipid components using supercritical CO2 coupled with cross-flow reverse osmosis membrane filtration," *Journal of Membrane Science,* vol. 551, pp. 333-340, 2018/04/01/ 2018.

[341] R. R. Bhave, "Chapter 9 - Cross-Flow Filtration," in *Fermentation and Biochemical Engineering Handbook (Third Edition)*, H. C. Vogel and C. M. Todaro, Eds., ed Boston: William Andrew Publishing, 2014, pp. 149-180.

[342] L. Mir, S. L. Michaels, and V. Goel, "Crossflow microfiltration: Applications, design, and cost," *Membrane Handbook,* pp. 571-594, 1992.

[343] J. Song, W. Zou, Y. Bian, F. Su, and R. Han, "Adsorption characteristics of methylene blue by peanut husk in batch and column modes," *Desalination,* vol. 265, pp. 119-125, 2011/01/15/ 2011.

[344] H. A. Alalwan, M. N. Abbas, Z. N. Abudi, and A. H. Alminshid, "Adsorption of thallium ion (Tl+3) from aqueous solutions by rice husk in a fixed-bed column: Experiment and prediction of breakthrough curves," *Environmental Technology & Innovation,* vol. 12, pp. 1-13, 2018/11/01/ 2018.

[345] M. J. Ahmed and B. H. Hameed, "Removal of emerging pharmaceutical contaminants by adsorption in a fixed-bed column: A review," *Ecotoxicology and Environmental Safety,* vol. 149, pp. 257-266, 2018/03/01/ 2018.

[346] T. Tanaka, T. Nishimoto, K. Tsukamoto, M. Yoshida, T. Kouya, M. Taniguchi*, et al.*, "Formation of depth filter microfiltration membranes of poly(l-lactic acid) via phase separation," *Journal of Membrane Science,* vol. 396, pp. 101-109, 2012/04/01/ 2012.

[347] P. Ncube, M. Pidou, T. Stephenson, B. Jefferson, and P. Jarvis, "Consequences of pH change on wastewater depth filtration using a multimedia filter," *Water Research,* vol. 128, pp. 111-119, 2018/01/01/ 2018.

[348] A. W. Z. Chew and A. W.-K. Law, "DRFM hybrid model to optimize energy performance of pre-treatment depth filters in desalination facilities," *Applied Energy,* vol. 220, pp. 576-597, 2018/06/15/ 2018.

[349] E. Sikorska, J. M. Gac, and L. Gradoń, "Performance of a depth fibrous filter at particulate loading conditions. Description of temporary and local phenomena with structure development," *Chemical Engineering Research and Design,* vol. 132, pp. 743-750, 2018/04/01/ 2018.

CHAPTER 2

ENGINEERING CELLULOSE FIBRE INORGANIC COMPOSITES FOR DEPTH FILTRATION AND ADSORPTION

THIS PAGE HAS BEEN INTENTIONALLY LEFT BLANK

PREFACE

Although depth filters have been studied in the literature, it is not clear how we can improve the performance of depth filters further. In particular, the contribution of each component in depth filters must be investigated to identify the role of each one of them much clearly. This is because they can be delivering different functionalities to the filters with their own unique properties, resulting in an enhanced filter performance. Therefore, this chapter explores the preparation of depth filters comprised of cellulose fibres, perlite and a charged wet strength polymer, polyamideamine-epichlorohydrin (PAE). Following filter preparation, the structural properties were obtained by mercury porosimetry and scanning electron microscopy. Separation by surface interactions and size-exclusion was investigated with a dead-end stirred cell. The effect of perlite and PAE as well as increased fibrillation in cellulose fibres was investigated on these properties.

This chapter follows the first objective.

THIS PAGE HAS BEEN INTENTIONALLY LEFT BLANK

CHAPTER 2 ENGINEERING CELLULOSE FIBRE INORGANIC COMPOSITES FOR DEPTH FILTRATION AND ADSORPTION

ENGINEERING CELLULOSE FIBRE INORGANIC COMPOSITES FOR DEPTH FILTRATION AND ADSORPTION

Aysu Onur[1], Aaron Ng[2], Gil Garnier[1*], Warren Batchelor[1*]

[1] Bioresource Processing Research Institute of Australia (BioPRIA), Chemical Engineering Department, Monash University, Clayton, Australia

[2] 3M Australia, Sydney, Australia

*** Corresponding authors at:** Bioresource Processing Research Institute of Australia (BioPRIA), Chemical Engineering Department, Monash University, 3800

Email addresses: gil.garnier@monash.edu (G. Garnier), warren.batchelor@monash.edu (W. Batchelor).

2.1. ABSTRACT

Depth type composite filters are porous materials heavily loaded with adsorbents. They are intended to remove contaminants from liquids by combining mechanical entrapment and adsorption. There is still a need for developing high performance filters by controlling the internal structure at micro and nano level. In this study, highly fibrillated cellulose fibres with increased surface area was used as partial substitute for the fibre matrix to tailor the filter structure as well as the adsorption and filtration performance. Polyamideamine-epichlorohydrin (PAE) was added both to adjust the charge of medium and provide wet strength. Filters were fabricated by embedding perlite particles into the cellulose fibre matrix by papermaking technique. The structure of composites was characterised for pore size distribution and surface morphology. Adsorption and filtration characteristics were quantified using two model dyes and silicon dioxide particles. Adsorption was found to be electrostatically controlled and dependent on the charge of the dye molecules and the filter medium. The addition of nanofibrillated cellulose (NFC) doubled the removal of a cationic dye by increasing the surface area and the available negative charges; it however decreased the removal of an anionic dye by 75%. PAE addition decreased the adsorption of the cationic methylene blue dye, while increasing the adsorption of the anionic metanil yellow

dye. Rejection by filtration of 1 µm particles was over 90% for all filters. This study demonstrates that NFC combined with a cationic wet strength polyelectrolyte can be used to tailor the filter structure and properties.

2.2. KEYWORDS

Depth filter; adsorption; filtration; nanofibrillated cellulose; composite

2.3. INTRODUCTION

Liquid filtration is used in a vast range of applications such as water treatment, beverage and juice filtration, pharmaceutical and industrial chemical filtration as well as medical purposes such as blood filtration [1]. Membrane technology plays an important role in liquid filtration applications and polymeric membranes made of polyamide, polysulfone and polyimide are widely used [2] due to their mechanical and chemical resistances. However, these membranes suffer environmental drawbacks as they are petroleum based, non-biodegradable and large quantities of solvents and chemicals [3] are required for their production. These membranes perform separation only by filtration/size exclusion and remain inefficient for the separation of small charged molecules. In addition, membrane technology mainly relies on separation at the surface which is very susceptible to fouling [4]. There is a need for environmentally benign products with improved functionalities that can be reprocessed, recycled or will biodegrade at the end of their life. Depth type composites using cellulose fibres provide a solution. Depth filters are porous materials heavily loaded with adsorbents. These filters retain molecules not only on the surface but also within the media [5]. They can remove contaminants from liquids by combining mechanical entrapment with adsorption, resulting in a higher removal capacity.

Nanofibrillated cellulose (NFC) has widely been explored as an alternative polymer in membranes/filters due to unique properties such as high surface area, high strength, wettability, ease of chemical functionalization and low environmental impact [6]. Cellulose is the most abundant polymer and can be used in the form of fibres and derivatives in a vast range of products [7-10]. NFC technology has significantly progressed in the last decade; the applications of NFC were reviewed by Salas *et al.* [11]. The potential of NFC in filtration applications and its excellent adsorption

capacity due to its high surface area-to-volume ratio have long been identified [12-18]. Even though NFC performance for water treatment was demonstrated, most studies have focused on functionalized NFC fibres with a variety of chemistries, improving pollutants binding efficiency [13, 19, 20]. This functionalization often requires expensive and toxic chemical treatments and can be difficult to scale up, limiting industrial applications. Also, regulations for some applications, such as food and beverage, often restrict filters' chemical modification. The filters should be as chemical modification free as possible.

Some studies have quantified adsorption with NFC based adsorbents using static experiments [13, 16, 18]; however, very few have reported particle rejection with dynamic experiments [14, 15]. This is unfortunate as industry typically operates filters in a continuous mode instead of in a batch mode. NFC composites with nano-ranged pore sizes have been explored for separation applications [21]. Keshavarzi *et al.* [22] investigated odour elimination with NFC-zeolite composites in separation processes. However, limited number of studies have quantified NFC composite performance in liquid filtration/adsorption. The following section gives an overview of dynamic studies of liquid filtration or adsorption with NFC composites.

Varanasi *et al.* [23] reported the preparation of NFC composite membranes and showed their potential in ultrafiltration. Silica nanoparticles were used to control the pore size of the nanofibre network. The pure NFC membranes had high flux but the rejection of polyethylene glycol (PEG) was low because of the large pores. Composite membranes showed better rejection performance as the pore size was controlled by the silica nanoparticles. Control of composite pore size by nano particles addition is a promising avenue in ultrafiltration. However, this study focused on molecular weight cut off (MWCO) and ignored composite adsorption capability.

Karim *et al.* [24] investigated cellulose nano composites with functional cellulose nanocrystals added on a supporting layer of micro-sized cellulose fibres for adsorbing heavy metal ions from waste water. Nanocrystals promoted adsorption and the membranes showed excellent removal of metal ions. However, particle filtration was ignored, and the cellulose nanocrystals used in membrane preparation were isolated from a cellulose sludge using sulphuric acid hydrolysis. This a tedious process requiring chemical treatment.

There is a lack of fundamental separation understanding in terms of combining adsorption and size exclusion for NFC composites under dynamic conditions. However, separation combining both adsorption and size exclusion is needed for some applications. In beer and wine filtration, for instance, it is necessary to remove bacteria and yeast particles to eliminate haziness [25] as well as removing some ionic compounds to avoid bitter taste [26-28].

This study aims developing microporous filters with mechanically-treated NFC fibres and perlite, a low-cost inorganic adsorbent. Composite filters combining adsorption and filtration are prepared with a simple and scalable papermaking process. The performance of NFC as a partial substitute for the fibre matrix of the filters is studied. Polyamideamine-epichlorohydrin (PAE), a cationic and cross-linking polyelectrolyte, is selected to provide wet strength and control the charge of the medium; PAE is food grade when fully crosslinked. Filtration and adsorption performances are evaluated dynamically with two model dyes and silicon dioxide particles and analysed in the context of food and pharmaceutical applications.

2.4. MATERIALS AND METHODS

2.4.1. Materials

The cellulose fibres used for the composites are unrefined northern softwood NIST RM 8495 bleached kraft pulp (with a typical fibre length of around 2.5-4 mm and 30 µm wide) and bleached radiata pine softwood kraft pulp refined to 400 Canadian standard freeness (CSF) in a disk refiner. NFC fibres were prepared by processing refined pulp in a GEA Niro Soavi homogenizer at 800 bar at both 1 pass and 3 passes.

Expanded perlite supplied by Dicalite Minerals Corp was used as an inorganic adsorbent. Commercial PAE provided from Nopcobond Paper Technology Pty Ltd was used as wet strength resin.

Methylene blue (MB) and metanil yellow (MY) dyes supplied from Sigma Aldrich were used to test adsorption. 1 µm monodisperse silicon dioxide particles from Sigma Aldrich were used to test filtration capability of the composites.

2.4.2. Methods

2.4.2.1. Preparation of filters

Prior to sheet preparation, dry pulp was soaked in 2 L deionised water overnight and then disintegrated by a model MKIIIC, Messmer Instruments Ltd for 75,000 revolutions. Following disintegration, sheet suspensions were prepared by adding perlite suspensions to the pulp suspensions. PAE (0.22% w/v) was then added at a rate of 100 mg/g fibre and the mixtures were hand mixed before sheet making. 5 different composites and a control cellulose sheet were prepared; the fibre component was varied as described with only 1/3 of the cellulose fibre component. Composites were labelled based on the fibre composition and presence of perlite and polymer as follow:

1) **Refined** -100% Fibre (1/3 refined pulp + 2/3 unrefined pulp)

2) **Refined/Per/PAE** -30% Fibre (1/3 refined pulp + 2/3 unrefined pulp) + 70% Perlite + 120 mg PAE

3) **Unrefined/Per/PAE** – 30% Fibre (3/3 unrefined pulp) + 70% Perlite + 120 mg PAE

4) **Homogenized(1pass)/Per/PAE**–

30% Fibre (1/3 homogenized (1 pass) + 2/3 unrefined pulp) + 70% Perlite + 120 mg PAE

5) **Homogenized(3pass)/Per/PAE**–

30% Fibre (1/3 homogenized (3 pass) + 2/3 unrefined pulp) + 70% Perlite + 120 mg PAE

6) **Homogenized(3pass)/Per** – 30% Fibre (1/3 homogenized (3 pass) + 2/3 unrefined pulp) +

70% Perlite

The cellulose component was always kept constant at 60 grams per square metre (gsm). For the composites with perlite, the target total gsm was 200 gsm- assuming full retention.

A British hand sheet maker was used to form the composite filters. A wet strengthened qualitative filter paper was deposited over the 150 micron size mesh and the suspension was poured into the chamber and then drained through the filter paper to form the sheets uniformly. After sheet formation, the wet sheet was separated from the mesh, placed between dry blotting papers and pressed under 345 kPa for 5 minutes. The composites containing PAE were heated 30 minutes at

105°C for curing and then air-dried in a humidity room (23˚C, 50% relative humidity) overnight. The sheets without PAE were air-dried in the humidity room for at least 24 hours without any oven treatment.

2.4.2.2. Mercury porosimetry

Composite pore size distribution was measured with a Micromeritics' AutoPore IV 9500 series. This technique quantifies a material's pore size distribution and porosity by applying increasing pressures (up to 60,000 psia) to a sample immersed in mercury and recording the volume of mercury intruded into pores. Samples were cut into approximately 5 mm × 5 mm small pieces and degassed for at least two days prior to characterization. A penetrometer with 0.412 mL stem volume was used to carry out the measurements. After degassing, approximately 0.1 g of sample was placed in the penetrometer and the analysis conducted. The volume of mercury intruded into pores is converted to equivalent pore sizes using the instrument software [29].

2.4.2.3. Scanning electron microscopy

A FEI Nova NanoSEM 450 FEG SEM and a FEI Magellan 400 FEG SEM were used to characterize surface and bulk morphology of composites and estimate fibre diameter. Samples were mounted onto a metal substrate using carbon tape and coated with a thin layer of Iridium. Secondary electron images of composites were captured. 2kV of accelerating voltage was applied for magnification up to 100,000. For fibre diameter measurement, silicon chips were used to cast the fibres and iridium coating was applied.

2.4.2.4. Adsorption and filtration

A Merck Millipore, model UFSC40001 dead-end stirred cell was used for adsorption and filtration experiments. The stirred cell is pressure driven with a 0.00418 m^2 effective membrane area and 400 mL working volume. Samples were placed on the membrane holder at the bottom and the cell body was filled with the prepared solution. The system was closed and pressurized by a compressed air gas cylinder. Filtrate was passed through a quartz micro flow cell with 10 mm optical path length sitting in an ultraviolet-visible (UV-Vis) absorption spectrometer and transferred to a beaker on a balance. Both instantaneous absorbance and weight of the filtrate were measured every 10 seconds. The schematic system is illustrated in Figure 1.

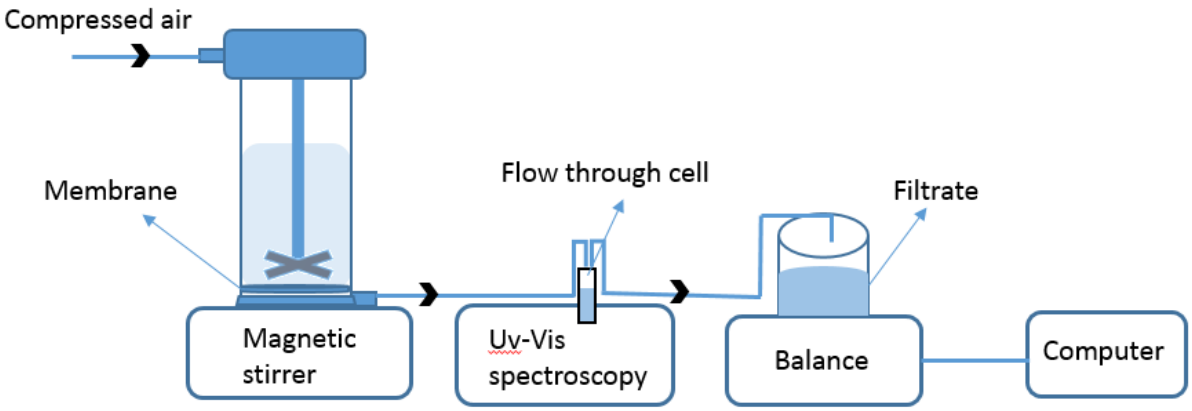

Figure 1: Schematic illustration of the stirred cell experimental setup.

Preliminary adsorption experiments, performed at pressures ranging from 1 to 3 bar, identified the optimum inlet pressure as 1.5 bar; data is provided in the supplementary section (Figure S1). Adsorption results were determined at 1.5 bar with 400 mL of 5 ppm dye solution. 5 ppm dye solutions were prepared by dissolving 5 mg of dye in 1 litre deionized water. Breakthrough curves were obtained by plotting the instantaneous concentration (normalized by the initial concentration) as a function of time. The calibration curves are provided in supplementary information (SI) (Figure S2). Dye removal was measured from the concentration of initial feed solution and filtrate:

$$Dye\ removal\ (\%) = \frac{\text{Initial dye concentration} - \text{filtrate dye concentration}}{\text{Initial dye concentration}} \times 100 \quad (1)$$

Adsorption capacity of each filter was calculated with the following equation. The integral was calculated from the area over the curve by trapeze method. Methylene blue and metanil yellow adsorption capacities of the filters were given in SI (Table SI and SII).

$$q = \frac{C_F \times \dot{Q}}{1000 \times m_s} \int_0^{t_{end}} \left(1 - \frac{C_{out}}{C_F}\right) dt \quad (2)$$

Where:

q: Capacity of the adsorbent (mg/g)

C_{out}: Concentration of MB in the filtrate (mg/g)

C_F: Concentration of MB in the feed (mg/g)

$\dot{Q}$: Volumetric flow rate (cm^3/s)

t_{end}: Time (s)

m_s: Weight of adsorbent (g)

Filtration efficiency was measured with a 0.05wt % suspension of 1 µm silicon dioxide particles. Experiments were also conducted at 1.5 bar and concentration of silicon dioxide in suspension was measured before and after filtration by UV-Vis spectroscopy to calculate filter rejection:

$$Rejection\ (\%) = \frac{\text{Initial feed concentration} - \text{Filtrate concentration}}{\text{Initial feed concentration}} \times 100 \quad (3)$$

Flux was calculated from the time to filter all of the suspension as:

$$FLUX\ (LMH) = \frac{Volume\ of\ filtrate\ (L)}{area(\text{m2}) \times time\ (h)} \quad (4)$$

Water was passed through the filters to remove any contaminants prior to adsorption and filtration experiments.

2.5. RESULTS

2.5.1. Filter structure

2.5.1.1. Fibre size distribution

Fibre diameter size distribution of refined and homogenized pulps was measured from SEM images. High magnification images (Figure 2) from completely different points of samples were acquired with at least 100 individual fibres in total and the diameter of every individual fibre in standard pictures was measured by image J, image processing software. The effect of increased fibrillation by mechanical treatment is seen on Figure 2a-c. Low magnification images show that large fibres are still present even after homogenization (SI, Figure S4). Histograms present fibre diameter size distributions estimated from the high magnification images in Figure 3.

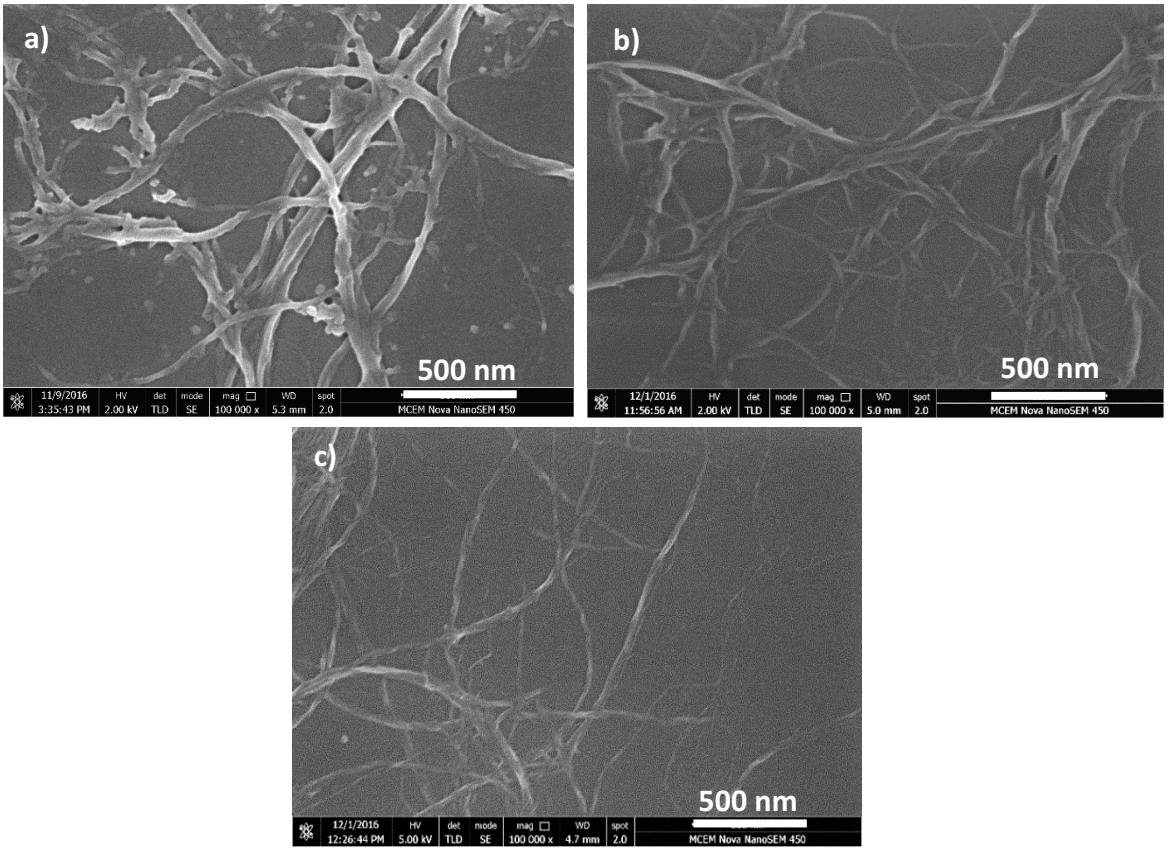

Figure 2: High magnification SEM images of: **a)** Refined pulp, **b)** Homogenized pulp by 1 pass and **c)** Homogenized pulp by 3 passes.

The majority of the refined fibres in the high magnification images have a diameter centred between 45 nm and 50 nm and the diameter is decreasing with the intensity of homogenization treatment. The average fibre diameters measured in these images fall to 25 nm to 40 nm after 1 pass and 20nm-25nm after 3 passes homogenization.

Additionally, particle size distribution of perlite particles was measured by the same technique and can be found in SI (Figure S5).

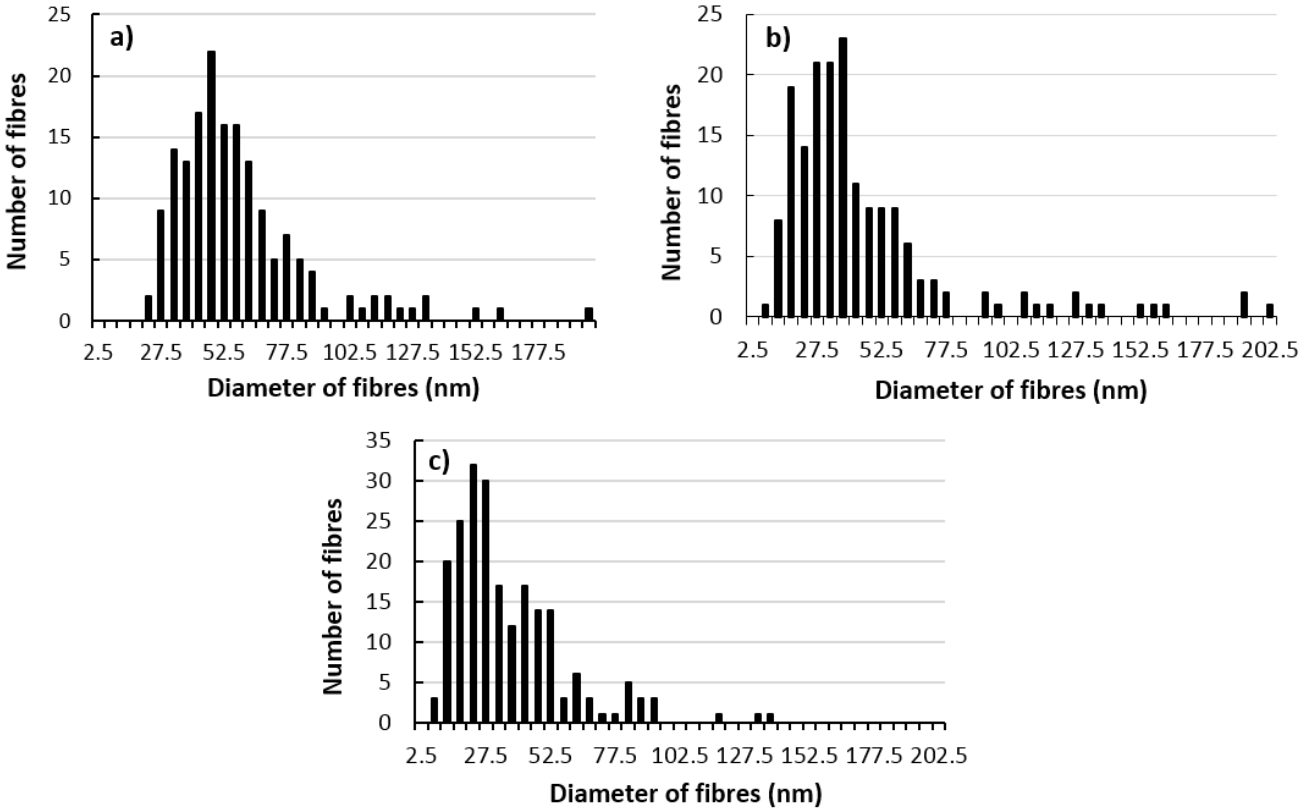

Figure 3: Fibre size distribution of **a)** Refined pulp **b)** Homogenized pulp by 1 pass **c)** Homogenized pulp by 3 passes.

2.5.1.2. Pore size distribution

Filter pore size distribution was measured by mercury porosimetry (Figure 4). The distribution of pore size ranges from 1 to 3 µm. Substitution of fibre composition with homogenized pulp resulted in smaller pore sizes.

The cellulose sheet (*Refined*) has a smaller pore size distribution compared to composite combining refined pulp, perlite and PAE (*Refined/Per/PAE*) even though the fibre content is identical. Perlite addition increased the composite pore size by adsorbing between fibres. The peak intensity is also significantly smaller which reflects that the number of pores at a specific pore size is lower.

The slight difference between pore sizes of composites *Homogenized(3pass)/Per* and *Homogenized(3pass)/Per/PAE* demonstrates the effect of PAE addition. The sample with PAE (*Homogenized(3pass)/Per/PAE*) has a slightly smaller pore size.

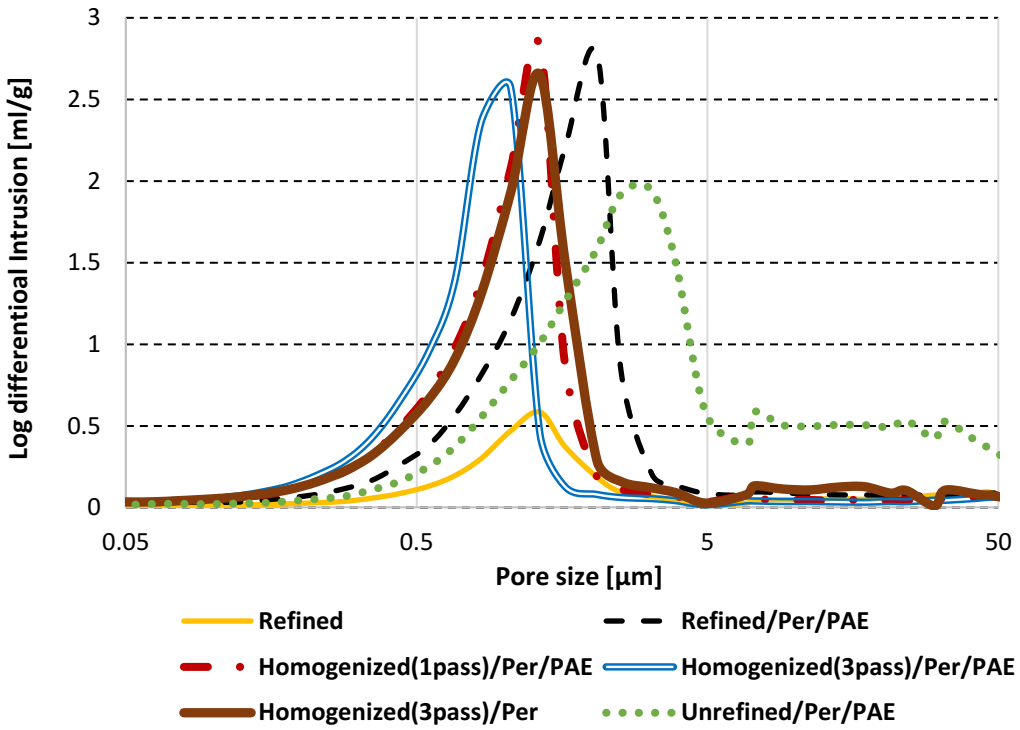

Figure 4: Pore size distributions of filters measured by mercury porosimetry; effect of homogenization intensity and addition of perlite and PAE.

2.5.1.3. Surface morphology

SEM images of filters made with different pulps homogenized to different intensities are shown in Figure 5. Connectivity between fibres and perlite particles increases with the entangled network created by NFC addition (Figure 5a-d). This connectivity results in a smoother, more closed surface and a decrease in composite porosity.

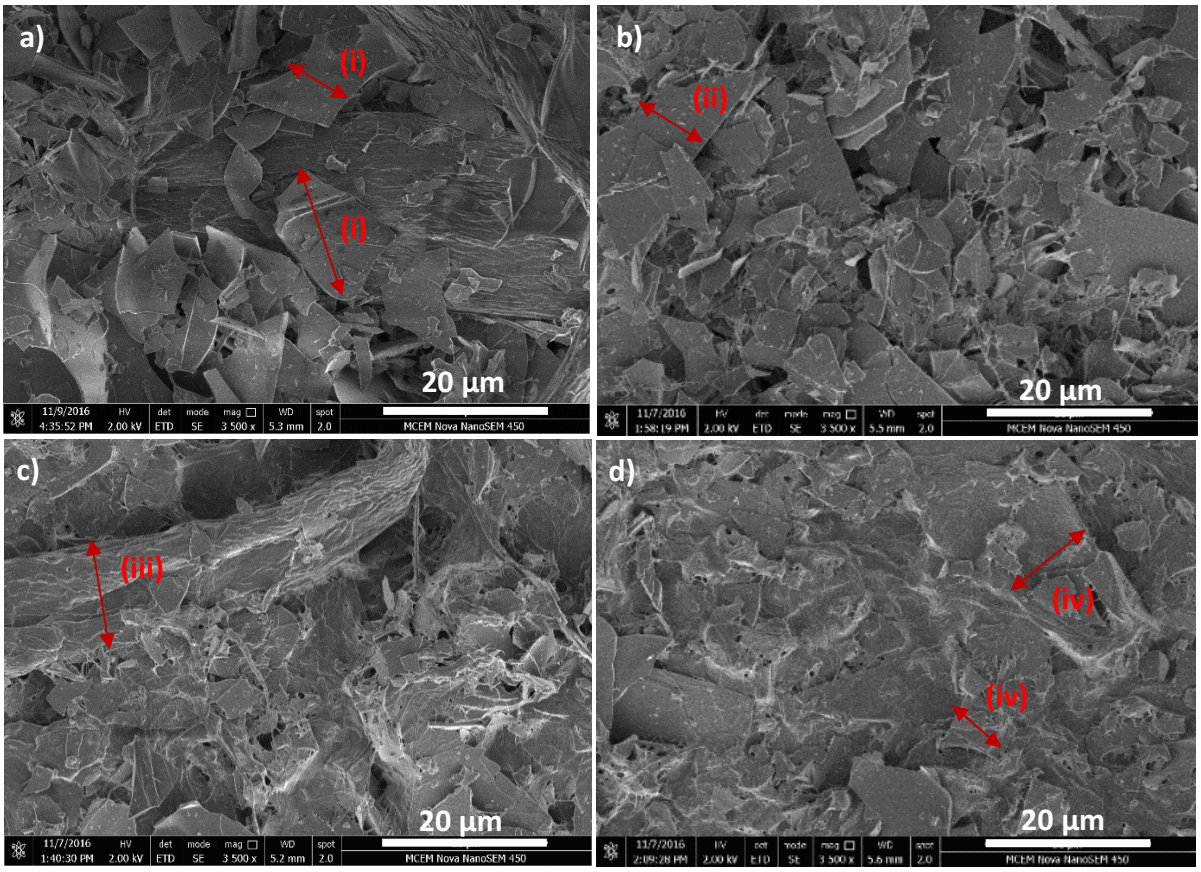

Figure 5: SEM images of composites: **a)** Unrefined/Per/PAE, **b)** Refined/Per/PAE, **c)** Homogenized(1pass)/Per/PAE and **d)** Homogenized(3pass)/Per/PAE.

The arrows in Figure 5 highlight the changes in surface morphology. Arrows (i) and (ii) show the perlite particles with sharp edges which became blurred with homogenized pulp addition in arrows (iv). Addition of NFC smooths the edges and binds the perlite particles. Arrow (iii) shows the presence of some remaining large fibres in sample *Homogenized(1pass)/Per/PAE*.

2.5.2. Adsorption and filtration

2.5.2.1. Adsorption with breakthrough curves

The breakthrough curves measured at 1.5 bar for all samples with MY and MB dye solutions are shown in Figure 6a and 6b, respectively. Breakthrough curves present the normalized concentrations as a function of time or effluent volume. They usually show a characteristic S shape with varying degrees of steepness. All outlet concentrations are presented normalized with the inlet

concentration: C/Co ranges from 0, for full adsorption, to 1, for no adsorption. Initially, the dye molecules are adsorbed very effectively on the fresh adsorbent and the outlet concentration equals zero. As the filters start to saturate, the outlet concentration gradually approaches the inlet concentration and the normalized concentration (C/Co) increases to eventually level-off at one.

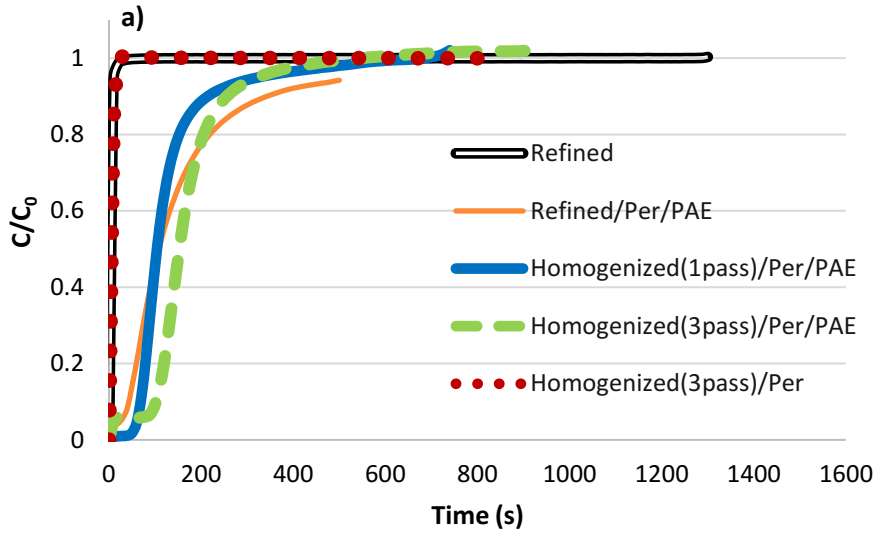

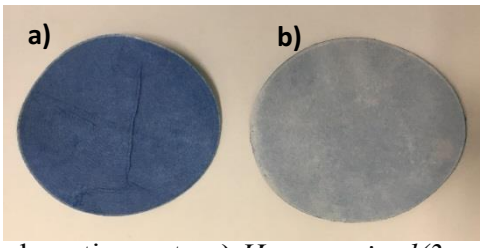

5 ppm MB adsorption onto **a)** *Homogenized(3pass)/Per* and **b)** *Refined/Per/PAE*

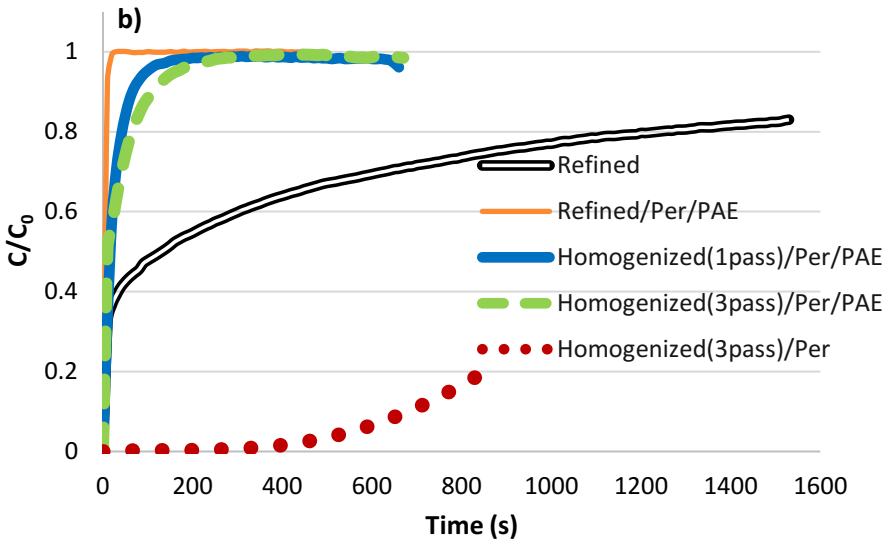

Figure 6: Adsorption breakthrough curves for **a)** Metanil yellow and **b)** Methylene blue at 1.5 bar for filters of different charges and extent of mechanical treatment.

The two oppositely charged dyes showed two opposite adsorption behaviours onto the composites (Figure 6a and 6b). Basically, no adsorption was recorded for the cationic MY dye onto cellulose sheet (*Refined*) or composite made with homogenized fibres (3 passes) with no PAE (*Homogenized(3pass)/Per*) (Figure 6a). By contrast, the cationic MB showed some affinity and retention onto these same composites (Figure 6b). Here, *Homogenized(3pass)/Per* presents the straightest breakthrough curve which indicates very strong attractive forces with MB- in the absence of positively charged PAE. The very intense blue colour of the saturated filter after adsorption (Figure 6b) indicates more MB adsorbed onto the composite with highly fibrillated pulp content (*Homogenized(3pass)/Per*).

Adsorption occurs slightly differently for composites made only with refined pulp and those made with two different homogenized pulps treated at different intensities. As fibre fibrillation increases (homogenization or more passes in homogenization), composites increasingly repel the anionic dye-metanil yellow and attract the cationic dye (MB). From *Refined/Per/PAE* through *Homogenized(3pass)/Per/PAE* sample, attraction with MB (Figure 6b) and repulsion with MY (Figure 6a) increases with the fibrillation and increased surface area.

Flux and total dye removal were measured (Figure 7). A maximum of 94% MB removal was achieved with composites made with highly fibrillated cellulose but without PAE (*Homogenized(3pass)/Per*); the maximum removal of MY was around 28% for the composites with refined fibres and PAE (*Refined/Per/PAE*). Flux remained identical for both dyes for all composites. Flux remarkably decreases with addition of homogenized pulps. The flow rates for each sample and both dyes are reported in SI (Figure S3a-d).

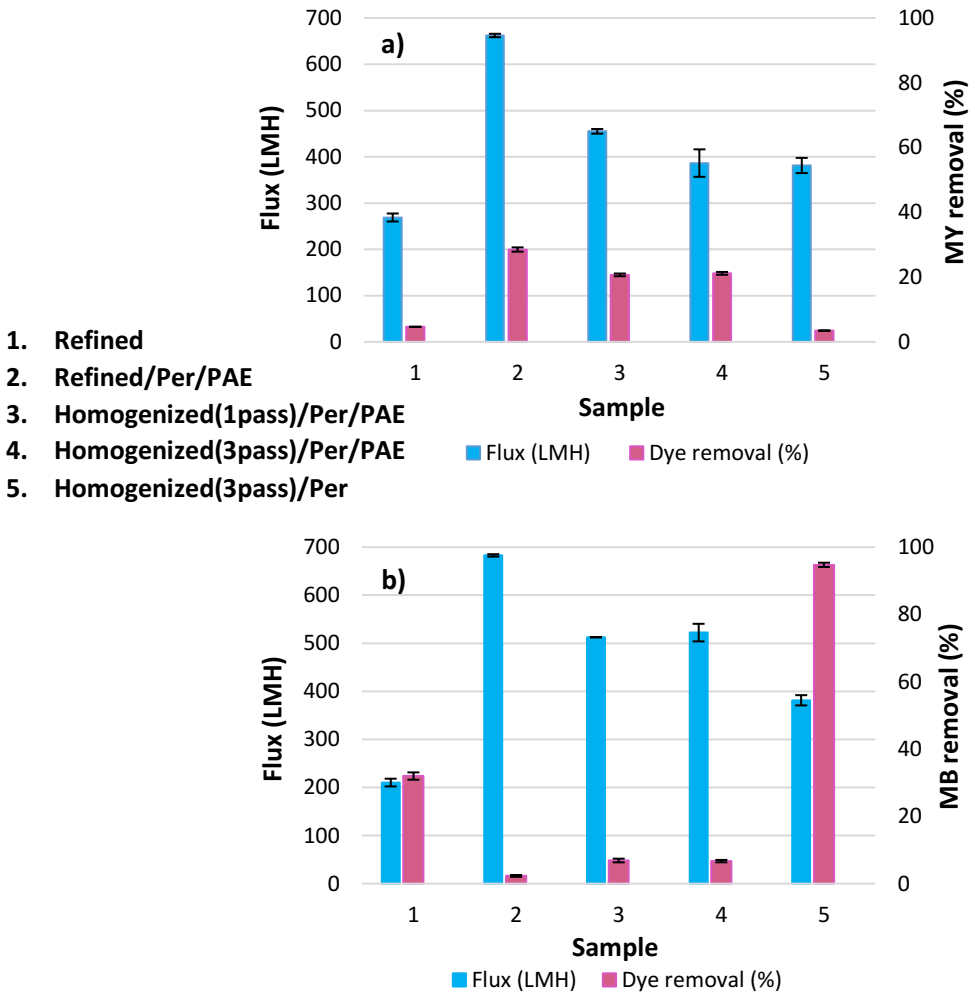

Figure 7: Flux and total dye removal (%) of samples with **a)** Metanil yellow and **b)** Methylene blue dye solutions.

2.5.2.2. Filtration

The rejection rate of suspensions with 1 µm SiO_2 particles was determined for the four different filters at an inlet pressure of 1.5 bar. 1 µm particles were selected as model bacteria (1 µm and

bigger) to be removed from food streams such as beer, wine or juice [27]. The effect of homogenization, filter medium charge, inlet pressure and suspension pH on filtration performance was measured. The rejection rate and flux are presented at pHs of 5.8 and 7.2 in Figure 8. The effect of pH was tested as it is an important variable in applications such as food and pharmaceutical; pH can affect cellulosic fibre pore structure and porosity through swelling and modifying bond strength. Filters have more than 90% particle rejection rate at both pH; pH had no effect on rejection. Charge of filter medium and inlet pressure also did not affect filtration efficiency. Rejection is around 99% for the negatively charged cellulose composites made with homogenized fibres (3 pass) (*Homogenized(3pass)/Per)*. The same rejection rate of around 99% was measured for the composites treated with PAE (*Homogenized(3pass)/Per/PAE*) at 2 different pressures (1 and 2 bar) (Figure 8a).

(Figure 8b) Flux decreased remarkably after only 1/3 of the fibre fraction substituted with homogenized fibres. Filtration flux decreased by 30% to 70% compared to dye solution adsorption flux.

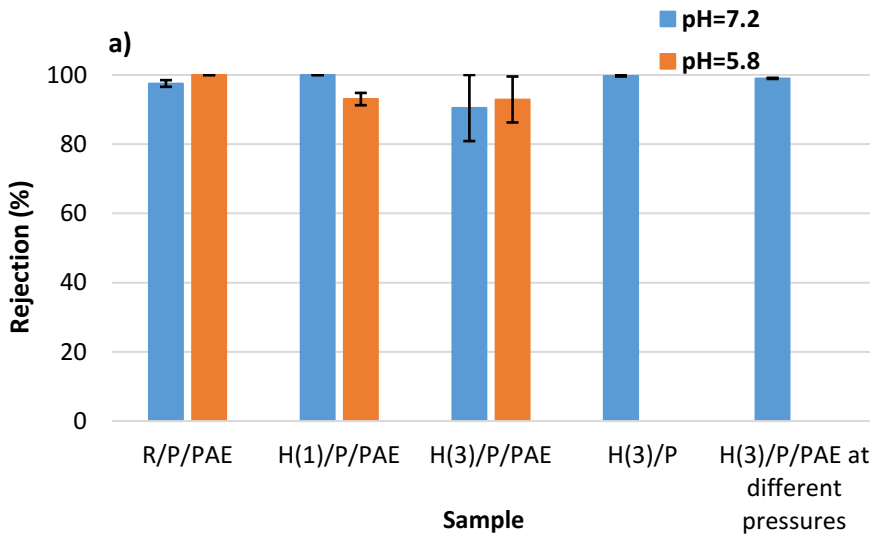

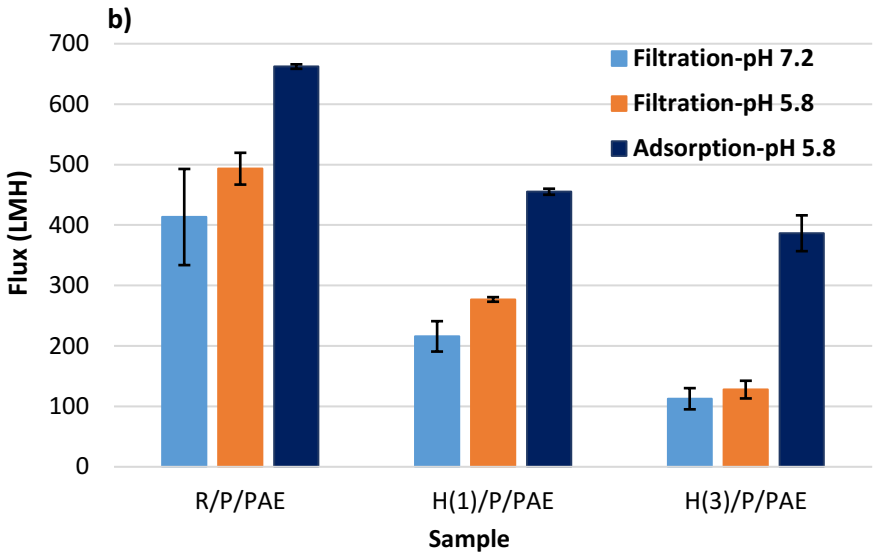

Figure 8: **a)** SiO_2 particle rejection rate (%) of Refined/Per/PAE, Homogenized(1pass)/Per/PAE, Homogenized(3pass)/Per/PAE, Homogenized(3pass)/Per at 1.5 bar and Homogenized (3pass)/Per/PAE at 1 and 2 bar **b)** Adsorption and filtration flux of Refined/Per/PAE, Homogenized(1pass)/Per/PAE, Homogenized(3pass)/Per/PAE at 1.5 bar.

2.6. DISCUSSION

The adsorption of dye onto the perlite-cellulose composites is electrostatically controlled. The major effect of homogenization on adsorption is to increase surface area which also increases the surface and density of accessible charges. An increase in negatively charged sites contributes either to stronger repulsive or attractive forces between filter medium and dye depending on the system. The effect of surface area is revealed by the breakthrough curves of composites made with refined and homogenized pulps. Composites with refined pulp (*Refined/Per/PAE*) have less repulsive forces with negatively charged dye (MY, Figure 6a) and less attractive forces with the cationic dye (MB, Figure 6b) compared to other PAE treated composites. As homogenization is applied and the extent of homogenization increases, increasing accessible negative charges on surface remarkably changes the adsorption behaviour of dye molecules onto the composites.

Adding the cationic PAE both modifies the filter charge which changes its adsorption capacity and improves the composite wet strength by cross linking cellulose fibres. For the cationic dye (MB), the

electrostatic interactions, maximized by the elimination of PAE, yield higher adsorption capacity. In contrast, PAE triggers higher adsorption of anionic dye (MY) onto the composites. The addition of negatively charged perlite particles also changes the adsorption behaviour significantly; this is similar to the effect of mechanical treatment of fibres and cationic polymer. The remarkably improved breakthrough curve of *Homogenized(3pass)/Per* (Figure 6b) is attributed to perlite acting as an excellent filter aid [30].

Nanofibrillated cellulose addition, achieved by fiberizing a fraction of cellulose fibres (1/3), did not affect the filtration performance significantly. (Figure 8a). The slight decrease in SiO_2 rejection rate by composites made of highly homogenized fibres (*Homogenized(3pass)/Per/PAE)* at 1.5 bar) is within experimental error. Increasing fibrillation through mechanical treatment intensity did not increase filtration performance.

Homogenization on refined pulp creates a dense and highly fibrillated NFC network with a decrease in fibre diameters. The filters made with a small fraction of nanofibres have a more compact and connected structure. The pore size distribution changed remarkably by only substituting 1/3 of the pulp by homogenized fibres. This is due to the web like entangled structure of NFC. The more fibrillated the fibres are, the denser the structure is and the less and the smaller the voids developed between fibres are. Composite porosity and pore size distribution can be controlled by modifying fibre diameters. As the homogenization forms smaller pores with denser fibre packing, liquid flux through the composites filters decreases with homogenized pulp addition.

The presence of inorganic particle in the filters also affects porosity and pore size distribution. Pure cellulose sheet has the lowest flux value (Figure 4a and b). This is due to two phenomena: low porosity as there is no settlement of particles between fibres; decreasing flow rate in time as the fibres compress under pressure (Figure S3a-d). This compressibility of fibres is well known [31] and leads to poor flux. High loading of inorganic particles prevents this compression so the composites retain high flow rates with very slight change over time.

There is only a weak relation between flux and dye removal capacity – as measured with both dyes (Figure 7). While less adsorption generally occurs at high fluxes, adsorption is mostly affected by the charge of the filter medium and the solute molecules (Figure7a), regardless of flux. Similarly, there

was no correlation between rejection rate of 1 µm particles and flux. *Homogenized(3pass)/Per/PAE* successfully removed 99% of the particles at both 1 and 2 bar.

The high filtration rejection of 1 µm particles achieved by the nanofibrillated cellulose/perlite depth composites is important to the pharmaceutical, food and beverage industry. This brings a new perspective in cold pasteurization to remove microorganisms ranging from 1 to 2 µm [26] and remove ionic compounds [32] (acids and phenolic compounds) without heat treatment which affects taste or denaturing active ingredients. The concept is to rely on the inorganic particles for the selective adsorption of organic molecules, PAE treatment for the retention of colloids- based on charge and filtration for the pasteurization. Nanofibrillated cellulose-inorganic depth composites can easily be engineered for specific liquid stream purification.

2.7. CONCLUSION

Cellulose fibre-perlite composites were prepared using a papermaking technique for liquid filtration and adsorption applications. Perlite content was maintained at 70wt % and the fibre composition was varied with partial substitution of pulp homogenized to different intensities; this was to control fibre structure by increased bonding area and decreasing porosity. A well-known wet strength agent, polyamideamine-epichlorohydrin (PAE), was used for two purposes; first to provide wet strength; second, to control charge and capacity of filter medium. Additionally, PAE acts as a retention aid by holding small particles on the surface of cellulose during papermaking process. Two oppositely charged dyes were investigated as models to characterize the adsorption behaviour. The adsorption of dye is electrokinetically controlled and selective adsorption can be achieved by engineering the attractive and repulsive forces. The presence of NFC increased the surface area and also the amount of negative charges accessible in the medium. Increase in negatively charged sites contributed to attractive/repulsive forces depending on the type of dye. Homogenized pulp also yielded smaller pore sizes which decreased flux. PAE addition controls and can reverse the charge of filters which substantially affected adsorption performance, but it had no effect on filtration efficiency. The composites were efficient in filtration with 90% rejection rate of 1 µm particles. The high filtration capability of the composites at high flux is promising for cold pasteurization in which bacteria (1 µm) are removed at higher than 99% efficiency. Nanofibrillated cellulose-depth composites provide new

purification opportunities in pharmaceutical and food product stream by combining adsorption and filtration to remove interfering elements and colloids.

2.8. ACKNOWLEDGEMENTS

This work was supported by 3M Australia. The authors also acknowledge the Monash Centre for electron microscopy for the facilities used.

2.9. REFERENCES

[1] I. M. Hutten, "Chapter 7 - Liquid Filter Applications," in *Handbook of Nonwoven Filter Media (Second Edition)*, ed Oxford: Butterworth-Heinemann, 2016, pp. 409-450.

[2] M. F. Jimenez-Solomon, P. Gorgojo, M. Munoz-Ibanez, and A. G. Livingston, "Beneath the surface: Influence of supports on thin film composite membranes by interfacial polymerization for organic solvent nanofiltration," *Journal of Membrane Science,* vol. 448, pp. 102-113, 12/15/ 2013.

[3] S. Ramaswamy, A. R. Greenberg, and W. B. Krantz, "Fabrication of poly (ECTFE) membranes via thermally induced phase separation," *Journal of Membrane Science,* vol. 210, pp. 175-180, 12/1/ 2002.

[4] S. Jiang, Y. Li, and B. P. Ladewig, "A review of reverse osmosis membrane fouling and control strategies," *Science of The Total Environment,* vol. 595, pp. 567-583, 10/1/ 2017.

[5] A. Mukhopadhyay, "8 - Composite nonwovens in filters: applications," in *Composite Non-Woven Materials*, ed: Woodhead Publishing, 2014, pp. 164-210.

[6] D. Klemm, F. Kramer, S. Moritz, T. Lindström, M. Ankerfors, D. Gray*, et al.*, "Nanocelluloses: A New Family of Nature-Based Materials," *Angewandte Chemie International Edition,* vol. 50, pp. 5438-5466, 2011.

[7] R. Andrade, O. Skurtys, F. Osorio, R. Zuluaga, P. Gañán, and C. Castro, "Wettability of gelatin coating formulations containing cellulose nanofibers on banana and eggplant epicarps," *LWT - Food Science and Technology,* vol. 58, pp. 158-165, 9// 2014.

[8] K. Dimic-Misic, C. Ridgway, T. Maloney, J. Paltakari, and P. Gane, "Influence on Pore Structure of Micro/Nanofibrillar Cellulose in Pigmented Coating Formulations," *Transport in Porous Media,* vol. 103, pp. 155-179, 2014.

[9] J. Kim, G. Montero, Y. Habibi, J. P. Hinestroza, J. Genzer, D. S. Argyropoulos*, et al.*, "Dispersion of cellulose crystallites by nonionic surfactants in a hydrophobic polymer matrix," *Polymer Engineering & Science,* vol. 49, pp. 2054-2061, 2009.

[10] G. Rodionova, M. Lenes, Ø. Eriksen, and Ø. Gregersen, "Surface chemical modification of microfibrillated cellulose: improvement of barrier properties for packaging applications," *Cellulose,* vol. 18, pp. 127-134, 2011.

[11] C. Salas, T. Nypelö, C. Rodriguez-Abreu, C. Carrillo, and O. J. Rojas, "Nanocellulose properties and applications in colloids and interfaces," *Current Opinion in Colloid & Interface Science,* vol. 19, pp. 383-396, 10// 2014.

[12] Z. Karim, S. Claudpierre, M. Grahn, K. Oksman, and A. P. Mathew, "Nanocellulose based functional membranes for water cleaning: Tailoring of mechanical properties, porosity and metal ion capture," *Journal of Membrane Science,* vol. 514, pp. 418-428, 9/15/ 2016.

[13] H. Ma, B. S. Hsiao, and B. Chu, "Ultrafine Cellulose Nanofibers as Efficient Adsorbents for Removal of UO22+ in Water," *ACS Macro Letters,* vol. 1, pp. 213-216, 2012/01/17 2012.

[14] A. Mautner, K. Y. Lee, P. Lahtinen, M. Hakalahti, T. Tammelin, K. Li*, et al.*, "Nanopapers for organic solvent nanofiltration," *Chemical Communications,* vol. 50, pp. 5778-5781, 2014.

[15] A. Mautner, K.-Y. Lee, T. Tammelin, A. P. Mathew, A. J. Nedoma, K. Li*, et al.*, "Cellulose nanopapers as tight aqueous ultra-filtration membranes," *Reactive and Functional Polymers,* vol. 86, pp. 209-214, 1// 2015.

[16] H. Sehaqui, A. Mautner, U. Perez de Larraya, N. Pfenninger, P. Tingaut, and T. Zimmermann, "Cationic cellulose nanofibers from waste pulp residues and their nitrate, fluoride, sulphate and phosphate adsorption properties," *Carbohydrate Polymers,* vol. 135, pp. 334-340, 1/1/ 2016.

[17] H. Sehaqui, B. Michen, E. Marty, L. Schaufelberger, and T. Zimmermann, "Functional Cellulose Nanofiber Filters with Enhanced Flux for the Removal of Humic Acid by Adsorption," *ACS Sustainable Chemistry & Engineering,* vol. 4, pp. 4582-4590, 2016/09/06 2016.

[18] H. Sehaqui, U. Perez de Larraya, P. Tingaut, and T. Zimmermann, "Humic acid adsorption onto cationic cellulose nanofibers for bioinspired removal of copper(ii) and a positively charged dye," *Soft Matter,* vol. 11, pp. 5294-5300, 2015.

[19] S. Srivastava, A. Kardam, and K. R. Raj, "Nanotech Reinforcement onto Cellulosic Fibers: Green Remediation of Toxic Metals," *International Journal of Green Nanotechnology,* vol. 4, pp. 46-53, 2012/01/01 2012.

[20] X. Yu, S. Tong, M. Ge, L. Wu, J. Zuo, C. Cao*, et al.*, "Adsorption of heavy metal ions from aqueous solution by carboxylated cellulose nanocrystals," *Journal of Environmental Sciences,* vol. 25, pp. 933-943, 2013/05/01 2013.

[21] J. J. Blaker, K.-Y. Lee, and A. Bismarck, "Hierarchical Composites Made Entirely from Renewable Resources," *Journal of Biobased Materials and Bioenergy,* vol. 5, pp. 1-16, // 2011.

[22] N. Keshavarzi, F. Mashayekhy Rad, A. Mace, F. Ansari, F. Akhtar, U. Nilsson*, et al.*, "Nanocellulose–Zeolite Composite Films for Odor Elimination," *ACS Applied Materials & Interfaces,* vol. 7, pp. 14254-14262, 2015/07/08 2015.

[23] S. Varanasi, Z.-X. Low, and W. Batchelor, "Cellulose nanofibre composite membranes – Biodegradable and recyclable UF membranes," *Chemical Engineering Journal,* vol. 265, pp. 138-146, 4/1/ 2015.

[24] Z. Karim, A. P. Mathew, V. Kokol, J. Wei, and M. Grahn, "High-flux affinity membranes based on cellulose nanocomposites for removal of heavy metal ions from industrial effluents," *RSC Advances,* vol. 6, pp. 20644-20653, 2016.

[25] G. J. Freeman, "11 - Reducing microbial spoilage of beer using filtration," in *Brewing Microbiology*, A. E. Hill, Ed., ed Oxford: Woodhead Publishing, 2015, pp. 241-251.

[26] V. Millet and A. Lonvaud-Funel, "The viable but non-culturable state of wine micro-organisms during storage," *Letters in Applied Microbiology,* vol. 30, pp. 136-141, 2000.

[27] C. Peri, M. Riva, and P. Decio, "Crossflow Membrane Filtration of Wines: Comparison of Performance of Ultrafiltration, Microfiltration, and Intermediate Cut-Off Membranes," *American Journal of Enology and Viticulture,* vol. 39, pp. 162-168, 1988.

[28] T. M. Toland, K. C. Fugelsang, and C. J. Muller, "Methods for Estimating Protein Instability in White Wines: A Comparison," *American Journal of Enology and Viticulture,* vol. 47, pp. 111-112, 1996.

[29] H. Giesche, "Mercury Porosimetry: A General (Practical) Overview," *Particle & Particle Systems Characterization,* vol. 23, pp. 9-19, 2006.

[30] M. Doğan, M. Alkan, and Y. Onganer, "Adsorption of Methylene Blue from Aqueous Solution onto Perlite," *Water, Air, and Soil Pollution,* vol. 120, pp. 229-248, June 01 2000.

[31] P. Orsolini, B. Michen, A. Huch, P. Tingaut, W. R. Caseri, and T. Zimmermann, "Characterization of Pores in Dense Nanopapers and Nanofibrillated Cellulose Membranes: A Critical Assessment of Established Methods," *ACS Applied Materials & Interfaces,* vol. 7, pp. 25884-25897, 2015/11/25 2015.

[32] J. A. Considine and E. Frankish, "Chapter 3 - Wine Chemistry," in *A Complete Guide to Quality in Small-Scale Wine Making*, ed San Diego: Academic Press, 2014, pp. 23-50.

THIS PAGE HAS BEEN INTENTIONALLY LEFT BLANK

CHAPTER 3

MULTI-LAYER FILTERS: ADSORPTION AND FILTRATION MECHANISMS FOR IMPROVED SEPARATION

THIS PAGE HAS BEEN INTENTIONALLY LEFT BLANK

PREFACE

New developments in membrane structures have long been studied for membrane technology to improve the efficiency of membrane processes. Even though new membrane structures have been found to be promising for producing high performance membranes, none of these innovative developments has ever been adapted to depth filters. However, engineering new structures would potentially allow us to impart additional functionalities to the filters. Therefore, this chapter presents a new concept in filter structures. Multi-layered filter structure was engineered to control the structural properties as well as separation performance of the filters. Filters were prepared from the same total quantity of components (cellulose, perlite and polyamideamine-epichlorohydrin) either as one thick single layer or as a pile of equal multi-layers. Structural properties were obtained by 3D X-ray tomography imaging technique. Adsorption capacity was quantified with methylene blue dye molecules, while size-based rejection rates were quantified with silicon dioxide (SiO_2) and polyethylene glycol (PEG), respectively in a dead-end filtration unit. Furthermore, the effect of constant flow rate and constant pressure operations was analysed on adsorption performance.

This chapter follows the second objective.

THIS PAGE HAS BEEN INTENTIONALLY LEFT BLANK

CHAPTER 3 MULTI-LAYER FILTERS: ADSORPTION AND FILTRATION MECHANISMS FOR IMPROVED SEPARATION

MULTI-LAYER FILTERS: ADSORPTION AND FILTRATION MECHANISMS FOR IMPROVED SEPARATION

Aysu Onur[1], Aaron Ng[2], Warren Batchelor[1] and Gil Garnier[1*]

[1] Bioresource Processing Research Institute of Australia, Chemical Engineering Department, Monash University, Clayton, Australia

[2] 3M Australia, Sydney, Australia

*** Corresponding author at:** Bioresource Processing Research Institute of Australia, Chemical Engineering Department, Monash University, Clayton, Australia, 3800

Email address: gil.garnier@monash.edu (G. Garnier).

3.1. ABSTRACT

Filters made of cellulose fibre and perlite particles were prepared using a wet laying papermaking technique. Polyamideamine-epichlorohydrin (PAE) was added to provide wet strength. Filters were prepared at two different total basis weights of 200 and 400 grams per square metre (gsm). Single and multi-layered filters were structured for each total basis weight. The effect of total basis weights and multi-layered structure on methylene blue adsorption and silicon dioxide (SiO_2) particle filtration was investigated. Methylene blue adsorption was performed in two modes: constant pressure and constant flow rate. In both operation modes, the adsorption capacity of multi-layered filters was significantly higher (16 to 100%) than for single-layer filters at the same overall weight. The effect of layer separation was also characterized using polypropylene separators and tested under constant flow rate operation. Separators provided more effective methylene blue adsorption by generating a well distributed flow. Filtration performance was quantified with 0.5 µm silicon dioxide particles under constant pressure conditions; this is to mimic bacteria rejection. Filtration capability of SiO_2 particles was reduced slightly (12%) with decreasing individual filter layer thickness regardless of the multi-layered structure. Filtering polyethylene glycol (PEG) molecules with two different molecular weights was performed; however, no rejection was recorded. The filter internal pore structure was visualised by 3D-X ray computed tomography and the void fraction was

quantified. 400 gsm single layer presented areas of low fibre density forming pores, while the pore volume decreased for thinner filter layers.

3.2. KEYWORDS

Composite; multi-layer; adsorption; filtration; cellulose fibre, channelling

3.3. INTRODUCTION

Depth filters [1] are porous filtering mediums composed of cellulose fibres and inorganic absorbents. Unlike surface filtration, they can retain contaminants through the thickness as well as on the surface during liquid filtration. These composite structures combine two different separation principles and technologies in a single medium. Filtration by particle rejection is provided by forming an intricate mesh, where selective adsorption is achieved by a functional inorganic particle. Separation can further be improved by combining other additives, such as charged polyelectrolytes in the network [2]. The medium can be modified with a cationic polymer adsorbing the common negatively charged dissolved contaminants significantly smaller than the average pore size. However, depth filtration analysis reported in literature has mostly focused on the modelling of membrane separations [1, 3-7]; there is a lack of experimental studies optimizing depth type filter operation especially in terms of membrane structure.

Filtration performance can be tailored in many ways by controlling filter structure/composition and operation mode. Two efficient modes of operation are dead-end filtration and cross-flow filtration, where the flow is passed directly through the filter in dead-end and tangential to the filter in cross-flow filtration [8], respectively. Furthermore, these processes can be controlled under modes of constant pressure or constant flow rate. In either case, the non-constant parameter is being monitored, and the extent of filter fouling or clogging is assessed by the recorded parameters [3, 9]. Filtration performance can also be altered by modifying the structure and configuration of filters. Multi-layer structured filters with varying pore sizes stacked on top of another offer a simple way of sequentially separating cells or particles [10, 11]. In a recent study by Griffiths et al. [12], filtration was modelled on a multi-layered membrane structure with each layer having varying pore sizes stacked on one another. The efficiency of multi-layered filter structure was analysed by developing

a model simulating the transport and filtration of particles through a multi-layer structure. This model characterizes the filter and offers optimal design requirements in terms of number of filter layers, pore size in each layer and pore interconnectivity between layers.

Filtering bacteria with multi-layered filters to provide a greater capture of bacteria was also reported [13]. The study aimed at achieving higher bacteria rejection by mechanically attaching a layer to another, which contains a bacteria-destroying material. In another study [14], a nano fibre layer was attached to the initial layer of a fibrous filter. Filter media having a first layer and a nanofibre layer adhered onto exhibited advantageous properties including increased dust holding capacity.

Although multi-layered filters are well known in industry, very few studies have systematically quantified their adsorption and filtration mechanisms, and even less have characterized the effect of multi-layered structure on depth filter performance. In this study, we developed multi-layered and single-layered filter structures made from the same amount of filter media. Depth filter layer processing was inspired from papermaking technique and characterized for adsorption and particle rejection capability. The adsorption and filtration mechanisms behind the performance of single and multi-layered filters were analysed in terms of chemical engineering and internal filter structure using an advanced image technique and colloids and surface concepts.

3.4. MATERIALS AND METHODS

3.4.1. Materials

Cellulose fibres used for the composites are unrefined northern softwood NIST RM 8495 bleached Kraft pulp and bleached radiata pine softwood Kraft pulp refined to 400 Canadian standard freeness (CSF) in a disk refiner. Expanded perlite was provided by Dicalite Minerals Corp. Commercial PAE was provided from Nopcobond Paper Technology Pty Ltd.

Methylene blue (MB) in powder form and 0.5 µm monodispersed silicon dioxide (SiO_2) particles of density 1.8 g/cm^3 were purchased from Sigma Aldrich. Polyethylene glycol (PEG) of two molecular weights (600 and 5,000 kDa) was provided by Dow Chemical. Polypropylene separators with 0.45 µm pore size and diameter of 47 mm was purchased from CUNO Inc. Meriden, USA.

3.4.2. Methods

3.4.2.1. Fabrication of filters

The dry northern softwood NIST pulp was wetted by soaking in deionized water overnight. The pulp was transferred to a disintegrator (Model MKIIIC, Messmer Instruments Ltd.) and disintegrated for 75,000 revolutions. Filters were prepared using a standard British hand sheet maker at three different total basis weights: 100, 200 and 400 gsm. The step by step preparation method was published in a previous study [15]. The filter chemical composition is similar to that of standard industrial filters: it consists of 30% Fibre (1/3 refined pulp + 2/3 unrefined pulp) and 70% perlite with PAE (0.22% w/v) added at a rate of 100 mg/g fibre on top of the suspension (0.26 wt%) before papermaking. Composites were prepared either as one single layer or in the form of stacked equal multilayers that is equivalent to the total targeted basis weight. 5 different filters prepared according to different layer configurations and different total basis weights are shown in Figure 1. Samples were coded with the corresponding labels. The criteria for material selection are based on industrial filters for food and beverage applications; food grade filters usually contain these materials.

PAE is used to provide wet strength to the filters. It crosslinks with the carboxyl group of cellulose and itself to create an irreversible covalent bond network and provides some waterproof barrier around fibres [16]. However, in our case the major crosslinking is provided by self-crosslinking of PAE as our source of cellulose does not contain much carboxyl groups. PAE also adsorbs onto the fibres and particles of the suspension which introduces positive charges to the anionic surfaces of cellulose fibres and perlite particles. Addition of PAE to the suspension results in the partial surface coverage of perlite and cellulose fibres by positively charged polymer. This induces electrostatic interactions between negatively charged contaminants and the filter medium. Using PAE is allowed by food regulations at low concentrations (up to 2.5 wt. % of the dry sheet); it is considered an indirect food additive and the concentration of PAE of this study is around this limit [17].

Perlite is a low cost adsorbent made from a glassy volcanic rock; it is known as an excellent filter aid [18]. Perlite is an anionic adsorbent of zeta potential ranging between -40 to -50 mV [19]. The particle size distribution of perlite and its effect on the structure and porosity of filters was reported in a previous study [15].

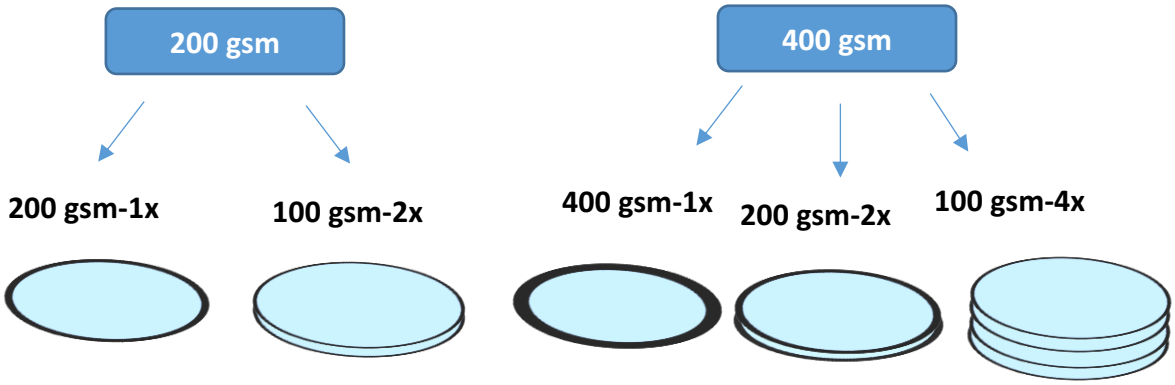

Figure 1: Schematic representation of the different filter configurations investigated at two different basis weights.

3.4.2.2. Adsorption and filtration with constant pressure

Adsorption and filtration experiments under constant pressure mode were performed with a dead-end stirred cell from Merck Millipore Australia. The closed setup has 400 mL of working volume and is pressurized by a compressed air gas cylinder. Samples were placed on the membrane holder at the bottom of the cell body with an O–ring. For multilayers, the O-ring pressed layers from the edges so the interlayer gap was negligible. The cell body was filled with the desired solution following sample placement. Filtrate that passes through filters was transferred to an ultraviolet-visible (UV-Vis) absorption spectrometer via a quartz micro flow cell with 10 mm optical path length. Instantaneous absorbance was measured here every 10 seconds at a specific wavelength. After measurement in UV-Vis, filtrate was transferred to a beaker on a balance. Before conducting any experiments, water was flushed through samples to ensure equilibration. After equilibrium has been reached, either 5 ppm MB solution or 0.05 wt. % SiO_2 suspension were passed through the filters at 1.5 bar. Two replicates of filters were tested for both adsorption and filtration. Here, *adsorption* corresponds to the accumulation of model cationic or anionic molecules onto a surface by electrostatic attraction, while *filtration* is measured as the rejection of particles in suspension by size exclusion. MB preferentially adsorbs onto negatively charged surfaces; it can also diffuse through the pores of the negatively charged perlite particles. However, there is no electrostatic attraction between MB molecules and the positively charged filter medium after adsorption of the PAE cationic polymer. MB was therefore selected as standard dye to quantify improvement in breakthrough curves due to the multi-layered filter structure as unable to adsorb.

Mass flux for the effective membrane area (0.00418 m^2) was calculated by measuring the volume of permeate per unit area and time; Litre per Square Metre per Hour (LMH). Mass flow rate of filtrate as a function of time was also continuously recorded by a computer. Total flux was calculated with equation 1.

$$FLUX\ (LMH) = \frac{Volume\ of\ filtrate\ (L)}{area(\mathrm{m}^2) \times time\ (h)} \quad (1)$$

Adsorption experiments were run with 400 mL MB dye solution at a concentration of 5 ppm at pH 5.8 (This is the characteristic pH of MB). Breakthrough curves were plotted by normalized concentrations as a function of time. Additional solution was added for filters that did not reach saturation with 400 mL solution. Area over the curve was calculated for each filter to determine the adsorption capacity of filters. Capacity was calculated based on equation 2 [20]. The integral was calculated from the area over the curve using the trapezoidal method.

$$q = \frac{C_F \times \dot{Q}}{1000 \times m_s} \int_0^{t_{end}} \left(1 - \frac{C_{out}}{C_F}\right) dt \quad (2)$$

Where:

q: Capacity of the adsorbent (mg/g)

C_{out}: Concentration of MB in the filtrate (mg/g)

C_F: Concentration of MB in the feed (mg/g)

$\dot{Q}$: Volumetric flow rate (cm^3/s)

t_{end}: Time (s)

m_s: Weight of adsorbent (g)

Rejection of 0.5 µm SiO_2 particles was determined by filtering 0.05 wt. % SiO_2 suspension at the same pH value as dye molecules (pH=5.8) through the filters. pH of 5.8 is desirable as increasing pH would dissociate carboxylic acids leading to repulsive forces between charged groups. These repulsive forces also lead to swelling of the cellulose fibre with collapse of the filter pore structure. SiO_2 concentration of suspension before and after filtration was estimated by UV-Vis absorption spectroscopy and the equation 3 was used to calculate rejection capability of filters. UV-Vis

spectroscopy calibration curves of MB dye molecules and SiO_2 particles are shown in the supplementary information (Figure S5).

$$Rejection\ (\%) = 1 - \left(\frac{\text{Filtrate concentration}}{\text{Initial feed concentration}}\right) \times 100 \quad (3)$$

PEG molecules were also filtered through the composites to quantify their microfiltration capability. The MWCO range for microfiltration applications usually starts from 500 kDa up to big particle filtration such as yeast and bacteria; the filtration spectrum can be found in the study [21]. Total carbon analyser was used to measure the concentration of PEG molecules in the suspension before and after filtration.

3.4.2.3. Adsorption with constant flow rate

Adsorption performance was additionally tested using 47 mm (corresponds to diameter of filter housings) stainless steel filter housings with 0.00132 m^2 effective membrane area to verify the performance under constant flow rate operation mode. A peristaltic pump was used at a constant flow rate (12 mL/min) such that the same total flux as the constant pressure experiments for the same sample was obtained. Experiments were performed with and without presence of polypropylene separators. Separators are used to provide a well distributed and uniform flow through a filter; they do not adsorb MB. Separators were placed in the housings as previously described (2.2.2.). The only gap created between multilayers is the thickness of the separator which is well below 1 mm. 47 mm separators were placed between the layers as well as on top of initial layers. Filtrate was transferred to UV-Vis spectroscopy via quartz micro flow cell to obtain the concentration at a regular time interval. Total mass flux and flow rate as a function of time were recorded by the same setup as constant pressure mode. Adsorption capacities were calculated form the experimental breakthrough curves as explained above. The experimental setup for constant flow rate operation is shown in Figure 2.

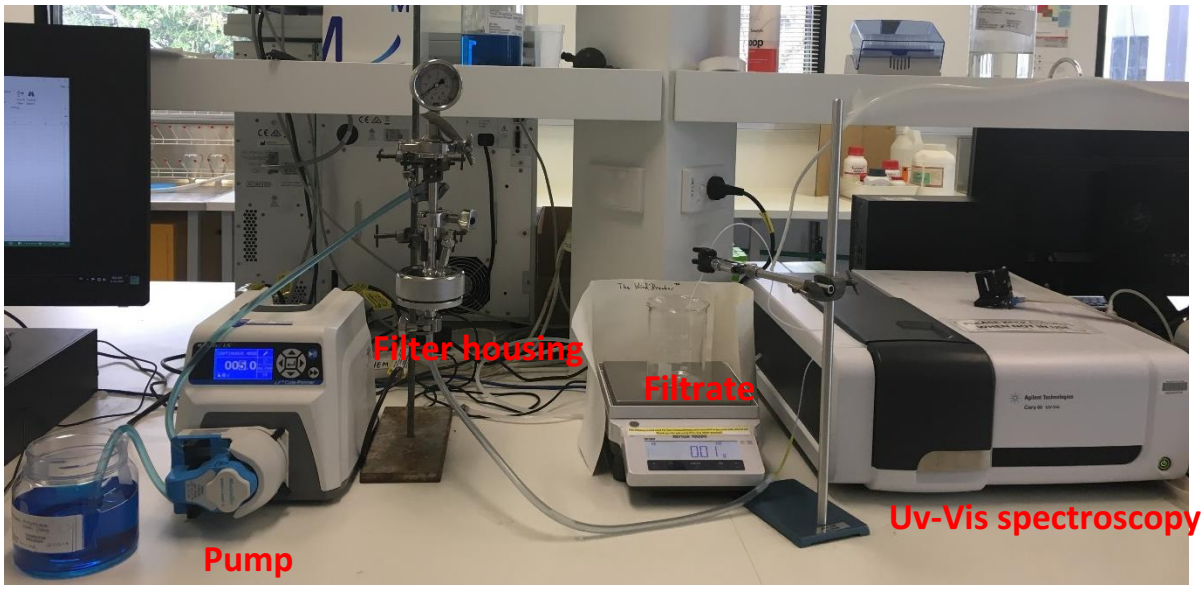

Figure 2: Experimental setup shown for 47 mm filter housings under constant flow rate mode.

3.4.2.4. 3D X-ray tomography

X-ray computed 3D tomography was used to make a quantitative and qualitative analysis on the internal structure of filters about how the fibre network differently built up to form a sheet according to different basis weights. This technique provides a non-destructive 3D imaging. The basic principle is based on the set of images of beam transmitted through the sample while the sample is rotated to different positions for each image taken [22]. Samples with 2 mm×8 mm of size were visualized by Zeiss Xradia 520 Versa. The X-ray source was operated at 30 kV. Distance from source to sample and sample to detector was set to 15 mm. The number of images taken per scan was 1601 and the image resolution was 2022×2022 pixels. Avizo and Image J software were used to reconstruct images and to quantify the total void fraction and void fraction distribution through the thickness (SI). Thresholding is done by comparing grayscale and thresholded image with a judgement. The threshold was meticulously selected with trial and error such that we do not lose any materials. Detailed information on scanning settings can be found in supplementary materials (Figure S6).Void structure and how the void structure is changing through the thickness were analysed qualitatively as well.

3.5. RESULTS

Cellulosic membranes of two different thicknesses (200 and 400 gsm) were tested under different filter configurations. The filters were examined under two operating conditions: at a constant flow rate (12 mL/min) or at a constant pressure (1.5 bar). The effect of polypropylene separators between the layers on adsorption performance was tested with 400 gsm single layer (400 gsm-1x) and four layers of 100 gsm filters (100gsm-4x) under constant flow operation. Filtration of 0.1 wt. % PEG molecules of molecular weight of 600 and 5,000 kDa was performed under constant pressure (1.5 bar) mode for each filter configuration. Filters were also tested with suspensions of 0.5 µm SiO_2 particles (0.05 wt.%) under constant pressure (1.5 bar). Finally, the internal structure of 400 gsm filters made of single and multiple layers was analysed by 3D X-ray tomography combined with image analysis.

3.5.1. Methylene blue adsorption under constant pressure

Methylene blue was used as a model for the cationic organic dissolved contaminants. Constant pressure adsorption testing identifies filter compaction and saturation by measuring flowrate. Breakthrough curves were recorded under constant pressure (1.5 bar) for different filter configurations using two types of cellulose filters differing in thickness (gsm) (Figure 2a). The adsorption capacity for each configuration was calculated using the breakthrough curves. The adsorption capacity of each filter is shown in Figure 2b.

Multilayer filters provided improved breakthrough curves and higher adsorption capacities than single layer filters as tested under constant pressure (Figure 3). Adsorption capacity of 400 gsm filter drastically increased by 54% and 118% by forming two layers (200gsm-2x) and four layers (100gsm-4x), respectively (Figure 3b), all at the same filter weight. Adsorption capacity of 200 gsm filter also increased significantly by forming two layers of 100 gsm (100gsm-2x).

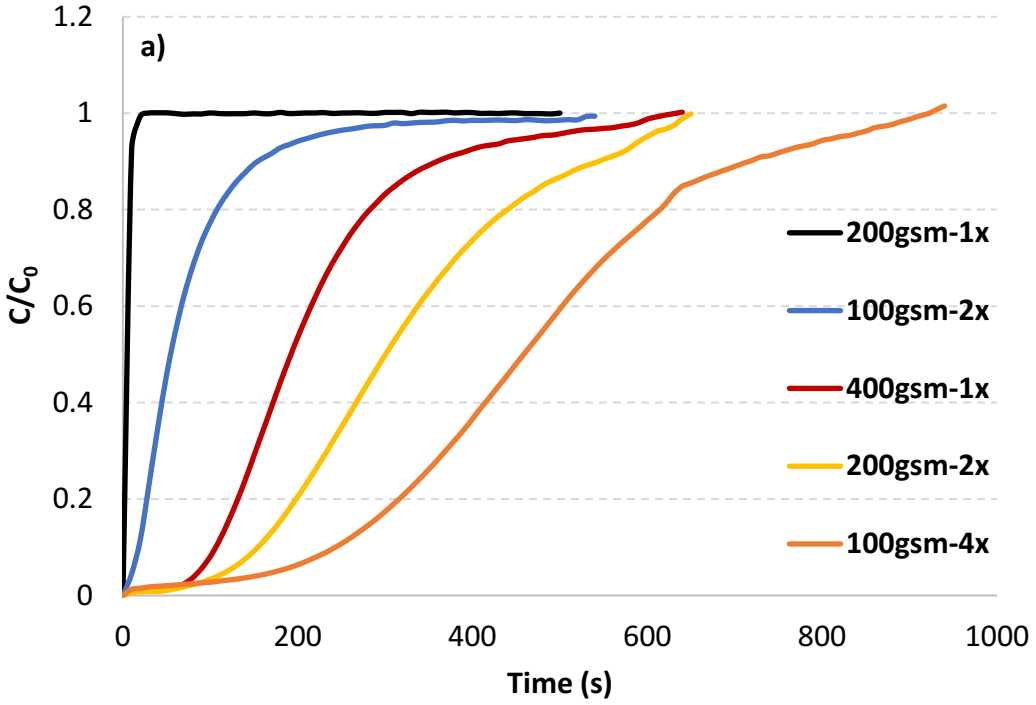

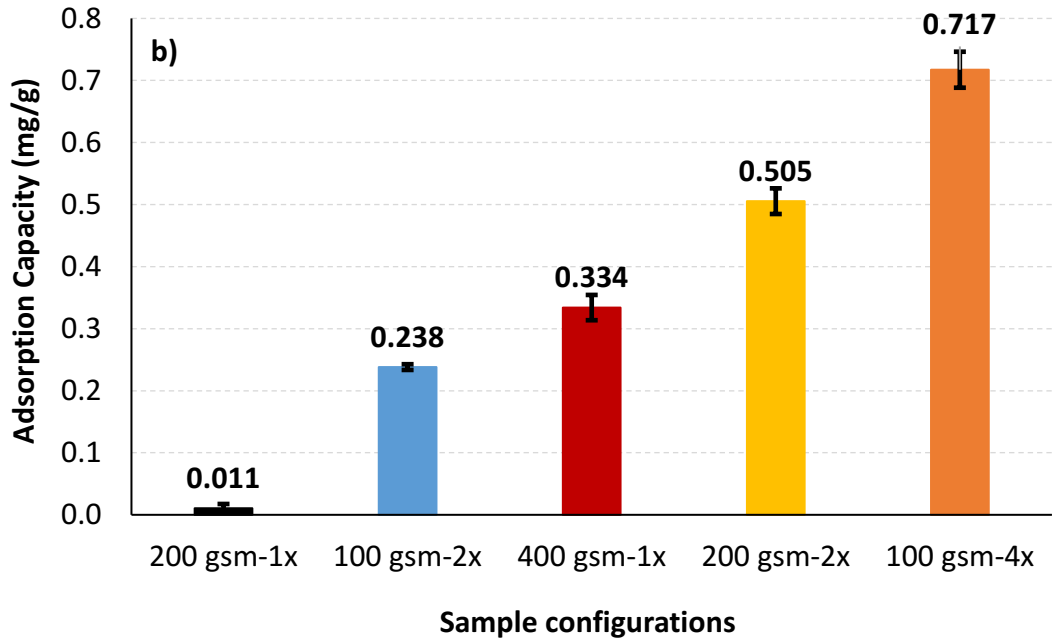

Figure 3: Effect of filter configuration and number of interfaces on the **a)** methylene blue breakthrough curves and **b)** methylene blue adsorption capacities. Tests were performed at 1.5 bar and 22°C.

The effect of filter configuration, including number and basis weight of layers, on filtration flux and filter thickness is shown in Figure 4 under constant pressure mode. At a given basis weight or amount of filter media, filter thickness increases slightly with multi-layered configuration. Flux decreased with increased gsm and the number of layers at a given gsm. Flux decreased from 682 to 600 LMH (Litres per Square Metre per Hour) for 200 gsm filters by introducing two layers of 100 gsm. However, flux slightly dropped for 400 gsm filters from 574 to 569 LMH for 4 layers of 100 gsm. For multi layered filters, an increased flux is expected according to Kozeny-Carman and Darcy [23]. These equations provide the mathematical relationships describing the flow of a fluid in a uniform porous media. Pressure loss between the layers might lead the flow travelling in the planar direction to find the path of least resistance through the next layer, resulting in an increased flux. However, this analysis does not fully apply to the space between layers. Once the stirred cell is pressurized by compressed air, the layers are being compressed and the flow is somewhat forced to flow through the next layer with little chance to flow in the planar direction. However, it might still have an impact, considering the low pressure used in the experiments, and result in lower flux values.

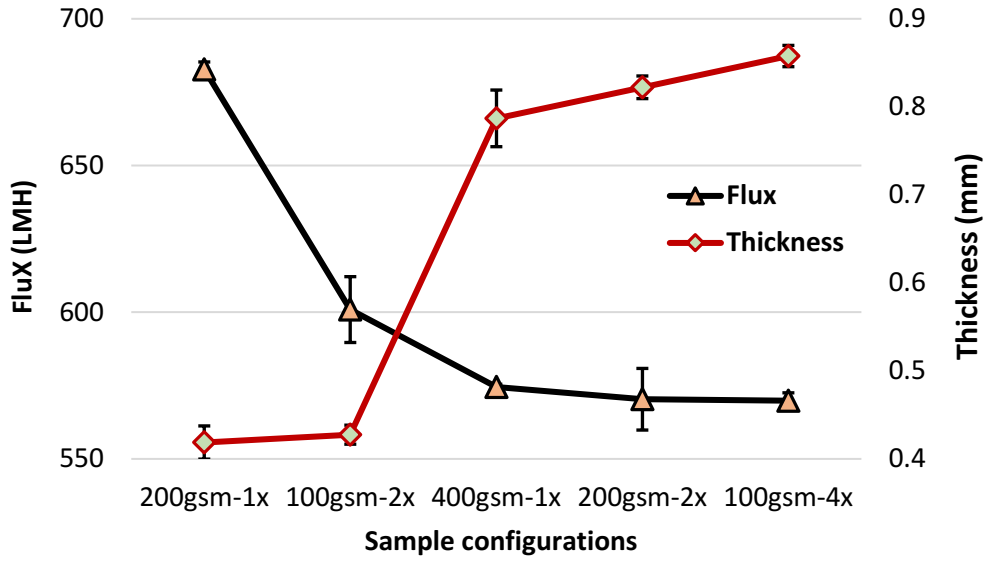

Figure 4: Effect of filter configuration and number of interfaces on the flux and thickness under 1.5 bar, 22°C.

3.5.2. Methylene blue adsorption under constant flow rate

Methylene blue adsorption breakthrough curves of 400 gsm filters comparing single layer configuration with four layers are presented in Figure 5. Breakthrough curves were obtained under constant flow rate with and without polypropylene separators between layers and on top of the first layer. Flow rate was set such that the flux is matching the flux values from constant pressure experiments for the same samples (12 mL/min).

Adsorption capacity is also much higher with multilayered filters under constant flow mode. The saturation occurred much quicker for both filters without separators. However, adsorption capacity decreased for both type of filters without separators. The capacity decreased by almost 15% for multilayered filter (100gsm-4x) and 29% for single layer filter (400gsm-1x) by removing separators. Adsorption capacities are found in Table I.

The offset at the beginning of the curves without separators needs further study to better understand the phenomenon involved.

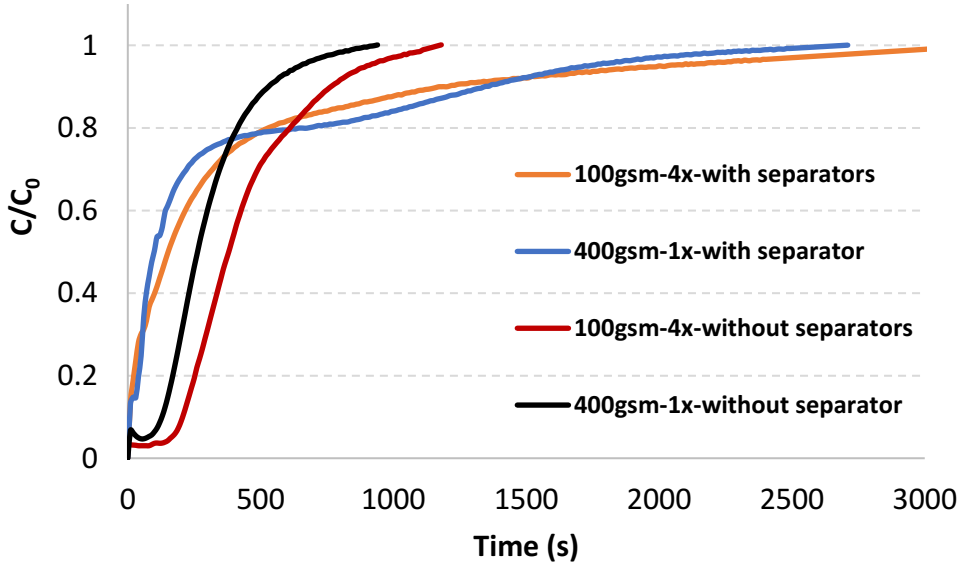

Figure 5: Methylene blue breakthrough curves of 47 mm 100gsm-4x and 400gsm-1x filters in a single filter housing with and without separators at 12 mL/min, 22°C.

Table I: Methylene blue adsorption capacities of single layer and multi-layered filters with and without separators under constant flow rate (12 mL/min).

Filters	Adsorption capacity (mg/g)
100gsm-4x-with separators	0.51 ± 0.04
400gsm-1x-with separators	0.44 ± 0.01
100gsm-4x	0.43 ± 0.05
400gsm-1x	0.31 ± 0.05

3.5.3. 3D X-ray tomography

3D X-ray tomography image analysis was conducted on single layer 400 gsm (400gsm-1x), two layers of 200 gsm (200gsm-2x) and four layers of 100 gsm (100gsm-4x). Grayscale and thresholded cross section images of 400gsm-1x are given in Figure 6. 3D images of all filters are shown with intersection of three different planes (Figure 7). The white sections represent voids in thresholded images. Animations on voids change locations through thickness are provided for all samples in supplementary information.

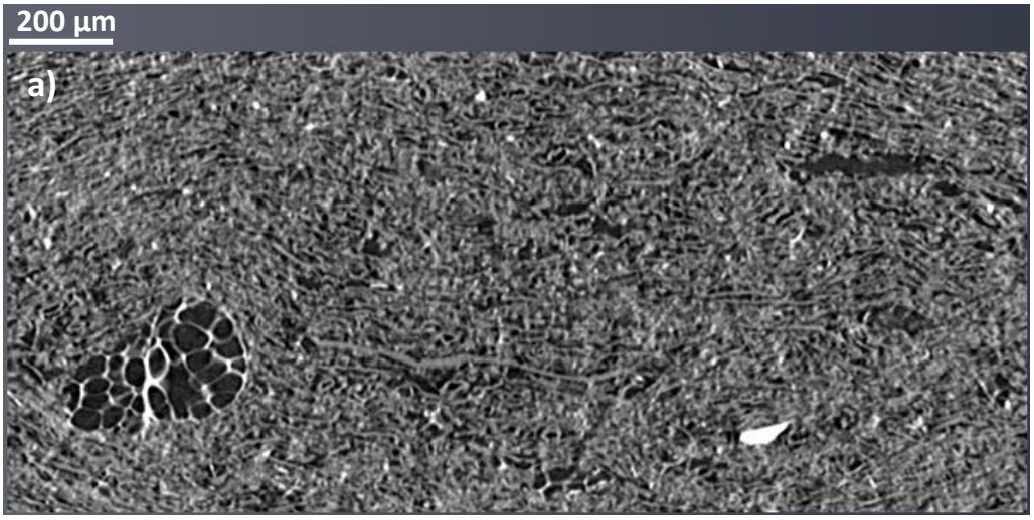

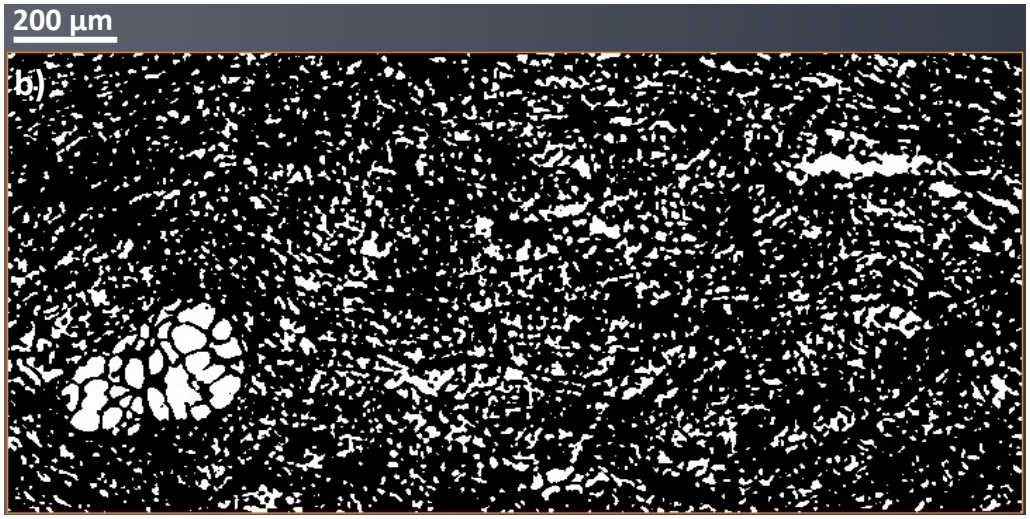

Figure 6: 3D X-ray reconstituted images of 400 gsm sample (400gsm-1x). **a)** Grayscale and **b)** Thresholded cross section images.

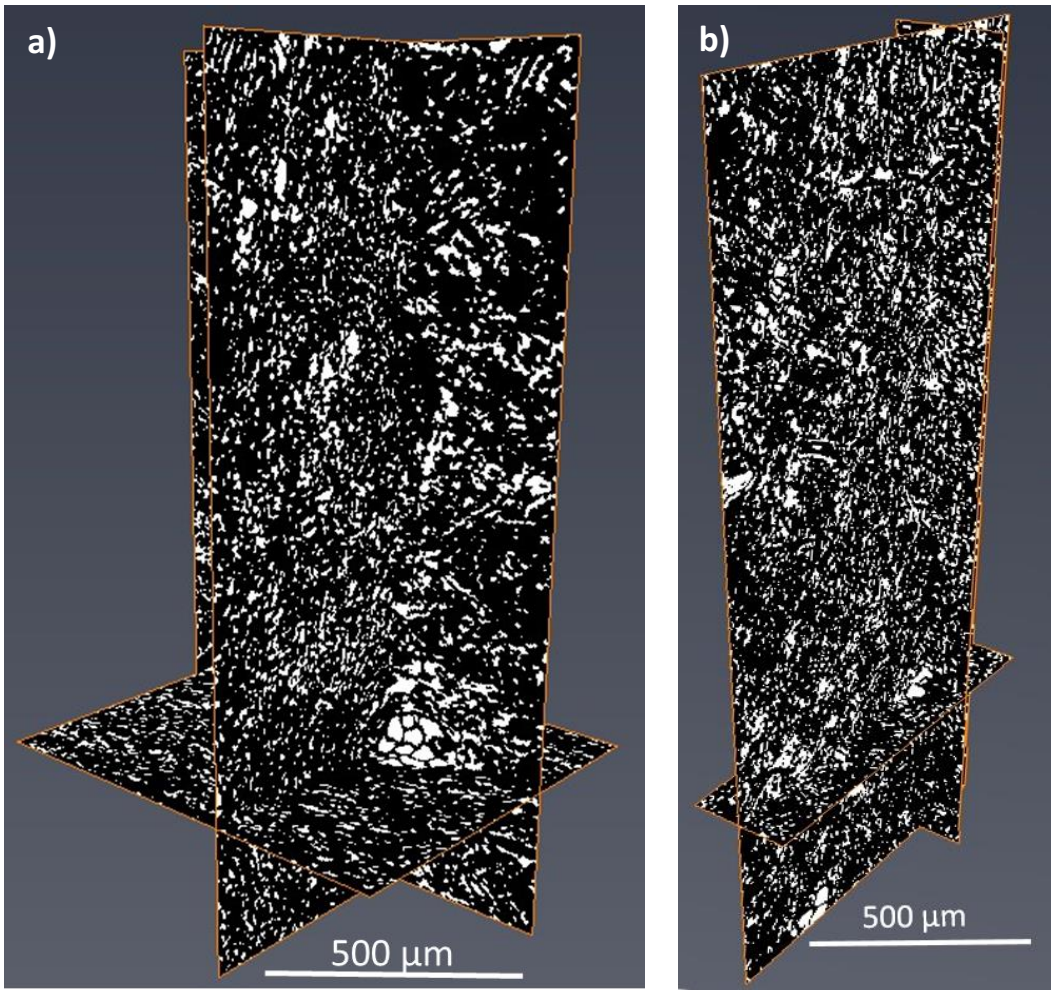

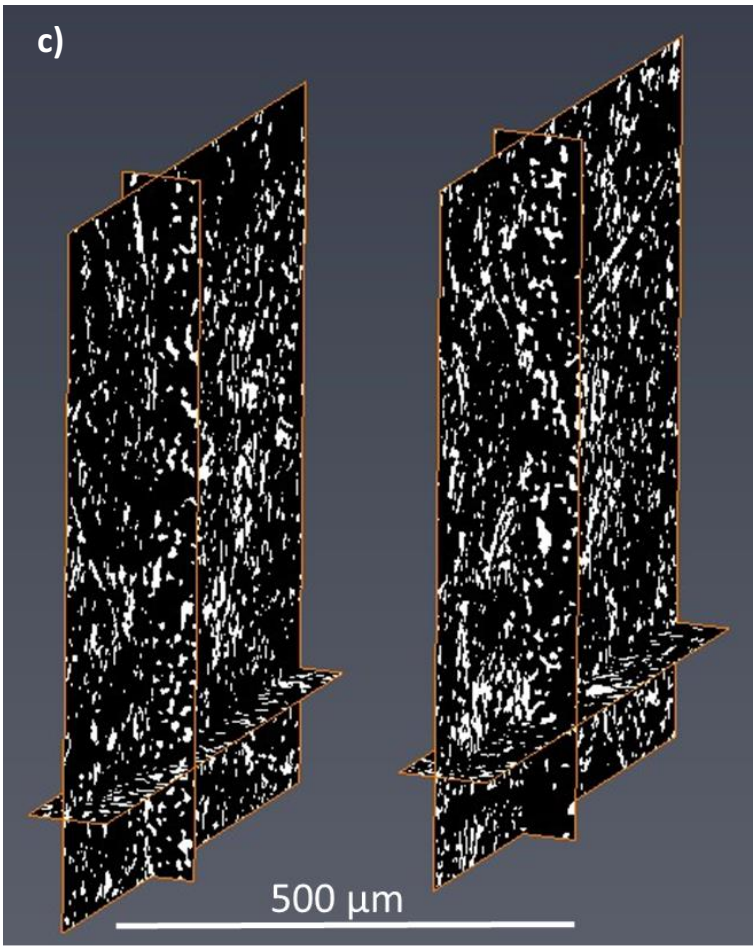

Figure 7: 3D X-ray images of **a)** 400 gsm sample **b)** 200 gsm sample and **c)** 100 gsm sample presented with some of layers with intersection of three different planes.

The total void fraction of the composites calculated by image analysis is 20% for the 400 and 200 gsm filters and 14% for the 100 gsm filters. However, all void fractions are similar, as expected for filters of identical composition. The main difference lies in the pore structure, which differs with thicknesses, despite having a similar void fraction. The probability of forming bigger voids increases with the composite thickness. There are some zones of low density, creating flow channels in the 400 gsm single layer sample (Figure 6 and 7). These channels appear to propagate through the thickness and then to disappear. Channels are best observed in the animations provided in SI. These massive void concentration decreases at lower basis weights, particularly in 100 gsm composites.

The void distribution through thickness of an individual layer (200gsm-2x) is shown in Figure 8. The composite mesh side is at the high number (88) and the air side is at the origin. Void distribution of 200 gsm filter through the thickness is decreasing from top to bottom (Figure 8); this density

gradient is inherent to the papermaking technique. The density gradient across filter thickness with the highest composite density (lowest volume fraction) on the mesh side are expected from papermaking. The void distributions for all composites are provided in supplementary information (Figure S.1-S.4). However, it was not possible to visualize density gradient in all samples; this suggests that the subtle differences in structure affecting density are below the resolution of the X-ray tomography used. Sample properties based on different gsm were calculated using the properties of fibre and perlite and are shown in supplementary materials (Table III). The calculated porosities are comparable to the porosities measured by X-ray tomography. However, these calculations suggest that the structure would be slightly denser with the increasing basis weights.

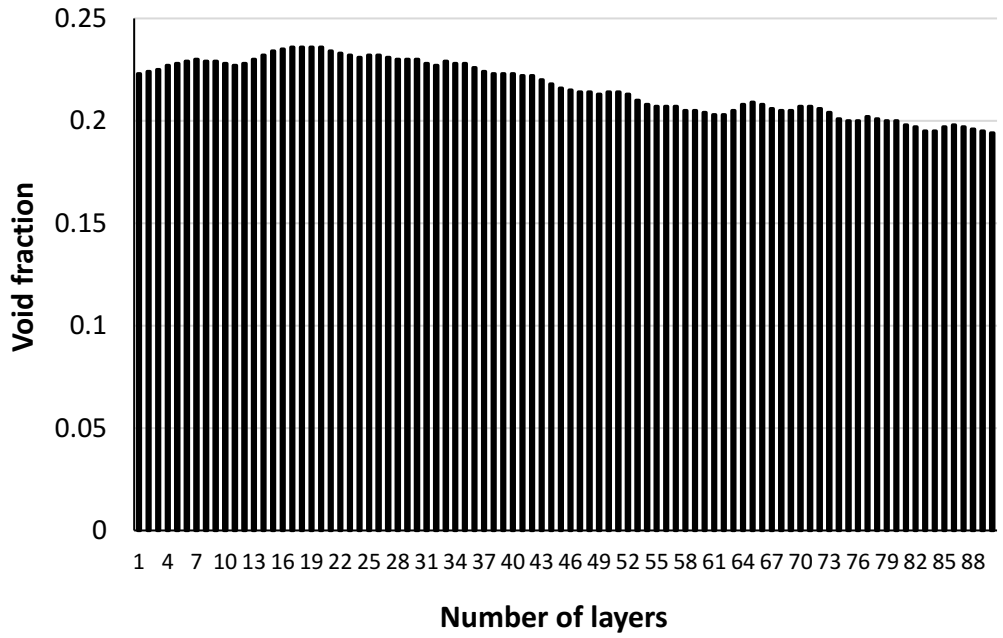

Figure 8: Void fraction distribution through the thickness of an individual layer (200 gsm). The composite mesh side is at the high number (88) and the air side is at the origin.

3.5.4. Filtration

The filtration ability of filters was quantified for the different configurations using polyethylene glycol polymers (PEG) of two molecular weights (600 and 5,000 kDa) and 0.5 µm SiO_2 colloids. Both PEGs passed through the filters without showing any cut off. Total organic carbon content (TOC) of PEG solutions before and after filtration were identical and given in SI (Table I and II). These filters

are unable to provide microfiltration. The particle rejection of 0.5 µm SiO_2 particles was then measured. Very high particle rejection was recorded for the 400 and 200 gsm single layer filters. Particle rejection rate however dropped down for 100 gsm 2 layers (100gsm-2x) and 4 layers (100gsm-4x) filters. This shows that the actual thickness of the layers plays an important role in particle capture, regardless of the number of layers. SiO_2 particle rejection results are given in Table II. Besides, 100gsm-4x filter also shows higher variation in rejection results. This variance potentially shows that multi-layered filters formed by low gsm layers cannot be relied upon for rejecting particles. The better performance of single thick layers (200 and 400 gsm) might be explained by the slightly denser structure that helps trap particles. However, further studies on filtration are needed to fully characterize the mechanism behind the rejection capability of multi-layered filters.

Table II: 0.5 µm SiO_2 particle rejection of 400gsm-1x, 200gsm-1x, 100gsm-2x and 100gsm-4x filters.

Filters	**SiO_2 rejection (%)**
100gsm-4x	87 ± 11
100gsm-2x	87 ± 3
200gsm-1x	98 ± 0.9
400gsm-1x	99 ± 0.2

3.6. DISCUSSION

3.6.1. Effect of operation modes: Constant pressure or constant flow

Under constant flow, pressure drop builds up across the filter to maintain the flow as fouling occurs over time [3]. However, during constant pressure operations, flux decreases gradually as the filter fouls [3] and initial high flux in constant pressure mode can result in severe fouling in processes with suspended particles. High flux at the beginning of filtration causes much faster deposition of particles on the membrane surface than are back transported, resulting in faster particle deposition than in constant flow rate mode [24]. This reduces the overall capacity of the filter. Therefore, industrial processes are mainly operated under constant flow mode to maximize the available filter area by avoiding sudden fouling. However, filtering solute molecules can be different with constant

pressure as there is no particle involved; our experiments are conducted with solute dye molecules and the main mechanism for separation is by electrostatic adsorption.

During our constant pressure adsorption experiments with multilayer filters, flow rate decreased compared to single layer as a result of the resistance created by multi-layers. Decreased flow rate results in an increased residence time for liquid, which provides more time for dye molecules to adsorb. In contrast, residence time does not change for multi-layers under constant flow as flow rate is constant. This explains why adsorption capacities at a given basis weight is so dependent upon layer configuration under constant pressure mode.

3.6.2. Effect of multi-layered filter structure

Heterogeneous composite filters combining fibres and adsorbent particles can develop heterogeneity at small length scales, creating channels. This is accentuated by the agglomeration of adsorbent particles and poor fibre distribution (formation). Liquid flows through such channels with little resistance and saturates the surrounding filter medium of this preferential flow path; this reduces the effectiveness of filters substantially.

By introducing multi-layers, tortuosity is increased and channelling mostly avoided as multi-layers offsets the channel alignment between consecutive layers. This prevents preferential flow through continuous channels across the entire filter medium. Multi-layers have also increased external surface area maximizing filter-liquid contact (Figure 9).

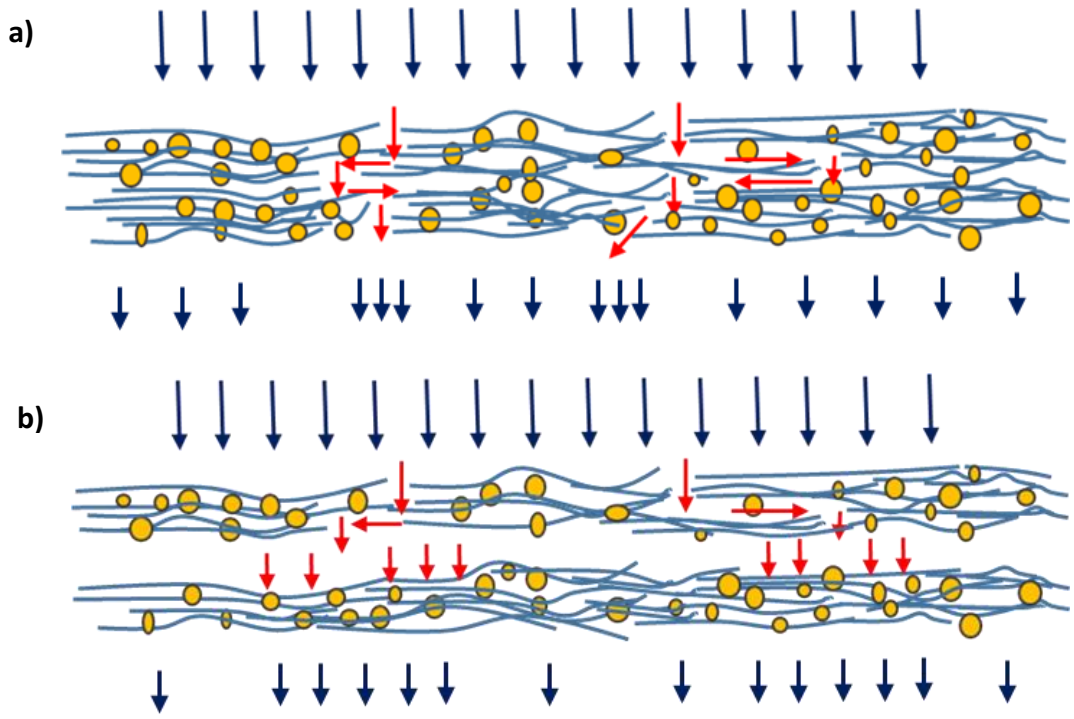

Figure 9: Schematic illustration of flow through a single layer **(a)** and two layers **(b)** filters.

Figure 9 shows liquid streams following the tortuous path of least resistance in a single layer structure **(a)**. This pattern is distorted between two stacked layers as liquid contacts the filtering medium of the next layer **(b)**. This explains the improved breakthrough curves as a result of operating multi-layered filters for the same basis weight.

Analysis of 3D X-ray tomography images and animations (SI) reveals that a single thick layer of filter (400gsm-1x) is more likely to contain macro voids than thinner filters; these massive gaps are absent at lower basis weights. Macro voids are defects reported in literature mainly for membranes prepared by phase-inversion methods. The presence of such macro voids results in compaction or collapse of the membranes that reduces flux [25, 26]. In our case, these defects cause preferential liquid flow through these gaps in single layer that results in a poor adsorption capacity. However, the filtering efficiency decreases with multiple layers of thinner filter layers (100gsm-4x & 100gsm-2x). Thicker depth filters can better hold particles and prevent any particle escape; filter density gradient across the thickness can be an explanation. Usually, cellulosic fibre composites are formed by wet papermaking laying technique with a density gradient across the thickness. The density increases from top to bottom. The decreasing void fraction through the thickness can be seen in

Figure 8. This is due to the preferential distribution of fines away from the mesh and their varying degrees of compaction through the sheet thickness [27]. Thick single layer filters are expected to have a higher density variance through thickness than smaller basis weights. Also, thick samples are expected to have higher densities than low basis weight samples (the density and porosity calculations based on thickness of the samples are given in the supplementary section.) Another explanation could be the denser structure of thick samples better trapping particles.

3.6.3. Effect of separators

The improved adsorption capacity with separators under constant flow operation is attributed to a uniformly distributed flow between the layers. Well distributed flow increases the probability of liquid to follow through the entire filter medium instead of following some preferential pathway and saturating local areas. The operations schematic is illustrated with and without separators in Figure 10.

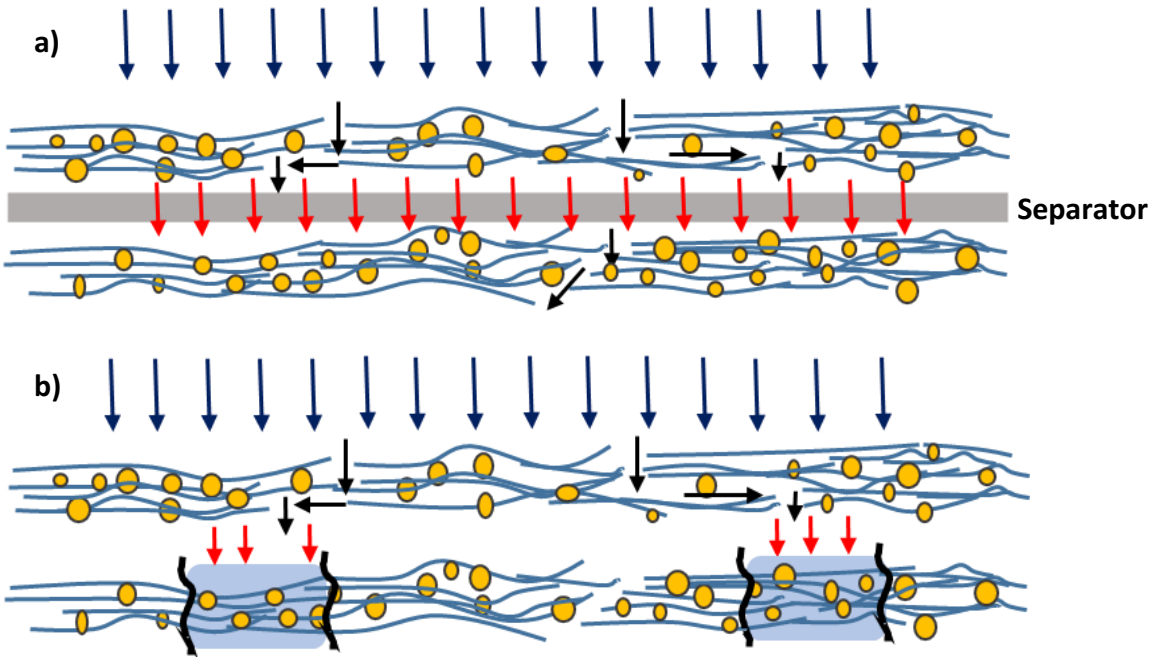

Figure 10: Schematic illustration of flow of liquid through filters with (**a**) and without (**b**) separators.

3.7. PERSPECTIVE

A thermal process, pasteurization is usually used for food preservation in the food industry. Treatment temperature ranges from less than one minute up to several minutes at temperatures varying from 100 to 150°C, based on products [28]. However, this process can alter the organoleptic characteristics and degrade the quality of food, specifically in heat-sensitive foods such as juices and wine [28]. Removal of microbial spoilage from liquid foods at low temperatures through filtration is a promising method for food and beverage industry [29]. In this work, we developed food grade filters made from cellulose, a naturally abundant, biocompatible and low-cost material. These filters can remove spoilage as small as 0.5 μm (in the size range of bacteria [30]) by up to 98% with 200 gsm two layers and 400 gsm single layer and at least by 87% rejection rate with 100 gsm two and four layers. Filtration can also serve as a preliminary step before any further treatment – including pasteurization [31, 32]. The contaminants smaller than the pore size also retained through adsorption combining electrostatic interactions; these interactions are further improved via multi-layer filter configurations. Depth filters can provide a good alternative for “cold” pasteurization process.

3.8. CONCLUSION

The effect of multi-ply and inter-ply spacing of novel inorganic-cellulosic depth filters was investigated in terms of adsorption capacity and filtration efficiency. Cellulose fibre-perlite composite layers were prepared at three different thicknesses (basis weights) using a papermaking technique. Perlite and fibre content was maintained at 70 wt% and 30 wt%, respectively. Polyamideamine-epichlorohydrin (PAE) was used for wet strength, filler retention and charge control. Filters were constructed as single-layer and multi-layers for different total basis weights. Methylene blue (MB) was selected as a cationic solute molecule to characterize adsorption under constant pressure and constant flow rate modes for the different filter configurations. Filtration efficiency was measured with PEG molecules of two molecular weights (600 and 5,000 kDa) and 0.5 μm silicon dioxide (SiO_2) particles. The filter structure was quantified by 3D X-ray tomography.

MB adsorption capacity increased by multi- layered filter structures at a given basis weight for both operation modes (constant pressure/flowrate). The constant pressure mode is a better option for

multi-layer filters as it maximizes adsorption capacity. The adsorption capacity of multi-layered filters (over single layer) increased by preventing flow channelling by off-setting macro voids-channels through the thickness of the filter; these local heterogeneities are often inherent to papermaking. The probability of forming continuous macro voids-channels through the full thickness of paper sharply decreases as the number of layers increases. Distorted channel alignment by multi-layered structure results in an increase in contact surface area that provides a more efficient adsorption. The presence of separators between layers increased adsorption capacity thanks to a well distributed liquid flow in constant flow mode. Filters had no rejection capability for PEG molecules. The thickest (400gsm-1x) and half thickness (200gsm-1x) filter structures filtered 0.5 µm particles at a very high rejection rate (98%). The rejection rate however decreased with multi-layer structures. Multi-layered composites provide better adsorption performances while filtration is best with single thick layers. This work highlights how engineering materials and operation can improve and change filtration and adsorption performance in filters. A novel generation of multi-layer depth inorganic-cellulose filters can provide new avenues for purification of temperature sensitive suspensions such as food and pharmaceutical streams. However, further studies are still required to fully characterize the filtration mechanisms of multi-layered filters.

3.9. ACKNOWLEDGEMENTS

This work was supported by the Graduate Research Industry Partnership (GRIP), Victorian Government, Monash University and 3M Australia. Thanks to the X-ray Microscopy Facility for Imaging Geo materials (XMFIG) for the image acquisition, Civil Engineering, Monash University. Daniel Pelliccia is acknowledged for expertise on 3D X-ray tomography image analysis.

3.10. REFERENCES

[1] K. Sutherland, "Depth filtration: Efficient separation processes through depth filtration," *Filtration + Separation,* vol. 48, pp. 12-15, 2011.

[2] N. Dizge, D. Y. Koseoglu-Imer, A. Karagunduz, and B. Keskinler, "Effects of cationic polyelectrolyte on filterability and fouling reduction of submerged membrane bioreactor (MBR)," *Journal of Membrane Science,* vol. 377, pp. 175-181, 2011.

[3] S. Goldrick, A. Joseph, M. Mollet, R. Turner, D. Gruber, S. S. Farid*, et al.*, "Predicting performance of constant flow depth filtration using constant pressure filtration data," *Journal of Membrane Science,* vol. 531, pp. 138-147, 2017.

[4] Y. S. Polyakov, "Depth filtration approach to the theory of standard blocking: Prediction of membrane permeation rate and selectivity," *Journal of Membrane Science,* vol. 322, pp. 81-90, 2008.

[5] P. Bedrikovetsky, Z. You, A. Badalyan, Y. Osipov, and L. Kuzmina, "Analytical model for straining-dominant large-retention depth filtration," *Chemical Engineering Journal,* vol. 330, pp. 1148-1159, 2017.

[6] M. Kuhn and H. Briesen, "Dynamic Modeling of Filter-Aid Filtration Including Surface- and Depth-Filtration Effects," *Chemical Engineering & Technology,* vol. 39, pp. 425-434, 2016.

[7] Y. S. Polyakov, "Effect of operating parameters and membrane characteristics on the permeate rate and selectivity of ultra- and microfiltration membranes in the depth filtration model," *Theoretical Foundations of Chemical Engineering,* vol. 43, p. 926, December 12 2009.

[8] J. Liderfelt and J. Royce, "Chapter 14 - Filtration Principles," in *Biopharmaceutical Processing*, ed: Elsevier, 2018, pp. 279-293.

[9] E. Iritani, N. Katagiri, T. Takenaka, and Y. Yamashita, "Membrane pore blocking during cake formation in constant pressure and constant flux dead-end microfiltration of very dilute colloids," *Chemical Engineering Science,* vol. 122, pp. 465-473, 2015.

[10] C. J. M. V. Rijn, "Membrane filter and a method of manufacturing the same as well as a membrane," US Patent No. US5753014A, May 19, 1998.

[11] K. H. W. M. W. K. Saefkow, "Filter for liquor filtration," US Patent No. US5462667A, Oct. 31, 1995.

[12] I. M. Griffiths, A. Kumar, and P. S. Stewart, "Designing asymmetric multilayered membrane filters with improved performance," *Journal of Membrane Science,* vol. 511, pp. 108-118, 2016.

[13] E. Koch, "Multi-layer filter," US Patent No. US4483771A, Nov. 20, 1984.

[14] J. A. Wertz, Guimond, D.M., "Filter media with a multi-layer structure," US Patent No. US 20140144113A1, May 29, 2014.

[15] A. Onur, A. Ng, G. Garnier, and W. Batchelor, "Engineering cellulose fibre inorganic composites for depth filtration and adsorption," *Separation and Purification Technology,* vol. 203, pp. 209-216, 9/12/ 2018.

[16] T. Obokata and A. Isogai, "The mechanism of wet-strength development of cellulose sheets prepared with polyamideamine-epichlorohydrin (PAE) resin," *Colloids and Surfaces A: Physicochemical and Engineering Aspects,* vol. 302, pp. 525-531, 7/20/ 2007.

[17] *CFR - Code of Federal Regulations Title 21*. Available: https://www.accessdata.fda.gov/scripts/cdrh/cfdocs/cfcfr/cfrsearch.cfm?fr=176.170

[18] M. Doğan, M. Alkan, and Y. Onganer, "Adsorption of Methylene Blue from Aqueous Solution onto Perlite," *Water, Air, and Soil Pollution,* vol. 120, pp. 229-248, June 01 2000.

[19] M. Alkan, Ö. Demirbaş, and M. Dogˇan, "Zeta potential of unexpanded and expanded perlite samples in various electrolyte media," *Microporous and Mesoporous Materials,* vol. 84, pp. 192-200, 2005.

[20] M. A. S. D. Barros, P. A. Arroyo, and E. A. Silva, "General Aspects of Aqueous Sorption Process in Fixed Beds," in *Mass Transfer - Advances in Sustainable Energy and Environment Oriented Numerical Modeling*, H. Nakajima, Ed., ed Rijeka: InTech, 2013, p. Ch. 14.

[21] G. Pearce, "Introduction to membranes: Filtration for water and wastewater treatment," *Filtration & Separation,* vol. 44, pp. 24-27, 2007.

[22] R. Holmstad, "Methods for paper structure characterisation by means of image analysis," Doctorate, Norges teknisk-naturvitenskapelige universitet, 2004.

[23] W. G. Siegfried Ripperger, Christian Alt, "Ullmann's Encyclopedia of Industrial Chemistry: Filtration, 1. Fundamentals," ed, 2000.

[24] S.-H. Yoon, *Membrane Bioreactor Processes Principles and Applications: Membrane Fouling*, 2016.

[25] F. G. Paulsen, S. S. Shojaie, and W. B. Krantz, "Effect of evaporation step on macrovoid formation in wet-cast polymeric membranes," *Journal of Membrane Science,* vol. 91, pp. 265-282, 1994.

[26] V. A. Kosma and K. G. Beltsios, "Macrovoids in solution-cast membranes: Direct probing of systems exhibiting horizontal macrovoid growth," *Journal of Membrane Science,* vol. 407-408, pp. 93-107, 2012.

[27] M. R. Rosenthal, S. United, and L. Forest Products, *Effective thickness of paper: appraisal and further development*. Madison, Wis.: Dept. of Agriculture, Forest Service, Forest Products Laboratory, 1977.

[28] R. P. Lopes, M. J. Mota, I. Delgadillo, and J. A. Saraiva, "Pasteurization: Effect on Sensory Quality and Nutrient Composition," in *Encyclopedia of Food and Health*, ed Oxford: Academic Press, 2016, pp. 246-263.

[29] E. Papafotopoulou-Patrinou, A. I. Gialleli, M. Kallis, S. Plessas, A. Alexopoulos, I. Mantzourani*, et al.*, "Microbiological assessment of tubular cellulose filters used for liquid foods cold pasteurization," *LWT - Food Science and Technology,* vol. 67, pp. 151-158, 2016.

[30] *MICROBIOLOGICAL HAZES AND DEPOSITS*. Available: https://www.awri.com.au/industry_support/winemaking_resources/fining-stabilities/hazes_and_deposits/microbiological/

[31] P. M. Tomasula, S. Mukhopadhyay, N. Datta, A. Porto-Fett, J. E. Call, J. B. Luchansky*, et al.*, "Pilot-scale crossflow-microfiltration and pasteurization to remove spores of Bacillus anthracis (Sterne) from milk1," *Journal of Dairy Science,* vol. 94, pp. 4277-4291, 2011.

[32] E. Wray, "12 - Reducing microbial spoilage of beer using pasteurisation," in *Brewing Microbiology*, A. E. Hill, Ed., ed Oxford: Woodhead Publishing, 2015, pp. 253-269.

THIS PAGE HAS BEEN INTENTIONALLY LEFT BLANK

CHAPTER 4

CELLULOSE FIBRE-PERLITE DEPTH FILTERS WITH NANOFIBRILLATED CELLULOSE TOP COATING FOR IMPROVED FILTRATION

THIS PAGE HAS BEEN INTENTIONALLY LEFT BLANK

PREFACE

In the previous Chapter, multi-layered filter structure was investigated and improved adsorption capacity was achieved. However, filters were still not capable of performing polyethylene glycol (PEG) molecule rejection. Also, filters inherently do not adsorb positively charged molecules due to the repulsive forces against positive charges of the filter medium. Therefore, there is still need for new functionalities developed in filters with small modifications on the structure.

This chapter explores coating a nanofibrillated cellulose (NFC) barrier layer on top of depth filters to achieve improved filtration performance. Depth filters were prepared as base sheets by cellulose fibres, perlite and polyamideamine-epichlorohydrin (PAE), using a papermaking technique. NFC barrier layers were coated on filters by spray coating technique. Different thicknesses of NFC layer were investigated on different properties of filters. Water flux, PEG molecule rejection and positively charged methylene blue (MB) dye adsorption were quantified with a dead-end filtration unit in a model system with no additional salt. Scanning electron microscopy (SEM) was used to characterise surface and cross-section morphologies. Air permeability of the filters was obtained to investigate the air barrier properties.

This chapter follows the third objective.

THIS PAGE HAS BEEN INTENTIONALLY LEFT BLANK

CHAPTER 4 CELLULOSE FIBRE-PERLITE DEPTH FILTERS WITH NANOFIBRILLATED CELLULOSE TOP COATING FOR IMPROVED FILTRATION

CELLULOSE FIBRE-PERLITE DEPTH FILTERS WITH NANOFIBRILLATED CELLULOSE TOP COATING FOR IMPROVED FILTRATION

Aysu Onur[1], Kirubanandan Shanmugam[1], Aaron Ng[2], Gil Garnier[1], Warren Batchelor[1*]

[1] Bioresource Processing Research Institute of Australia, Chemical Engineering Department, Monash University, Clayton, Australia

[2] 3M Australia, Sydney, Australia

*** Corresponding author at:** Bioresource Processing Research Institute of Australia, Chemical Engineering Department, Monash University, Clayton, Australia, 3800

Email address: warren.batchelor@monash.edu (W. Batchelor).

4.1. ABSTRACT

Depth type composite filters are used to remove contaminants from liquids by combining mechanical entrapment and adsorption. Commonly, depth filters can adsorb either anionic or cationic charged contaminants, but not both, as well as filter micron-sized particles. They can also adsorb any charged particles where mechanical filtration is not efficient to trap them. Therefore, there is still a need to improve the existing depth filter performance. In this study, we developed a two-layer filters with enhanced functionality by spray coating an anionically charged nanofibrillated cellulose (NFC) layer onto a cationically charged depth filter base sheet prepared via papermaking technique from wood pulp fibres, perlite adsorbent and cationic polyamideamine-epichlorohydrin (PAE) wet strength resin. The NFC coat weight ranged from 4 to 30 grams per square metre (gsm). The two layer filters were proven to have triple functionality, capable of adsorbing anionic molecules in the cationic depth filter layer, while the anionic NFC layer could adsorb cationic molecules and was also a microfiltration membrane. Increasing NFC coat weight improved performance but at the cost of lower flux. The optimum performance was found at an 8 gsm NFC coat weight, where the membrane layer rejected 80% of 5,000 kDa molecular weight polyethylene glycol, at a flux of 133 Litres per square meter per hour (LMH) under 1.5 bar pressure, while still achieving a good breakthrough curve when adsorbing cationic methylene blue dye.

4.2. KEYWORDS

Nanofibrillated cellulose; Spray coating; Depth filters; Filtration; Adsorption

4.3. INTRODUCTION

Depth filters are porous filtering mediums that are retaining contaminants throughout the thickness by both size-based and adsorption-based separations [1]. These filters are composed of cellulose fibres, a type of filter aid and a charged wet-strength polymer and they are mainly used for clarification of food and beverages as well as pharmaceuticals [2, 3]. Even though they are commercially available and used, there is still a need to improve the performance of the depth filters due to some limitations. For example, these filters are able to adsorb either anionic or cationic charged contaminants, but not both into one filter medium under very low salt concentrations [4]. Furthermore, the current depth filters still have unresolved challenges with the cost-effective removal of relatively small molecules. These limitations particularly were identified in our previous studies [5, 6]. Ideally, all these challenges should be addressed with the aid of renewable and sustainable materials to reduce the impact on the environment. Recently, nanofibrillated cellulose (NFC) is seen as a good candidate to meet these challenges.

The use of NFC in filters can particularly be seen in thin film nanofibrous composite (TFNC) membranes [7-11]. TFNC membranes typically consists of a multi-layered fibrous structure; a thin top barrier layer offering filtration function; a mid-layer fibrous scaffold made of electrospun nanofibres with large porosity and uniform continuous void structure minimizing the resistance of the membrane and giving a delicate support; and a bottom layer of a non-woven microfibrous substrate such as polyethylene terephthalate (PET) providing an overall mechanical support to the TFNC. However, the top barrier layer is the key component in these membranes for separation of solute and permeates and here the use of NFC as a barrier layer has been widely researched. NFC not only can have a similar performance to conventional materials as a top barrier layer, but also be able to offer new opportunities in water purification [12]. For example, the ultrafine cellulose nanofibres can be used as an adsorbent with a high adsorption efficiency to remove charged molecules, such as positively charged contaminant adsorption [13]. TFNC membrane concept has

been proven to be energy efficient for membrane filtration, and a nanocomposite cellulose barrier layer could potentially further help in improving energy efficiency [14-17].

In a recent study, Roy et al. studied the NFC coating on top of a tissue paper to add excellent membrane separation functionality to tissue paper [18]. Modified NFC was coated on tissue paper by spray coating technique and they reported that coated tissue papers showed outstanding separation performances towards a variety of oil/water mixtures. Additionally, coated tissue papers exhibited improved dye absorption capacity from aqueous solutions.

Following that, the same top layer approach could be applied to depth filters to improve their performance. Use of NFC as a barrier layer could be a route for the performance improvement with a low impact on environment thanks to the biodegradable and renewable feature of cellulose. Furthermore, an easy, rapid and eco-friendly technique, such as spray coating, should be employed for the coating of barrier layer. Spray coating was recently shown to be a rapid and inexpensive method for NFC film preparation [19, 20]. In this study, we spray-coated NFC barrier layers with weights per unit area ranging from 4 to 30 g/m^2 onto depth filter base sheets and have investigated water permeation flux, cationic and anionic dye adsorption and polyethylene glycol (PEG) rejection to characterise the performance of the two layer filters.

4.4. MATERIAL AND METHODS

4.4.1. Material

Unrefined northern softwood NIST RM 8495 bleached Kraft pulp from Procter and Gamble and Bleached radiata pine softwood Kraft pulp refined to 400 Canadian standard freeness (CSF) in a disk refiner are used for the base sheet preparation. Microfibrillated cellulose (MFC) purchased from DAICEL Chemical Industries Limited, Japan, (grade Celish KY-100S) was used as received for the top barrier layer preparation. MFC has 25% solids content and an average aspect ratio of 142 ± 28 with mean fibre diameter of 73 nm as reported in Varanasi et al. [21]. The MFC suspension, containing only cellulose and water, has a zeta potential of −22.3 mV [22]. Additionally, no chemical treatment such as TEMPO was applied on any type of cellulose fibres in this study.

Expanded perlite supplied by Dicalite Minerals Corp was used as inorganic fillers. Perlite is a low cost and an excellent filter aid made from a glassy volcanic rock [23]. It is an anionic adsorbent; the zeta potential is ranging between -40 to -50 mV [24]. The particle size distribution of perlite and its effect on the structure and porosity of filters was reported in a previous study [5]. Commercial PAE provided from Nopcobond Paper Technology Pty Ltd was used as a wet strength resin.

Positively charged methylene blue (MB) and negatively charged metanil yellow (MY) dyes supplied from Sigma Aldrich were used to characterise the adsorption properties. Polyethylene glycol (PEG) of two molecular weights (600 and 5,000 kDa) was provided by Dow Chemical for characterising the ultrafiltration and microfiltration capabilities of the filters. Dye and PEG solutions for testing were prepared using ultrapure water.

4.4.2. Methods

4.4.2.1. Preparation of base sheets

200 gsm base sheets were prepared by using a standard British hand sheet maker. A particular fibre and perlite composition with a constant polymer (PAE) dosage was used to form the sheets. The composition is given below.

- 30% Fibre (1/3 refined pulp + 2/3 unrefined pulp) + 70% Perlite + 120 mg PAE

This composition was used in our previous studies [5, 6]; however, due to its overall cationic charge it does not adsorb positively charged MB [5]. Preliminary experiments were also unable to detect any retention of PEG up to a molecular weight of 5,000 kDa.

To prepare the base sheet, the perlite suspension (1.4 wt%) was mixed with refined pulp suspension (0.1 wt%). Following that, the mixture is added to the unrefined pulp suspension (0.08 wt%) and PAE (0.22% w/v) was added at a rate of 100 mg/g fibre on top of the finished slurry. As the last stage, the slurry was hand mixed and poured into British hand sheet maker chamber. A 150 micron size mesh was used in the chamber with a wet strengthened qualitative filter paper deposited on top. Filter paper is used to obtain uniformity and maximise the retention. The sheets were formed on top of the filter paper by draining water. After sheet formation, the wet sheets were taken out from the mesh and placed between dry blotting papers for pressing under 345 kPa for 5 minutes in sheet

pressing machine. This is followed by curing for 5 minutes at 150°C. Cured sheets were further air-dried in a humidity-controlled room (23˚C, 50% relative humidity) for at least 24 hours.

4.4.2.2. Spray coating onto base sheets

NFC suspension for coating was prepared using MFC from DAICEL. 1 wt. % pulp suspension was prepared and disintegrated by a model MKIIIC, Messmer Instruments Ltd for 15,000 revolutions. Spray coating was performed using a Professional Wagner spray system (Model number 117) at a pressure of 200 bar. Before coating, the base sheets were placed onto stainless steel circular plates (diameter of 159 mm) and pre-wetted with water to improve the adhesion of the NFC layer. The detailed description of experimental system for spray coating can be found in Shanmugam et al. [19, 20]. The spray nozzle used in this work is Wagner 415, producing a spray jet angle and a beam width around 50° and 22.5 cm, respectively. The spray distance from spray nozzle to the circular steel plate is 30.0 ± 1.0 cm. NFC suspension consistency was kept constant at 1 wt. % and deposited mass of the NFC layer was controlled with varying conveyor speed levels which are 20, 40, 60, 80 and 100. The measured actual speeds of each level are respectively 533, 1333, 2182, 2667, 3429 mm/min. After spray coating, the filters were left on the circular plates and air-dried for 24 hours. Following air-drying, samples were kept in the humidity-controlled room for another 24 hours before any further testing.

4.4.2.3. Thickness and air flow testing

Thickness of the filters was measured before and after spray coating using L&W thickness tester. Average thickness of ten points was used to calculate the thickness of each sample. The weight of coated NFC layer was measured by weighing filters before and after spray coating. The grammage of each coating was then measured by dividing the weight of NFC layers by surface area of the filters. A L&W air permeance tester with an operating range from 0.003 to 100 µm/Pa.S was used to measure air permeance before and after coating. Two replicates were tested for each filter.

4.4.2.4. Scanning electron microscopy

FEI Magellan 400 FEG SEM were used to characterize surface and cross section morphology of filters. Samples were mounted onto a metal substrate using carbon tape and coated with a thin layer of

Iridium. Secondary electron images of composites were captured. 2kV of accelerating voltage was applied for magnification up to 10,000 X.

4.4.2.5. Adsorption and filtration properties

Adsorption and filtration experiments were carried out with a dead-end stirred cell from Merck Millipore Australia. For PEG filtration, TOC (Total Organic Carbon) analyser was used to analyse the PEG content of the filtrate. Dye concentration was measured at 10 second intervals with an ultraviolet-visible (UV-Vis) spectrometer with a quartz micro flow cell with 10 mm optical path length. Mass flux for the effective membrane area (0.00418 m^2) was calculated by measuring the mass of permeate as a function of time. The experimental procedure with a comprehensive schematic and flux equation can be found in our previous studies [5, 6].

The experiments were performed at 1.5 bar for both adsorption and filtration experiments. Before any adsorption and filtration testing, water flux was measured on the sheets at 1.5 bar with 400 ml ultra-pure water. Adsorption experiments were conducted with 400 mL of either 5 ppm MY or MB dye solutions and PEG filtration was done with 50 ml of 0.1% (wt./v) of either 600 or 5,000 kDa PEG. 0.1% (wt./v) PEG solution was prepared by adding 1 gram of polymer into 1000 ml pure water and stirring overnight. Two replicates were tested for each sample.

4.5. RESULTS

4.5.1. Nanofibrillated cellulose layer structure

4.5.1.1. Coated layer grammage

Figure 1 shows the different grammage of NFC layer coated on top of the base sheets as a function of conveyor speed.

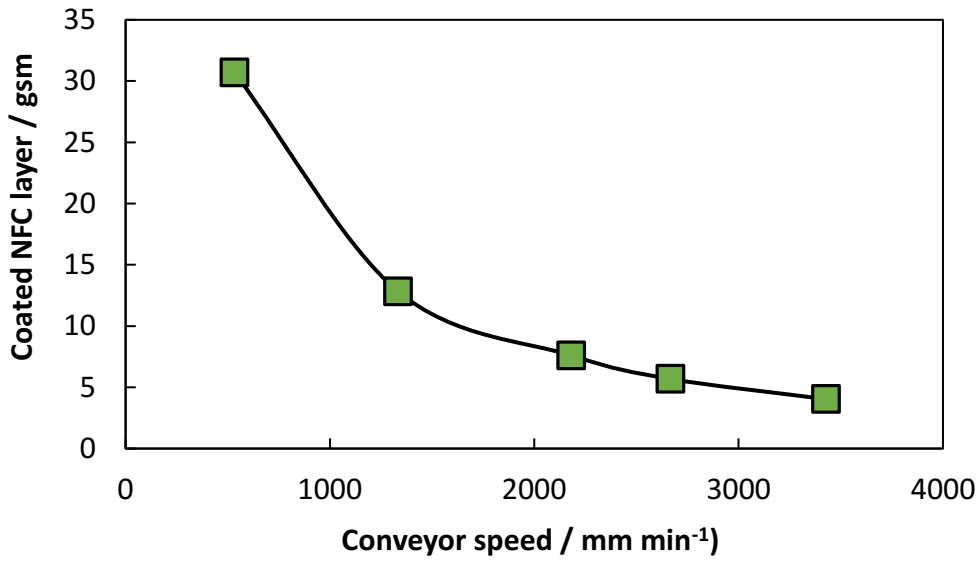

Figure 1: The grammage of top coating according to increasing conveyor speeds.

Figure 1 shows that we could get a 30 gsm NFC layer coated onto base sheet with the slowest speed (533 mm/min). However, increasing speeds result in less material transfer onto base sheets, which in turn decrease the total gsm of final products. The lowest gsm coated onto filters is around 4 gsm with the highest speed (3429 mm/min).

The thickness of coated layers onto base sheets is shown is Figure 2 in mm according to different coating grammages. The original base sheet thicknesses are ranging between 0.43 and 0.45 mm. The coated layer thicknesses onto base sheets are in the range of 0.0112 to 0.0405 mm; these thicknesses were obtained by NFC grammage between 4 and 30 gsm. The increase in thickness at 4 gsm is 28% of the increase in thickness at 30 gsm. The gradual increase indicates that NFC is not likely to intrude into the base layer. This can be also seen from the cross-section SEM image in the next section (Figure 4). Moreover, this is also consistent with measurements of the gel-point [21], which show that at the sprayed solids content of 1 wt.%, the fibres in the suspension will form a connected network, preventing them from adsorbing into the base sheet layer.

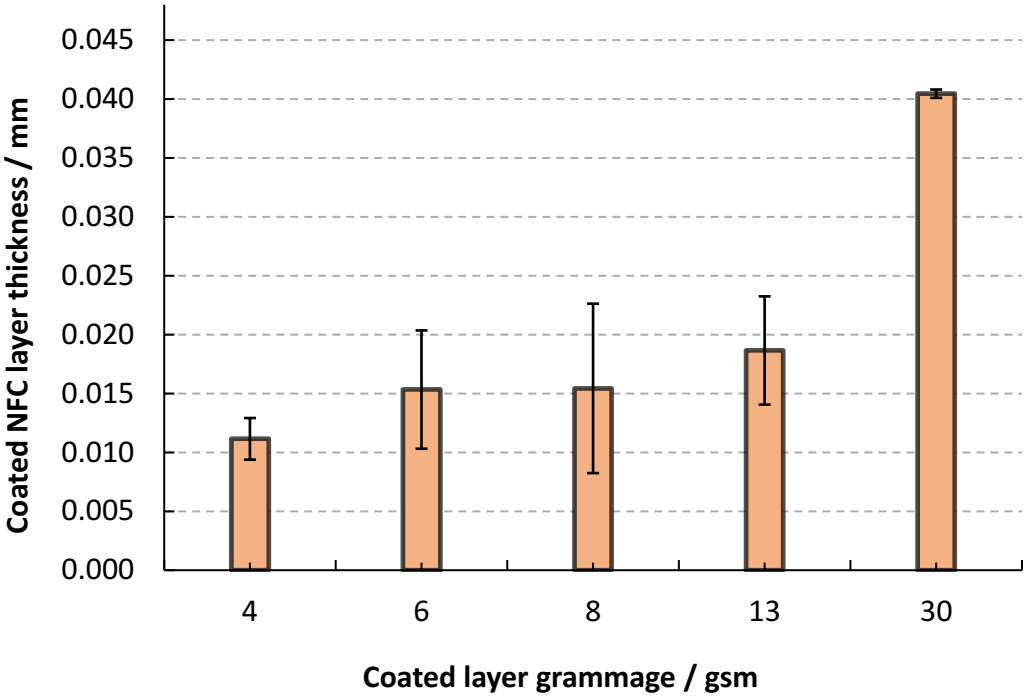

Figure 2: Thickness of coated layers according to different grammages.

4.5.1.2. Surface and cross section scanning electron microscopy images

Figure 3 shows the surface morphology of base sheet and samples coated with different grammages of NFC layer. The base sheet has a lot of perlite particles protruding from the surface. However, NFC layer successfully provides almost full surface coverage from 8 gsm coating upwards; neither of the high gsm coatings (13 and 30 gsm) show visible protruding through the coating. However, as the NFC layer thickness decreases, perlite particles begin to visibly protrude from the surface.

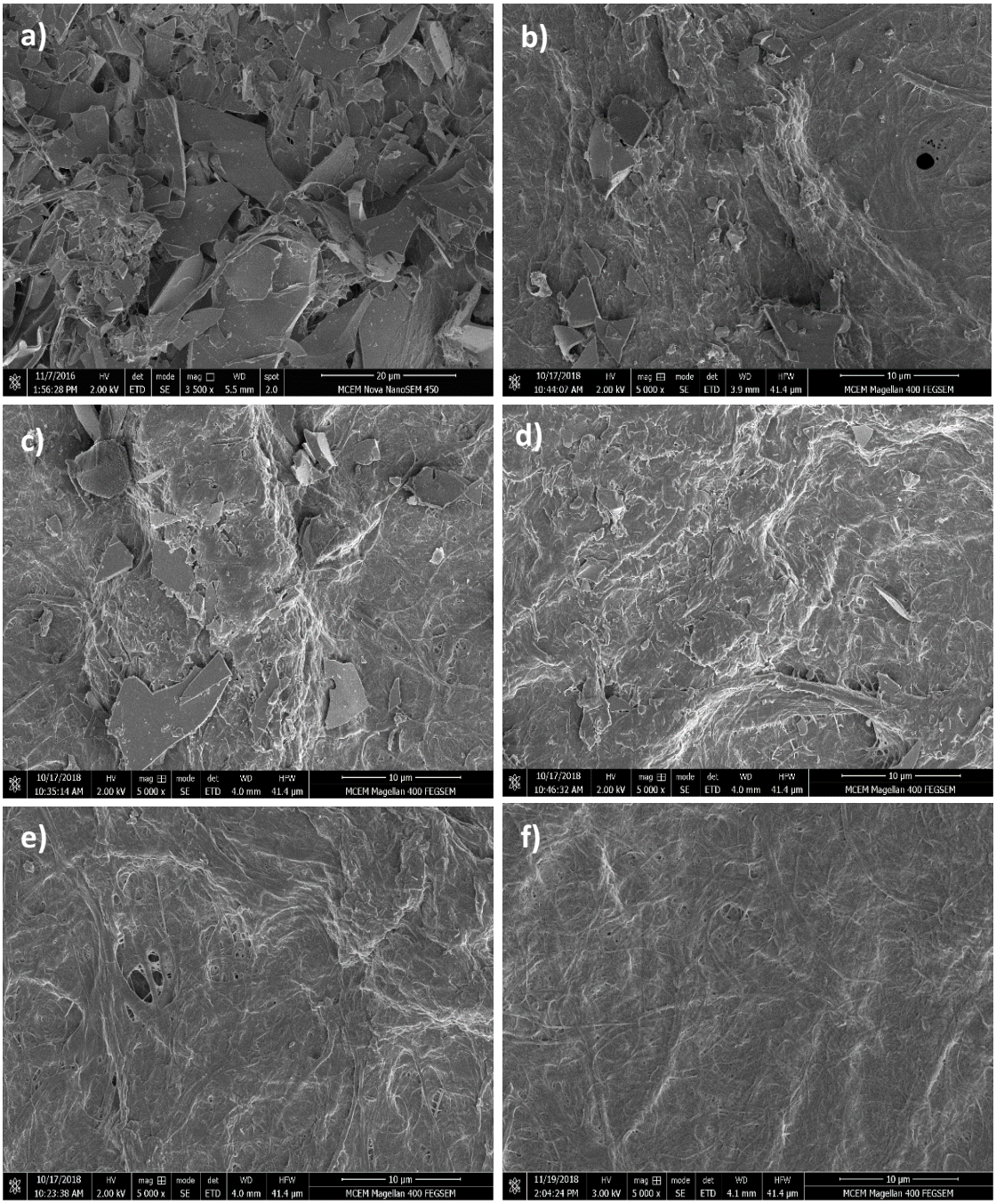

Figure 3: Surface SEM images of **a)** base sheet **b)** 4 gsm **c)** 6 gsm) **d)** 8 gsm **e)** 13 gsm **f)** 30 gsm NFC layers.

Figure 4 shows a cross-section of the sample with 6 gsm NFC layer, with the NFC layer on the right hand side of the image. The internal bonding between the NFC coating and base sheet can be seen in the image; the NFC layer is connected to the base sheet with extensive amount of bonding provided by high surface area of NFC. However, there is no evidence of fibres intruding into the base

sheet. The fibres seem to form a discrete smooth surface providing a full surface coverage on the base sheet. This is also in agreement with the gradual thickness increase of layers with increasing grammages (Figure 2).

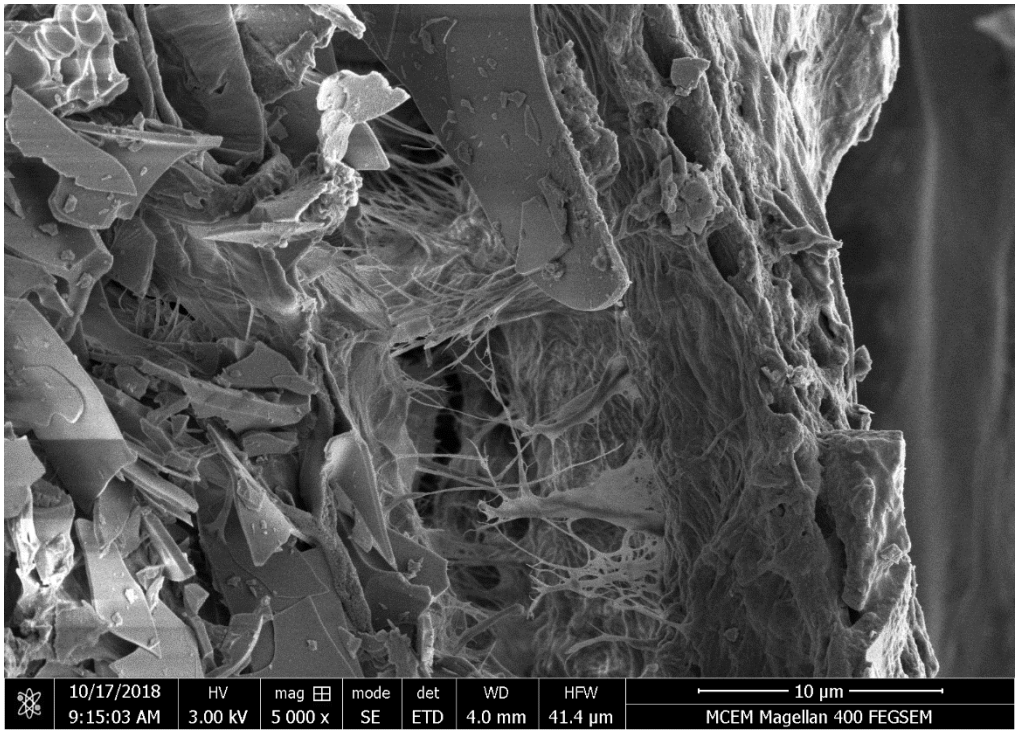

Figure 4: Cross section images of 6 gsm coated sample.

4.5.1.3. Air flow testing

Air flow testing is done to investigate the air barrier properties of samples that might be potentially improved by NFC coating. Figure 5 shows the air permeability of each filter in µm/Pa.s. Base sheet is quite porous with high permeability around 2.39 µm/Pa.s. 4 gsm coating on top of base sheet reduced the air permeability significantly by 83%. The thickest coating, 30 gsm, has a permeability of less than 0.003 µm/Pa.s, which is the lower measurement limit of the instrument. All these results confirm that even the thinnest 4 gsm sprayed NFC layer has successfully formed a continuous barrier layer.

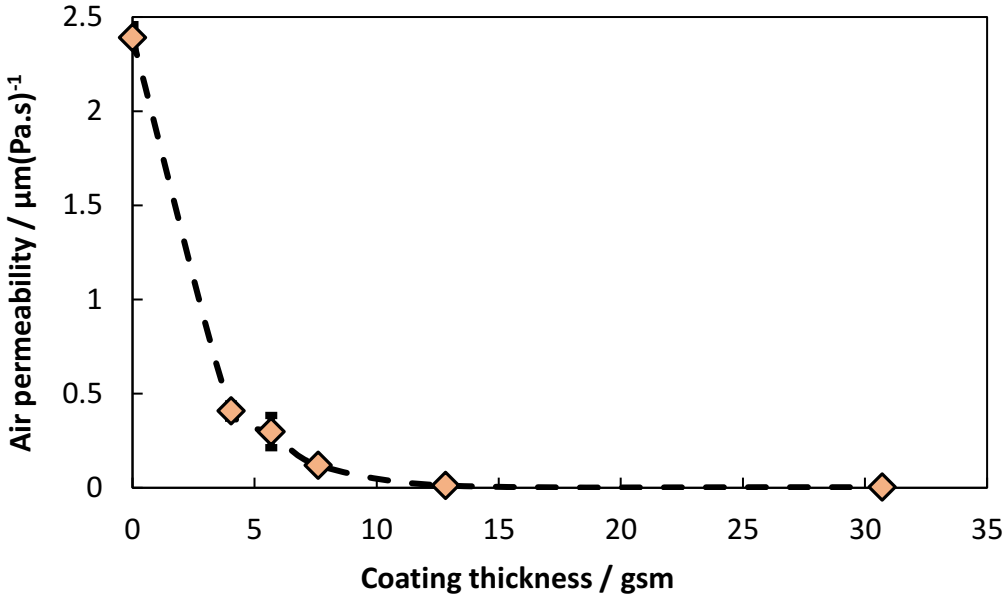

Figure 5: Air permeability of filters versus coating layer grammage.

4.5.2. Filtration performance

4.5.2.1. Water flux

Water flux of samples, as a function of coating layer grammage, is shown in Figure 6. The base sheet without any NFC layer (0 gsm) has the highest flux around 690 LMH. Even the lowest coating grammage (4 gsm) dropped flux by 51%. The gradual increase in the coating layer grammage decreased the water flux gradually where the thickest coating layer (30 gsm) only has a flux of around 15 LMH, which is a substantial decrease by 98% compared to base sheet. Our flux results are in a similar range with NFC membranes reported by Varanasi et al. [25].

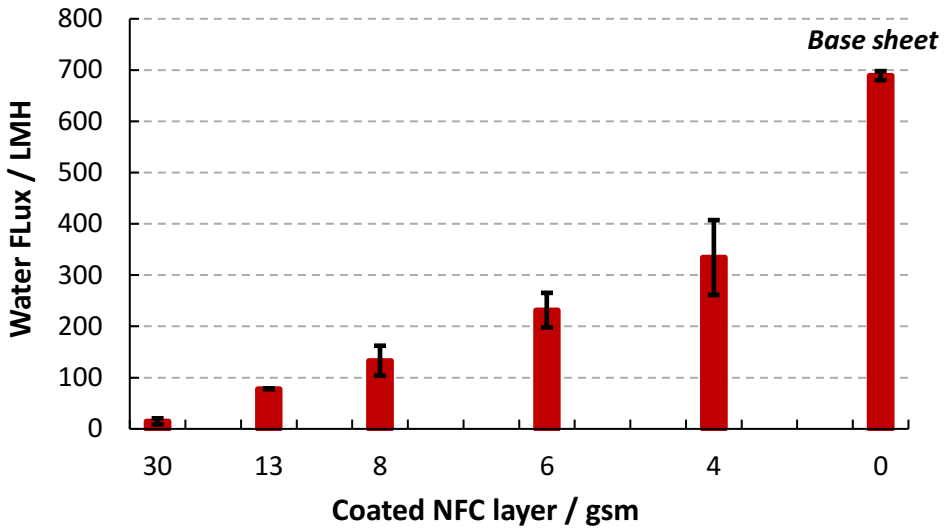

Figure 6: Water flux of samples versus coating layer grammage.

4.5.2.2. Polyethylene glycol filtration

Separation experiments by molecular weight were conducted with two different molecular weights of polyethylene glycol (PEG) (600 kDa and 5,000 kDa). The percentage rejected for each molecular weight is given in Figure 7 as a function of the grammage of NFC coating. The highest rejection achieved was 84% and 86% for 600 and 5,000 kDa PEG, respectively, at the thickest coating (30 gsm). The rejection for 5,000 kDa PEG is slightly higher than 600 kDa for 6 and 8 gsm coatings. This is expected as 5,000 kDa PEG molecules would be larger and more likely to be held by the filters. However, there is no rejection obtained with the base sheets for any of these molecular weights; these experiments were performed in our previous study [6]. Ultrafiltration membranes have MWCO reported in Dalton, ranging from 1000 Da to 1 MDa [26]. MWCO refers to the lowest molecular weight of a solute of which at least 90% can be retained by a membrane. 600 kDa can easily fall under ultrafiltration, where 5,000 kDa is in the smaller size ranges of microfiltration. Therefore, these results indicate that we could improve the rejection of different molecular weights by spraying NFC layer on top of the base filters. The full set of TOC results for each sample are given in SI (Table S1).

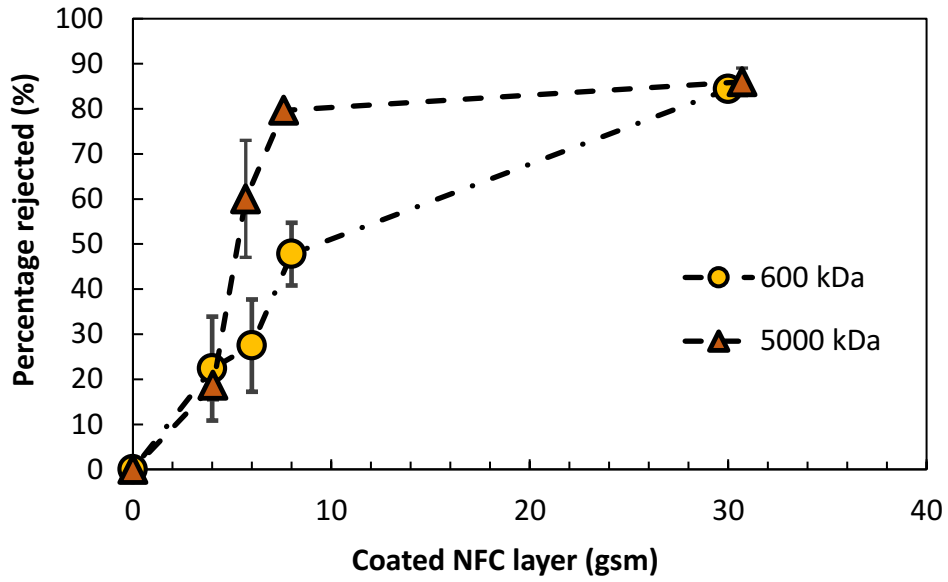

Figure 7: PEG rejection results with respect to different coating layer grammage and two different molecular weights of PEG.

4.5.2.3. Methylene blue adsorption

MB adsorption breakthrough curves are shown in Figure 8. Base sheets originally have very steep adsorption breakthrough curves which correspond to very poor adsorption. This can be attributed to the positive charge characteristics of the filters due to the presence of positively charged polymer PAE. As a result of repulsion between the filter media and positively charged methylene blue, very little adsorption occurs onto filters. However, our filters are very successful in terms of adsorbing negatively charged contaminants thanks to the presence of PAE. The negatively charged metanil yellow adsorption breakthrough curve of base sheet can be found in our previously published work [5]. In this study, we also aim to improve the positively charged contaminant adsorption onto filters besides adding filtration capabilities. Figure 8 shows that with the increasing NFC layer thickness, MB breakthrough curves are improving and more adsorption occurs onto filters. This can be also seen with the pictures taken after adsorption onto filters (Figure 9a). The layers become darker from left to right with increasing NFC thicknesses which indicates more MB adsorption on filters. On the other hand, figure 9b demonstrates the back side of the filters after adsorption. The back side is the base sheet and they all have the same very light intensity of blue colour; this proves that the

adsorption is mainly dependent on the top layer coating. The poor base sheet MB adsorption characteristics were not been impacted by the top coating in the manner suggested by the hypothesis stated earlier.

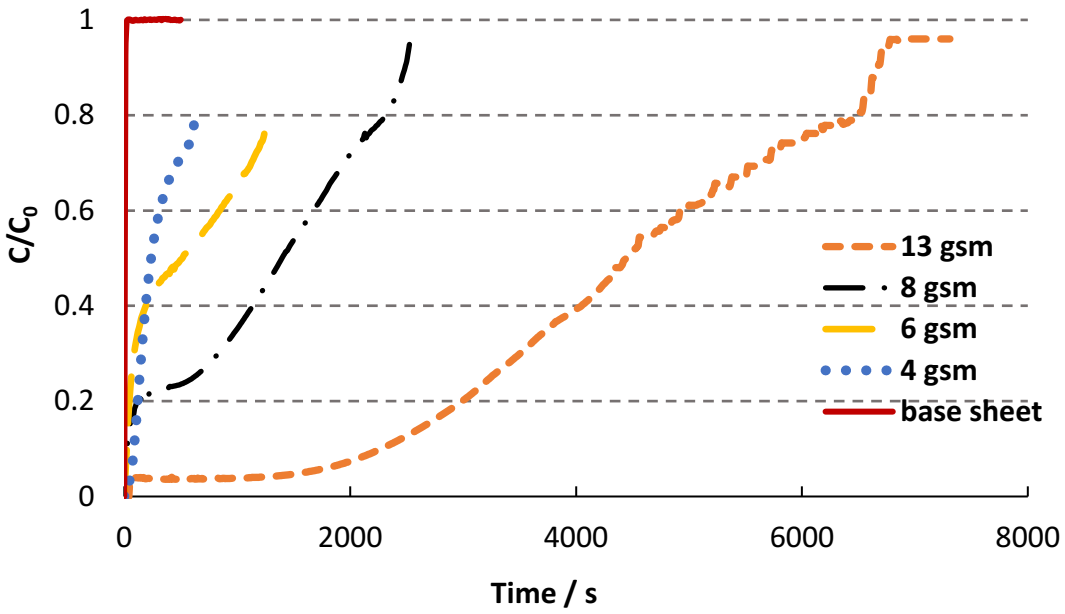

Figure 8: Methylene blue adsorption breakthrough curves as a function of NFC layer thicknesses.

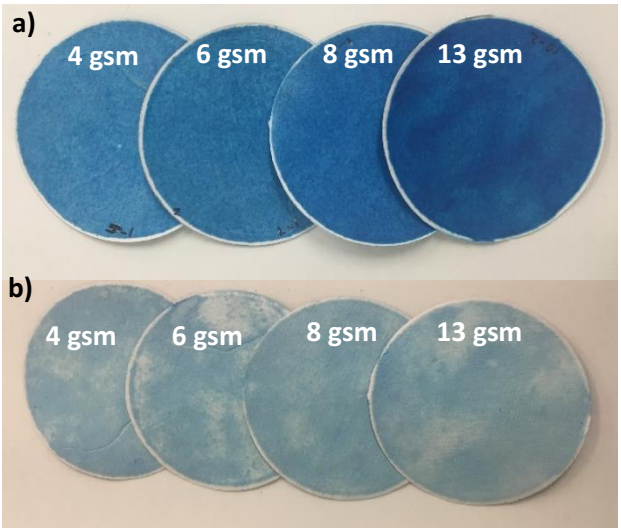

Figure 9: Pictures taken after methylene blue adsorption from **a)** the front side **b)** the back side of filters with different thicknesses of NFC layer.

Pictures of the sheet with 13 gsm NFC coating and the base sheet after MY adsorption are shown in Figure 10a and 10b, respectively. There is no adsorption onto NFC layer; metanil yellow is adsorbed onto the base sheet only.

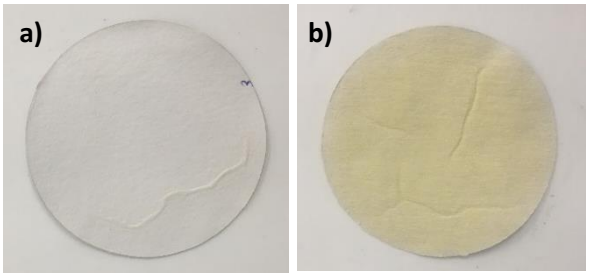

Figure 10: **a)** Composite sheet 13 gsm NFC layer after metanil yellow (MY) adsorption **b)** base sheet after MY adsorption.

4.6. DISCUSSION AND FUTURE PERSPECTIVE

This new two-layer filter developed here shows remarkable performance. While the positively charged cellulose-perlite depth filters are a well-established solution for adsorbing negatively charged contaminants, we have previously established that they have no adsorption of positively charged contaminants. In addition, the pore size distribution of our base sheet measured by mercury autopore technique is around 1-3 µm [5], which means that filtration by size exclusion is restricted to very large particles. In this work, we have prepared a dual layer system by spraying a second layer onto the previously developed depth filters. Spraying is a scalable and could readily be adapted for the production of these materials on an industrial scale.

Furthermore, the sprayed NFC layer is naturally negatively charged. The performance achieved has not required the use of any additional polyelectrolytes to control the charge. These negatively charged NFC fibres have formed a layer that has effectively bonded to the depth filter layer due to firstly, the small size of the fibres, which means that they are able to conform to the base layer. Secondly, the electrostatic interaction between the positively charged base layer and the negatively charged NFC layer provides additional bonding between the layers.

The new dual layer structure gives a highly promising triple functionality: microfiltration performance to reject particles by size, adsorption of positively charged contaminants in the negatively charged NFC membrane layer and adsorption of negatively charged contaminants in the

depth filter layer. In addition, the membrane layer protects the depth filter layer from becoming clogged from suspended particles. However, addition of such a barrier layer could also make the system susceptible to fouling in some cases where micron-sized particles are being separated as well. In this case, a NFC barrier layer might cause a rapid surface fouling. When using a barrier layer, the decision should be made based on the contaminants that are contained in the suspension.

The performance trade-off is also in the reduction of flux. Selection of the appropriate barrier layer grammage needs to be made. After consideration of all the results, the best grammage to balance separation performance against flux would be an 8 gsm layer. While this layer has reduced the flux at 1.5 bar pressure from 689 to 133 LMH, the two layer structure has achieved nearly 80% rejection of 5,000 kDa PEG and has not been fully saturated when filtering the positively charged dye.

4.7. CONCLUSION

This study has focused on the development of new functionalities for depth type filters by coating a top barrier layer. Depth filters were made by papermaking technique and used as base sheets. Following this, NFC was coated on top of the base sheets by spray coating technique. Different thickness of NFC layer was investigated for a variety of properties; water flux, adsorption and rejection of molecules by molecular weight. NFC is advantageous as a top barrier layer thanks to its highly connected network and smaller pore size distribution. This helps holding smaller molecules that base sheets individually are not able to do. We could obtain around 84% cut-off for two different molecular weights of PEG only with 30 gsm top coating. Moreover, negatively charged nature of NFC helps attracting positively charged molecules. MB dye breakthrough curves showed a remarkable improvement with increasing grammage of NFC layer. Surface and cross section morphologies were observed by SEM images and they indicate that NFC provides a smoother and more discrete surface coverage by increasing thickness of NFC.

Our study shows that NFC is a promising material to be used as a barrier layer on top of the filters. NFC's biodegradable and renewable nature also ensure that our filters are tailored without any chemical impact on the environment.

4.8. ACKNOWLEDGEMENTS

This work was supported by the Graduate Research Industry Partnership (GRIP), Victorian Government, Monash University and 3M Australia. The authors would like to acknowledge the Monash Centre for Electron Microscopy for the facilities used. The authors also would like to thank Prof. Huanting Wang for allowing us to use the facilities in his research lab and Ms Shasha Liu for the help with TOC analysis.

4.9. REFERENCES

[1] I. M. Hutten, "Chapter 7 - Liquid Filter Applications," in *Handbook of Nonwoven Filter Media (Second Edition)*Oxford: Butterworth-Heinemann, 2016, pp. 409-450.

[2] A. Bennett, "Pharmaceuticals and fine chemicals: Filtration and separation in the diverse fine chemical sectors," *Filtration + Separation,* vol. 50, no. 6, pp. 30-33, 2013/11/01/ 2013.

[3] K. Sutherland, "Filtration overview: A closer look at depth filtration," *Filtration & Separation,* vol. 45, no. 8, pp. 25-28, 2008/10/01/ 2008.

[4] H. Sehaqui, P. Spera, A. Huch, and T. Zimmermann, "Nanoparticles capture on cellulose nanofiber depth filters," *Carbohydrate Polymers,* vol. 201, pp. 482-489, 2018/12/01/ 2018.

[5] A. Onur, A. Ng, G. Garnier, and W. Batchelor, "Engineering cellulose fibre inorganic composites for depth filtration and adsorption," *Separation and Purification Technology,* vol. 203, pp. 209-216, 2018.

[6] A. Onur, A. Ng, W. Batchelor, and G. Garnier, "Multi-Layer Filters: Adsorption and Filtration Mechanisms for Improved Separation," (in English), *Frontiers in Chemistry,* Original Research vol. 6, no. 417, 2018-September-12 2018.

[7] H. Ma, C. Burger, B. S. Hsiao, and B. Chu, "Fabrication and characterization of cellulose nanofiber based thin-film nanofibrous composite membranes," *Journal of Membrane Science,* vol. 454, pp. 272-282, 2014/03/15/ 2014.

[8] H. Ma *et al.*, "High-flux thin-film nanofibrous composite ultrafiltration membranes containing cellulose barrier layer," *Journal of Materials Chemistry,* 10.1039/B922536F vol. 20, no. 22, pp. 4692-4704, 2010.

[9] X. Wang, H. Ma, B. Chu, and B. S. Hsiao, "Thin-film nanofibrous composite reverse osmosis membranes for desalination," *Desalination,* vol. 420, pp. 91-98, 2017/10/15/ 2017.

[10] X. Wang, D. Fang, B. S. Hsiao, and B. Chu, "Nanofiltration membranes based on thin-film nanofibrous composites," *Journal of Membrane Science,* vol. 469, pp. 188-197, 2014/11/01/ 2014.

[11] Z. Wang, H. Ma, B. S. Hsiao, and B. Chu, "Nanofibrous ultrafiltration membranes containing cross-linked poly(ethylene glycol) and cellulose nanofiber composite barrier layer," *Polymer,* vol. 55, no. 1, pp. 366-372, 2014/01/14/ 2014.

[12] H. Ma, C. Burger, B. S. Hsiao, and B. Chu, "Ultrafine Polysaccharide Nanofibrous Membranes for Water Purification," *Biomacromolecules,* vol. 12, no. 4, pp. 970-976, 2011/04/11 2011.

[13] H. Ma, B. S. Hsiao, and B. Chu, "Ultrafine Cellulose Nanofibers as Efficient Adsorbents for Removal of UO22+ in Water," *ACS Macro Letters,* vol. 1, no. 1, pp. 213-216, 2012/01/17 2012.

[14] H. Ma, C. Burger, B. S. Hsiao, and B. Chu, "Highly permeable polymer membranes containing directed channels for water purification," *ACS Macro Letters,* Article vol. 1, no. 6, pp. 723-726, 2012.

[15] K. Yoon, B. S. Hsiao, and B. Chu, "Functional nanofibers for environmental applications," *Journal of Materials Chemistry,* Article vol. 18, no. 44, pp. 5326-5334, 2008.

[16] H. Ma, C. Burger, B. S. Hsiao, and B. Chu, "Ultra-fine cellulose nanofibers: new nano-scale materials for water purification," *Journal of Materials Chemistry,* 10.1039/C0JM04308G vol. 21, no. 21, pp. 7507-7510, 2011.

[17] H. Ma, B. Chu, and B. S. Hsiao, "Functional nanofibers for water purification," in *Functional Nanofibers and their Applications*, 2012, pp. 331-370.

[18] S. Roy *et al.*, "One-step nanocellulose coating converts tissue paper into an efficient separation membrane," *Cellulose,* journal article vol. 25, no. 9, pp. 4871-4886, September 01 2018.

[19] K. Shanmugam, H. Doosthosseini, S. Varanasi, G. Garnier, and W. Batchelor, "Flexible spray coating process for smooth nanocellulose film production," *Cellulose,* journal article vol. 25, no. 3, pp. 1725-1741, March 01 2018.

[20] K. Shanmugam, S. Varanasi, G. Garnier, and W. Batchelor, "Rapid preparation of smooth nanocellulose films using spray coating," *Cellulose,* journal article vol. 24, no. 7, pp. 2669-2676, July 01 2017.

[21] S. Varanasi, R. He, and W. Batchelor, "Estimation of cellulose nanofibre aspect ratio from measurements of fibre suspension gel point," *Cellulose,* journal article vol. 20, no. 4, pp. 1885-1896, August 01 2013.

[22] P. Raj, A. Blanco, E. de la Fuente, W. Batchelor, C. Negro, and G. Garnier, "Microfibrilated cellulose as a model for soft colloid flocculation with polyelectrolytes," *Colloids and Surfaces A: Physicochemical and Engineering Aspects,* vol. 516, pp. 325-335, 2017/03/05/ 2017.

[23] M. Doğan, M. Alkan, and Y. Onganer, "Adsorption of Methylene Blue from Aqueous Solution onto Perlite," *Water, Air, and Soil Pollution,* journal article vol. 120, no. 3, pp. 229-248, June 01 2000.

[24] M. Alkan, Ö. Demirbaş, and M. Dogˇan, "Zeta potential of unexpanded and expanded perlite samples in various electrolyte media," *Microporous and Mesoporous Materials,* vol. 84, no. 1, pp. 192-200, 2005.

[25] S. Varanasi, Z.-X. Low, and W. Batchelor, "Cellulose nanofibre composite membranes – Biodegradable and recyclable UF membranes," *Chemical Engineering Journal,* vol. 265, pp. 138-146, 2015/04/01/ 2015.

[26] J. Liderfelt and J. Royce, "Chapter 14 - Filtration Principles," in *Biopharmaceutical Processing*: Elsevier, 2018, pp. 279-293.

THIS PAGE HAS BEEN INTENTIONALLY LEFT BLANK

CHAPTER 5

THE USE OF NANOFIBRILLATED CELLULOSE TO REDUCE THE WET STRENGTH POLYMER QUANTITY FOR DEVELOPMENT OF CLEANER FILTERS

THIS PAGE HAS BEEN INTENTIONALLY LEFT BLANK

PREFACE

In the previous Chapters, function of each component was investigated and we gained an insight into engineering internal structure and separation performance of the filters with different components. Furthermore, new advanced filters were structured for developing high performance filter products with additional functionalities. However, with the increasing demands towards sustainability and green chemistry, filters need to be in agreement with the regulations more. Current filters comprise the toxic wet strength chemical, polyamideamine-epichlorohydrin (PAE), which creates a challenge for both environment and food grade applications. Therefore, there should be more efforts to develop filters with greener components.

This chapter presents reducing the quantity of wet strength polymer, PAE, for a reduced impact on the environment and food grade applications. Filters were prepared by cellulose fibres, perlite and PAE. A very minor cellulose fibre composition was substituted for nanofibrillated cellulose (NFC), while reducing the PAE quantity gradually. Wet tensile index of the composites was obtained by Instron tensile testing system. Charge characteristics were investigated by zeta potential measurements. Additional polymers, polyethylenimine (PEI) and cationic polyacrylamide (CPAM), were used to recover any potential charge difference occurring in the composites. Adsorption was investigated with methylene blue (MB) dye in a dead-end filtration unit.

This chapter follows the fourth objective.

THIS PAGE HAS BEEN INTENTIONALLY LEFT BLANK

CHAPTER 5 THE USE OF NANOFIBRILLATED CELLULOSE TO REDUCE THE WET STRENGTH POLYMER QUANTITY FOR DEVELOPMENT OF CLEANER FILTERS

THIS PAGE HAS BEEN INTENTIONALLY LEFT BLANK

THE USE OF NANOFIBRILLATED CELLULOSE TO REDUCE THE WET STRENGTH POLYMER QUANTITY FOR DEVELOPMENT OF CLEANER FILTERS

Aysu Onur[a], Aaron Ng[b], Gil Garnier[a] and Warren Batchelor[a*]

[a] Bioresource Processing Research Institute of Australia, Department of Chemical Engineering, Monash University, Clayton, Australia 3800

[b] 3M Innovation Centre, North Ryde, Australia 2113

*** Corresponding author at:** Bioresource Processing Research Institute of Australia, Chemical Engineering Department, Monash University, Clayton, Australia, 3800

Email address: warren.batchelor@monash.edu (W. Batchelor).

5.1. ABSTRACT

Polyamideamine-epichlorohydrin resin (PAE) is one of the most commonly used wet strength agents in the papermaking industry. However, adsorbable organic halogens (AOX) are known to be a toxic side product of the PAE manufacturing process; therefore, the use of PAE is restricted by regulation for food and medical applications. In this study, we investigated partially replacing the indirect food additive, PAE, with a renewable, biodegradable material, nanofibrillated cellulose (NFC), in order to drastically reduce the amount of PAE used while maintaining the same wet tensile strength. The concept is to replace covalent bonds by hydrogen bonds and to drastically increase bonding area. Depth-type filters were prepared with cellulose (30%), perlite (70%) and lesser amounts of PAE via papermaking technique. A small fraction of cellulose fibre composition was substituted with NFC while the PAE amount was gradually decreased. The substitution of positively charged PAE for negatively charged nanofibrillated cellulose switched the overall charge of the system from cationic to anionic. Therefore, two cationic polyelectrolytes, CPAM or PEI, were investigated to control the overall charge and adsorption performance of the filter system.

The substitution of NFC enabled PAE dosage to be reduced by over 95% while retaining the wet strength properties of the filters. The wet strength obtained from the small quantity of wet strength polymer could be further improved by increasing the curing temperature to 150 °C with a much shorter curing period. The filters with reduced PAE dosage have also improved adsorption of positively charged contaminants. However, for negatively charged contaminants a very minor amount (around 20 mg/g) of cationic polymer addition would be required to maintain the performance. Our study shows that partial replacement of conventional papermaking fibres with nanofibrillated cellulose allows us to reduce the quantity of wet strength polymer remarkably and achieve a sustainable and environmentally-friendly concept for filter manufacturing or for any paper product requiring wet strength.

5.2. KEYWORDS

Nanofibrillated cellulose; Wet strength; Composite; Filter; Adsorption

5.3. INTRODUCTION

Wet strength is a critical property of certain paper products; it measures the ability of fibre network to maintain its original strength when it is wetted with an aqueous solution. Wet strength is critical for hygiene products such as paper towel and tissue paper [1, 2]. Moreover, cellulosic filters that are used in liquid filtration require a substantial wet strength as well to remain robust during operations.

Polyamideamine-epichlorohydrin (PAE) is by far the most common additive to manufacture wet strengthened papers [3]. Wet strength is developed through cross-linking the azetidinium groups with each other and with the cellulose [4]. These reactions generate a partial water-proof barrier around the fibre to fibre contact point which restricts water from hydrolysing the hydrogen bonds when the sheets are re-wetted.

However, epichlorohydrin-based products, such as PAE, have significant drawbacks. Both the manufacture and use of epichlorohydrin can produce a high adsorbable organic halogen (AOX) content in the process wastewater [5]. The toxic effects of AOX range from carcinogenic and mutagenic effects to acute and chronic toxicity and can inhibit microorganism growth [6-9].

A further problem with PAE strengthened products is that the majority of papers strengthened with epoxy thermosets cannot be easily recycled due to their irreversible 3-D crosslinked networks [10]. The used epoxy thermosets can only be incinerated or landfilled, or degraded to small molecules directly using strong acidic or basic agents [10].

An ideal solution from a broad cleaner production perspective would be one that retains the required product performance while:

1. Replacing the epichlorohydrin resins, with their toxic by-products in manufacture and use, with a non-hazardous alternative.
2. Facilitating recycling.
3. Using a locally sourced bio-derived alternative.

During the last two decades, nanofibrillated cellulose (NFC) have emerged as a promising alternative that can meet all these requirements. Cellulose is the most abundant polymer on Earth; it is renewable, biodegradable, non-toxic and chemically versatile [11]. Nanofibrillated cellulose is formed by breaking down cellulose fibres into their nano-scale cellulose microfibril building blocks [12]. NFC is thus fully chemically compatible with cellulose and can be recycled with the cellulose fibres. Almost any source of cellulose can be used, including agricultural and food processing residues [13] as well as the fibre degradation products from paper-mill processing [14], thus utilising the principles of industrial ecology.

Furthermore NFC is an outstanding sustainable reinforcement material [15, 16]. Use of NFC has emerged as a wet-end additive with potential applications as wet and dry strength agents as well as a coating to improve the barrier properties [12]. The contribution of NFC to strength can be achieved by two mechanisms [15]. Firstly, NFC promotes the bridging between fibres which increases the fibre to fibre contact, and in turn increases the bonded area. Secondly, web-like entangled structure of NFC brings larger fibres together creating a network, which boosts the load-bearing capacity of the paper. As a result, the final paper strength is achieved by both fibre to fibre contact and the NFC network.

While NFC is a promising alternative to resin-bonded products, it must still be demonstrated that the product performance has been maintained. In this study, we investigated the development of

cleaner food grade filters with the least amount of wet strength resin while delivering the same wet strength and adsorption properties as original filters with high PAE dosage. To achieve this, a particular fibre fraction was substituted with NFC without changing the total fibre composition. Filters were prepared with a variety of PAE dosages. Performance of NFC was examined as a wet strength agent, where effect of different variables such as curing conditions and addition order of raw materials were investigated on wet strength development. Adsorption performance was examined by two different oppositely charged dye molecules. Positively charged polyelectrolytes were used to maintain the similar charge and adsorption characteristics of the filters.

5.4. MATERIAL AND METHODS

5.4.1. Material

The cellulose fibres used for the composites were:

- Unrefined northern softwood NIST RM 8495 bleached Kraft pulp from Procter and Gamble
- Bleached radiata pine softwood Kraft pulp refined to 400 Canadian standard freeness (CSF) in a disk refiner
- NFC prepared by processing a 0.3 wt. % suspension of bleached radiata pine softwood Kraft pulp, that had been refined to 400 Canadian standard freeness, in a GEA Niro Soavi homogeniser at 800 bar pressure for 3 passes.

The fibre diameter distributions of homogenised and refined pulp were previously reported in our study [17] and are almost 50 and 25 nm for the nanofibre fraction of the refined and homogenised pulp, respectively. Expanded perlite supplied by Dicalite Minerals Corp was used as the inorganic absorbent. Commercial PAE provided from Nopcobond Paper Technology Pty Ltd was used as wet strength resin.

Negatively charged metanil yellow (MY) and positively charged methylene blue (MB) dyes supplied from Sigma Aldrich were used to investigate adsorption characteristics. The cationic polyacrylamide (CPAM) polymer was supplied by AQUA + TECH. The F1 grade with 13MDa molecular weight and 40% charge density was used. Polyethylenimine (PEI), branched with 10,000 Da molecular weight was purchased from Sigma Aldrich.

5.4.2. Methods

5.4.2.1. Preparation of filters

Filters were prepared by using a standard British hand sheet maker. Detailed step by step explanation of sheet making procedure can be found in our previously published study [17]. Filter suspensions were prepared by mixing pulp suspension with perlite and PAE (0.22 w/v %) or PAE & CPAM (0.1 wt. %) or PAE & PEI (0.1 wt. %) combinations with a variety of compositions. Filters prepared with different compositions and curing conditions were listed below.

1) 30% Fibre **(1/3 refined pulp +** 2/3 unrefined pulp**) +** 70% Perlite **+ 120 mg PAE-half an hour at 105°C *(Reference sample)***

2) 30% Fibre **(1/3 NFC +** 2/3 unrefined pulp**) +** 70% Perlite **+ (0-5-10-30-60-90-120 mg PAE) –half an hour at 105°C**

3) 30% Fibre **(1/3 NFC +** 2/3 unrefined pulp**) +** 70% Perlite **+ 5 mg PAE- one hour at 105°C**

4) 30% Fibre **(1/3 NFC +** 2/3 unrefined pulp**) +** 70% Perlite **+ 5 mg PAE- 5 minutes at 150°C *(tried by two different order of addition methods)***

5) 30% Fibre **(1/3 NFC +** 2/3 unrefined pulp**) +** 70% Perlite **+ 5 mg PAE & 25 mg CPAM-5 minutes at 150°C**

6) 30% Fibre **(1/3 NFC +** 2/3 unrefined pulp**) +** 70% Perlite **+ 5 mg PAE & 25 mg PEI-5 minutes at 150°C**

Suspensions were mixed by the following the order of addition in Figure 1a. Figure 1b was only used to investigate the effect of different order of additions on wet strength development by 5 mg PAE added sample cured at 150°C for 5 min. Mixing procedures were shown in Figure 1.

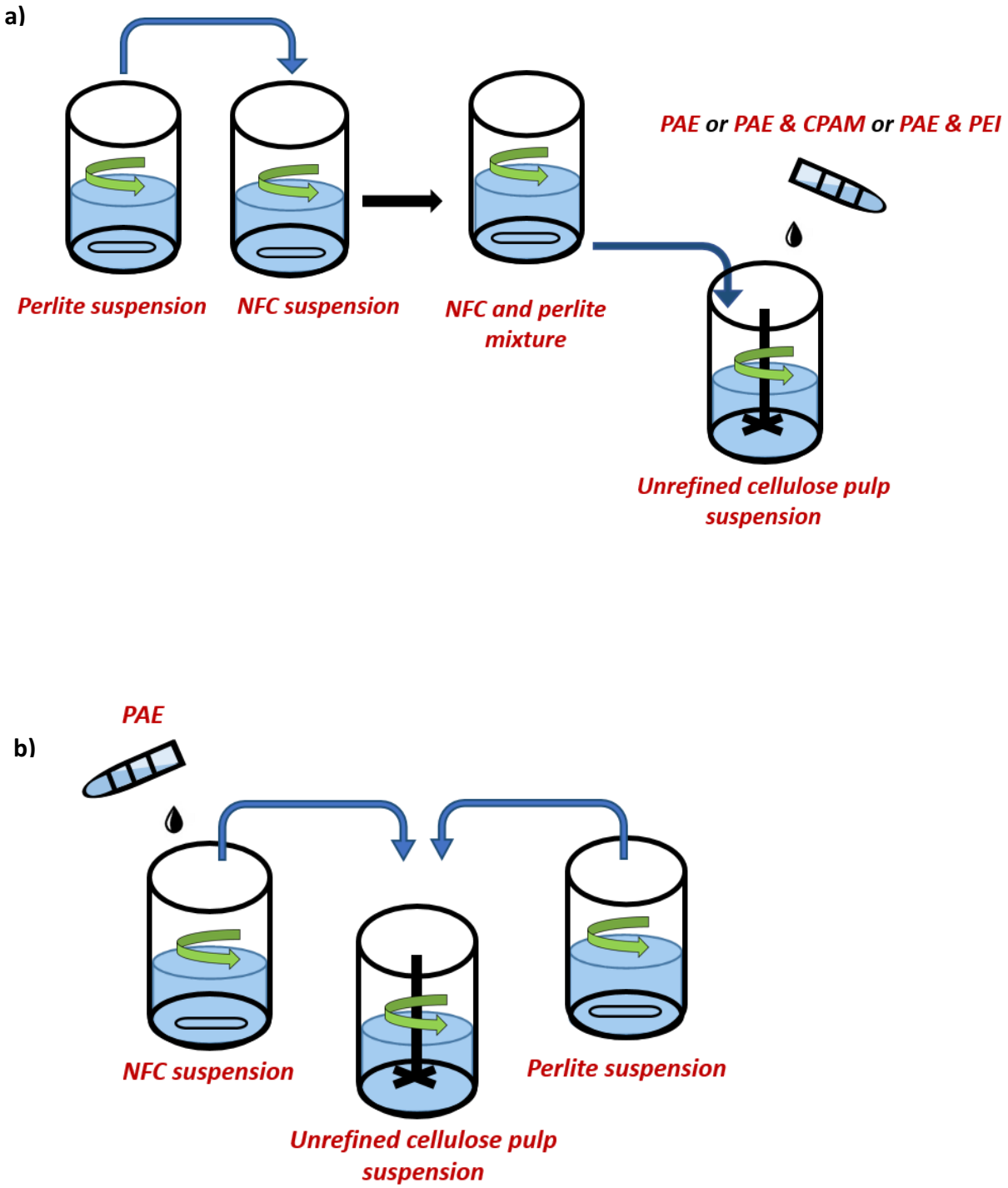

Figure 1: Graphical representation of mixture preparation procedures.

In Figure 1a, perlite is added to NFC suspension first and then the perlite and NFC mixture is added to unrefined cellulose pulp suspension. PAE or any other positively charged polymers used with PAE for charge modification were added at the end on top of the entire suspension. Combination of PAE

with other positively charged polymers was used to investigate the charge modification of the composites along with adsorption and wet strength properties.

In Figure 1b, PAE is added to NFC mixture first and then this mixture is added to unrefined pulp suspension. Perlite suspension was then added last.

All the filters were further air dried after oven treatment in a humidity controlled room for at least 24 hours prior to any further use.

5.4.2.2. Wet tensile strength measurements

Composites were conditioned in the humidity room at 23°C and 50% relative humidity at least for 24 hours prior to any mechanical testing. Thickness of the composites was measured using L&W thickness tester after conditioning. Average thickness of ten points was used to calculate the thickness of each sample. Following thickness measurements, each sample was cut into 15 mm wide strips using a sheet cutting machine. Wet strength measurements were conducted on an Instron model 5566 with a constant strain rate of 10 mm/min. At least 14 strips in total from two separately formed sheets for each sample was measured with a 100 ms test span. Sample strips were individually soaked in water for one minute before measurements. Tensile index for each sample was calculated as tensile load per unit width divided by grammage.

5.4.2.3. Zeta potential

Nanobrook Omni from Brookhaven Instruments was used to measure the zeta potential of suspensions. Small quantity of the suspensions was analysed in a cuvette cell at 25°C before papermaking. The electrophoretic mobility was determined using laser Doppler velocimetry and zeta potential was calculated based on the Smoluchowski equation.

5.4.2.4. Adsorption properties

A dead-end stirred cell working with constant pressure was used to carry out adsorption experiments with 400 mL MY and MB dye solutions. The experimental procedure was explained comprehensively in our previous study [17]. Effect of different compositions of charged polymers and NFC on charged dye molecule adsorption was investigated.

5.5. RESULTS

In this section, wet tensile index of the composites was measured as a function of critical variables: PAE dosage, curing conditions and PAE adsorption methodology. Charge characteristics of the composites were investigated by zeta potential measurements. Contaminant adsorption properties were tested using an anionic (MY) and a cationic (MB) dye. Cationic polyelectrolyte addition was also examined in terms of charge modification, adsorption characteristics as well as wet strength improvement.

5.5.1. Wet tensile index

5.5.1.1. Effect of PAE dosage

Wet tensile strength properties of composites with varying PAE dosages and pulp content are presented in Figure 2. The reference composite with refined pulp and 120 mg PAE has a wet tensile index of 5.78 Nm/g. Simultaneously substituting NFC for the refined pulp and eliminating PAE (Mixing procedure **(a)** in section 2.2.1 was used for sample preparation) reduced the wet tensile index to 2.80 Nm/g, showing that it is not possible to fully replace the PAE. The optimum PAE dosage with the NFC, which provides the reference wet strength, ranges between 5 mg and 7 mg under the usual curing condition and preparation technique.

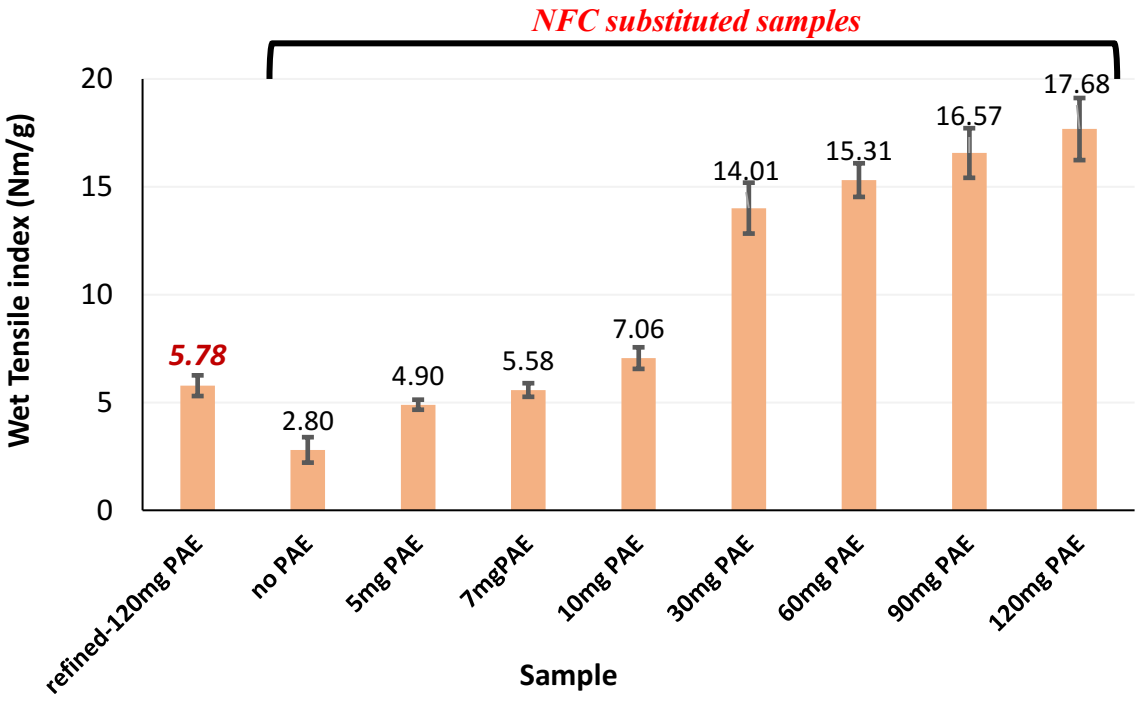

Figure 2: Effect of PAE dosage on wet tensile index of the composites. (Curing at 105˚C for 30 min).

5.5.1.2. Effect of curing conditions

The effect of curing condition was investigated with an addition level of 5 mg PAE. Samples were prepared with the procedure (Figure 1a) given in section 2.2.1. The composites were treated at 105°C for one hour and 150°C for 5 minutes, differing from the normal curing conditions (Figure 3). One hour treatment at 105°C and 5 minute curing at 150°C increased wet tensile index to 5.64 and 5.83 Nm/g, respectively. However, these differences are not statistically different from the reference material with 5.78 Nm/g. (T-test is given in supplementary material). It shows that either one hour treatment at 105°C or 5 minute treatment at 150°C can be selected with 5 mg PAE addition to achieve the same wet strength as the reference filter.

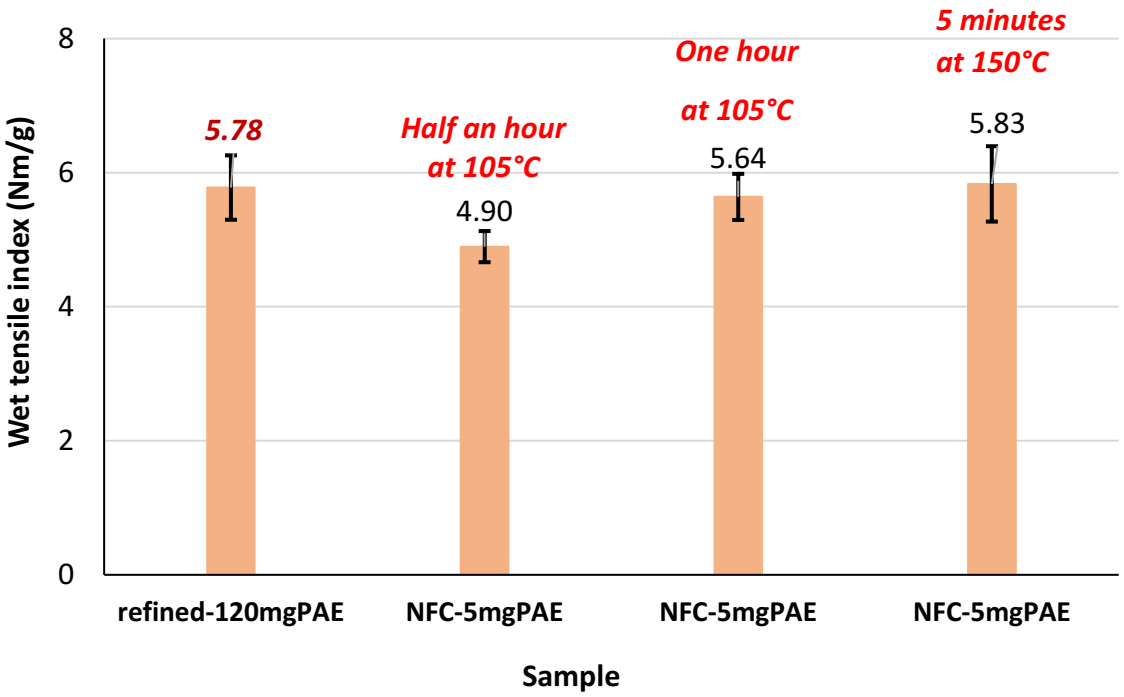

Figure 3: Effect of curing on wet tensile index of the composites (with 5 mg PAE dosage).

5.5.1.3. Effect of order of PAE addition

Here, PAE was added first to NFC and the mixture was then mixed to unrefined fibres (see section 2.2.1, Figure 1b); this differs from the previous method. Perlite suspension was added at the end and the resulting suspension was gently mixed before papermaking. Curing was set at 5 minutes, 150°C. The order of addition of resin to the fibres has no statistically significant effect (Figure 4; with T-test analysis in supplementary material).

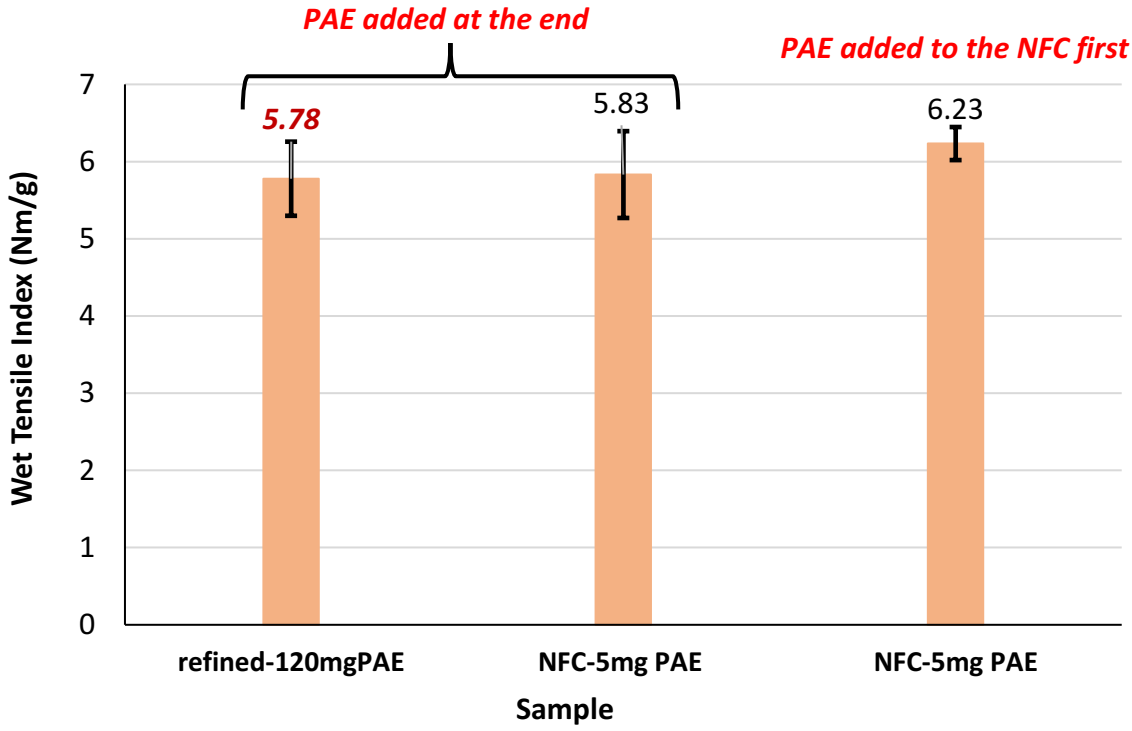

Figure 4: Effect of order of PAE addition on wet tensile index of the composites (Curing at 5 min., 150°C with 5 mg PAE).

5.5.2. Cationic polyelectrolyte addition: Zeta potential and wet strength improvement

As the reduction in PAE amount also changes the charge of filter medium, charge modification was investigated with two cationic polyelectrolytes, CPAM and PEI, differing in morphology to maintain the electrostatic adsorption properties. Sheets with CPAM and PEI were prepared by the method given in 2.1.1, Figure 1a. Zeta potential measurements of the critical composites are given in Figure 5. Results show that eliminating PAE dropped the electrical double layer net charge of the suspended particles from +30 mV to –37 mV, while charge is controlled from -27 mV to -15 mV by adding PAE up to 10 mg.

Substitution of 1/3 of the fibres by NFC decreased the zeta potential slightly, indicating an increase in negative charges from the surface of fibres upon homogenisation. Adding 25 mg of either CPAM or PEI with 5 mg PAE produced suspensions of zeta potential of +38 mV and +22 mV, respectively, which is essentially in the range of the reference material.

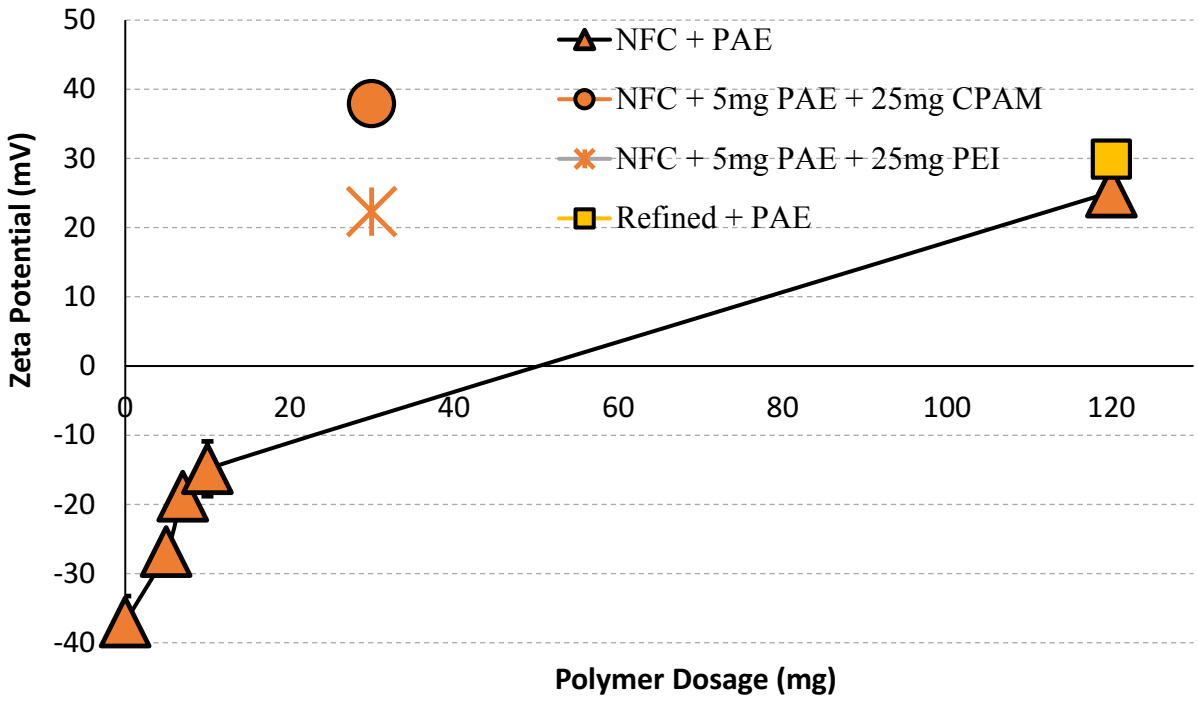

Figure 5: Zeta potential values of composites.

Addition of PEI or CPAM in combination with PAE was tested to investigate the contribution of polyelectrolytes on wet strength development (Figure 6). Adding 25 mg PEI with 5 mg PAE doubles the composite wet strength. However, CPAM did not improve the wet strength significantly.

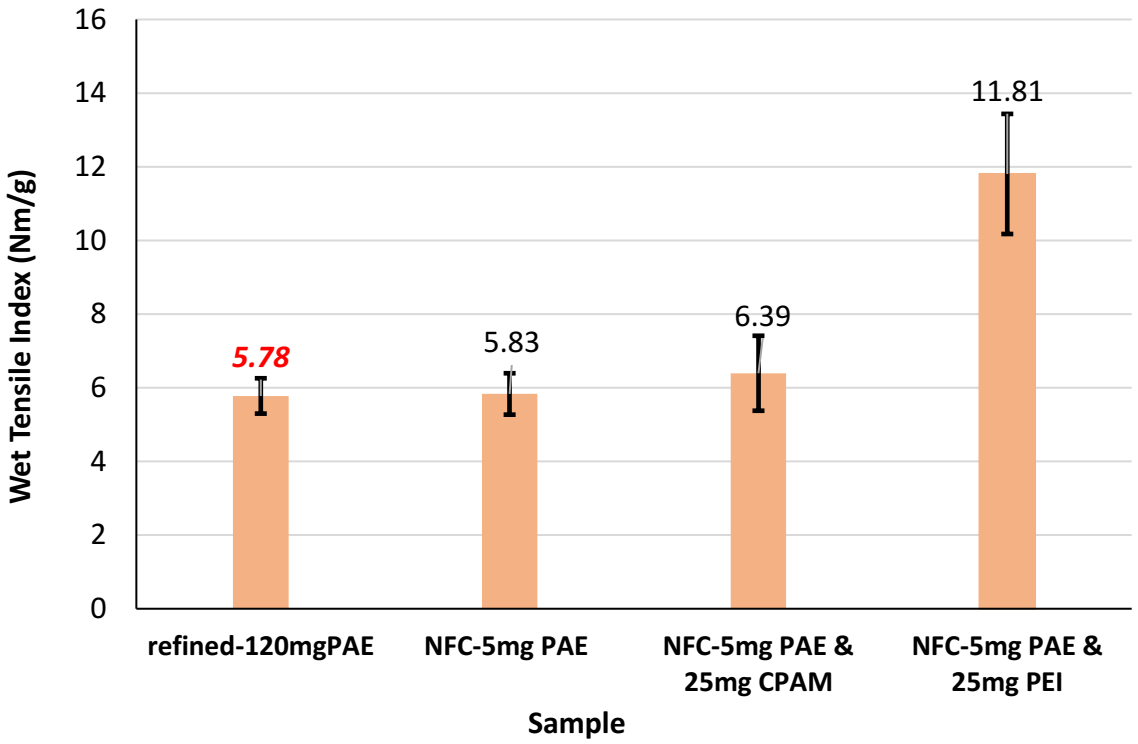

Figure 6: Wet tensile strength properties of composites with PAE & PEI and PAE & CPAM polymer mixtures.

5.5.3. Adsorption properties

The effect of adsorbing 400 mL of anionic metanil yellow (MY) or cationic methylene blue (MB) was quantified on different composites. Figure 7a and b show the metanil yellow and methylene blue adsorption breakthrough curves, respectively. The refined-120 mg PAE composite (reference sample) has a higher adsorption capacity for MY molecules than the composite with NFC, 5 mg PAE & 25 mg CPAM (Figure 7a). However, when CPAM is substituted for 25 mg PEI, the filter has a remarkable capacity for MY, even higher than that of the reference sample. Even though the zeta potential with combination of CPAM and PAE is similar to that of the reference sample, CPAM cannot provide the same adsorption characteristics with anionic MY. PEI addition (25 mg or less) combined with 5 mg PAE generates numerous positive charges, improving anionic contaminant adsorption onto the composites.

No additional polymer is needed for adsorbing the cationic methylene blue (Figure 7b). The sample with 5 mg PAE and NFC provides an improved adsorption capacity shown by the breakthrough curve.

Composites combining 5 mg PAE with NFC provide a remarkable separation of any cationic contaminant while retaining their original wet strength.

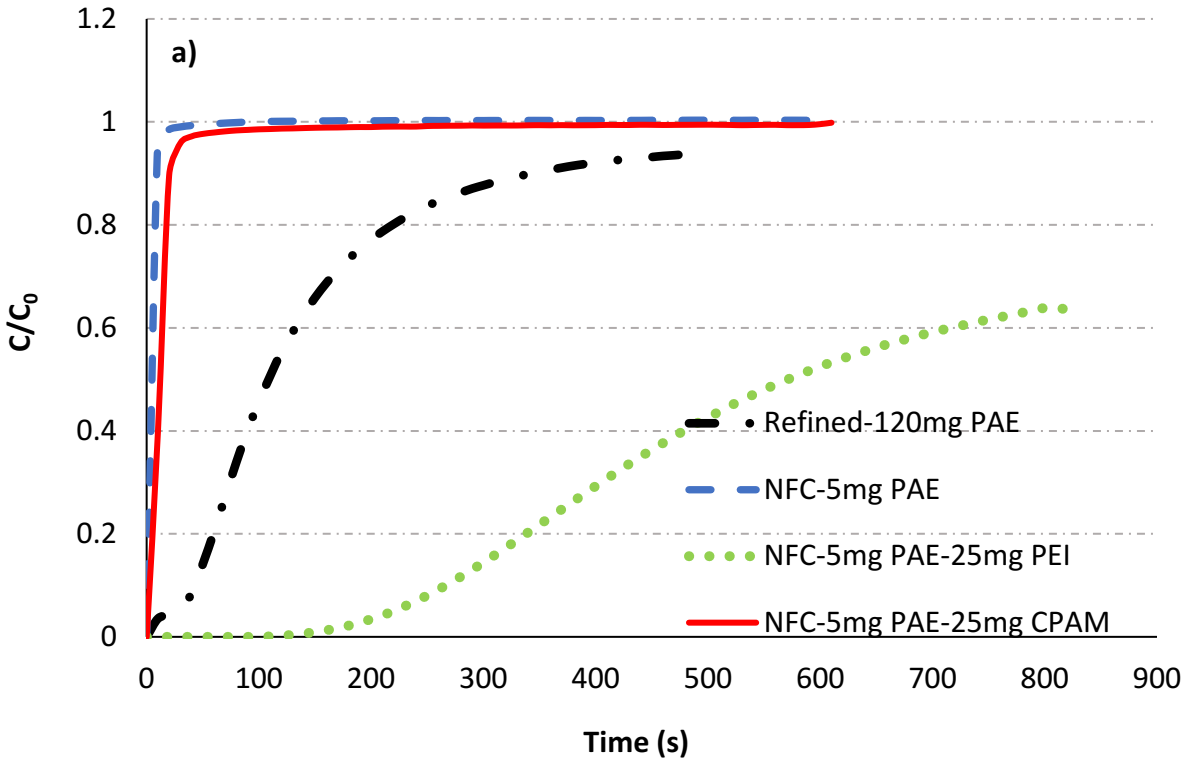

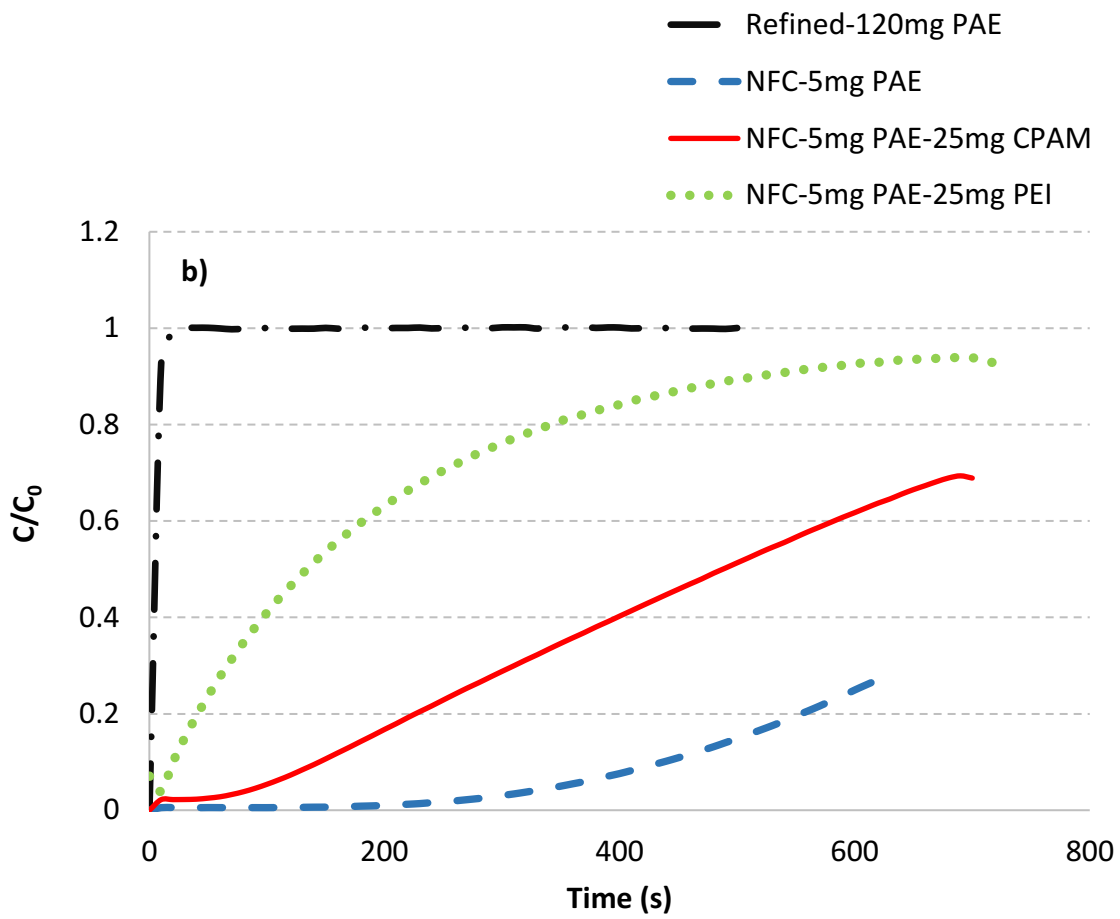

Figure 7: Adsorption breakthrough curves of composites with (**a)** metanil yellow (**b)** methylene blue.

5.6. DISCUSSION

Curing time and temperature are important variables affecting cellulosic composite wet strength at a given resin dosage. Optimising temperature and curing time can maximize the curing and crosslinking for the same amount of wet strength resin. The crosslinking of all PAE molecules on cellulose also minimizes their possible diffusion into the filtrate, an important requirement of filters in food or pharmaceutical applications. By efficient curing, either 5 min. at 150°C or 1 hour at 105°C, and substituting the refined fibre for NFC, the desired wet strength level was maintained while reducing the PAE usage by 95% (Figure 2 and 3). This is a substantial contribution from a broad cleaner production perspective. As discussed in the introduction, NFC can be made from any cellulosic material including agricultural waste and degradation products from paper-mill processing.

The straight-forward mechanical treatment we used here to produce NFC, with mechanical refining in a disk mill followed by homogenisation, does not require large factory floor area to implement and can be readily designed to any required capacity, thus allowing for on-site manufacture and use.

Adsorption in our filters is driven by electrostatic attractions between negatively and positively charged molecules. The original anionic charge of both cellulose and perlite favours the adsorption of cationic contaminants onto filters. On the other hand, cationic polymers can be adsorbed onto the fibres and perlite particles to promote anionic molecule adsorption onto filters. Charge modification is one of the reasons that PAE is used in filters in addition to the wet strength development. CPAM and PEI are the cationic polymers used in our study after PAE reduction to compensate for the loss of the positively charged PAE. Both polymers successfully helped regaining the charge characteristics. However, there is a significant difference between the adsorption behaviour of negatively charged molecules onto different samples prepared with either CPAM or PEI. CPAM is a linear and high molecular weight polymer forming flexible random coil configurations, whereas PEI is a highly branched polymer with a high charge density and much lower molecular weight. These two polymers have been previously studied and the effect of polyelectrolyte morphology on the adsorption and flocculation of micro fibrillated cellulose (MFC) was analysed [18]. Polyelectrolytes adsorb onto surfaces of opposite charges by electrostatic attractions. Equilibrium conformation of an adsorbed linear polymer chain is as a tails and loops configuration [19]. The size of the loops can be reduced if the strength of the electrostatic interaction with the surface increases. CPAM bridges with a flattened conformation onto cellulose resulting in a smaller accessible area for negatively charged molecule adsorption. However, a branched polymer, such as PEI, adsorbs onto fibres as large rigid bridges by maintaining its shape without reconformation and flattening [20] and leaving both the polymer and the surface more accessible to interact with the surrounding molecules. Anionic MY adsorbs onto PEI treated composites more efficiently than on CPAM treated composites; this is because most of the charges remain accessible in contrast to CPAM. PEI is a promising dendrimer to be used in conjunction with 5 mg PAE to retain adsorption characteristics. PEI also contributes to wet strength significantly (Fig. 6); a minute amount of PEI alone should be enough for both negatively charged molecule adsorption as well as wet strength

development. While the contribution of cationic polymers to paper strength was already reported [21, 22], the significant effect of PEI on wet strength was unexpected.

In the work here, we have shown that we can almost entirely replace PAE wet strength resin with NFC. That is, we are substituting a product with a long supply chain, a short shelf life and toxic by-products in manufacture and use with NFC, a biodegradable, renewable material which can be produced on-site from waste, thus promoting both industrial ecology and the circular economy.

This innovation also addresses the aspect of design for recycling. NFC, being composed only of cellulose is thus fully chemically compatible with micron-diameter cellulose fibres that are used to make paper. In fact, NFC has been widely investigated as a reinforcing fibre to improve the strength of conventional paper sheets [23, 24], due to its outstanding web-like entangled structure, high aspect ratio and high strength [25]. The achievement of the required wet-strength, largely using only cellulose fibre-NFC hydrogen bonding and minimising cross-linking will allow re-dispersion in water. Thus filters wet-strengthened with NFC should be recyclable within a conventional paper recycling process, possibly with enhanced initial dispersion, because of the high wet strength.

5.7. CONCLUSION

This study investigated reducing the quantity of wet strength resin, PAE used in cellulosic filter products by substituting a renewable, biodegradable material, nanofibrillated cellulose (NFC). Substituting NFC for refined fibre allowed us to reduce PAE content by 95% while retaining full wet strength. In addition, the use of PEI to substitute for the cationic charge lost upon removal of the PAE was found to allow for the adsorption of both negatively and positively charged contaminants, in comparison to filters prepared with PAE, which only adsorbed negatively charged contaminants. This substantial reduction in PAE usage is particularly interesting for cellulosic filters used in beverage filtration applications. PAE is used as an indirect food additive in these type of filter products and the allowed concentration is very limited. Therefore, NFC substitution is a promising strategy for high performance cellulose fibre based filters while reducing PAE usage by 95%, drastically reducing AOX generation in PAE production and application. NFC's biodegradable and renewable nature provides cleaner products by significantly reducing the chemical impact on the

environment and should be further investigated for any paper product currently using PAE to develop the required wet-strength.

5.8. ACKNOWLEDGEMENTS

This work was supported by the Graduate Research Industry Partnership (GRIP), Victorian Government, Monash University and 3M Australia.

5.9. REFERENCES

[1] P. Bajpai, "Chapter 4 - Additives for Papermaking," in *Biermann's Handbook of Pulp and Paper (Third Edition)*, P. Bajpai, Ed., ed: Elsevier, 2018, pp. 77-94.

[2] S. Zakaria, "Development of wet-strength paper with dianhydride and diacid," *Materials Chemistry and Physics,* vol. 88, pp. 239-243, 2004/12/15/ 2004.

[3] T. Obokata, M. Yanagisawa, and A. Isogai, "Characterization of polyamideamine-epichlorohydrin (PAE) resin: Roles of azetidinium groups and molecular mass of PAE in wet strength development of paper prepared with PAE," *Journal of Applied Polymer Science,* vol. 97, pp. 2249-2255, 2005.

[4] T. Obokata and A. Isogai, "The mechanism of wet-strength development of cellulose sheets prepared with polyamideamine-epichlorohydrin (PAE) resin," *Colloids and Surfaces A: Physicochemical and Engineering Aspects,* vol. 302, pp. 525-531, 7/20/ 2007.

[5] J. W. J. Cornel Hagiopol, *Chemistry of Modern Papermaking*: CRC Press, 2011.

[6] N. S. Deshmukh, K. L. Lapsiya, D. V. Savant, S. A. Chiplonkar, T. Y. Yeole, P. K. Dhakephalkar*, et al.*, "Upflow anaerobic filter for the degradation of adsorbable organic halides (AOX) from bleach composite wastewater of pulp and paper industry," *Chemosphere,* vol. 75, pp. 1179-1185, 2009/05/01/ 2009.

[7] W. H. W. Osman, S. R. S. Abdullah, A. B. Mohamad, A. A. H. Kadhum, and R. A. Rahman, "Simultaneous removal of AOX and COD from real recycled paper wastewater using GAC-SBBR," *Journal of Environmental Management,* vol. 121, pp. 80-86, 2013/05/30/ 2013.

[8] D. V. Savant, R. Abdul-Rahman, and D. R. Ranade, "Anaerobic degradation of adsorbable organic halides (AOX) from pulp and paper industry wastewater," *Bioresource Technology,* vol. 97, pp. 1092-1104, 2006/06/01/ 2006.

[9] G. Müller, "Sense or no-sense of the sum parameter for water soluble “adsorbable organic halogens” (AOX) and “absorbed organic halogens” (AOX-S18) for the assessment of organohalogens in sludges and sediments," *Chemosphere,* vol. 52, pp. 371-379, 2003/07/01/ 2003.

[10] Y. Min, S. Huang, Y. Wang, Z. Zhang, B. Du, X. Zhang*, et al.*, "Sonochemical Transformation of Epoxy–Amine Thermoset into Soluble and Reusable Polymers," *Macromolecules,* vol. 48, pp. 316-322, 2015/01/27 2015.

[11] A. Dufresne, "Nanocellulose: a new ageless bionanomaterial," *Materials Today,* vol. 16, pp. 220-227, 6// 2013.

[12] N. Lavoine, I. Desloges, A. Dufresne, and J. Bras, "Microfibrillated cellulose – Its barrier properties and applications in cellulosic materials: A review," *Carbohydrate Polymers,* vol. 90, pp. 735-764, 10/1/ 2012.

[13] S. Varanasi, L. Henzel, S. Sharman, W. Batchelor, and G. Garnier, "Producing nanofibres from carrots with a chemical-free process," *Carbohydrate Polymers,* vol. 184, pp. 307-314, 2018.

[14] T. Gunawardhana, P. Banham, D. E. Richardson, A. F. Patti, and W. Batchelor, "Upgrading waste whitewater fines from a pinus radiata thermomechanical pulping mill," *Nord. Pulp Pap. Res. J.,* vol. 32, pp. 656-665, 2017.

[15] S. Boufi, I. González, M. Delgado-Aguilar, Q. Tarrès, M. À. Pèlach, and P. Mutjé, "Nanofibrillated cellulose as an additive in papermaking process: A review," *Carbohydrate Polymers,* vol. 154, pp. 151-166, 2016/12/10/ 2016.

[16] M. R. Sanjay, P. Madhu, M. Jawaid, P. Senthamaraikannan, S. Senthil, and S. Pradeep, "Characterization and properties of natural fiber polymer composites: A comprehensive review," *Journal of Cleaner Production,* vol. 172, pp. 566-581, 2018/01/20/ 2018.

[17] A. Onur, A. Ng, G. Garnier, and W. Batchelor, "Engineering cellulose fibre inorganic composites for depth filtration and adsorption," *Separation and Purification Technology,* vol. 203, pp. 209-216, 2018.

[18] P. Raj, W. Batchelor, A. Blanco, E. de la Fuente, C. Negro, and G. Garnier, "Effect of polyelectrolyte morphology and adsorption on the mechanism of nanocellulose flocculation," *Journal of Colloid and Interface Science,* vol. 481, pp. 158-167, 2016/11/01/ 2016.

[19] J. Gregory and S. Barany, "Adsorption and flocculation by polymers and polymer mixtures," *Advances in Colloid and Interface Science,* vol. 169, pp. 1-12, 2011/11/14/ 2011.

[20] Á. Blanco, E. Fuente, M. C. Monte, N. Cortés, and C. Negro, "Polymeric Branched Flocculant Effect on the Flocculation Process of Pulp Suspensions in the Papermaking Industry," *Industrial & Engineering Chemistry Research,* vol. 48, pp. 4826-4836, 2009/05/20 2009.

[21] M. Rahmaninia, M. Rohi, M. A. Hubbe, S. M. Zabihzadeh, and O. Ramezani, "The performance of chitosan with bentonite microparticles as wet-end additive system for paper reinforcement," *Carbohydrate Polymers,* vol. 179, pp. 328-332, 2018/01/01/ 2018.

[22] M. C. Rice, L. Pal, R. Gonzalez, and M. A. Hubbe, "Wet-end addition of nanofibrillated cellulose pretreated with cationic starch to achieve paper strength with less refining and higher bulk," *Tappı Journal* vol. 17, pp. 395-403, 2018.

[23] J. Su, W. K. J. Mosse, S. Sharman, W. J. Batchelor, and G. Garnier, "Effect of tethered and free microfibrillated cellulose (MFC) on the properties of paper composites," *Cellulose,* vol. 20, pp. 1925-1935, 2013/05/28 2013.

[24] T. Taipale, M. Österberg, A. Nykänen, J. Ruokolainen, and J. Laine, "Effect of microfibrillated cellulose and fines on the drainage of kraft pulp suspension and paper strength," *Cellulose,* vol. 17, pp. 1005-1020, 2010.

[25] Q. Li, W. Chen, Y. Li, X. Guo, S. Song, Q. Wang*, et al.*, "Comparative study of the structure, mechanical and thermomechanical properties of cellulose nanopapers with different thickness," *Cellulose,* vol. 23, pp. 1375-1382, 2016.

CHAPTER 6

CONCLUSION AND PERSPECTIVES

THIS PAGE HAS BEEN INTENTIONALLY LEFT BLANK

CHAPTER 6 CONCLUSION AND PERSPECTIVES

THIS PAGE HAS BEEN INTENTIONALLY LEFT BLANK

6.1. CONCLUSION

Even though depth filters have been widely used in industrial clarification processes and studied in the literature, there is very little understanding on how to improve performance of depth filters. Depth filters are commonly made of cellulose fibres, a filter aid and a charged polymer. However, effect of each component on the final filter performance is not known. Therefore, understanding the effect of different components on depth filter performance in separation as well as observing structural changes is required. Moreover, there is another clear gap regarding applying the new advances in the filter structures that could potentially add different capabilities to the filters. Although membrane technology has been strongly developed, depth filter concept that combines different separation principles has not been explored in this manner. Finally, the use of toxic chemicals in the current depth filters is challenging due to the limited concentration allowed for food grade applications and the environmental concerns surrounding the use of these chemicals. Therefore, greener components are required for the development of a new generation of more sustainable and less toxic depth filters.

This thesis has reported three main interrelated research topics that have addressed the three current major gaps regarding depth filters. Firstly, the effect on separation performance of each component used in the filters was investigated. Secondly, new advanced filter structures were developed and the effect on filtration performance was quantified. Lastly, the performance of nanofibrillated cellulose (NFC) was investigated as a potential partial substitute for the toxic wet strength polymer, PAE.

6.1.1. Understanding depth filter concept with the role of each component

In Chapter 2, composite depth filters were prepared with refined and unrefined cellulose fibres, perlite and a well-known wet strength agent, polyamideamine-epichlorohydrin (PAE). A papermaking technique was used to prepare the composites. Different composites with a variety of components and compositions were prepared to investigate the effect of each component. Effect of fibre structure was also investigated by systematically substituting some of the pulp content for homogenised pulp. Adsorption characterisation was conducted with two oppositely charged dye molecules: methylene blue (MB) and metanil yellow (MY). Particle rejection experiments were

carried out with 1 µm silicon dioxide (SiO_2) particles. Mercury porosimetry and scanning electron microscopy (SEM) techniques were used to observe structural properties.

Increasing homogenisation intensity increased the fibrillation of NFC and reduced the fibre diameter. The increased NFC fibrillation resulted in a higher surface area and a higher quantity of negative charges accessible in the medium. Since adsorption is charge driven, an increase in accessible negatively charged sites contributed to attractive or repulsive forces depending on the type of dye tested and changed the adsorption properties accordingly. PAE has no impact on particle rejection properties; however, it substantially affected the charge of filters, and in turn the adsorption performance. The perlite content changed the structural properties such as pore size of filters increased as perlite particles adsorbed between the fibres. Also, the perlite content improved the dye adsorption due to the high surface area and highly porous structure of the perlite. Even though different variations of composites resulted in different pore size distributions, the composites were overall very efficient in particle rejection with at least 90% rejection rate of SiO_2 particles.

This study shows that each component contributes to the overall functionality of the depth filter. The internal structure as well as filtration performance can be controlled by adding different components.

6.1.2. Engineering new filter structures for improved filtration performance

With the understanding obtained through Chapter 2 on the role of different filter components, the next two Chapters (Chapter 3 and 4) of this thesis aimed at engineering novel structured depth filters, comprising all the components, for improved performance.

In Chapter 3, the effect of multi-layered and single-layered depth filter structures was investigated in terms of adsorption capacity as well as size-based rejection. Filters were again prepared from cellulose fibre, perlite and PAE, using a papermaking technique. The perlite and fibre content was kept constant at 70 wt% and 30 wt%, respectively, along with 100 mg PAE per gram of fibre. Filters were prepared at two different total basis weights; 200 and 400 gsm. Different configurations were structured either as single layer or multi-layers within each of the total basis weight. In the case of multi-layered filters, all individual layers were prepared from equal quantities and the final filters were achieved by piling up all the individual layers on top of each other, resulting in the total basis

weight. MB was used to characterise adsorption properties. Particle and polymer rejection rates were measured with 0.5 μm SiO_2 particles and PEG molecules of two molecular weights (600 and 5,000 kDa), respectively. The filter structure was quantified by 3D X-ray tomography.

MB adsorption capacity increased when using a multi-layered filter configuration. Higher adsorption capacities were achieved by increasing number of layers within the same total basis weight. The structural characterisation by 3D X-ray tomography revealed the presence of macro voids/channels through the thickness of high basis weight single-layered filters. Macro-voids would lead a preferential flow of liquid through the voids as they will offer path of least resistance. Structuring multi-layers by piling up individual layers prevents these defects from aligning. Therefore, multi-layered filter structure with less voids within the thickness results in higher adsorption capacities by providing an increased contact surface area. None of the filters showed any rejection of PEG molecules. However, SiO_2 particle rejection rates were more than 85% for each configuration in each total basis weight without any improvement observed with the multi-layered filter structure.

In Chapter 4, NFC was explored as a barrier layer on top of depth filters. Depth filters were prepared as base sheets by the usual preparation method and this is followed by NFC coating. NFC was spray-coated on top of the filters with the grammage of the sprayed layer ranging from 4 to 30 gsm. With a barrier layer concept, it was aimed to develop different functionalities which were not originally possessed by the filters. MB and MY dyes were used as positively and negatively charged model molecules to characterise the adsorption performance. PEG molecules with two different molecular weights (600 and 5,000 kDa) were used to test the molecule rejection. Surface and cross section morphologies were observed by SEM.

This study indicates that a barrier layer can be successfully added on to the existing filters to develop new functionalities. With the barrier layer, 84% rejection for two different molecular weights of PEG (600 and 5,000 kDa) was obtained by only 30 gsm top coating. MB dye adsorption onto top layer increased significantly by increasing NFC layer thickness. The optimum performance was found at an 8 gsm NFC coat weight, where we could achieve 80% rejection of 5,000 kDa molecular weight PEG, while still achieving a good breakthrough curve, adsorbing cationic MB dye. The anionic MY dye was absorbed in the depth filter layer. The results showed that the two layer structure was able to achieve triple functionality, absorbing both positively and negatively charged dye molecules and

rejecting PEG molecules by size. PEG molecule rejection and MB adsorption are the two functionalities that were not achievable in the depth filters that were prepared in the previous chapters of the thesis.

These two works highlight how engineering new advanced structures can improve and control the filter performance by adding new functionalities.

6.1.3. Development of cleaner filters by partially replacing the toxic polymer with nanofibrillated cellulose

The last study of this thesis focuses on reducing the impact of filter manufacture and use on the environment and expanding filter functionality for food grade applications by reducing the quantity of wet strength resin, PAE. A renewable and biodegradable material, NFC was investigated to partially substitute the refined cellulose fibre component, while the quantity of PAE was gradually reduced. Wet tensile index of the composites was obtained using an Instron tensile testing system. Adsorption properties were again tested by two oppositely charged dye molecules: MB and MY. Zeta potential of the composite suspensions was also measured to investigate charge characteristics. Polyethylenimine (PEI) and cationic polyacrylamide (CPAM) were used to recover the overall cationic charge loss as the PAE content was reduced.

The strength provided by the highly connected NFC network allowed us to reduce PAE content by 95% while retaining the same wet strength. However, the reduction in the quantity of PAE used shifted the overall system charge from positive to negative. Adsorption capacity on positively charged methylene blue increased tremendously with the reduction of PAE. It was possible to restore the overall positive charge in the system using a small quantity of positively charged polymer (around 5 mg per 1.2 gram of fibre) of either PEI or CPAM. The results showed that adsorption was not only controlled by overall charge, but also by the conformation of the adsorbed polymer and that the dendrimer PEI is more effective than the high molecular weight linear CPAM to attract the negatively charged dye molecules onto composites.

This study indicates that 95% reduction in the quantity of PAE was obtained only by substituting the refined fibres with NFC. This result shows that NFC is an outstanding material to create greener filters.

6.2. PERSPECTIVES

Even though dynamic filtration with a dead-end filtration unit provides us a detailed insight regarding separation performance, this setup is limited to a certain volume. This usually prevents us from continuing filtration until the actual saturation point is reached, something which is particularly important to establish a full breakthrough curve. Since a constant pressure filtration unit has a closed setup where the feed solution is transferred into cell before it is pressurised, they commonly come with a set volume. Therefore, it is worthwhile to work with a constant flux setup which commonly works with a peristaltic pump with the feed solution kept outside. Also, it is more realistic as industrial applications are usually performed under constant flux conditions. Additionally, experiments in this thesis were somewhat limited with respect to the variables, such as pressure and volume. These variables should be further investigated in future work.

Additionally, we have shown that NFC is a remarkable reinforcement material for wet strength and we could get 95% reduction in the amount of PAE by substituting NFC for the refined fibre component. However, this study was limited to one type of mechanical treatment intensity. If we increase the fibre fibrillation further with more treatment, we would expect to be able to have more strength with the same quantity of NFC substitution. Also, PEI is shown to be very effective for wet strength development in this thesis. A very small quantity of PEI could provide enough strength and help in eliminating PAE completely. However, it should be noted that in our study PEI was used with PAE and CNF resulting in a polymer complex. The behaviour of PEI alone could be completely different in terms of wet strength. Future studies should be carried out on this topic, so as to be able to completely remove PAE and to be able to manufacture cleaner filters.

Lastly, the barrier layer on top of depth filters is proven to improve microfiltration significantly. This concept can be combined with the multi-layered filter structure where higher adsorption capacities can be achieved. Therefore, it is also worthwhile to focus on combining both concepts in one depth filter in a future work, in order to make filters with enhanced adsorption capacity of both positively and negatively charged molecules, with superior breakthrough curves and with the ability to microfilter larger contaminants. However, a NFC barrier layer should be used based on the size of contaminants as filtering suspensions with micron-sized particles might lead to rapid surface fouling.

THIS PAGE HAS BEEN INTENTIONALLY LEFT BLANK

APPENDIX I

SUPPLEMENTARY INFORMATION

THIS PAGE HAS BEEN INTENTIONALLY LEFT BLANK

ENGINEERING CELLULOSE FIBRE INORGANIC COMPOSITES FOR DEPTH FILTRATION AND ADSORPTION

Aysu Onur[1], Aaron Ng[2], Gil Garnier[1], Warren Batchelor[1]

[1] Chemical Engineering Department, Monash University, Australia

[2] 3M Australia, Sydney, Australia

*** Corresponding authors at:** Bioresource Processing Research Institute of Australia (BioPRIA), Chemical Engineering Department, Monash University, 3800

Email addresses: gil.garnier@monash.edu (G. Garnier), warren.batchelor@monash.edu (W. Batchelor).

A1: Calibration curves

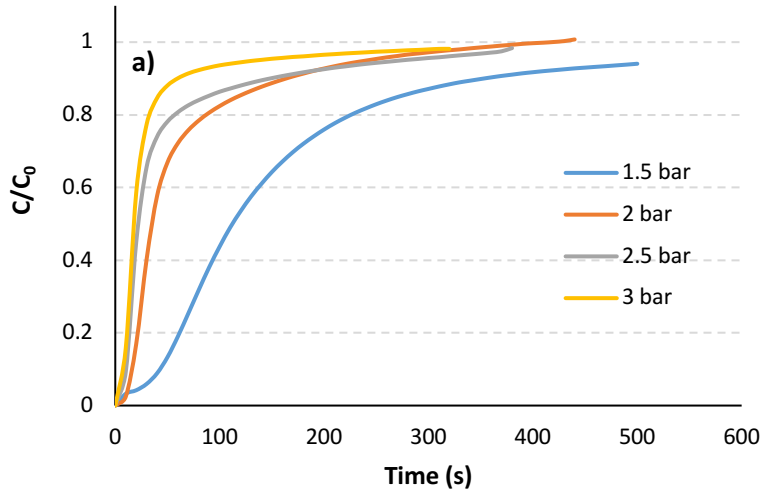

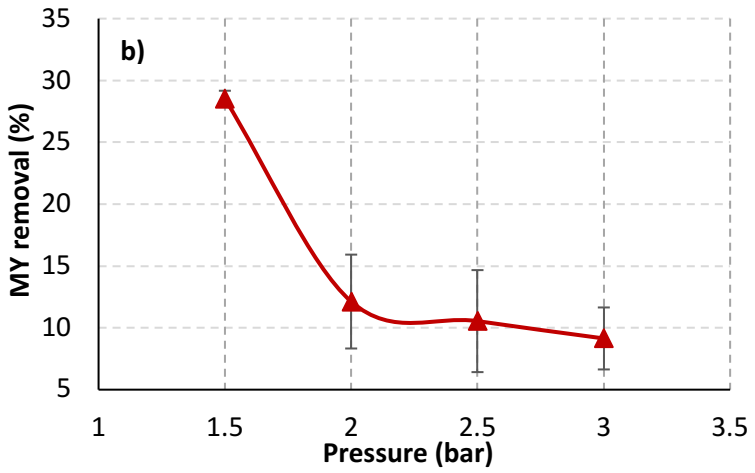
b)
MY removal (%)
35
30
25
20
15
10
5
1
1.5
2
2.5
3
3.5
Pressure (bar)

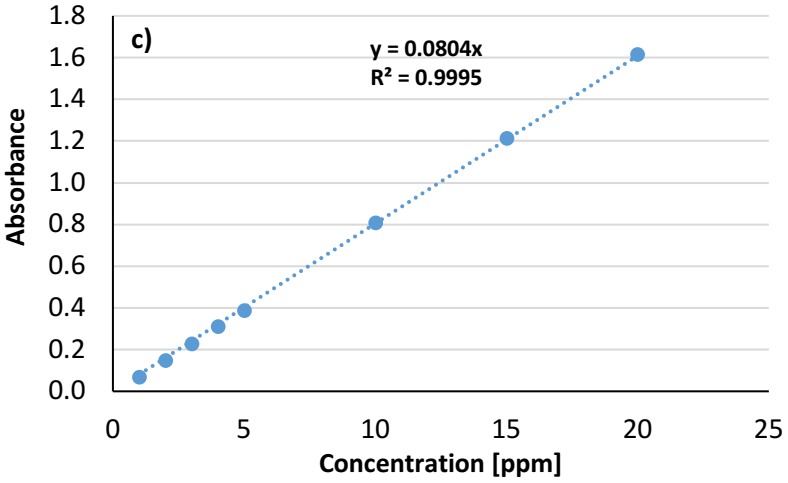
c)
y = 0.0804x
R² = 0.9995
Absorbance
1.8
1.6
1.4
1.2
1.0
0.8
0.6
0.4
0.2
0.0
0
5
10
15
20
25
Concentration [ppm]

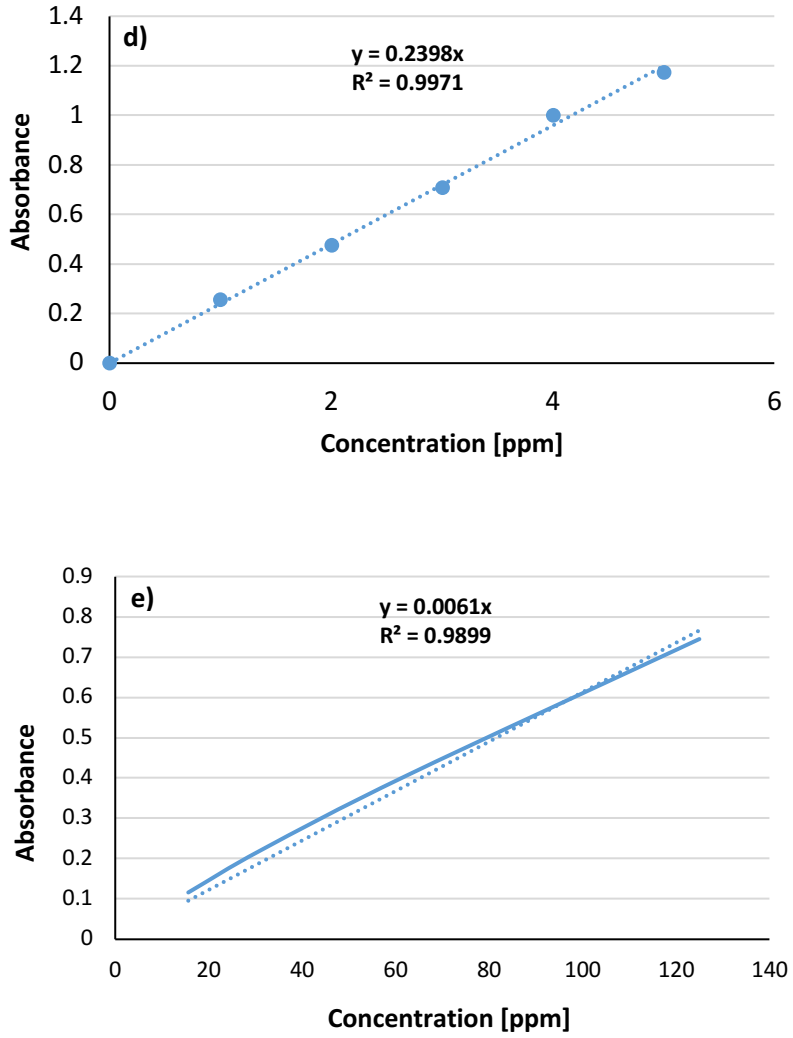

Figure A1: **a)** Metanil yellow (MY) breakthrough curves and **b)** Metanil yellow dye removal of Refined/Per/PAE as a function of pressure **c)** Metanil yellow, **d)** Methylene blue (MB) and **e)** Silicon dioxide calibration curves.

A2: Flow rate of samples

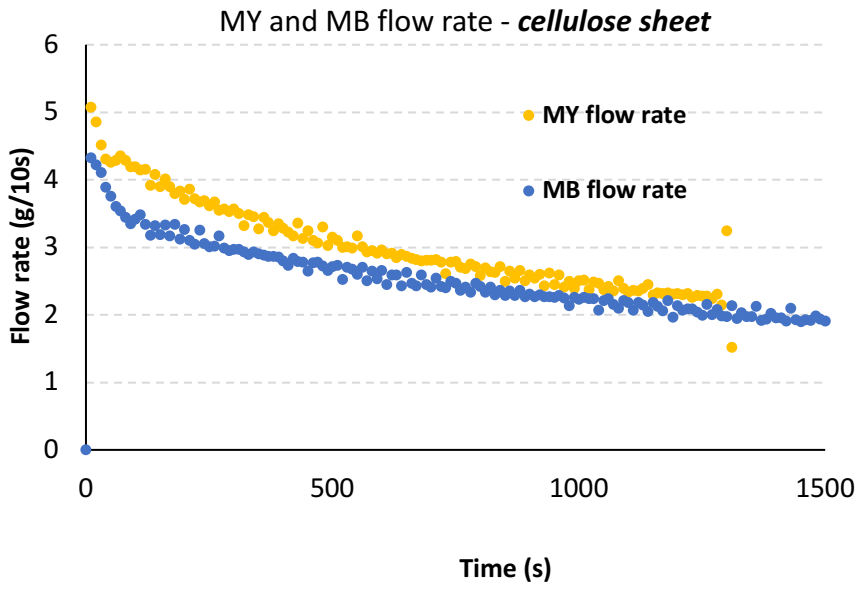

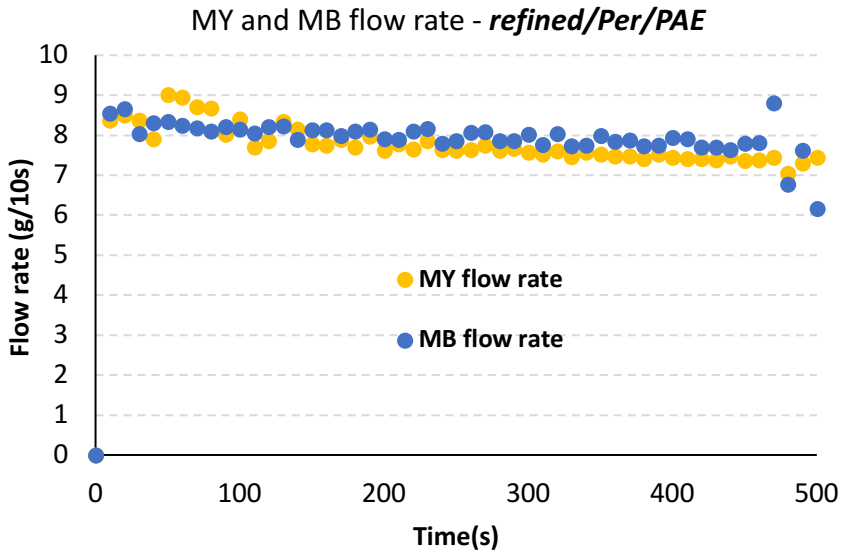

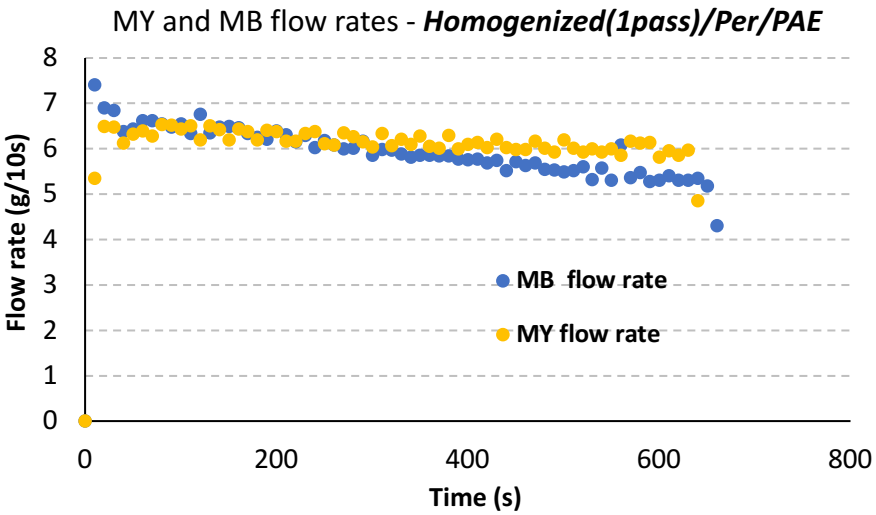

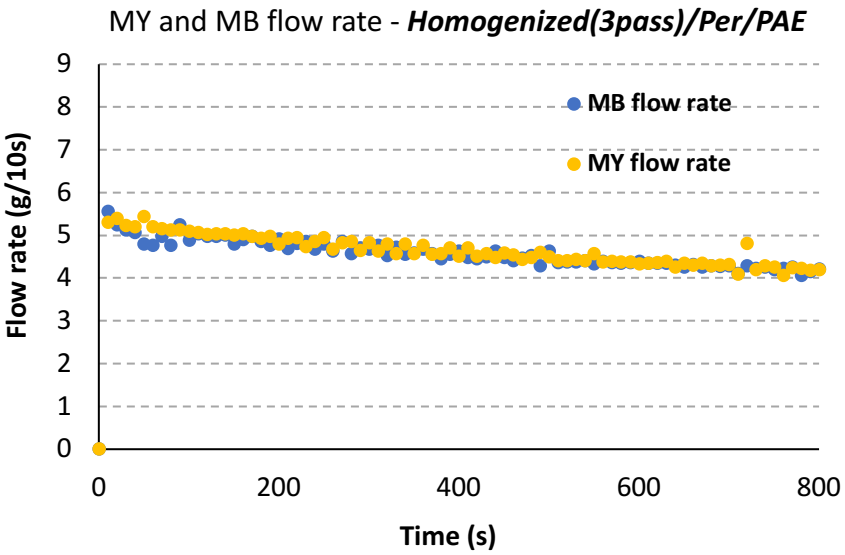

Figure A2: Metanil yellow and methylene blue flow rate of samples.

A3: Low magnification SEM images

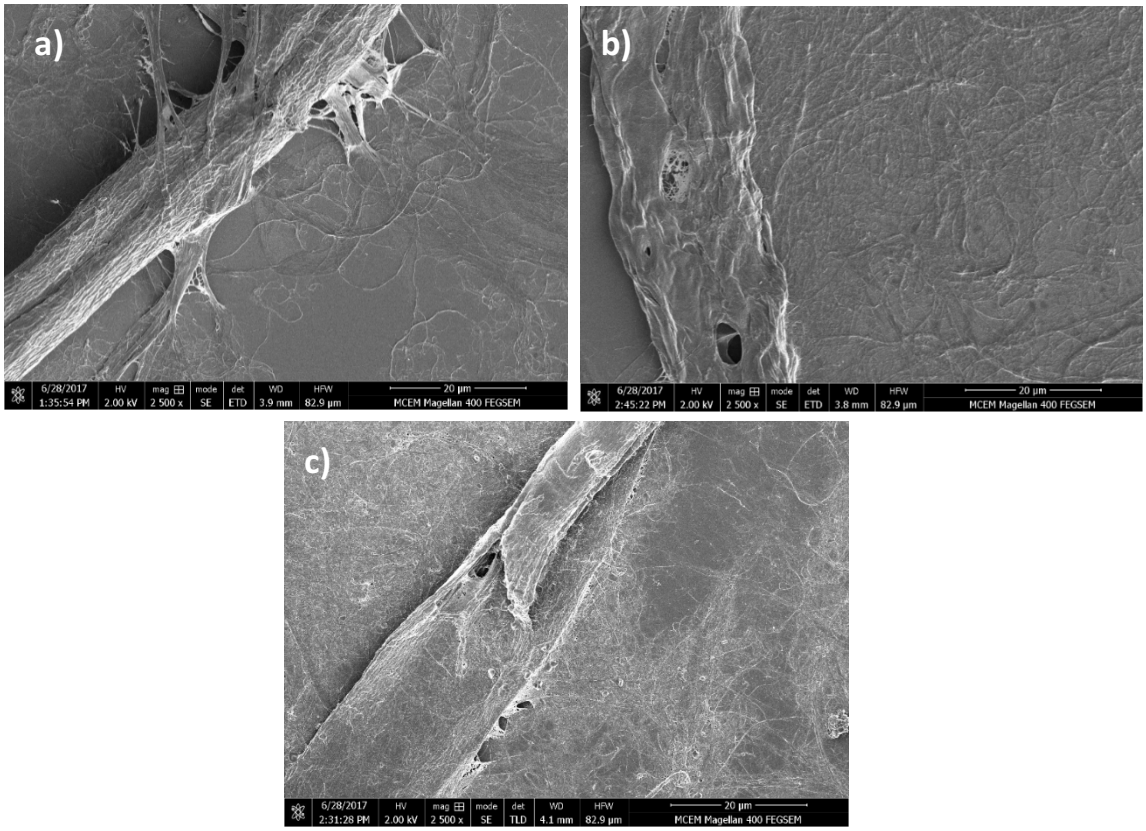

Figure A3: Low magnification SEM images of **a)** Refined pulp **b)** Homogenized pulp by 1 pass **c)** Homogenized pulp by 3 pass.

A4: Perlite particle size distribution

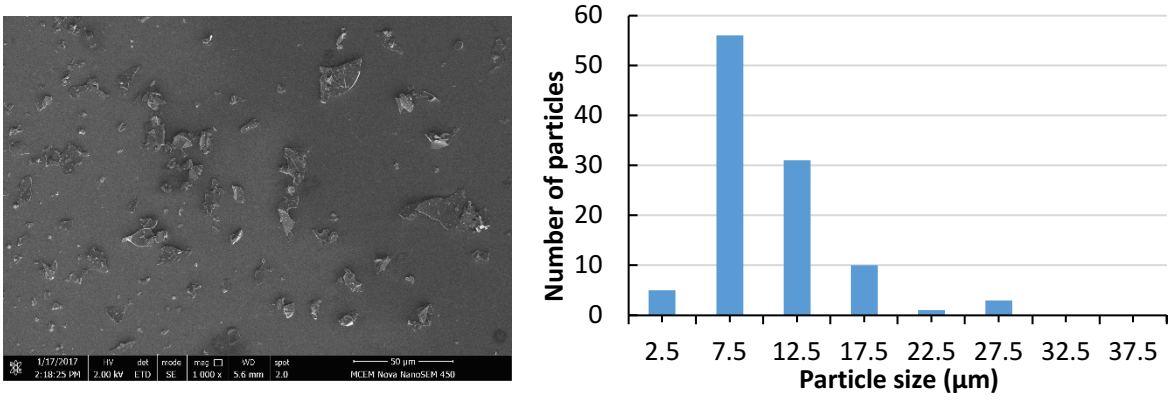

Figure A4: **a)** SEM image and **b)** particle size distribution of perlite particles.

A5: Methylene blue and metanil yellow adsorption capacity of the filters

Table AI. Methylene blue adsorption capacity of filters.

Sample	MB Adsorption Capacity (mg/g)
Refined	0.3672
Refined/Per/PAE	0.0016
Homogenized(1pass)/Per/PAE	0.0072
Homogenized(3pass)/Per/PAE	0.0386
Homogenized(3pass)/Per	1.5280

Table AII. Metanil yellow adsorption capacity of filters.

Sample	MY Adsorption Capacity (mg/g)
Refined	0.0008
Refined/Per/PAE	0.3448
Homogenized(1pass)/Per/PAE	0.1861
Homogenized(3pass)/Per/PAE	0.1825
Homogenized(3pass)/Per	0.0024

THIS PAGE HAS BEEN INTENTIONALLY LEFT BLANK

MULTI-LAYER FILTERS: ADSORPTION AND FILTRATION MECHANISMS FOR IMPROVED SEPARATION

Aysu Onur[1], Aaron Ng[2], Warren Batchelor[1], Gil Garnier[1*]

[1] Bioresource Processing Research Institute of Australia, Chemical Engineering Department, Monash University, Clayton, Australia

[2] 3M Australia, Sydney, Australia

*** Corresponding author at:** Bioresource Processing Research Institute of Australia, Chemical Engineering Department, Monash University, Clayton, Australia, 3800

Email address: gil.garnier@monash.edu (G. Garnier).

B1: Void fraction distribution of samples through thickness

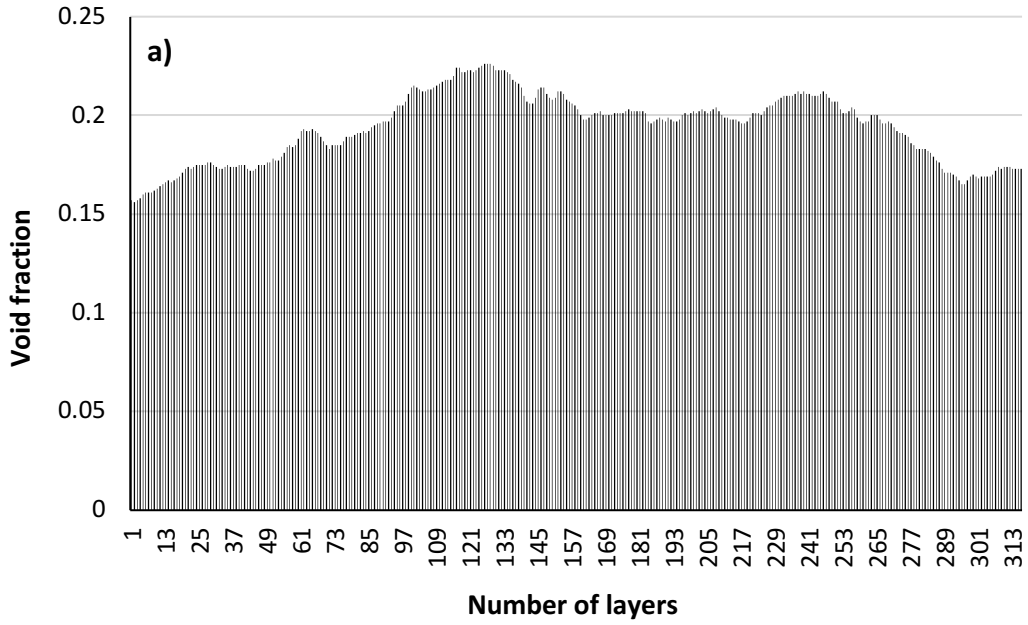

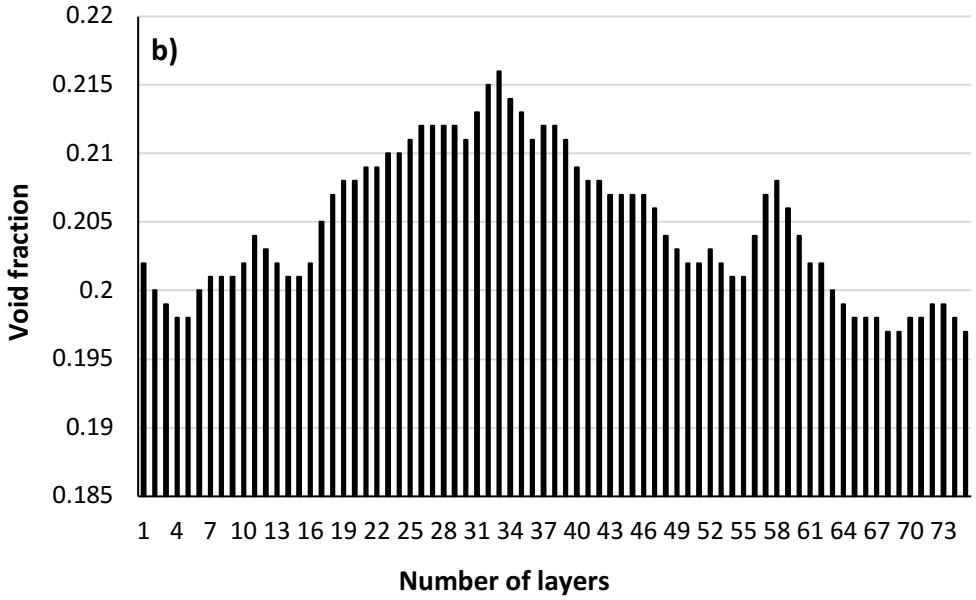
b)
Void fraction
0.22
0.215
0.21
0.205
0.2
0.195
0.19
0.185
1 4 7 10 13 16 19 22 25 28 31 34 37 40 43 46 49 52 55 58 61 64 67 70 73
Number of layers

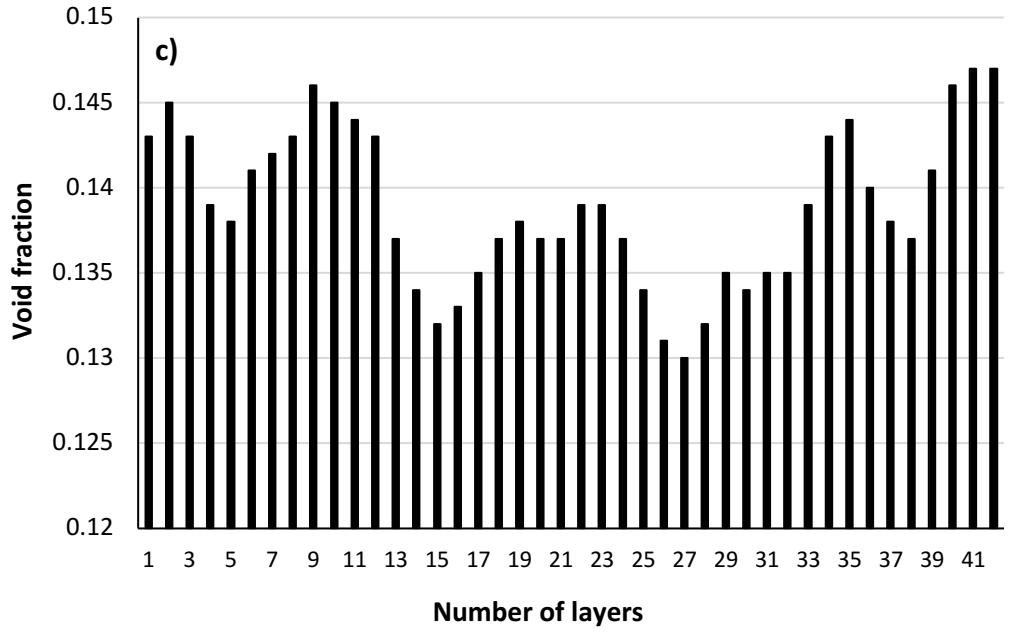
c)
Void fraction
0.15
0.145
0.14
0.135
0.13
0.125
0.12
1 3 5 7 9 11 13 15 17 19 21 23 25 27 29 31 33 35 37 39 41
Number of layers

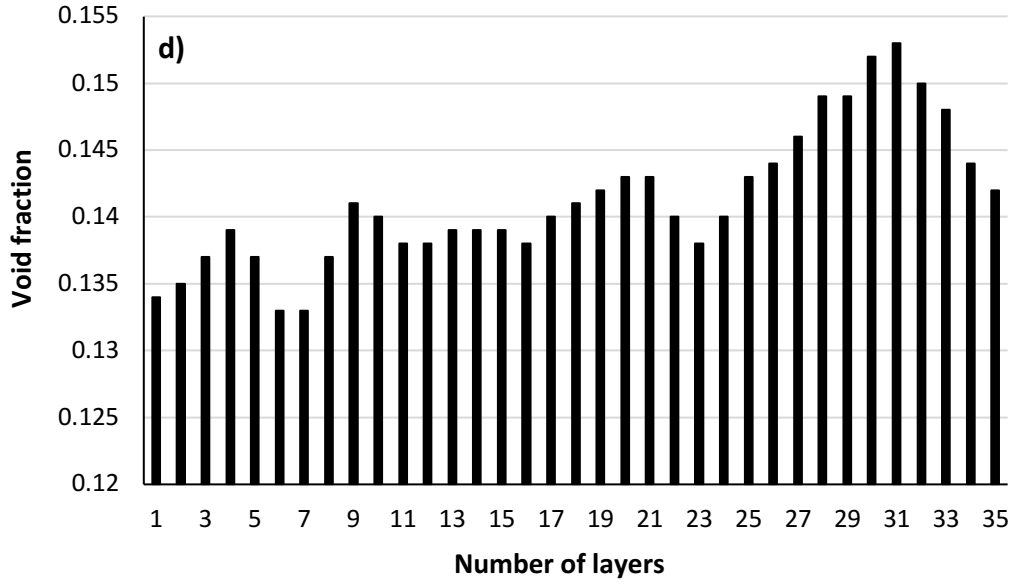

Figure B1: Void Fraction Distribution of **a)** 400gsm-1x **b)** 200gsm-2x (first layer) **c)** 100gsm-4x (second layer) and **d)** 100gsm-4x (third layer).

B2: Polyethylene glycol (PEG) filtration

Table B2-I: 600 kDa PEG Filtration TOC Results.

Sample	Analysis	Result
Control	TOC	TOC:51.92 mg/L TC:52.07 mg/L IC:0.1465 mg/L
200gsm-1x-1	TOC	TOC:48.98 mg/L TC:49.14 mg/L IC:0.1632 mg/L
100gsm-2x-1	TOC	TOC:51.92 mg/L TC:52.09 mg/L IC:0.1725 mg/L
200gsm-2x-2	TOC	TOC:51.59 mg/L TC:51.75 mg/L IC:0.1581 mg/L
100gsm-2x-2	TOC	TOC:50.57 mg/L TC:50.74 mg/L IC:0.1684 mg/L
400gsm-1x-1	TOC	TOC:49.18 mg/L TC:49.37 mg/L IC:0.1936 mg/L
400gsm-1x-2	TOC	TOC:52.46 mg/L TC:52.69 mg/L IC:0.2297 mg/L
200gsm-2x-1	TOC	TOC:53.05 mg/L TC:53.23 mg/L IC:0.1872 mg/L
200gsm-2x-2	TOC	TOC:49.29 mg/L TC:49.47 mg/L IC:0.1843 mg/L
100gsm-4x-1	TOC	TOC:52.59 mg/L TC:52.77 mg/L IC:0.1759 mg/L
100gsm-4x-2	TOC	TOC:50.76 mg/L TC:50.96 mg/L IC:0.1971 mg/L

Table B2-II: 5,000 kDa PEG Filtration TOC Results.

Sample	Analysis	Result
Control	TOC	TOC:53.97 mg/L TC:54.16 mg/L IC:0.1851 mg/L
200gsm-1x-1	TOC	TOC:51.70 mg/L TC:51.91 mg/L IC:0.2024 mg/L
200gsm-2x-2	TOC	TOC:49.80 mg/L TC:50.00 mg/L IC:0.2013 mg/L
100gsm-2x-1	TOC	TOC:52.19 mg/L TC:52.41 mg/L IC:0.2171 mg/L

100gsm-2x-2	TOC	TOC:50.87 mg/L TC:51.12 mg/L IC:0.2446 mg/L
400gsm-1x-1	TOC	TOC:51.76 mg/L TC:52.05 mg/L IC:0.2954 mg/L
400gsm-1x-2	TOC	TOC:51.96 mg/L TC:52.20 mg/L IC:0.2414 mg/L
200gsm-2x-1	TOC	TOC:52.62 mg/L TC:52.82 mg/L IC:0.1989 mg/L
200gsm-2x-2	TOC	TOC:53.61 mg/L TC:53.80 mg/L IC:0.1841 mg/L
100gsm-4x-1	TOC	TOC:52.41 mg/L TC:52.58 mg/L IC:0.1728 mg/L
100gsm-4x-2	TOC	TOC:52.18 mg/L TC:52.32 mg/L IC:0.1471 mg/L

B3: Calibration curves

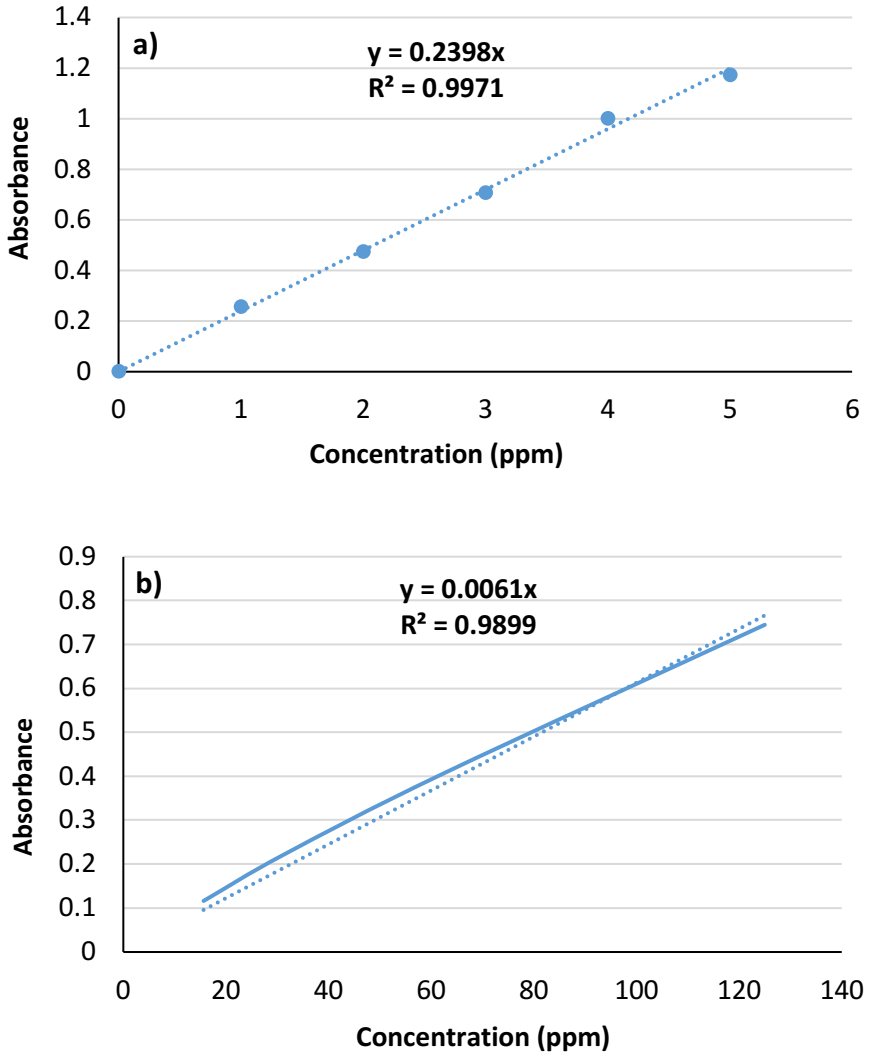

Figure B3: **a)** methylene blue and **b)** silicon dioxide calibration curves.

B4: 3D X-ray computed tomography data acquisition recipe

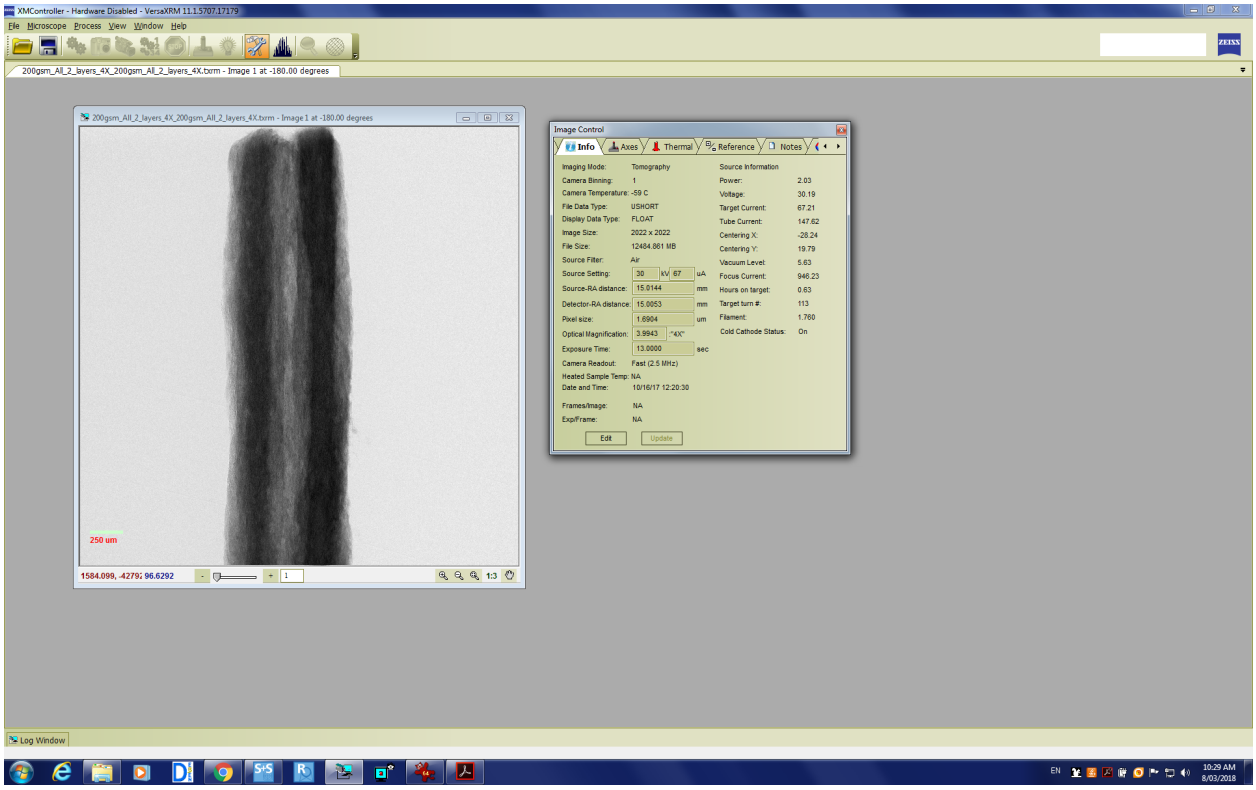

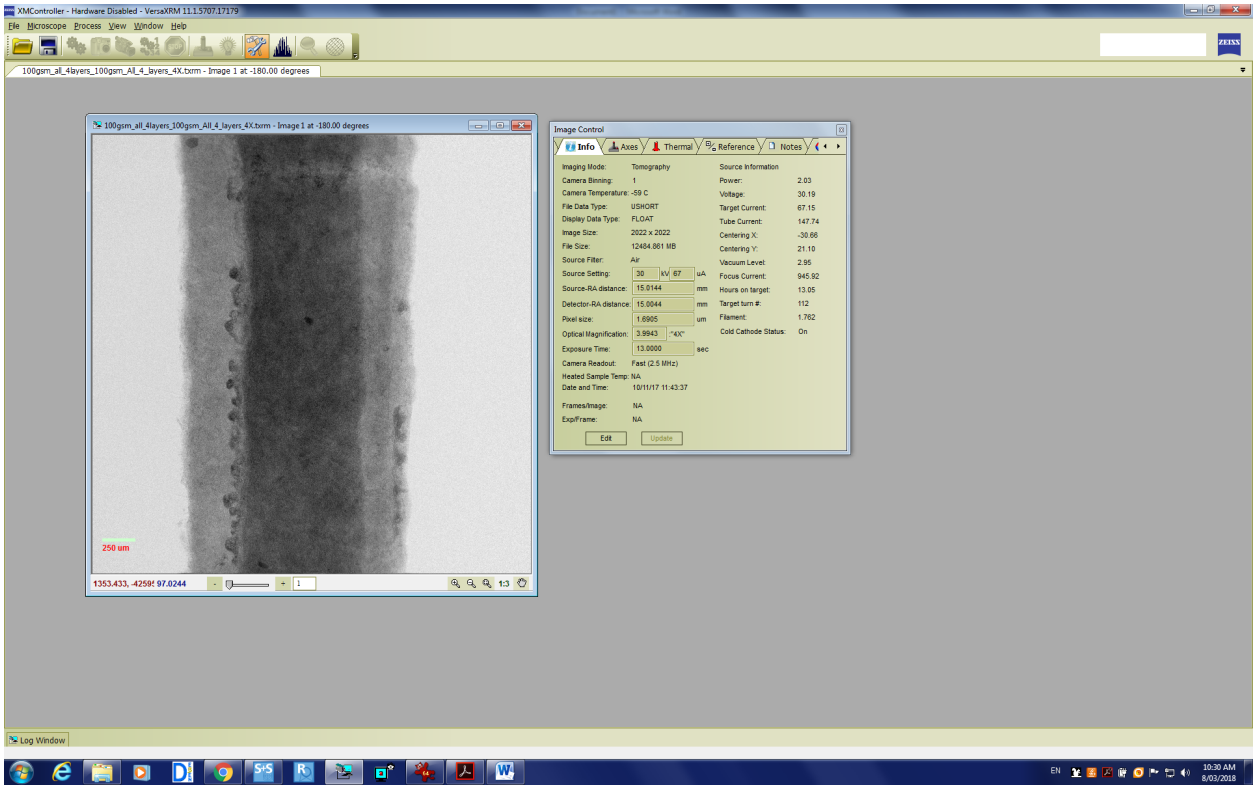

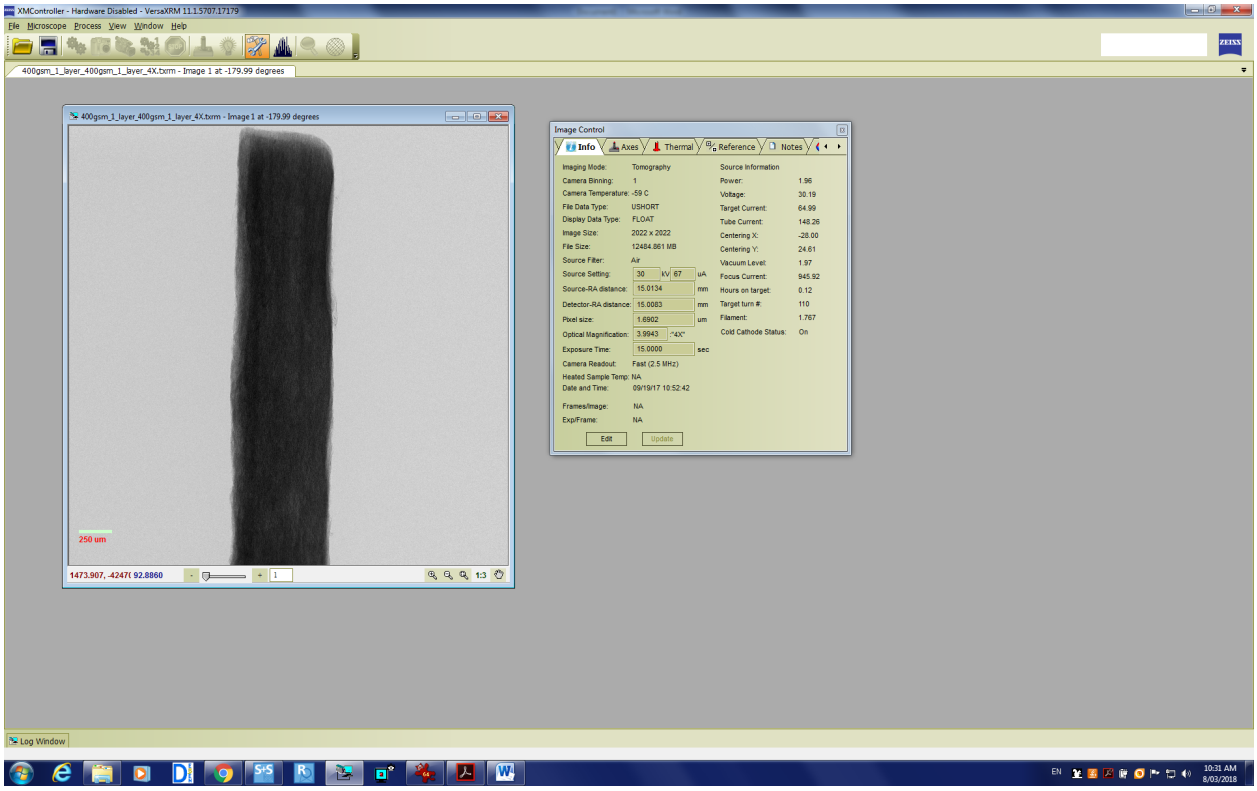

Figure B4: 3D X-ray scanning and image analysis settings of 200gsm-2x, 100gsm-4x and 400gsm-1x, respectively.

B5: Properties of samples

Table B5: Properties of samples based on different basis weights (gsm).

	100 gsm	200 gsm	400 gsm
Thickness (mm)	0.224	0.419	0.787
Weight (g)	0.470	0.930	1.87
Theoretical density (g/cm^3)	0.555	0.555	0.555
Bulk density (g/cm^3)	0.446	0.477	0.508
Porosity (%)	0.20	0.14	0.08
Flux (LMH)	711	683	574

CELLULOSE FIBRE-PERLITE DEPTH FILTERS WITH NANOFIBRILLATED CELLULOSE TOP COATING FOR IMPROVED FILTRATION

Aysu Onur[1], Kirubanandan Shanmugam[1], Aaron Ng[2], Gil Garnier[1], Warren Batchelor[1*]

[1] Bioresource Processing Research Institute of Australia, Chemical Engineering Department, Monash University, Clayton, Australia

[2] 3M Australia, Sydney, Australia

*** Corresponding author at:** Bioresource Processing Research Institute of Australia, Chemical Engineering Department, Monash University, Clayton, Australia, 3800

Email address: warren.batchelor@monash.edu (W. Batchelor).

C1: PEG filtration TOC results

Table C1: PEG filtration: TOC analysis raw data.

Samples based on conveyor speed level	Results		
Control-1-600 kDa	**TOC:** 53.54 mg/L	**TC:** 53.79mg/L	**IC:** 0.2428mg/L
60-1	**TOC:** 30.60 mg/L	**TC:** 30.85mg/L	**IC:** 0.2447mg/L
60-2	**TOC:** 25.33 mg/L	**TC:** 25.52mg/L	**IC:** 0.1965mg/L
80-1	**TOC:** 34.96 mg/L	**TC:** 35.21mg/L	**IC:** 0.2496mg/L
80-2	**TOC:** 42.71 mg/L	**TC:** 42.96mg/L	**IC:** 0.2456mg/L
100-1	**TOC:** 37.20 mg/L	**TC:** 37.47mg/L	**IC:** 0.2709mg/L
100-2	**TOC:** 45.93 mg/L	**TC:** 46.16mg/L	**IC:** 0.2346mg/L
20-1	**TOC:** 8.380 mg/L	**TC:** 8.628mg/L	**IC:** 0.2428mg/L
Control-2-5,000 kDa	**TOC:** 54.63 mg/L	**TC:** 54.82mg/L	**IC:** 0.1848mg/L
60-1	**TOC:** 11.05 mg/L	**TC:** 11.30mg/L	**IC:** 0.2565mg/L
60-2	**TOC:** 11.15 mg/L	**TC:** 11.36mg/L	**IC:** 0.2128mg/L
80-1	**TOC:** 26.85 mg/L	**TC:** 27.06mg/L	**IC:** 0.2108mg/L
80-2	**TOC:** 16.82 mg/L	**TC:** 17.07mg/L	**IC:** 0.2468mg/L
100-1	**TOC:** 45.69 mg/L	**TC:** 45.91mg/L	**IC:** 0.2151mg/L
100-2	**TOC:** 43.19 mg/L	**TC:** 43.39mg/L	**IC:** 0.1961mg/L
20-1	**TOC:** 8.838 mg/L	**TC:** 9.053mg/L	**IC:** 0.2158mg/L
20-2	**TOC:** 6.472 mg/L	**TC:** 6.679mg/L	**IC:** 0.2077mg/L

THIS PAGE HAS BEEN INTENTIONALLY LEFT BLANK

THE USE OF NANOFIBRILLATED CELLULOSE TO REDUCE THE WET STRENGTH POLYMER QUANTITY FOR DEVELOPMENT OF CLEANER FILTERS

Aysu Onur[1], Aaron Ng[2], Gil Garnier[1], Warren Batchelor[1*]

[1] Bioresource Processing Research Institute of Australia, Chemical Engineering Department, Monash University, Clayton, Australia

[2] 3M Australia, Sydney, Australia

*** Corresponding author at:** Bioresource Processing Research Institute of Australia, Chemical Engineering Department, Monash University, Clayton, Australia, 3800

Email address: warren.batchelor@monash.edu (W. Batchelor).

T-Test data analysis

D1: Comparison of different curing conditions

Comparison of *105°C & 1/2 hour* vs *105°C & 1 hour*
t-Test: Two-Sample Assuming Unequal Variances

	Variable 1	*Variable 2*
Mean	4.406428571	5.074285714
Variance	0.058209341	0.12738022
Observations	14	14
Hypothesized Mean Difference	0	
df	23	
t Stat	-5.800571994	
P(T<=t) one-tail	3.27795E-06	
t Critical one-tail	1.713871528	
P(T<=t) two-tail	6.5559E-06	
t Critical two-tail	2.06865761	

Comparison of *105°C & 1/2 hour* vs *150°C & 5min*

t-Test: Two-Sample Assuming Unequal Variances

	Variable 1	*Variable 2*
Mean	4.406429	5.248571
Variance	0.058209	0.331873
Observations	14	21
Hypothesized Mean Difference	0	
df	29	
t Stat	-5.96062	
P(T<=t) one-tail	8.87E-07	
t Critical one-tail	1.699127	
P(T<=t) two-tail	1.77E-06	
t Critical two-tail	2.04523	

Comparison of *105°C & 1 hour* vs *150°C & 5min*

t-Test: Two-Sample Assuming Unequal Variances

	Variable 1	*Variable 2*
Mean	5.074285714	5.248571
Variance	0.12738022	0.331873
Observations	14	21
Hypothesized Mean Difference	0	
df	33	
	-	
t Stat	1.104445229	
P(T<=t) one-tail	0.13869411	
t Critical one-tail	1.692360309	
P(T<=t) two-tail	0.277388219	
t Critical two-tail	2.034515297	

D2: Comparison of different order of additions

Comparison of PAE addition*: PAE added to the fibres first* vs *added on top of entire suspension at the end*

t-Test: Two-Sample Assuming Unequal Variances

	Variable 1	*Variable 2*
Mean	5.613333333	5.248571
Variance	0.86109697	0.331873
Observations	12	21
Hypothesized Mean Difference	0	
df	16	
t Stat	1.232686824	
P(T<=t) one-tail	0.117749458	
t Critical one-tail	1.745883676	
P(T<=t) two-tail	0.235498915	
t Critical two-tail	2.119905299	

THIS PAGE HAS BEEN INTENTIONALLY LEFT BLANK

APPENDIX II

PUBLICATIONS INCLUDED IN THESIS IN THEIR PUBLISHED FORMAT

THIS PAGE HAS BEEN INTENTIONALLY LEFT BLANK

Separation and Purification Technology 203 (2018) 209–216

Contents lists available at ScienceDirect

Separation and Purification Technology

journal homepage: www.elsevier.com/locate/seppur

Engineering cellulose fibre inorganic composites for depth filtration and adsorption

Aysu Onur[a], Aaron Ng[b], Gil Garnier[a,*], Warren Batchelor[a,*]

[a] BioProcessing Research Institute of Australia (BioPRIA), Chemical Engineering Department, Monash University, Clayton, Australia
[b] 3M Australia, Sydney, Australia

ARTICLE INFO

Keywords:
Depth filter
Adsorption
Filtration
Cellulose nanofibre
Composite

ABSTRACT

Depth type composite filters are porous materials heavily loaded with adsorbents and can remove contaminants from liquids by combining mechanical entrapment and adsorption. There is still a need for developing high performance filters by controlling the internal structure at micro and nano level. In this study, highly fibrillated nanocellulose (NC) with increased surface area was used as partial substitute for the fibre matrix to tailor the filter structure as well as the adsorption and filtration performance. Polyamide-amine-epichlorohydrin (PAE) was added both to adjust the charge of medium and provide wet strength. Filters were fabricated by embedding perlite particles into the cellulose fibre matrix by papermaking technique. The structure of composites was characterized for pore size distribution and surface morphology. Adsorption and filtration characteristics were quantified using two model dyes and silicon dioxide particles. Adsorption was found to be electrostatically controlled and dependent on the charge of the dye molecules and the filter medium. The addition of NC doubled the removal of a cationic dye by increasing the surface area and the available negative charges; it however decreased the removal of an anionic dye by 75%. PAE addition decreased the adsorption of the cationic methylene blue dye, while increasing the adsorption of the anionic metanil yellow dye. Rejection by filtration of 1 μm particles was over 90% for all filters. This study demonstrates that highly fibrillated NC fibres combined with a cationic wet strength polyelectrolyte can be used to tailor the filter structure and properties.

1. Introduction

Liquid filtration is used in a vast range of applications such as water treatment, beverage and juice filtration, pharmaceutical and industrial chemical filtration as well as medical purposes such as blood filtration [1]. Membrane technology plays an important role in liquid filtration applications and polymeric membranes made of polyamide, polysulfone and polyimide are widely used [2] due to their mechanical and chemical resistances. However, these membranes suffer environmental drawbacks as they are petroleum based, non-biodegradable and large quantities of solvents and chemicals [3] are required for their production. These membranes perform separation only by filtration/size exclusion and remain inefficient for the separation of small charged molecules. In addition, membrane technology mainly relies on separation at the surface which is very susceptible to fouling [4]. There is a need for environmentally benign products with improved functionalities that can be reprocessed, recycled or will biodegrade at the end of their life. Depth type composites using cellulose fibres provide a solution. Depth filters are porous materials heavily loaded with adsorbents. These filters retain molecules not only on the surface but also within the media [5]. They can remove contaminants from liquids by combining filtration/mechanical entrapment with adsorption, resulting in a higher removal capacity.

Nanocellulose (NC) has widely been explored as an alternative polymer in membranes/filters due to unique properties such as high surface area, high strength, wettability, ease of chemical functionalization and low environmental impact [6]. Cellulose is the most abundant polymer and can be used in the form of fibres and derivatives in a vast range of products [7–10]. NC technology has significantly progressed in the last decade; the applications of NC were reviewed by Salas et al. [11]. The potential of NC in filtration applications and its excellent adsorption capacity due to its high surface area-to-volume ratio have long been identified [12–18]. Even though NC performance for water treatment was demonstrated, most studies have focused on functionalized NC fibres with a variety of chemistries, improving pollutants binding efficiency [13,19,20]. This functionalization often requires expensive and toxic chemical treatments and can be difficult to scale up, limiting industrial applications. Also, regulations for some

* Corresponding authors at: BioProcessing Research Institute of Australia (BioPRIA), Chemical Engineering Department, Monash University, 3800, Australia.
E-mail addresses: gil.garnier@monash.edu (G. Garnier), warren.batchelor@monash.edu (W. Batchelor).

https://doi.org/10.1016/j.seppur.2018.04.038
Received 13 December 2017; Received in revised form 12 April 2018; Accepted 15 April 2018
Available online 17 April 2018
1383-5866/ Crown Copyright © 2018 Published by Elsevier B.V. All rights reserved.

applications, such as food and beverage, often restrict filters' chemical modification. The filters should be as chemical modification free as possible.

Some studies have quantified adsorption with NC based adsorbents using static experiments [13,16,18]; however, very few have reported particle rejection with dynamic experiments [14,15]. This is unfortunate as industry typically operates filters in a continuous mode instead of in a batch mode. NC composites with nano-ranged pore sizes have been explored for separation applications [21]. Keshavarzi et al. [22] investigated odour elimination with NC-zeolite composites in separation processes. However, limited number of studies have quantified NC composite performance in liquid filtration/adsorption. The following section gives an overview of dynamic studies of liquid filtration or adsorption with NC composites.

Varanasi et al. [23] reported the preparation of NC composite membranes and showed their potential in ultrafiltration. Silica nanoparticles were used to control the pore size of the nanofiber network. The pure NC membranes had high flux but the rejection of polyethylene glycol (PEG) was low because of the large pores. Composite membranes showed better rejection performance as the pore size was controlled by the silica nanoparticles. Control of composite pore size by nano particles addition is a promising avenue in ultrafiltration. However, this study focused on molecular weight cut off (MWCO) and ignored composite adsorption capability.

Karim et al. [24] investigated cellulose nano composites with functional cellulose nanocrystals added on a supporting layer of micro-sized cellulose fibres for adsorbing heavy metal ions from waste water. Nanocrystals promoted adsorption and the membranes showed excellent removal of metal ions. However, filtration was ignored and the isolation of cellulose nanocrystals from cellulose sludge is a tedious process requiring chemical treatment.

There is a lack of fundamental separation understanding in terms of combining adsorption and size exclusion for NC fibre composites under dynamic conditions. However, separation combining both adsorption and size exclusion is needed for some applications. In beer and wine filtration, for instance, it is necessary to remove bacteria and yeast particles to eliminate haziness [25] as well as removing some ionic compounds to avoid bitter taste [26–28].

This study aims developing microporous filters with mechanically-treated NC fibres and perlite, a low cost inorganic adsorbent. Composite filters combining adsorption and filtration are prepared with a simple and scalable papermaking process. The performance of highly fibrillated NC as a partial substitute for the fibre matrix of the filters is studied. Polyamide-amine-epichlorohydrin (PAE), a cationic and cross-linking polyelectrolyte was selected to provide wet strength and control the charge of the medium; PAE is food grade when fully crosslinked. Filtration and adsorption performances are evaluated dynamically with two model dyes and silicon dioxide particles and analysed in the context of food and pharmaceutical applications.

2. Materials and methods

2.1. Materials

The cellulose fibres used for the composites are unrefined northern softwood NIST RM 8495 bleached kraft pulp (with a typical fibre length of around 2.5–4 mm and 30 μm wide) and bleached radiata pine softwood kraft pulp refined to 400 Canadian standard freeness (CSF) in a disk refiner. Highly fibrillated NC fibres were prepared by processing refined pulp in a GEA Niro Soavi homogenizer at 800 bar at both 1 pass and 3 passes.

Expanded perlite supplied by Dicalite Minerals Corp was used as an inorganic adsorbent. Commercial PAE provided from Nopcobond Paper Technology Pty Ltd was used as wet strength resin.

Methylene blue (MB) and metanil yellow (MY) dyes supplied from Sigma Aldrich were used to test adsorption. 1 μm monodisperse silicon dioxide particles from Sigma Aldrich were used to test filtration capability of the composites.

2.2. Methods

2.2.1. Preparation of filters

Prior to sheet preparation, dry pulp was soaked in 2 L deionised water overnight and then disintegrated by a model MKIIIC, Messmer Instruments Ltd for 75,000 revolutions. Following disintegration, sheet suspensions were prepared by adding perlite suspensions to the pulp suspensions. PAE (0.22% w/v) was then added at a rate of 100 mg/g fibre and the mixtures were hand mixed before sheet making. 5 different composites and a control cellulose sheet were prepared; the fibre component was varied as described with only 1/3 of the cellulose fibre component. Composites were labelled based on the fibre composition and presence of perlite and polymer as follow:

(1) **Refined** – 100% Fibre (1/3 refined pulp + 2/3 unrefined pulp)
(2) **Refined/Per/PAE** – 30% Fibre (1/3 refined pulp + 2/3 unrefined pulp) + 70% Perlite + 120 mg PAE
(3) **Unrefined/Per/PAE** – 30% Fibre (3/3 unrefined pulp) + 70% Perlite + 120 mg PAE
(4) **Homogenized(1pass)/Per/PAE** – 30% Fibre (1/3 homogenized (1 pass) + 2/3 unrefined pulp) + 70% Perlite + 120 mg PAE
(5) **Homogenized(3pass)/Per/PAE** – 30% Fibre (1/3 homogenized (3 pass) + 2/3 unrefined pulp) + 70% Perlite + 120 mg PAE
(6) **Homogenized(3pass)/Per** – 30% Fibre (1/3 homogenized (3 pass) + 2/3 unrefined pulp) + 70% Perlite

The cellulose component was always kept constant at 60 g per square metre (gsm). For the composites with perlite, the target total gsm was 200 gsm- assuming full retention.

A British hand sheet maker was used to form the composite filters. A wet strengthened qualitative filter paper was deposited over the 150 μm size mesh and the suspension was poured into the chamber and then drained through the filter paper to form the sheets uniformly. After sheet formation, the wet sheet was separated from the mesh, placed between dry blotting papers and pressed under 345 kPa for 5 min. The composites containing PAE were heated 30 min at 105 °C for curing and then air-dried in a humidity room (23 °C, 50% relative humidity) overnight. The sheets without PAE were air-dried in the humidity room for at least 24 h without any oven treatment.

2.2.2. Mercury porosimetry

Composite pore size distribution was measured with a Micromeritics' AutoPore IV 9500 series. This technique quantifies a material's pore size distribution and porosity by applying increasing pressures (up to 60,000 psia) to a sample immersed in mercury and recording the volume of mercury intruded into pores. Samples were cut into approximately 5 mm × 5 mm small pieces and degassed for at least two days prior to characterization. A penetrometer with 0.412 mL stem volume was used to carry out the measurements. After degassing, approximately 0.1 g of sample was placed in the penetrometer and the analysis conducted. The volume of mercury intruded into pores is converted to equivalent pore sizes using the instrument software [29].

2.2.3. Scanning electron microscopy (SEM)

A FEI Nova NanoSEM 450 FEG SEM and a FEI Magellan 400 FEG SEM were used to characterize surface and bulk morphology of composites and estimate fibre diameter. Samples were mounted onto a metal substrate using carbon tape and coated with a thin layer of Iridium. Secondary electron images of composites were captured. 2 kV of accelerating voltage was applied for magnification up to 100,000. For fibre diameter measurement, silicon chips were used to cast the fibres and iridium coating was applied.

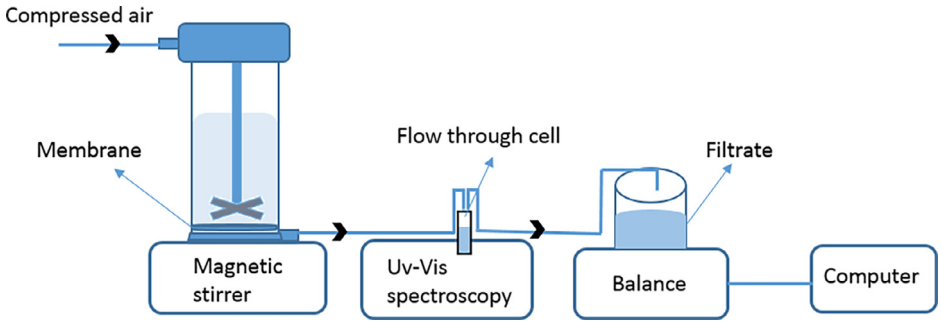

Fig. 1. Schematic illustration of the stirred cell experimental setup.

2.2.4. Adsorption and filtration

A Merck Millipore, model UFSC40001 dead-end stirred cell was used for adsorption and filtration experiments. The stirred cell is pressure driven with a 0.00418 m^2 effective membrane area and 400 mL working volume. Samples were placed on the membrane holder at the bottom and the cell body was filled with the prepared solution. The system was closed and pressurized by a compressed air gas cylinder. Filtrate was passed through a quartz micro flow cell with 10 mm optical path length sitting in an ultraviolet-visible (UV–vis) absorption spectrometer and transferred to a beaker on a balance. Both instantaneous absorbance and weight of the filtrate were measured every 10 s. The schematic system is illustrated in Fig. 1.

Preliminary adsorption experiments, performed at pressures ranging from 1 to 3 bar, identified the optimum inlet pressure as 1.5 bar; data is provided in the supplementary section (Fig. S1). Adsorption results were determined at 1.5 bar with 400 mL of 5 ppm dye solution. 5 ppm dye solutions were prepared by dissolving 5 mg of dye in 1 L deionized water. Breakthrough curves were obtained by plotting the instantaneous concentration (normalized by the initial concentration) as a function of time. The calibration curves are provided in supplementary information (SI) (Fig. S2). Dye removal was measured from the concentration of initial feed solution and filtrate:

$$Dye\ removal\ (\%) = \frac{\text{Initial dye concentration} - \text{filtrate dye concentration}}{\text{Initial dye concentration}} \times 100 \quad (1)$$

Adsorption capacity of each filter was calculated with the following equation. The integral was calculated from the area over the curve by trapeze method. Methylene blue and metanil yellow adsorption capacities of the filters were given in SI (Table SI and SII)

$$q = \frac{CF*Q}{1000*ms} \int \frac{1-\text{Cout}}{CF} \quad (2)$$

where:

q: Capacity of the adsorbent (mg/g)
C_{out}: Concentration of filtrate (mg/g)
C_F: Concentration of feed (mg/g)
Q: Volumetric flow rate (cm^3/s)
t: Time (s)
m_s: Weight of adsorbent (g)

Filtration efficiency was measured with a 0.05 wt% suspension of 1 μm silicon dioxide particles. Experiments were also conducted at 1.5 bar and concentration of silicon dioxide in suspension was measured before and after filtration by UV–vis spectroscopy to calculate filter rejection:

$$Rejection\ (\%) = \frac{\text{Initial feed concentration} - \text{Filtrate concentration}}{\text{Initial feed concentration}} \times 100 \quad (3)$$

Flux was calculated from the time to filter all of the suspension as:

$$FLUX\ (LMH) = \frac{Volume\ of\ filtrate\ (L)}{area\ (\text{m2}) \times time\ (h)} \quad (4)$$

Water was passed through the filters to remove any contaminants prior to adsorption and filtration experiments.

3. Results

3.1. Filter structure

3.1.1. Fibre size distribution

Fibre diameter size distribution of refined and homogenized pulps was measured from SEM images. High magnification images (Fig. 2) from completely different points of samples were acquired with at least 100 individual fibres in total and the diameter of every individual fibre in standard pictures was measured by image J, image processing software. The effect of increased fibrillation by mechanical treatment is seen on Fig. 2a–c. Low magnification images show that large fibres are still present even after homogenization (SI, Fig. S4). Histograms present fibre diameter size distributions estimated from the high magnification images in Fig. 3.

The majority of the refined fibres in the high magnification images have a diameter centred between 45 nm and 50 nm and the diameter is decreasing with the intensity of homogenization treatment. The average fibre diameters measured in these images fall to 25 to 40 nm after 1 pass and 20–25 nm after 3 passes homogenization.

Additionally, particle size distribution of perlite particles was measured by the same technique and can be found in SI (Fig S5).

3.1.2. Pore size distribution

Filter pore size distribution was measured by mercury porosimetry (Fig. 4). The distribution of pore size ranges from 1 to 3 μm. Substitution of fibre composition with homogenized pulp resulted in smaller pore sizes.

The cellulose sheet (*Refined*) has a smaller pore size distribution compared to composite combining refined pulp, perlite and PAE (*Refined/Per/PAE*) even though the fibre content is identical. Perlite addition increased the composite pore size by adsorbing between fibres. The peak intensity is also significantly smaller which reflects that the number of pores at a specific pore size is lower.

The slight difference between pore sizes of composites *Homogenized (3pass)/Per* and *Homogenized(3pass)/Per/PAE* demonstrates the effect of PAE addition. The sample with PAE (*Homogenized(3pass)/Per/PAE*) has a slightly smaller pore size.

3.1.3. Surface morphology

SEM images of filters made with different pulps homogenized to different intensities are shown in Fig. 5. Connectivity between fibres and perlite particles increases with the entangled network created by highly fibrillated NC addition (Fig. 5a–d). This connectivity results in a smoother, more closed surface and a decrease in composite porosity.

The arrows in Fig. 5 highlight the changes in surface morphology.

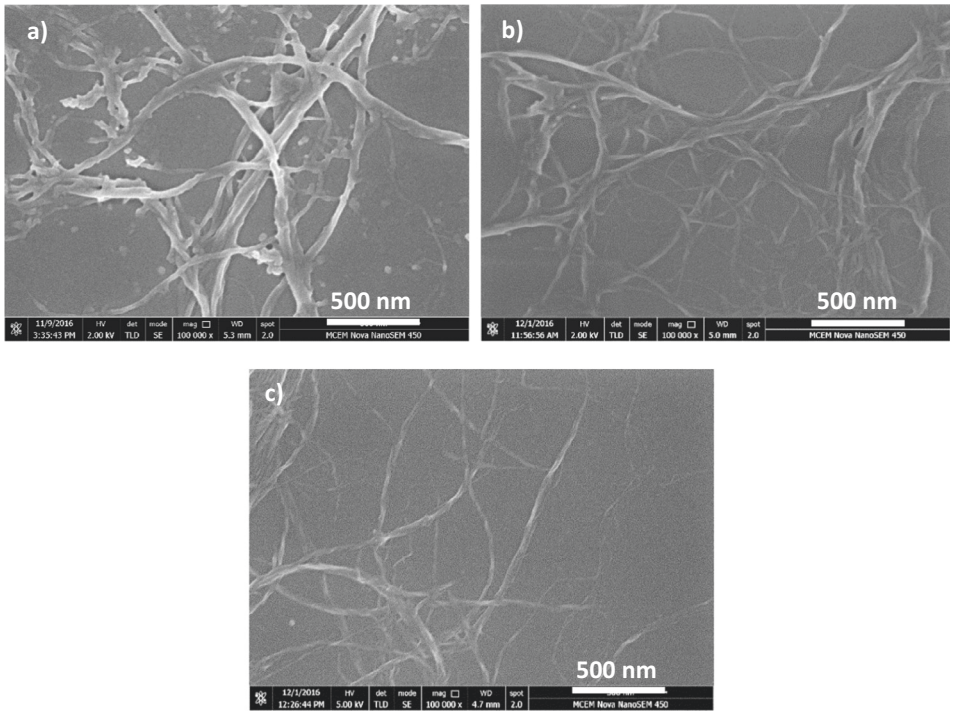

Fig. 2. High magnification SEM images of: **(a)** Refined pulp, **(b)** Homogenized pulp by 1 pass and **(c)** Homogenized pulp by 3 passes.

Arrows (i) and (ii) show the perlite particles with sharp edges which became blurred with homogenized pulp addition in arrows (iv). Addition of highly fibrillated NC smooths the edges and binds the perlite particles. Arrow (iii) shows the presence of some remaining large fibres in sample *Homogenized(*1*pass)/Per/PAE*.

3.2. Adsorption and filtration

3.2.1. Adsorption with breakthrough curves

The breakthrough curves measured at 1.5 bar for all samples with MY and MB dye solutions are shown in Fig. 6a and b, respectively. Breakthrough curves present the normalized concentrations as a function of time or effluent volume. They usually show a characteristic S shape with varying degrees of steepness. All outlet concentrations are presented normalized with the inlet concentration: C/Co ranges from 0, for full adsorption, to 1, for no adsorption. Initially, the dye molecules are adsorbed very effectively on the fresh adsorbent and the outlet concentration equals zero. As the filters start to saturate, the outlet concentration gradually approaches the inlet concentration and the normalized concentration (C/Co) increases to eventually level-off at

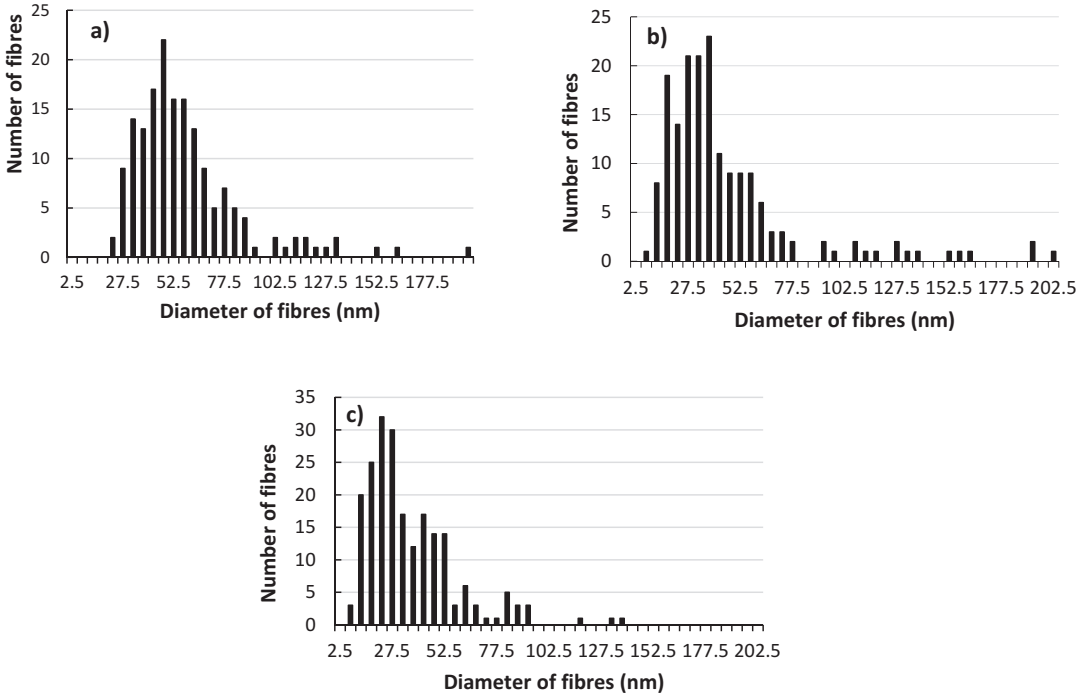

Fig. 3. Fibre size distribution of **(a)** Refined pulp **(b)** Homogenized pulp by 1 pass **(c)** Homogenized pulp by 3 passes.

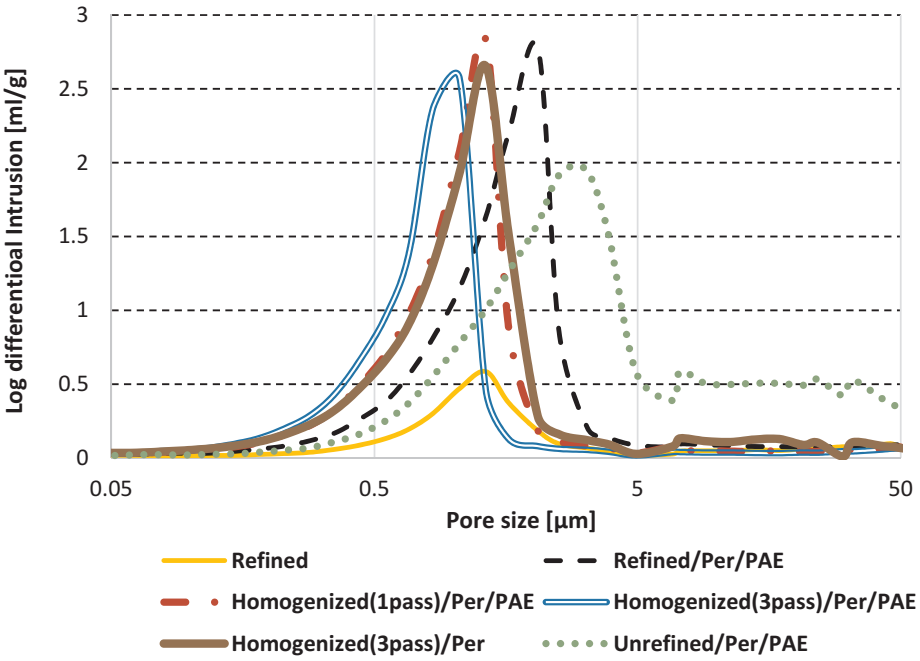

Fig. 4. Pore size distributions of filters measured by mercury porosimetry; effect of homogenization intensity and addition of perlite and PAE.

one.

The two oppositely charged dyes showed two opposite adsorption behaviours onto the composites (Fig. 6a and b). Basically no adsorption was recorded for the cationic MY dye onto cellulose sheet (*Refined*) or composite made with homogenized fibres (3 passes) with no PAE (*Homogenized(3pass)/Per*) (Fig. 6a). By contrast, the cationic MB showed some affinity and retention onto these same composites (Fig. 6b). Here, *Homogenized(3pass)/Per* presents the straightest breakthrough curve which indicates very strong attractive forces with MB- in the absence of positively charged PAE. The very intense blue colour of the saturated filter after adsorption (Fig. 6b) indicates more MB adsorbed onto the composite with highly fibrillated pulp content (*Homogenized(3pass)/Per*).

Adsorption occurs slightly differently for composites made only with refined pulp and those made with two different homogenized pulps treated at different intensities. As fibre fibrillation increases (homogenization or more passes in homogenization), composites increasingly repel the anionic dye- metanil yellow and attract the cationic dye (MB). From *Refined/Per/PAE* through *Homogenized(3pass)/Per/PAE* sample, attraction with MB (Fig. 6b) and repulsion with MY (Fig. 6a) increases with the fibrillation and increased surface area.

Flux and total dye removal were measured (Fig. 7). A maximum of

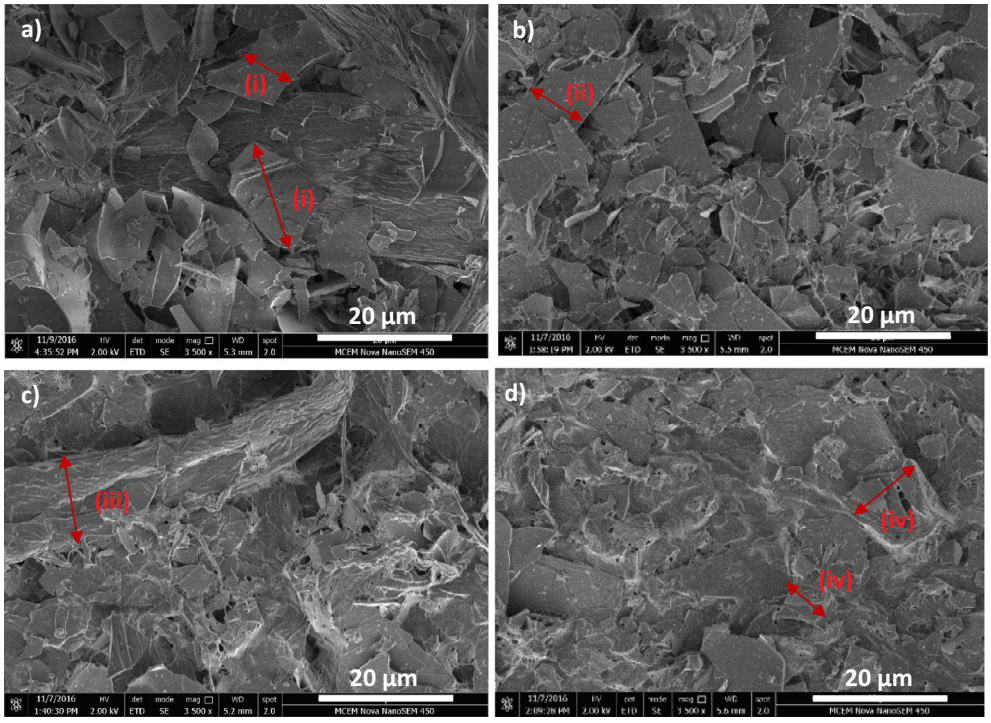

Fig. 5. SEM images of composites: **(a)** Unrefined/Per/PAE, **(b)** Refined/Per/PAE, **(c)** Homogenized(1pass)/Per/PAE and **(d)** Homogenized(3pass)/Per/PAE.

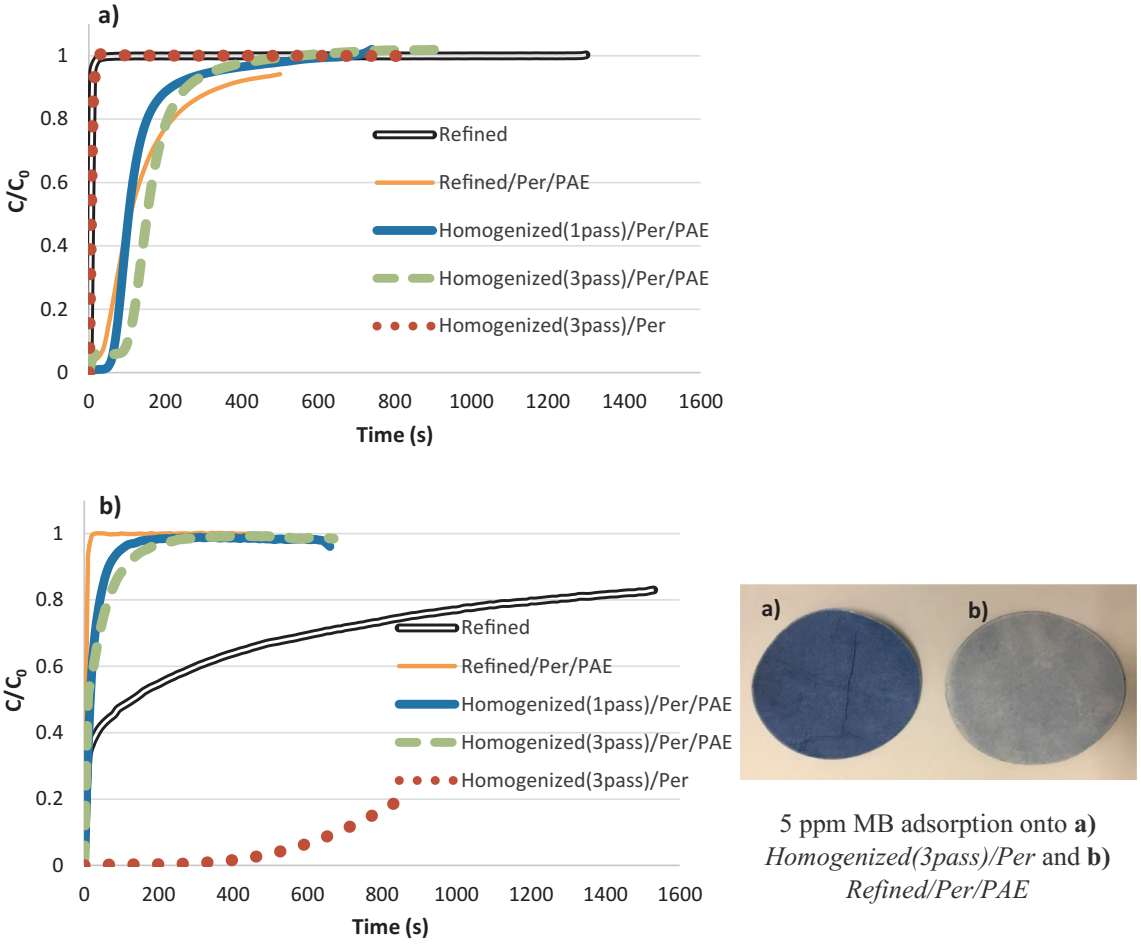

Fig. 6. Adsorption breakthrough curves for **(a)** Metanil yellow and **(b)** Methylene blue at 1.5 bar for filters of different charges and extent of mechanical treatment.

94% MB removal was achieved with composites made with highly fibrillated cellulose but without PAE (*Homogenized(3pass)/Per*); the maximum removal of MY was around 28% for the composites with refined fibres and PAE (*Refined/Per/PAE*). Flux remained identical for both dyes for all composites. Flux remarkably decreases with addition of homogenized pulps. The flow rates for each sample and both dyes are reported in SI (Fig. S3a–d).

3.2.2. Filtration

The rejection rate of suspensions with 1 μm SiO_2 particles was determined for the four different filters at an inlet pressure of 1.5 bar. 1 μm particles were selected as model bacteria (1 μm and bigger) to be removed from food streams such as beer, wine or juice [27]. The effect of homogenization, filter medium charge, inlet pressure and suspension pH on filtration performance was measured. The rejection rate and flux are presented at pHs of 5.8 and 7.2 in Fig. 8. The effect of pH was tested as it is an important variable in applications such as food and pharmaceutical; pH can affect cellulosic fibre pore structure and porosity through swelling and modifying bond strength. Filters have more than 90% particle rejection rate at both pH; pH had no effect on rejection. Charge of filter medium and inlet pressure also did not affect filtration efficiency. Rejection is around 99% for the negatively charged cellulose composites made with homogenized fibres (3 pass) (*Homogenized (3pass)/Per)*. The same rejection rate of around 99% was measured for the composites treated with PAE (*Homogenized(3pass)/Per/PAE*) at 2 different pressures (1 and 2 bar) (Fig. 8a).

(Fig. 8b) Flux decreased remarkably after only 1/3 of the fibre fraction substituted with homogenized fibres. Filtration flux decreased by 30–70% compared to dye solution adsorption flux.

4. Discussion

The adsorption of dye onto the perlite-cellulose composites is electrostatically controlled. The major effect of homogenization on adsorption is to increase surface area which also increases the surface and density of accessible charges. An increase in negatively charged sites contributes either to stronger repulsive or attractive forces between filter medium and dye depending on the system. The effect of surface area is revealed by the breakthrough curves of composites made with refined and homogenized pulps. Composites with refined pulp (*Refined/Per/PAE*) have less repulsive forces with negatively charged dye (MY, Fig. 6a) and less attractive forces with the cationic dye (MB, Fig. 6b) compared to other PAE treated composites. As homogenization is applied and the extent of homogenization increases, increasing accessible negative charges on surface remarkably changes the adsorption behaviour of dye molecules onto the composites.

Adding the cationic PAE both modifies the filter charge which changes its adsorption capacity and improves the composite wet strength by cross linking cellulose fibres. For the cationic dye (MB), the electrostatic interactions, maximized by the elimination of PAE, yield higher adsorption capacity. In contrast, PAE triggers higher adsorption of anionic dye (MY) onto the composites. The addition of negatively charged perlite particles also changes the adsorption behaviour significantly; this is similar to the effect of mechanical treatment of fibres and cationic polymer. The remarkably improved breakthrough curve of *Homogenized(3pass)/Per* (Fig. 6b) is attributed to perlite acting as an excellent filter aid [30].

Nanocellulose addition, achieved by fiberizing a fraction of cellulose fibres (1/3), did not affect the filtration performance significantly.

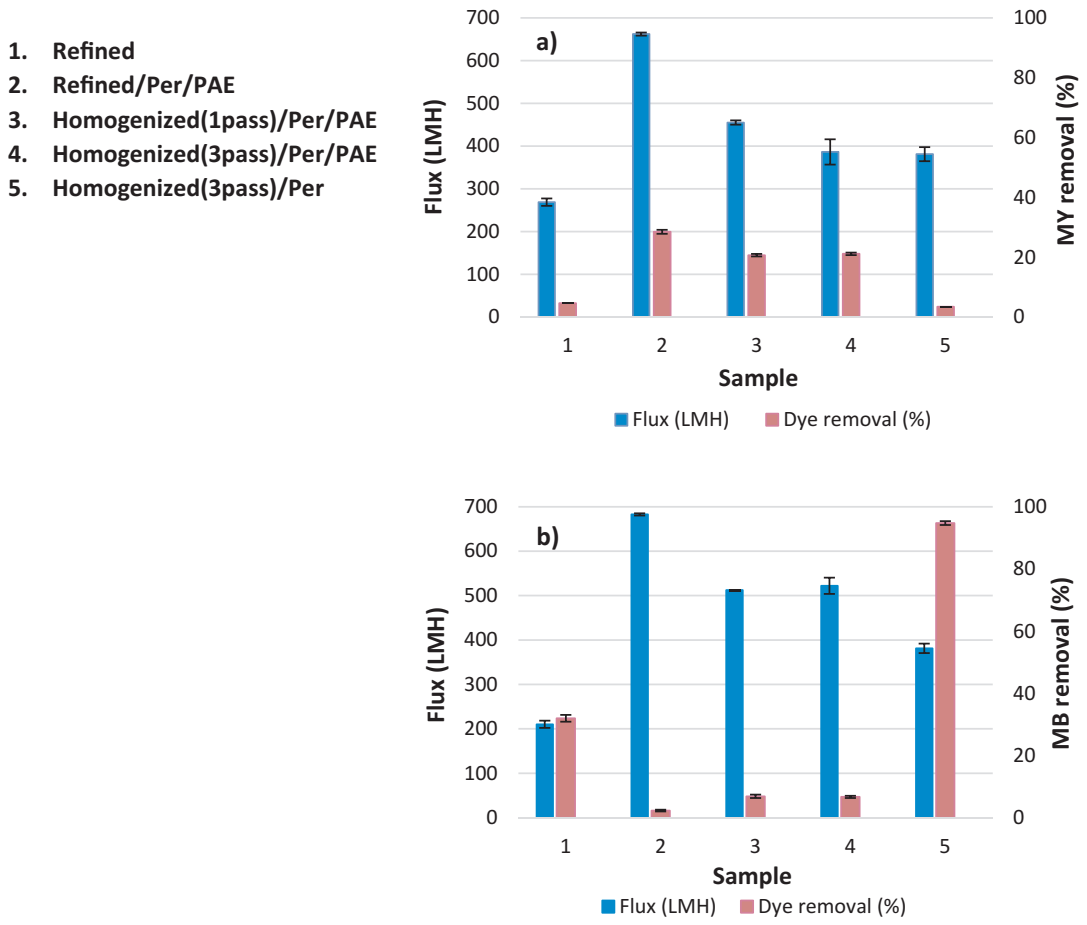

Fig. 7. Flux and total dye removal (%) of samples with **(a)** Metanil yellow and **(b)** Methylene blue dye solutions.

(Fig. 8a). The slight decrease in SiO_2 rejection rate by composites made of highly homogenized fibres (*Homogenized(3pass)/Per/PAE)* at 1.5 bar) is within experimental error. Increasing fibrillation through mechanical treatment intensity did not increase filtration performance.

Homogenization on refined pulp creates a dense and highly fibrillated NC network with a decrease in fibre diameters. The filters made with a small fraction of nano fibres have a more compact and connected structure. The pore size distribution changed remarkably by only substituting 1/3 of the pulp by homogenized fibres. This is due to the web like entangled structure of NC. The more fibrillated the fibres are, the denser the structure is and the less and the smaller are the voids developed between fibres. Composite porosity and pore size distribution can be controlled by modifying fibre diameters. As the homogenization forms smaller pores with denser fibre packing, liquid flux through the composites filters decreases with homogenized pulp addition.

The presence of inorganic particle in the filters also affects porosity and pore size distribution. Pure cellulose sheet has the lowest flux value (Fig. 4a and b). This is due to two phenomena: low porosity as there is no settlement of particles between fibres; decreasing flow rate in time as the fibres compress under pressure (Fig. S3a–d). This compressibility of fibres is well known [31] and leads to poor flux. High loading of inorganic particles prevents this compression so the composites retain high flow rates with very slight change over time.

There is only a weak relation between flux and dye removal capacity – as measured with both dyes (Fig. 7). While less adsorption generally occurs at high fluxes, adsorption is mostly affected by the charge of the filter medium and the solute molecules (Fig. 7a), regardless of flux. Similarly, there was no correlation between rejection rate of 1 μm particles and flux. *Homogenized(3pass)/Per/PAE* successfully removed 99% of the particles at both 1 and 2 bar.

The high filtration rejection of 1 μm particles achieved by the nanocellulose/perlite depth composites is important to the pharmaceutical, food and beverage industry. This brings a new perspective in cold pasteurization to remove microorganisms ranging from 1 to 2 μm [26] and remove ionic compounds [32] (acids and phenolic compounds) without heat treatment which affects taste or denaturing active ingredients. The concept is to rely on the inorganic particles for the selective adsorption of organic molecules, PAE treatment for the retention of colloids- based on charge and filtration for the pasteurization. Nanocellulose-inorganic depth composites can easily be engineered for specific liquid stream purification.

5. Conclusion

Cellulose fibre-perlite composites were prepared using a paper making technique for liquid filtration and adsorption applications. Perlite content was maintained at 70 wt% and the fibre composition was varied with partial substitution of pulp homogenized to different intensities; this was to control fibre structure by increased bonding area and decreasing porosity. A well-known wet strength agent, polyamide-amine-epichlorohydrin (PAE), was used for two purposes; first to provide wet strength; second, to control charge and capacity of filter medium. Two oppositely charged dyes were investigated as models to characterize the adsorption behaviour. The adsorption of dye is electrokinetically controlled and selective adsorption can be achieved by engineering the attractive and repulsive forces. The presence of highly fibrillated NC increased the surface area and also the amount of negative charges accessible in the medium. Increase in negatively charged sites contributed to attractive/repulsive forces depending on the type of

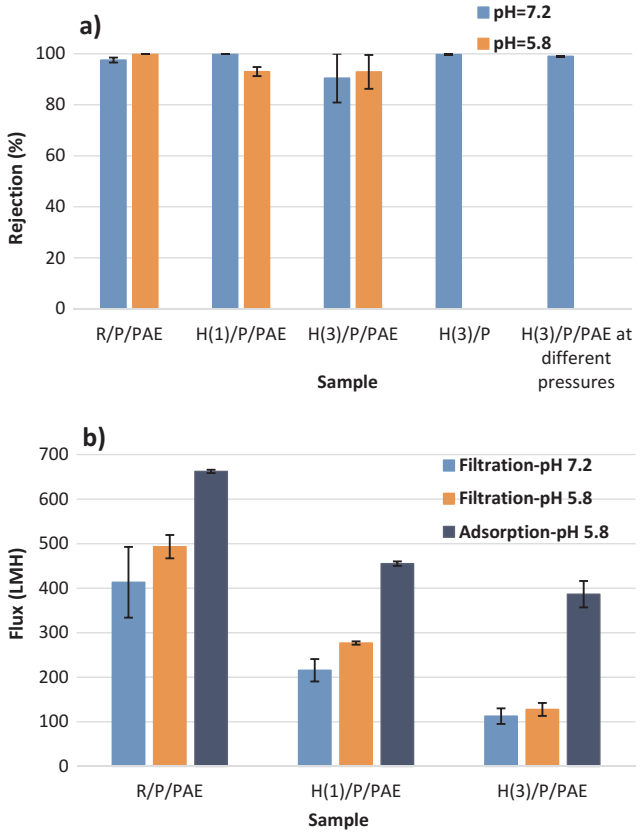

Fig. 8. (a) SiO_2 particle rejection rate (%) of Refined/Per/PAE, Homogenized (1pass)/Per/PAE, Homogenized(3pass)/Per/PAE, Homogenized(3pass)/Per at 1.5 bar and Homogenized (3pass)/Per/PAE at 1 and 2 bar **(b)** Adsorption and filtration flux of Refined/Per/PAE, Homogenized(1pass)/Per/PAE, Homogenized(3pass)/Per/PAE at 1.5 bar.

dye. Homogenized pulp also yielded smaller pore sizes which decreased flux. PAE addition controls and can reverse the charge of filters which substantially affected adsorption performance but it had no effect on filtration efficiency. The composites were efficient in filtration with 90% rejection rate of 1 μm particles. The high filtration capability of the composites at high flux is promising for cold pasteurization in which bacteria (1 μm) are removed at higher than 99% efficiency. Nanocellulose-depth composites provide new purification opportunities in pharmaceutical and food product stream by combining adsorption and filtration to remove interfering elements and colloids.

Acknowledgements

This work was supported by 3M Australia. The authors also acknowledge the Monash Centre for electron microscopy for the facilities used.

Appendix A. Supplementary material

Supplementary data associated with this article can be found, in the online version, at https://doi.org/10.1016/j.seppur.2018.04.038.

References

[1] I.M. Hutten, Chapter 7 - liquid filter applications, Handbook of Nonwoven Filter Media, second ed., Butterworth-Heinemann, Oxford, 2016, pp. 409–450.
[2] M.F. Jimenez-Solomon, P. Gorgojo, M. Munoz-Ibanez, A.G. Livingston, Beneath the surface: influence of supports on thin film composite membranes by interfacial polymerization for organic solvent nanofiltration, J. Membr. Sci. 448 (2013) 102–113.
[3] S. Ramaswamy, A.R. Greenberg, W.B. Krantz, Fabrication of poly (ECTFE) membranes via thermally induced phase separation, J. Membr. Sci. 210 (2002) 175–180.
[4] S. Jiang, Y. Li, B.P. Ladewig, A review of reverse osmosis membrane fouling and control strategies, Sci. Total Environ. 595 (2017) 567–583.
[5] A. Mukhopadhyay, 8 - Composite nonwovens in filters: applications, Composite Non-Woven Materials, Woodhead Publishing, 2014, pp. 164–210.
[6] D. Klemm, F. Kramer, S. Moritz, T. Lindström, M. Ankerfors, D. Gray, A. Dorris, Nanocelluloses: a new family of nature-based materials, Angew. Chem. Int. Ed. 50 (2011) 5438–5466.
[7] R. Andrade, O. Skurtys, F. Osorio, R. Zuluaga, P. Gañán, C. Castro, Wettability of gelatin coating formulations containing cellulose nanofibers on banana and eggplant epicarps, LWT – Food Sci. Technol. 58 (2014) 158–165.
[8] K. Dimic-Misic, C. Ridgway, T. Maloney, J. Paltakari, P. Gane, Influence on pore structure of micro/nanofibrillar cellulose in pigmented coating formulations, Transp. Porous Media 103 (2014) 155–179.
[9] J. Kim, G. Montero, Y. Habibi, J.P. Hinestroza, J. Genzer, D.S. Argyropoulos, O.J. Rojas, Dispersion of cellulose crystallites by nonionic surfactants in a hydrophobic polymer matrix, Polym. Eng. Sci. 49 (2009) 2054–2061.
[10] G. Rodionova, M. Lenes, Ø. Eriksen, Ø. Gregersen, Surface chemical modification of microfibrillated cellulose: improvement of barrier properties for packaging applications, Cellulose 18 (2011) 127–134.
[11] C. Salas, T. Nypelö, C. Rodriguez-Abreu, C. Carrillo, O.J. Rojas, Nanocellulose properties and applications in colloids and interfaces, Curr. Opin. Colloid Interface Sci. 19 (2014) 383–396.
[12] Z. Karim, S. Claudpierre, M. Grahn, K. Oksman, A.P. Mathew, Nanocellulose based functional membranes for water cleaning: tailoring of mechanical properties, porosity and metal ion capture, J. Membr. Sci. 514 (2016) 418–428.
[13] H. Ma, B.S. Hsiao, B. Chu, Ultrafine cellulose nanofibers as efficient adsorbents for removal of UO_2^{2+} in water, ACS Macro Lett. 1 (2012) 213–216.
[14] A. Mautner, K.Y. Lee, P. Lahtinen, M. Hakalahti, T. Tammelin, K. Li, A. Bismarck, Nanopapers for organic solvent nanofiltration, Chem. Commun. 50 (2014) 5778–5781.
[15] A. Mautner, K.-Y. Lee, T. Tammelin, A.P. Mathew, A.J. Nedoma, K. Li, A. Bismarck, Cellulose nanopapers as tight aqueous ultra-filtration membranes, React. Funct. Polym. 86 (2015) 209–214.
[16] H. Sehaqui, A. Mautner, U. Perez de Larraya, N. Pfenninger, P. Tingaut, T. Zimmermann, Cationic cellulose nanofibers from waste pulp residues and their nitrate, fluoride, sulphate and phosphate adsorption properties, Carbohydr. Polym. 135 (2016) 334–340.
[17] H. Sehaqui, B. Michen, E. Marty, L. Schaufelberger, T. Zimmermann, Functional cellulose nanofiber filters with enhanced flux for the removal of humic acid by adsorption, ACS Sustain. Chem. Eng. 4 (2016) 4582–4590.
[18] H. Sehaqui, U. Perez de Larraya, P. Tingaut, T. Zimmermann, Humic acid adsorption onto cationic cellulose nanofibers for bioinspired removal of copper(ii) and a positively charged dye, Soft Matter 11 (2015) 5294–5300.
[19] S. Srivastava, A. Kardam, K.R. Raj, Nanotech reinforcement onto cellulosic fibers: green remediation of toxic metals, Int. J. Green Nanotechnol. 4 (2012) 46–53.
[20] X. Yu, S. Tong, M. Ge, L. Wu, J. Zuo, C. Cao, W. Song, Adsorption of heavy metal ions from aqueous solution by carboxylated cellulose nanocrystals, J. Environ. Sci. 25 (2013) 933–943.
[21] J.J. Blaker, K.-Y. Lee, A. Bismarck, Hierarchical composites made entirely from renewable resources, J. Biobased Mater. Bioenergy 5 (2011) 1–16.
[22] N. Keshavarzi, F. Mashayekhy Rad, A. Mace, F. Ansari, F. Akhtar, U. Nilsson, L. Berglund, L. Bergström, Nanocellulose-zeolite composite films for odor elimination, ACS Appl. Mater. Interfaces 7 (2015) 14254–14262.
[23] S. Varanasi, Z.-X. Low, W. Batchelor, Cellulose nanofibre composite membranes – biodegradable and recyclable UF membranes, Chem. Eng. J. 265 (2015) 138–146.
[24] Z. Karim, A.P. Mathew, V. Kokol, J. Wei, M. Grahn, High-flux affinity membranes based on cellulose nanocomposites for removal of heavy metal ions from industrial effluents, RSC Adv. 6 (2016) 20644–20653.
[25] G.J. Freeman, 11 - Reducing microbial spoilage of beer using filtration A2, in: Annie E. Hill (Ed.), Brewing Microbiology, Woodhead Publishing, Oxford, 2015, pp. 241–251.
[26] V. Millet, A. Lonvaud-Funel, The viable but non-culturable state of wine microorganisms during storage, Lett. Appl. Microbiol. 30 (2000) 136–141.
[27] C. Peri, M. Riva, P. Decio, Crossflow membrane filtration of wines: comparison of performance of ultrafiltration, microfiltration, and intermediate cut-off membranes, Am. J. Enol. Viticult. 39 (1988) 162–168.
[28] T.M. Toland, K.C. Fugelsang, C.J. Muller, Methods for estimating protein instability in white wines: a comparison, Am. J. Enol. Viticult. 47 (1996) 111–112.
[29] H. Giesche, Mercury porosimetry: a general (practical) overview, Part. Part. Syst. Char. 23 (2006) 9–19.
[30] M. Doğan, M. Alkan, Y. Onganer, Adsorption of methylene blue from aqueous solution onto perlite, Water Air Soil Pollut. 120 (2000) 229–248.
[31] P. Orsolini, B. Michen, A. Huch, P. Tingaut, W.R. Caseri, T. Zimmermann, Characterization of pores in dense nanopapers and nanofibrillated cellulose membranes: a critical assessment of established methods, ACS Appl. Mater. Interfaces 7 (2015) 25884–25897.
[32] J.A. Considine, E. Frankish, Chapter 3 – wine chemistry, A Complete Guide to Quality in Small-Scale Wine Making, Academic Press, San Diego, 2014, pp. 23–50.

frontiers in Chemistry

ORIGINAL RESEARCH
published: 12 September 2018
doi: 10.3389/fchem.2018.00417

Multi-Layer Filters: Adsorption and Filtration Mechanisms for Improved Separation

*Aysu Onur[1], Aaron Ng[2], Warren Batchelor[1] and Gil Garnier[1]**

[1] Chemical Engineering Department, Bioresource Processing Research Institute of Australia, Monash University, Clayton, VIC, Australia, [2] 3M Australia, Sydney, NSW, Australia

Filters made of cellulose fiber and perlite particles were prepared using a wet laying papermaking technique. Polyamide-amine-epichlorohydrin (PAE) was added to provide wet strength. Filters were prepared at two different total basis weights of 200 and 400 grams per square meter (gsm). Single and multi-layered filters were structured for each total basis weights. The effect of total basis weights and multi-layered structure on methylene blue adsorption and silicon dioxide (SiO_2) particle filtration was investigated. Methylene blue adsorption was performed in two modes: constant pressure and constant flow rate. In both operation modes, the adsorption capacity of multi-layered filters was significantly higher (16–100%) than for single-layer filters at the same overall weight. The effect of layer separation was also characterized using polypropylene separators and tested under constant flow rate operation. Separators provided more effective methylene blue adsorption by generating a well-distributed flow. Filtration performance was quantified with 0.5 μm silicon dioxide particles under constant pressure conditions; this is to mimic bacteria rejection. Filtration capability of SiO_2 particles was reduced slightly (12%) with decreasing individual filter layer thickness regardless of the multi-layered structure. Filtering polyethylene glycol (PEG) molecules with two different molecular weights was performed; however, no rejection was recorded. The filter internal pore structure was visualized by 3D-X ray computed tomography and the void fraction was quantified. 400 gsm single layer presented areas of low fiber density forming pores, while the pore volume decreased for thinner filter layers.

Keywords: composite, multi-layer, adsorption, filtration, cellulose fiber, channeling

OPEN ACCESS

Edited by:
Alexei Lapkin, University of Cambridge, United Kingdom

Reviewed by:
Antti Ilmari Koponen, VTT Technical Research Centre of Finland Ltd, Finland
Omar Gonzalez-Ortega, Universidad Autónoma de San Luis Potosí, Mexico

***Correspondence:**
Gil Garnier
gil.garnier@monash.edu

Specialty section:
This article was submitted to Chemical Engineering, a section of the journal Frontiers in Chemistry

Received: *19 March 2018*
Accepted: *23 August 2018*
Published: *12 September 2018*

Citation:
Onur A, Ng A, Batchelor W and Garnier G (2018) Multi-Layer Filters: Adsorption and Filtration Mechanisms for Improved Separation. Front. Chem. 6:417. doi: 10.3389/fchem.2018.00417

INTRODUCTION

Depth filters (Sutherland, 2011) are porous filtering mediums composed of cellulose fibers and inorganic absorbents. Unlike surface filtration, they can retain contaminants through the thickness as well as on the surface during liquid filtration. These composite structures combine two different separation principles and technologies in a single medium. Filtration by particle rejection is provided by forming an intricate mesh, where selective adsorption is achieved by a functional inorganic particle. Separation can further be improved by combining other additives, such as charged polyelectrolytes in the network (Dizge et al., 2011). The medium can be modified with a cationic polymer adsorbing the common negatively charged dissolved contaminants significantly smaller than the average pore size. However, depth filtration analysis reported in literature has

mostly focused on the modeling of membrane separations (Polyakov, 2008, 2009; Sutherland, 2011; Kuhn and Briesen, 2016; Bedrikovetsky et al., 2017; Goldrick et al., 2017); there is a lack of experimental studies optimizing depth type filter operation especially in terms of membrane structure.

Filtration performance can be tailored in many ways by controlling filter structure/composition and operation mode. Two efficient modes of operation are dead-end filtration and cross-flow filtration, where the flow is passed directly through the filter in dead-end and tangential to the filter in cross-flow filtration (Liderfelt and Royce, 2018), respectively. Furthermore, these processes can be controlled under modes of constant pressure or constant flow rate. In either case, the non-constant parameter is being monitored, and the extent of filter fouling or clogging is assessed by the recorded parameters (Iritani et al., 2015; Goldrick et al., 2017). Filtration performance can also be altered by modifying the structure and configuration of filters. Multi-layer structured filters with varying pore sizes stacked on top of another offer a simple way of sequentially separating cells or particles (Saefkow, 1995; Rijn, 1998). In a recent study by Griffiths et al. (Griffiths et al., 2016), filtration was modeled on a multi-layered membrane structure with each layer having varying pore sizes stacked on one another. The efficiency of multi-layered filter structure was analyzed by developing a model simulating the transport and filtration of particles through a multi-layer structure. This model characterizes the filter and offers optimal design requirements in terms of number of filter layers, pore size in each layer and pore interconnectivity between layers.

Filtering bacteria with multi-layered filters to provide a greater capture of bacteria was also reported (Koch, 1984). The study aimed at achieving higher bacteria rejection by mechanically attaching a layer to another, which contains a bacteria-destroying material. In another study (Wertz and Guimond, 2014), a nano fiber layer was attached to the initial layer of a fibrous filter. Filter media having a first layer and a nanofiber layer adhered onto exhibited advantageous properties including increased dust holding capacity.

Although multi-layered filters are well-known in industry, very few studies have systematically quantified their adsorption and filtration mechanisms, and even less have characterized the effect of multi-layered structure on depth filter performance. In this study, we developed multi-layered and single-layered filter structures made from the same amount of filter media. Depth filter layer processing was inspired from papermaking technique and characterized for adsorption and particle rejection capability. The adsorption and filtration mechanisms behind the performance of single and multi-layered filters were analyzed in terms of chemical engineering and internal filter structure using an advanced image technique and colloids and surface concepts.

MATERIALS AND METHODS

Materials

Cellulose fibers used for the composites are unrefined northern softwood NIST RM 8495 bleached Kraft pulp and bleached radiata pine softwood Kraft pulp refined to 400 Canadian standard freeness (CSF) in a disk refiner. Expanded perlite was provided by Dicalite Minerals Corp. Commercial PAE was provided from Nopcobond Paper Technology Pty Ltd.

Methylene blue (MB) in powder form and 0.5 μm monodispersed silicon dioxide (SiO_2) particles of density 1.8 g/cm^3 were purchased from Sigma Aldrich. Polyethylene glycol (PEG) of two molecular weights (600 and 5,000 kDa) was provided by Dow Chemical. Polypropylene separators with 0.45 μm pore size and diameter of 47 mm was purchased from CUNO Inc. Meriden, USA.

Methods

Fabrication of Filters

The dry northern softwood NIST pulp was wetted by soaking in deionized water overnight. The pulp was transferred to a disintegrator (Model MKIIIC, Messmer Instruments Ltd.) and disintegrated for 75,000 revolutions. Filters were prepared using a standard British hand sheet maker at three different total basis weights: 100, 200, and 400 gsm. The step by step preparation method was published in a previous study (Onur et al., 2018). The filter chemical composition is similar to that of standard industrial filters: it consists of 30% fiber (1/3 refined pulp + 2/3 unrefined pulp) and 70% perlite with PAE (0.22% w/v) added at a rate of 100 mg/g fiber on top of the suspension (0.26 wt.%) before papermaking. Composites were prepared either as one single layer or in the form of stacked equal multilayers that is equivalent to the total targeted basis weight. Five different filters prepared according to different layer configurations and different total basis weights are shown in **Figure 1**. Samples were coded with the corresponding labels. The criteria for material selection are based on industrial filters for food and beverage applications; food grade filters usually contain these materials.

PAE is used to provide wet strength to the filters. It crosslinks with the carboxyl group of cellulose to create an irreversible covalent bond network and provides some waterproof barrier around fibers (Obokata and Isogai, 2007). PAE also adsorbs onto the fibers and particles of the suspension which introduces positive charges to the anionic surfaces of cellulose fibers and perlite particles. Addition of PAE to the suspension results in the partial surface coverage of perlite and cellulose fibers by positively charged polymer. This induces electrostatic interactions between negatively charged contaminants and the filter medium. Using PAE is allowed by food regulations at low concentrations (up to 2.5 wt.% of the dry sheet); it is considered an indirect food additive and the concentration of PAE of this study is around this limit (CFR–Code of Federal Regulations Title[1]).

Perlite is a low cost adsorbent made from a glassy volcanic rock; it is known as an excellent filter aid (Dogan et al., 2000). Perlite is an anionic adsorbent of zeta potential ranging between –40 and –50 mV (Alkan et al., 2005). The particle size distribution of perlite and its effect on the structure and porosity of filters was reported in a previous study (Onur et al., 2018).

[1]CFR–Code of Federal Regulations Title 21. Available online at: https://www.accessdata.fda.gov/scripts/cdrh/cfdocs/cfcfr/cfrsearch.cfm?fr=176.170.

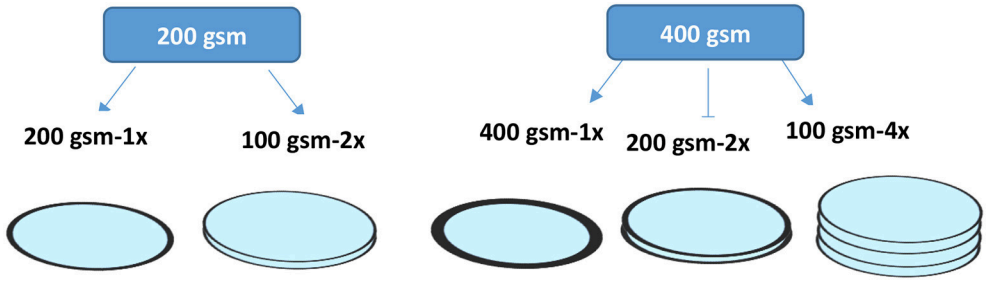

FIGURE 1 | Schematic representation of the different filter configurations investigated at two different basis weights.

Adsorption and Filtration With Constant Pressure

Adsorption and filtration experiments under constant pressure mode were performed with a dead-end stirred cell from Merck Millipore Australia. The closed setup has 400 mL of working volume and is pressurized by a compressed air gas cylinder. Samples were placed on the membrane holder at the bottom of the cell body with an O-ring. For multilayers, the O-ring pressed layers from the edges so the interlayer gap was negligible. The cell body was filled with the desired solution following sample placement. Filtrate that passes through filters was transferred to an ultraviolet-visible (UV–Vis) absorption spectrometer via a quartz micro flow cell with 10 mm optical path length. Instantaneous absorbance was measured here every 10 s at a specific wavelength. After measurement in UV–Vis, filtrate was transferred to a beaker on a balance. Before conducting any experiments, water was flushed through samples to ensure equilibration. After equilibrium has been reached, either 5 ppm MB solution or 0.05 wt.% SiO_2 suspension were passed through the filters at 1.5 bar. Two replicates of filters were tested for both adsorption and filtration. Here, *adsorption* corresponds to the accumulation of model cationic or anionic molecules onto a surface by electrostatic attraction, while *filtration* is measured as the rejection of particles in suspension by size exclusion. MB preferentially adsorbs onto negatively charged surfaces; it can also diffuse through the pores of the negatively charged perlite particles. However, there is no electrostatic attraction between MB molecules and the positively charged filter medium after adsorption of the PAE cationic polymer. MB was therefore selected as standard dye to quantify improvement in breakthrough curves due to the multi-layered filter structure as unable to adsorb.

Mass flux for the effective membrane area (0.00418 m^2) was calculated by measuring the volume of permeate per unit area and time; Liter per Square Meter per Hour (LMH). Mass flow rate of filtrate as a function of time was also continuously recorded by a computer. Total flux was calculated with Equation (1).

$$FLUX\ (LMH) = \frac{Volume\ of\ filtrate\ \ (L)}{area\ \left(m^2\right)\ \times\ time\ (h)} \tag{1}$$

Adsorption experiments were run with 400 mL MB dye solution at a concentration of 5 ppm at pH 5.8 (This is the characteristic pH of MB). Breakthrough curves were plotted by normalized concentrations as a function of time. Additional solution was added for filters that did not reach saturation with 400 mL solution. Area over the curve was calculated for each filter to determine the adsorption capacity of filters. Capacity was calculated based on Equation (2) (Barros et al., 2013). The integral was calculated from the area over the curve using the trapezoidal method.

$$q = \frac{C_F\ \times\ \dot{Q}}{1,000\ \times\ m_s} \int_0^{t_{end}} \left(1\ -\ \frac{C_{out}}{C_F}\right) dt \tag{2}$$

Where:

q: Capacity of the adsorbent (mg/g)
C_{out}: Concentration of MB in the filtrate (mg/g)
C_F: Concentration of MB in the feed (mg/g)
$\dot{Q}$: Volumetric flow rate (cm^3/s)
t_{end}: Time (s)
m_s: Weight of adsorbent (g)

Rejection of 0.5 μm SiO_2 particles was determined by filtering 0.05 wt.% SiO_2 suspension at the same pH value as dye molecules (pH = 5.8) through the filters. pH of 5.8 is desirable as increasing pH would dissociate carboxylic acids leading to repulsive forces between charged groups. These repulsive forces also lead to swelling of the cellulose fiber with collapse of the filter pore structure. SiO_2 concentration of suspension before and after filtration was estimated by UV–Vis absorption spectroscopy and the Equation (3) was used to calculate rejection capability of filters. UV–Vis spectroscopy calibration curves of MB dye molecules and SiO_2 particles are shown in the Supplementary information **(Figure S5)**.

$$Rejection\ (\%) = 1 - \left(\frac{\text{Filtrate concentration}}{\text{Initial feed concentration}}\right) \times 100 \tag{3}$$

PEG molecules were also filtered through the composites to quantify their microfiltration capability. The MWCO range for microfiltration applications usually starts from 500 kDa up to big particle filtration such as yeast and bacteria; the filtration spectrum can be found in the study (Pearce, 2007). Total carbon analyser was used to measure the concentration of PEG molecules in the suspension before and after filtration.

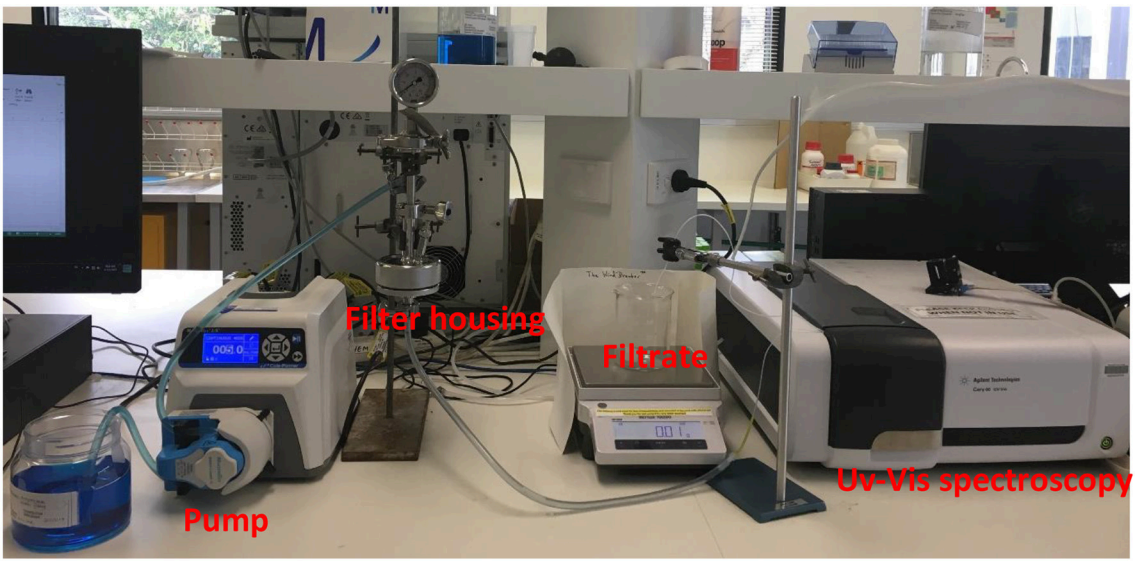

FIGURE 2 | Experimental setup shown for 47 mm filter housings under constant flow rate mode.

Adsorption With Constant Flow Rate

Adsorption performance was additionally tested using 47 mm (corresponds to diameter of filter housings) stainless steel filter housings with 0.00132 m^2 effective membrane area to verify the performance under constant flow rate operation mode. A peristaltic pump was used at a constant flow rate (12 mL/min) such that the same total flux as the constant pressure experiments for the same sample was obtained. Experiments were performed with and without presence of polypropylene separators. Separators are used to provide a well-distributed and uniform flow through a filter; they do not adsorb MB. Separators were placed in the housings as previously described (Adsorption and Filtration with Constant Pressure). The only gap created between multilayers is the thickness of the separator which is well below 1 mm. 47 mm separators were placed between the layers as well as on top of initial layers. Filtrate was transferred to UV-Vis spectroscopy via quartz micro flow cell to obtain the concentration at a regular time interval. Total mass flux and flow rate as a function of time were recorded by the same setup as constant pressure mode. Adsorption capacities were calculated form the experimental breakthrough curves as explained above. The experimental setup for constant flow rate operation is shown in **Figure 2**.

3D X-ray Tomography

X-ray computed 3D tomography was used to make a quantitative and qualitative analysis on the internal structure of filters about how the fiber network differently built up to form a sheet according to different basis weights. This technique provides a non-destructive 3D imaging. The basic principle is based on the set of images of beam transmitted through the sample while the sample is rotated to different positions for each image taken (Holmstad, 2004). Samples with 2 × 8 mm of size were visualized by Zeiss Xradia 520 Versa. The X-ray source was operated at 30 kV. Distance from source to sample and sample to detector was set to 15 mm. The number of images taken per scan was 1,601 and the image resolution was 2,022 × 2,022 pixels. Avizo and Image J software were used to reconstruct images and to quantify the total void fraction and void fraction distribution through the thickness (SI). Thresholding is done by comparing grayscale and thresholded image with a judgment. The threshold was meticulously selected with trial and error such that we do not lose any materials. Detailed information on scanning settings can be found in Supplementary materials **(Figure S6)**. Void structure and how the void structure is changing through the thickness were analyzed qualitatively as well.

RESULTS

Cellulosic membranes of two different thicknesses (200 and 400 gsm) were tested under different filter configurations. The filters were examined under two operating conditions: at a constant flow rate (12 mL/min) or at a constant pressure (1.5 bar). The effect of polypropylene separators between the layers on adsorption performance was tested with 400 gsm single layer (400 gsm-1x) and four layers of 100 gsm filters (100 gsm-4x) under constant flow operation. Filtration of 0.1 wt.% PEG molecules of molecular weight of 600 and 5,000 kDa was performed under constant pressure (1.5 bar) mode for each filter configuration. Filters were also tested with suspensions of 0.5 μm SiO_2 particles (0.05 wt.%) under constant pressure (1.5 bar). Finally, the internal structure of 400 gsm filters made of single and multiple layers was analyzed by 3D X-ray tomography combined with image analysis.

Methylene Blue Adsorption Under Constant Pressure

Methylene blue was used as a model for the cationic organic dissolved contaminants. Constant pressure adsorption testing

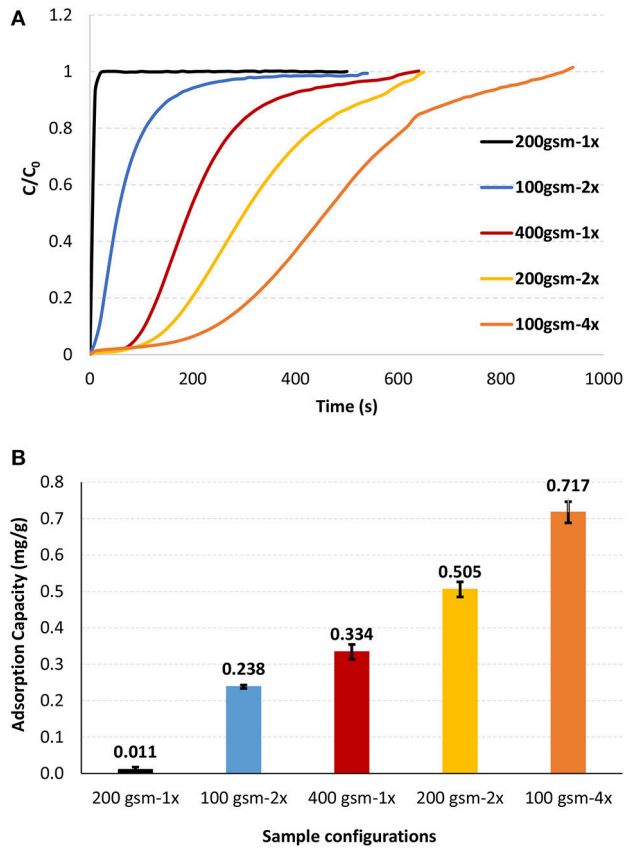

FIGURE 3 | Effect of filter configuration and number of interfaces on the **(A)** methylene blue breakthrough curves and **(B)** methylene blue adsorption capacities. Tests were performed at 1.5 bar and 22°C.

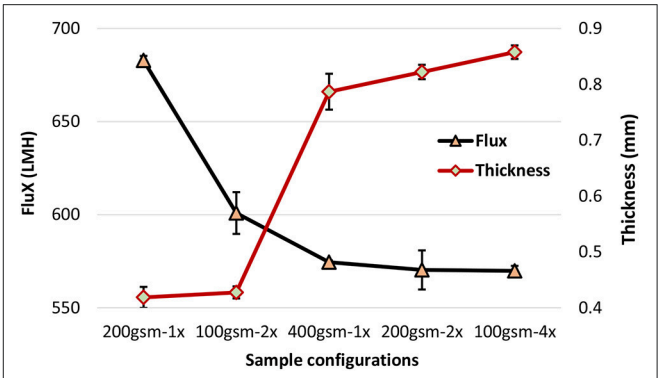

FIGURE 4 | Effect of filter configuration and number of interfaces on the flux and thickness under 1.5 bar, 22°C.

identifies filter compaction and saturation by measuring flowrate. Breakthrough curves were recorded under constant pressure (1.5 bar) for different filter configurations using two types of cellulose filters differing in thickness (gsm; **Figure 3A**). The adsorption capacity for each configuration was calculated using the breakthrough curves. The adsorption capacity of each filter is shown in **Figure 3B**.

Multilayer filters provided improved breakthrough curves and higher adsorption capacities than single layer filters as tested under constant pressure (**Figure 3**). Adsorption capacity of 400 gsm filter drastically increased by 54% and 118% by forming two layers (200 gsm-2x) and four layers (100 gsm-4x), respectively (**Figure 3B**), all at the same filter weight. Adsorption capacity of 200 gsm filter also increased significantly by forming two layers of 100 gsm (100 gsm-2x).

The effect of filter configuration, including number and basis weight of layers, on filtration flux and filter thickness is shown in **Figure 4** under constant pressure mode. At a given basis weight or amount of filter media, filter thickness increases slightly with multi-layered configuration. Flux decreased with increased gsm and the number of layers at a given gsm. Flux decreased from 682 to 600 LMH (Liters per Square Meter per Hour) for 200 gsm filters by introducing two layers of 100 gsm. However, flux slightly dropped for 400 gsm filters from 574 to 569 LMH for four layers of 100 gsm. For multi layered filters, an increased flux is expected according to Kozeny-Carman and Darcy (Siegfried Ripperger, 2000). These equations provide the mathematical relationships describing the flow of a fluid in a uniform porous media. Pressure loss between the layers might lead the flow traveling in the planar direction to find the path of least resistance through the next layer, resulting in an increased flux. However, this analysis does not fully apply to the space between layers. Once the stirred cell is pressurized by compressed air, the layers are being compressed and the flow is somewhat forced to flow through the next layer with little chance to flow in the planar direction. We believe that a slightly thicker layered structure would create a resistance and result in lower flux values.

Methylene Blue Adsorption Under Constant Flow Rate

Methylene blue adsorption breakthrough curves of 400 gsm filters comparing single layer configuration with four layers are presented in **Figure 5**. Breakthrough curves were obtained under constant flow rate with and without polypropylene separators between layers and on top of the first layer. Flow rate was set such that the flux is matching the flux values from constant pressure experiments for the same samples (12 mL/min).

Adsorption capacity is also much higher with multilayered filters under constant flow mode. The saturation occurred much quicker for both filters without separators. However, adsorption capacity decreased for both type of filters without separators. The capacity decreased by almost 15% for multilayered filter (100 gsm-4x) and 29% for single layer filter (400 gsm-1x) by removing separators. Adsorption capacities are found in **Table 1**.

The offset at the beginning of the curves without separators needs further study to better understand the phenomenon involved.

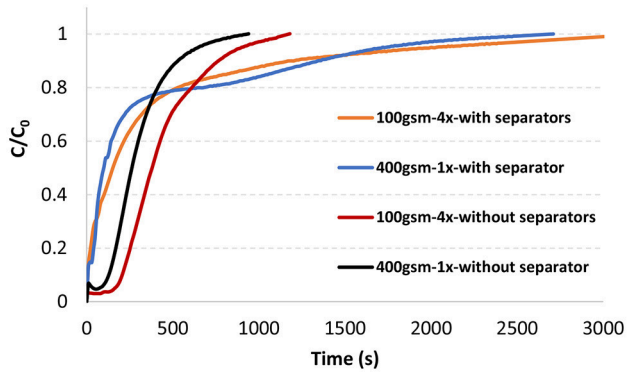

FIGURE 5 | Methylene blue breakthrough curves of 47 mm 100 gsm-4x and 400 gsm-1x filters in a single filter housing with and without separators at 12 mL/min, 22°C.

TABLE 1 | Methylene blue adsorption capacities of single layer and multi-layered filters with and without separators under constant flow rate (12 mL/min).

Filters	Adsorption capacity (mg/g)
100 gsm-4x-with separators	0.51 ± 0.04
400 gsm-1x-with separators	0.44 ± 0.01
100 gsm-4x	0.43 ± 0.05
400 gsm-1x	0.31 ± 0.05

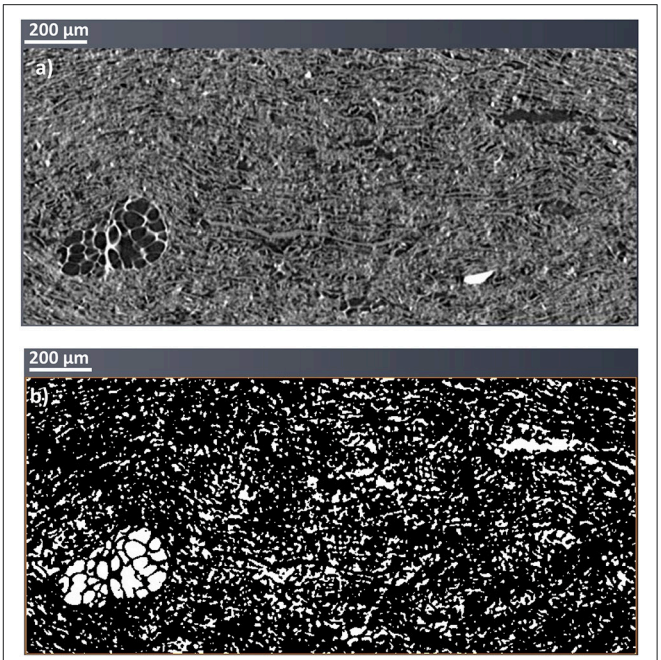

FIGURE 6 | 3D X-ray reconstituted images of 400 gsm sample (400 gsm-1x). **(a)** Grayscale and **(b)** Thresholded cross section images.

3D X-ray Tomography

3D X-ray tomography image analysis was conducted on single layer 400 gsm (400 gsm-1x), two layers of 200 gsm (200 gsm-2x) and four layers of 100 gsm (100 gsm-4x). Grayscale and thresholded cross section images of 400 gsm-1x are given in **Figure 6**. 3D images of all filters are shown with intersection of three different planes (**Figure 7**). The white sections represent voids in thresholded images. Animations on voids change locations through thickness are provided for all samples in **Supplementary information**.

The total void fraction of the composites calculated by image analysis is 20% for the 400 and 200 gsm filters and 14% for the 100 gsm filters. However, all void fractions are similar, as expected for filters of identical composition. The main difference lies in the pore structure, which differs with thicknesses, despite having a similar void fraction. The probability of forming bigger voids increases with the composite thickness. There are some zones of low density, creating flow channels in the 400 gsm single layer sample (**Figures 6**, **7**). These channels appear to propagate through the thickness and then to disappear. Channels are best observed in the animations provided in SI. These massive void concentration decreases at lower basis weights, particularly in 100 gsm composites.

The void distribution through thickness of an individual layer (200 gsm-2x) is shown in **Figure 8**. The composite mesh side is at the high number (88) and the air side is at the origin. Void distribution of 200 gsm filter through the thickness is decreasing from top to bottom (**Figure 8**); this density gradient is inherent to the papermaking technique. The density gradient across filter thickness with the highest composite density (lowest volume fraction) on the mesh side are expected from papermaking. The void distributions for all composites are provided in Supplementary information **(Figures S1–S4)**. However, it was not possible to visualize density gradient in all samples; this suggests that the subtle differences in structure affecting density are below the resolution of the X-ray tomography used. Sample properties based on different gsm were calculated using the properties of fiber and perlite and are shown in Supplementary material in **Table S3**. The calculated porosities are comparable to the porosities measured by X-ray tomography. However, these calculations suggest that the structure would be slightly denser with the increasing basis weights.

Filtration

The filtration ability of filters was quantified for the different configurations using polyethylene glycol polymers (PEG) of two molecular weights (600 and 5,000 kDa) and 0.5 µm SiO_2 colloids. Both PEGs passed through the filters without showing any cut off. Total organic carbon content (TOC) of PEG solutions before and after filtration were identical and given in Supplementary information **(Tables S1, S2)**. These filters are unable to provide microfiltration. The particle rejection of 0.5 µm SiO_2 particles was then measured. Very high particle rejection was recorded for the 400 and 200 gsm single layer filters. Particle rejection rate however dropped down for 100 gsm two layers (100 gsm-2x) and four layers (100 gsm-4x) filters. This shows that the actual thickness of the layers plays an important role in particle capture, regardless of the number of layers. SiO_2 particle rejection results

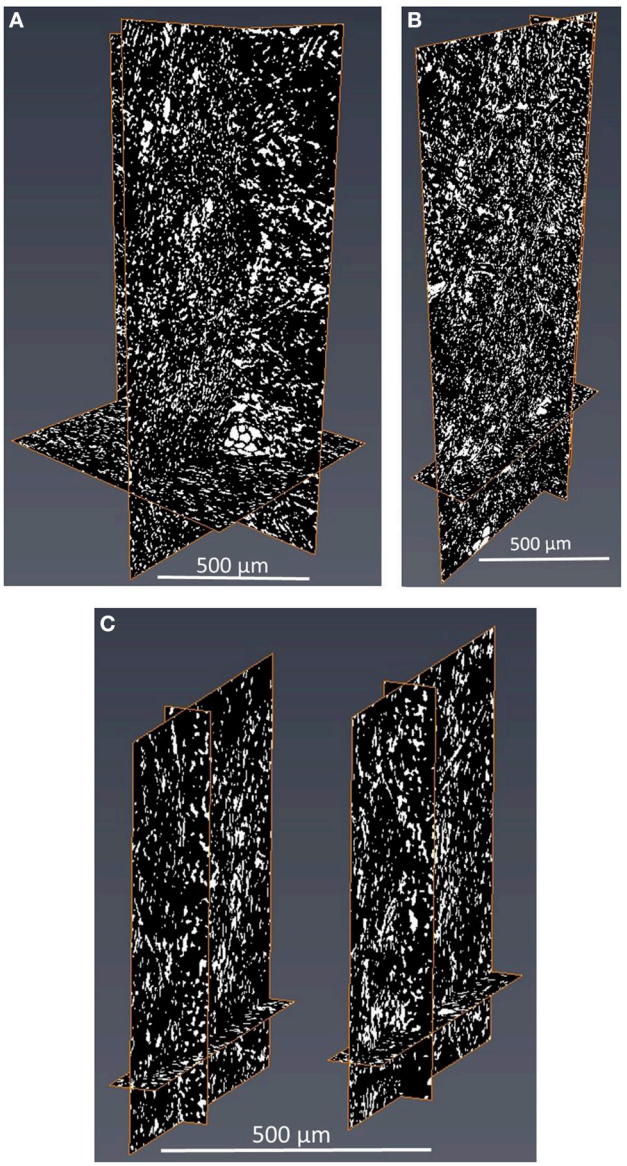

FIGURE 7 | 3D X-ray images of **(A)** 400 gsm sample **(B)** 200 gsm sample and **(C)** 100 gsm sample presented with some of layers with intersection of three different planes.

are given in **Table 2**. Besides, 100 gsm-4x filter also shows higher variation in rejection results. This variance potentially shows that multi-layered filters formed by low gsm layers cannot be relied upon for rejecting particles. However, further studies on filtration are needed to fully characterize the mechanism behind the rejection capability of multi-layered filters.

DISCUSSION

Effect of Operation Modes: Constant Pressure or Constant Flow

Under constant flow, pressure drop builds up across the filter to maintain the flow as fouling occurs over time (Goldrick et al., 2017). However, during constant pressure operations, flux decreases gradually as the filter fouls (Goldrick et al., 2017) and initial high flux in constant pressure mode can result in severe fouling in processes with suspended particles. High flux at the beginning of filtration causes much faster deposition of particles on the membrane surface than are back transported, resulting in faster particle deposition than in constant flow rate mode (Yoon, 2016). This reduces the overall capacity of the filter. Therefore, industrial processes are mainly operated under constant flow mode to maximize the available filter area by avoiding sudden fouling. However, filtering solute molecules can be different with constant pressure as there is no particle involved; our experiments are conducted with solute dye molecules and the main mechanism for separation is by electrostatic adsorption.

During our constant pressure adsorption experiments with multilayer filters, flow rate decreased compared to single layer as a result of the resistance created by the slightly increased thickness of multi-layers. Decreased flow rate results in an increased residence time for liquid, which provides more time for dye molecules to adsorb. In contrast, residence time does not change for multi-layers under constant flow as flow rate is constant. This explains why adsorption capacities at a given basis weight is so dependent upon layer configuration under constant pressure mode.

Effect of Multi-Layered Filter Structure

Heterogeneous composite filters combining fibers and adsorbent particles can develop heterogeneity at small length scales, creating channels. This is accentuated by the agglomeration of adsorbent particles and poor fiber distribution (formation). Liquid flows through such channels with little resistance and saturates the surrounding filter medium of this preferential flow path; this reduces the effectiveness of filters substantially.

By introducing multi-layers, tortuosity is increased and channeling mostly avoided as multi-layers offsets the channel alignment between consecutive layers. This prevents preferential flow through continuous channels across the entire filter medium. Multi-layers have also increased external surface area maximizing filter-liquid contact (**Figure 9**).

Figure 9 shows liquid streams following the tortuous path of least resistance in a single layer structure (A). This pattern is distorted between two stacked layers as liquid contacts the filtering medium of the next layer (B). This explains the improved breakthrough curves as a result of operating multi-layered filters for the same basis weight.

Analysis of 3D X-ray tomography images and animations (SI) reveals that a single thick layer of filter (400 gsm-1x) is more likely to contain macro voids than thinner filters; these massive gaps are absent at lower basis weights. Macro voids are defects reported in literature mainly for membranes prepared by phase-inversion methods. The presence of such macro voids results in compaction or collapse of the membranes that reduces flux (Paulsen et al., 1994; Kosma and Beltsios, 2012). In our case, these defects cause preferential liquid flow through these gaps in single layer that results in a poor adsorption capacity. However, the filtering efficiency decreases with multiple layers of thinner filter layers (100 gsm-4x and 100 gsm-2x). Thicker

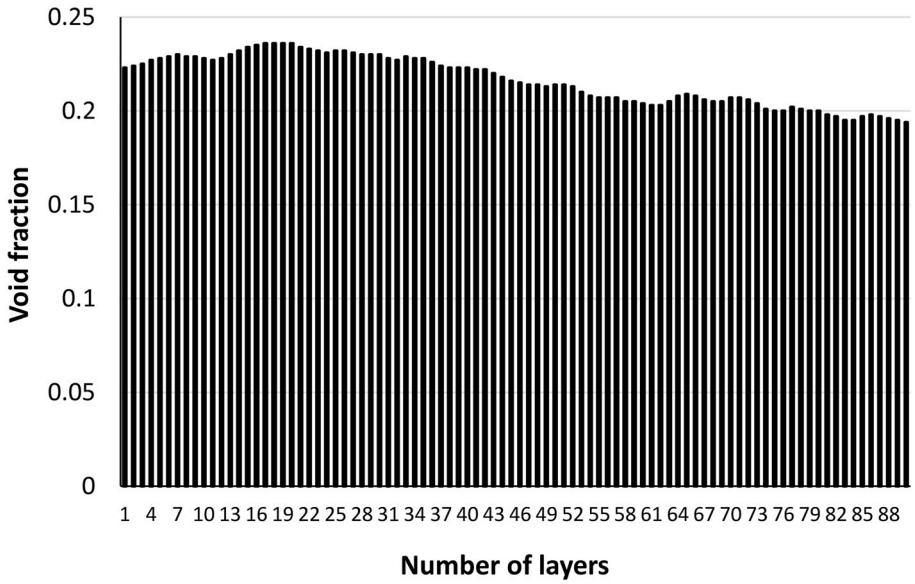

FIGURE 8 | Void fraction distribution through the thickness of an individual layer (200 gsm). The composite mesh side is at the high number (88) and the air side is at the origin.

TABLE 2 | 0.5 μm SiO_2 particle rejection of 400 gsm-1x, 200 gsm-1x, 100 gsm-2x, and 100 gsm-4x filters.

Filters	SiO_2 rejection (%)
100 gsm-4x	87 ± 11
100 gsm-2x	87 ± 3
200 gsm-1x	98 ± 0.9
400 gsm-1x	99 ± 0.2

depth filters can better hold particles and prevent any particle escape; filter density gradient across the thickness can be an explanation. Usually, cellulosic fiber composites are formed by wet papermaking laying technique with a density gradient across the thickness. The density increases from top to bottom. The decreasing void fraction through the thickness can be seen in **Figure 8**. This is due to the preferential distribution of fines away from the mesh and their varying degrees of compaction through the sheet thickness (Rosenthal et al., 1977). Thick single layer filters are expected to have a higher density variance through thickness than smaller basis weights. Also, thick samples are expected to have higher densities than low basis weight samples (the density and porosity calculations based on thickness of the samples are given in the **Supplementary section**). Another explanation could be the denser structure of thick samples better trapping particles.

Effect of Separators

The improved adsorption capacity with separators under constant flow operation is attributed to a uniformly distributed flow between the layers. Well-distributed flow increases the probability of liquid to follow through the entire filter medium instead of following some preferential pathway and saturating local areas. The operations schematic is illustrated with and without separators in **Figure 10**.

Perspective

A thermal process, pasteurization is usually used for food preservation in the food industry. Treatment temperature ranges from less than one minute up to several minutes at temperatures varying from 100 to 150°C, based on products (Lopes et al., 2016). However, this process can alter the organoleptic characteristics and degrade the quality of food, specifically in heat-sensitive foods such as juices and wine (Lopes et al., 2016). Removal of microbial spoilage from liquid foods at low temperatures through filtration is a promising method for food and beverage industry (Papafotopoulou-Patrinou et al., 2016). In this work, we developed food grade filters made from cellulose, a naturally abundant, biocompatible and low-cost material. These filters can remove spoilage as small as 0.5 μm [in the size range of bacteria (Microbiological hazes and deposits[2])] by up to 98% with 200 gsm two layers and 400 gsm single layer and at least by 87% rejection rate with 100 gsm two and four layers. Filtration can also serve as a preliminary step before any further treatment—including pasteurization (Tomasula et al., 2011; Wray, 2015). The contaminants smaller than the pore size also retained through adsorption combining electrostatic interactions; these interactions are further improved via multi-layer filter configurations. Depth

[2]Microbiological hazes and deposits. Available online at: https://www.awri.com.au/industry_support/winemaking_resources/fining-stabilities/hazes_and_deposits/microbiological/.)]

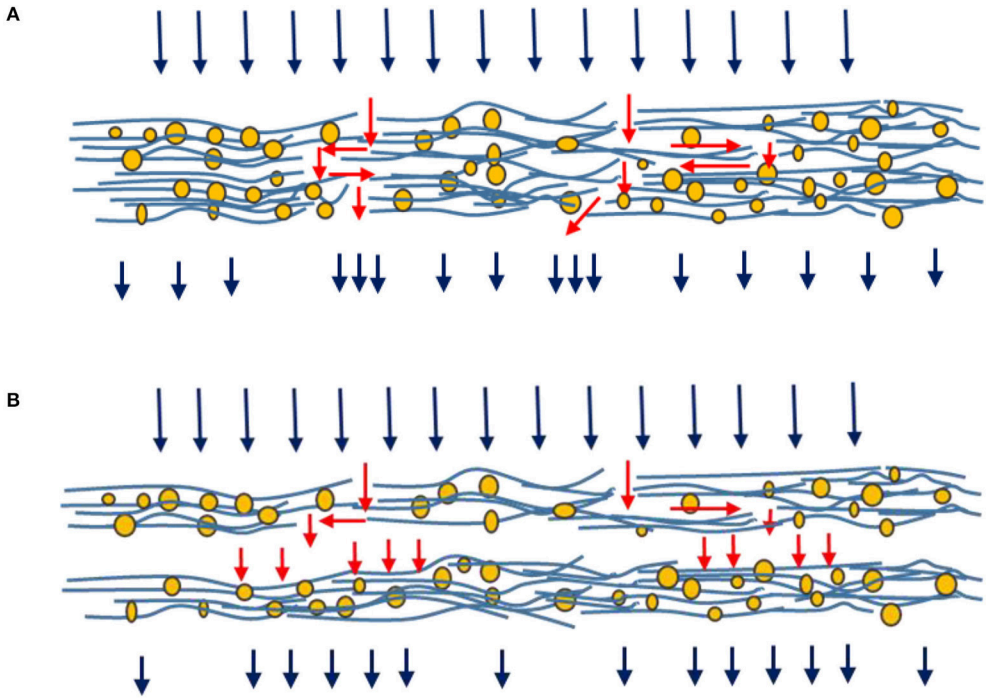

FIGURE 9 | Schematic illustration of flow through a single layer **(A)** and two layers **(B)** filters.

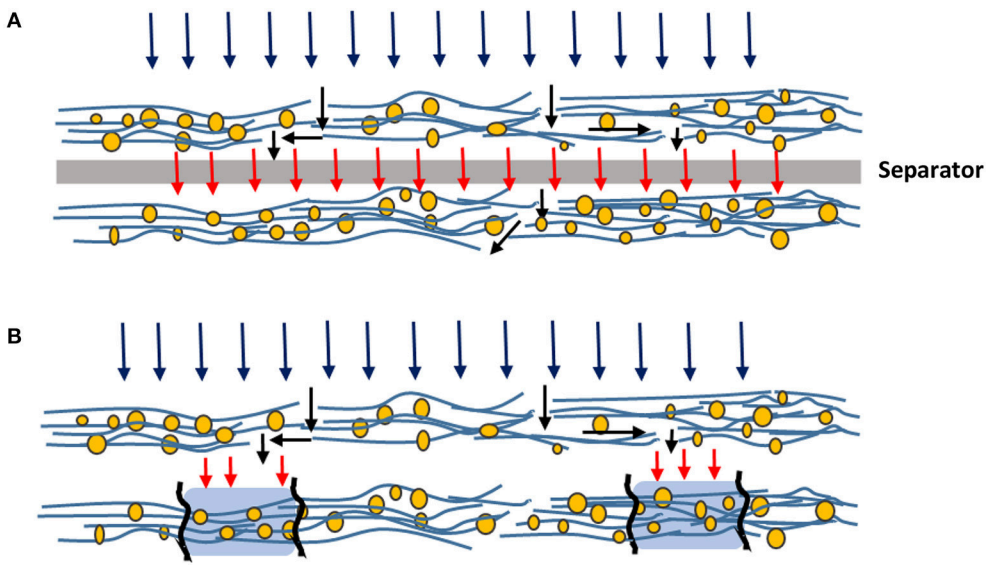

FIGURE 10 | Schematic illustration of flow of liquid through filters with **(A)** and without **(B)** separators.

filters can provide a good alternative for "cold" pasteurization process.

CONCLUSION

The effect of multi-ply and inter-ply spacing of novel inorganic-cellulosic depth filters was investigated in terms of adsorption capacity and filtration efficiency. Cellulose fiber-perlite composite layers were prepared at three different thicknesses (basis weights) using a papermaking technique. Perlite and fiber content was maintained at 70 and 30 wt.%, respectively. Polyamide-amine-epichlorohydrin (PAE) was used for wet strength, filler retention and charge control. Filters were constructed as single-layer and multi-layers for different total

basis weights. Methylene blue (MB) was selected as a cationic solute molecule to characterize adsorption under constant pressure and constant flow rate modes for the different filter configurations. Filtration efficiency was measured with PEG molecules of two molecular weights (600 and 5,000 kDa) and 0.5 μm silicon dioxide (SiO_2) particles. The filter structure was quantified by 3D X-ray tomography.

MB adsorption capacity increased by multi- layered filter structures at a given basis weight for both operation modes (constant pressure/flowrate). The constant pressure mode is a better option for multi-layer filters as it maximizes adsorption capacity. The adsorption capacity of multi-layered filters (over single layer) increased by preventing flow channeling by off-setting macro voids-channels through the thickness of the filter; these local heterogeneities are often inherent to papermaking. The probability of forming continuous macro voids-channels through the full thickness of paper sharply decreases as the number of layers increases. Distorted channel alignment by multi-layered structure results in an increase in contact surface area that provides a more efficient adsorption. The presence of separators between layers increased adsorption capacity thanks to a well-distributed liquid flow in constant flow mode. Filters had no rejection capability for PEG molecules. The thickest (400 gsm-1x) and half thickness (200 gsm-1x) filter structures filtered 0.5 μm particles at a very high rejection rate (98%). The rejection rate however decreased with multi-layer structures. Multi-layered composites provide better adsorption performances while filtration is best with single thick layers. This work highlights how engineering materials and operation can improve and change filtration and adsorption performance in filters. A novel generation of multi-layer depth inorganic-cellulose filters can provide new avenues for purification of temperature sensitive suspensions such as food and pharmaceutical streams. However, further studies are still required to fully characterize the filtration mechanisms of multi-layered filters.

AUTHOR CONTRIBUTIONS

AO carried out the experiment and wrote the manuscript with the support from AN, WB and GG. AN and WB supervised the project with the leadership of GG.

ACKNOWLEDGMENTS

This work was supported by the Graduate Research Industry Partnership (GRIP), Victorian Government, Monash University and 3M Australia. Thanks to the X-ray Microscopy Facility for Imaging Geo materials (XMFIG) for the image acquisition, Civil Engineering, Monash University. Daniel Pelliccia is acknowledged for expertise on 3D X-ray tomography image analysis.

SUPPLEMENTARY MATERIAL

The Supplementary Material for this article can be found online at: https://www.frontiersin.org/articles/10.3389/fchem.2018.00417/full#supplementary-material

REFERENCES

Alkan, M., Demirbaş, Ö., and Dogan, M. (2005). Zeta potential of unexpanded and expanded perlite samples in various electrolyte media. *Microporous Mesoporous Mater*. 84, 192–200. doi: 10.1016/j.micromeso.2005.05.023

Barros, M. A. S. D., Arroyo, P. A., and Silva, E. A. (2013). "General aspects of aqueous sorption process in fixed beds," in *Mass Transfer–Advances in Sustainable Energy and Environment Oriented Numerical Modeling*, ed H. Nakajima (Rijeka: InTech), 14.

Bedrikovetsky, P., You, Z., Badalyan, A., Osipov, Y., and Kuzmina, L. (2017). Analytical model for straining-dominant large-retention depth filtration. *Chem. Eng. J.* 330, 1148–1159. doi: 10.1016/j.cej.2017.08.031

Dizge, N., Koseoglu-Imer, D. Y., Karagunduz, A., and Keskinler, B. (2011). Effects of cationic polyelectrolyte on filterability and fouling reduction of submerged membrane bioreactor (MBR). *J. Memb. Sci.* 377, 175–181. doi: 10.1016/j.memsci.2011.04.048

Dogan, M., Alkan, M., and Onganer, Y. (2000). Adsorption of methylene blue from aqueous solution onto perlite. *Water Air Soil Pollut.* 120, 229–248. doi: 10.1023/A:1005297724304

Goldrick, S., Joseph, A., Mollet, M., Turner, R., Gruber, D., Farid, S. S., et al. (2017). Predicting performance of constant flow depth filtration using constant pressure filtration data. *J. Memb. Sci.* 531, 138–147. doi: 10.1016/j.memsci.2017.03.002

Griffiths, I. M., Kumar, A., and Stewart, P. S. (2016). Designing asymmetric multilayered membrane filters with improved performance. *J. Memb. Sci*. 511, 108–118. doi: 10.1016/j.memsci.2016.02.028

Holmstad, R. (2004). *Methods for Paper Structure Characterisation by Means of Image Analysis*. Doctorate thesis. Trondheim: Norges teknisk-naturvitenskapelige universitet.

Iritani, E., Katagiri, N., Takenaka, T., and Yamashita, Y. (2015). Membrane pore blocking during cake formation in constant pressure and constant flux dead-end microfiltration of very dilute colloids. *Chem. Eng. Sci.* 122. 465–473. doi: 10.1016/j.ces.2014.09.052

Koch, E. (1984). *Multi-Layer Filter*. US Patent No US4483771A.

Kosma, V. A., and Beltsios, K. G. (2012). Macrovoids in solution-cast membranes: direct probing of systems exhibiting horizontal macrovoid growth. *J. Memb. Sci.* 407–408, 93–107. doi: 10.1016/j.memsci.2012.03.021

Kuhn, M., and Briesen, H. (2016). Dynamic modeling of filter-aid filtration including surface- and depth-filtration effects. *Chem. Eng. Technol.* 39, 425–434. doi: 10.1002/ceat.201500347

Liderfelt, J., and Royce, J. (2018). "Chapter 14 – filtration principles," in *Biopharmaceutical Processing* (London, UK: Elsevier), 279–293.

Lopes, R. P., Mota, M. J., Delgadillo, I., and Saraiva, J. A. (2016). "Pasteurization: effect on sensory quality and nutrient composition," in *Encyclopedia of Food and Health* (Oxford: Academic Press), 246–263.

Obokata, T., and Isogai, A. (2007). The mechanism of wet-strength development of cellulose sheets prepared with polyamideamine-epichlorohydrin (PAE) resin. *Colloids Surf. A Physicochem. Eng. Asp.* 302, 525–531. doi: 10.1016/j.colsurfa.2007.03.025

Onur, A., Ng, A., Garnier, G., and Batchelor, W. (2018). Engineering cellulose fibre inorganic composites for depth filtration and adsorption. *Sep. Purif. Technol.* 203, 209–216. doi: 10.1016/j.seppur.2018.04.038

Papafotopoulou-Patrinou, E., Gialleli, A. I., Kallis, M., Plessas, S., Alexopoulos, A., Mantzourani, I., et al. (2016). Microbiological assessment of tubular cellulose filters used for liquid foods cold pasteurization. *LWT Food Sci. Technol. Res*. 67, 151–158. doi: 10.1016/j.lwt.2015.11.016

Paulsen, F. G., Shojaie, S. S., and Krantz, W. B. (1994). Effect of evaporation step on macrovoid formation in wet-cast polymeric membranes. *J. Memb. Sci.* 91, 265–282. doi: 10.1016/0376-7388(94)80088-X

Pearce, G. (2007). Introduction to membranes: filtration for water and wastewater treatment. *Filtr. Sep.* 44. 24–27. doi: 10.1016/S0015-1882(07)70052-6

Polyakov, Y. S. (2008). Depth filtration approach to the theory of standard blocking: Prediction of membrane permeation rate and selectivity. *J. Memb. Sci.* 322, 81–90. doi: 10.1016/j.memsci.2008.05.012

Polyakov, Y. S. (2009). Effect of operating parameters and membrane characteristics on the permeate rate and selectivity of ultra- and microfiltration membranes in the depth filtration model. *Theor. Found. Chem. Eng.* 43, 926. doi: 10.1134/S0040579509060104

Rijn, C. J. M. V. (1998). *Membrane Filter and a Method of Manufacturing the Same as Well as a Membrane*. US Patent No US5753014A.

Rosenthal, M. R., United, S., and Forest Products, L. (1977). *Effective Thickness of Paper: Appraisal and Further Development*. Madison: Dept. of Agriculture, Forest Service, Forest Products Laboratory.

Saefkow, K. H. W. M. W. K. (1995). *Filter for Liquor Filtration*. US Patent No US5462667A.

Siegfried Ripperger, W. G. (2000). *Christian Alt, Ullmann's Encyclopedia of Industrial Chemistry: Filtration, 1. Fundamentals*. Weinheim: Wiley-VCH Verlag GmbH.

Sutherland, K. (2011). Depth filtration: efficient separation processes through depth filtration. *Filtr. Sep.* 48, 12–15. doi: 10.1016/S0015-1882(11)70195-1

Tomasula, P. M., Mukhopadhyay, S., Datta, N., Porto-Fett, A., Call, J. E., Luchansky, J. B., et al. (2011). Pilot-scale crossflow-microfiltration and pasteurization to remove spores of *Bacillus anthracis* (Sterne) from milk1. *J. Dairy Sci.* 94, 4277–4291. doi: 10.3168/jds.2010-3879

Wertz, J. A., and Guimond, D. M. (2014). *Filter Media With a Multi-Layer Structure*. US Patent No US 20140144113A1.

Wray, E. (2015). "12–Reducing microbial spoilage of beer using pasteurization," in *Brewing Microbiology*, ed A. E Hill (Oxford: Woodhead Publishing), 253–269.

Yoon, S.-H. (2016). *Membrane Bioreactor Processes Principles and Applications: Membrane Fouling*. Boca Raton, FL: CRC Press.

Conflict of Interest Statement: The authors declare that the research was conducted in the absence of any commercial or financial relationships that could be construed as a potential conflict of interest.

Copyright © 2018 Onur, Ng, Batchelor and Garnier. This is an open-access article distributed under the terms of the Creative Commons Attribution License (CC BY). The use, distribution or reproduction in other forums is permitted, provided the original author(s) and the copyright owner(s) are credited and that the original publication in this journal is cited, in accordance with accepted academic practice. No use, distribution or reproduction is permitted which does not comply with these terms.

Journal of Cleaner Production 215 (2019) 226–231

Contents lists available at ScienceDirect

Journal of Cleaner Production

journal homepage: www.elsevier.com/locate/jclepro

The use of cellulose nanofibres to reduce the wet strength polymer quantity for development of cleaner filters

Aysu Onur [a], Aaron Ng [b], Gil Garnier [a], Warren Batchelor [a, *]

[a] Bioresource Processing Research Institute of Australia, Department of Chemical Engineering, Monash University, Clayton, 3800, Australia
[b] 3M Innovation Centre, North Ryde, 2113, Australia

ARTICLE INFO

Article history:
Received 19 October 2018
Received in revised form
10 December 2018
Accepted 2 January 2019
Available online 3 January 2019

Keywords:
Cellulose nanofibre
Wet strength
Composite
Filter
Adsorption

ABSTRACT

Polyamideamine-epichlorohydrin resin (PAE) is one of the most commonly used wet strength agents in the papermaking industry. However, adsorbable organic halogens (AOX) are known to be a toxic side product of the PAE manufacturing process; therefore, the use of PAE is restricted by regulation for food and medical applications. In this study, we investigated partially replacing the indirect food additive, PAE, with a renewable, biodegradable material, cellulose nanofibres (CNF), in order to drastically reduce the amount of PAE used while maintaining the same wet tensile strength. The concept is to replace covalent bonds by hydrogen bonds and to drastically increase bonding area. Depth-type filters were prepared with cellulose (30%), perlite (70%) and lesser amounts of PAE via papermaking technique. A small fraction of cellulose fibre composition was substituted with CNF while the PAE amount was gradually decreased. The substitution of positively charged PAE for negatively charged cellulose nanofibres switched the overall charge of the system from cationic to anionic. Therefore, two cationic polyelectrolytes, CPAM or PEI, were investigated to control the overall charge and adsorption performance of the filter system.

The substitution of CNF enabled PAE dosage to be reduced by over 95% while retaining the wet strength properties of the filters. The wet strength obtained from the small quantity of wet strength polymer could be further improved by increasing the curing temperature to 150 °C with a much shorter curing period. The filters with reduced PAE dosage have also improved adsorption of positively charged contaminants. However, for negatively charged contaminants a very minor amount (around 20 mg/g) of cationic polymer addition would be required to maintain the performance. Our study shows that partial replacement of conventional papermaking fibres with cellulose nanofibres allows us to reduce the quantity of wet strength polymer remarkably and achieve a sustainable and environmentally-friendly concept for filter manufacturing or for any paper product requiring wet strength.

© 2019 Elsevier Ltd. All rights reserved.

1. Introduction

Wet strength is a critical property of certain paper products; it measures the ability of fibre network to maintain its strength when it is wetted with an aqueous solution. Wet strength is critical for hygiene products such as paper towel and tissue paper (Zakaria, 2004; Bajpai, 2018). Moreover, cellulosic filters that are used in liquid filtration also require a substantial wet strength to remain robust during operations.

Polyamideamine-epichlorohydrin (PAE) is by far the most common additive to manufacture wet strengthened papers (Obokata et al., 2005). Wet strength is developed through cross-linking the azetidinium groups with each other and with the cellulose (Obokata and Isogai, 2007). These reactions generate a partial water-proof barrier around the fibre to fibre contact point which restricts water from hydrolysing the hydrogen bonds when the sheets are re-wetted.

However, epichlorohydrin-based products, such as PAE, have significant drawbacks. Both the manufacture and use of epichlorohydrin can produce a high adsorbable organic halogen (AOX) content in the process wastewater (Hagiopol and Johnston, 2011). The toxic effects of AOX range from carcinogenic and mutagenic effects to acute and chronic toxicity and can inhibit microorganism growth (Müller, 2003; Savant et al., 2006; Deshmukh et al., 2009; Osman et al., 2013).

A further problem with PAE strengthened products is that the

* Corresponding author.
E-mail address: warren.batchelor@monash.edu (W. Batchelor).

https://doi.org/10.1016/j.jclepro.2019.01.017
0959-6526/© 2019 Elsevier Ltd. All rights reserved.

majority of papers strengthened with epoxy thermosets cannot be recycled due to their irreversible 3-D crosslinked networks (Min et al., 2015). The used epoxy thermosets can only be incinerated or landfilled, or degraded to small molecules directly using strong acidic or basic agents (Min et al., 2015).

An ideal solution from a broad cleaner production perspective would be one that retains the required product performance while:

1. Replacing the epichlorohydrin resins, with their toxic by-products in manufacture and use, with a non-hazardous alternative.
2. Facilitating recycling.
3. Using a locally sourced bio-derived alternative.

During the last two decades, cellulose nanofibres (CNF) have emerged as a promising alternative that can meet all these requirements. Cellulose is the most abundant polymer on Earth; it is renewable, biodegradable, non-toxic and chemically versatile (Dufresne, 2013). Cellulose nanofibres are formed by breaking down cellulose fibres into their nano-scale cellulose microfibril building blocks (Lavoine et al., 2012). CNF is thus fully chemically compatible with cellulose and can be recycled with the cellulose fibres. Almost any source of cellulose can be used, including agricultural and food processing residues (Varanasi et al., 2018) as well as the fibre degradation products from paper-mill processing (Gunawardhana et al., 2017), thus utilising the principles of industrial ecology.

Furthermore CNF (Cellulose Nanofibre) is an outstanding sustainable reinforcement material (Boufi et al., 2016; Sanjay et al., 2018). Use of CNF has emerged as wet-end additive with potential applications as both a wet and dry strength agent as well as a coating to improve the barrier properties (Lavoine et al., 2012). The contribution of CNF to strength can be achieved by two mechanisms (Boufi et al., 2016). Firstly, CNF promotes the bridging between fibres which increases the fibre to fibre contact, and in turn increases the bonded area. Secondly, web-like entangled structure of CNF brings larger fibre together creating a network, which boosts the load-bearing capacity of the paper. As a result, the final paper strength is achieved by both fibre to fibre contact and the CNF network.

While CNF is a promising alternative to resin-bonded products, it must still be demonstrated that the product performance has been maintained. In this study, we investigated the development of cleaner food grade filters with the least amount of wet strength resin while delivering the same wet strength and adsorption properties as the original filters with high PAE dosage. To achieve this, a particular fibre fraction was substituted with CNF without changing the total fibre composition. Filters were prepared with a variety of PAE dosages. Performance of CNF was examined as a wet strength agent, where effect of different variables such as curing conditions and addition order of raw materials were investigated on wet strength development. Adsorption performance was examined using two different oppositely charged dye molecules. Positively charged polyelectrolytes were used to maintain the overall positive charge and adsorption characteristics of the filters.

2. Material and methods

2.1. Material

The cellulose fibres used for the composites were:

- Unrefined northern softwood bleached kraft pulp (NIST Reference Material 8495) from Procter and Gamble
- Bleached radiata pine softwood Kraft pulp refined to 400 Canadian standard freeness (CSF) in a disk refiner
- CNF prepared by processing a 0.3 wt % suspension of bleached radiata pine softwood Kraft pulp, that had been refined to 400 Canadian standard freeness, in a GEA Niro Soavi homogeniser at 800 bar pressure for 3 passes.

The fibre diameter distributions of homogenised and refined pulp were reported in our previous study (Onur et al., 2018) and are approximately 50 and 25 nm for the nanofibre fraction of the refined and homogenised pulp, respectively. Expanded perlite supplied by Dicalite Minerals Corp was used as the inorganic absorbent. Commercial PAE provided from Nopcobond Paper Technology Pty Ltd was used as wet strength resin.

Negatively charged metanil yellow (MY) and positively charged methylene blue (MB) dyes supplied from Sigma Aldrich was used to investigate adsorption characteristics. The cationic polyacrylamide (CPAM) polymer was supplied by AQUA + TECH. The F1 grade with 13 MDa molecular weight and 40% charge density was used. Polyethylenimine (PEI), branched with 10,000 Da molecular weight was purchased from Sigma Aldrich.

2.2. Methods

2.2.1. Preparation of filters

Filters were prepared by using a standard British hand sheet maker. A detailed step by step explanation of the sheet making procedure can be found in our previously published study (Onur et al., 2018). Filter suspensions were prepared by mixing pulp suspension with perlite and PAE (0.22 w/v %) or PAE & CPAM (0.1 wt %) or PAE & PEI (0.1 wt %) combinations. Filters prepared with different compositions and curing conditions are listed below.

1) 30% Fibre (1/3 refined pulp + 2/3 unrefined pulp) + 70% Perlite + 120 mg PAE-half an hour at 105 °C *(Reference sample)*
2) 30% Fibre (1/3 CNF + 2/3 unrefined pulp) + 70% Perlite + (0-5-10-30-60-90-120 mg PAE) —half an hour at 105 °C
3) 30% Fibre (1/3 CNF + 2/3 unrefined pulp) + 70% Perlite + 5 mg PAE-1 h at 105 °C
4) 30% Fibre (1/3 CNF + 2/3 unrefined pulp) + 70% Perlite + 5 mg PAE- 5 min at 150 °C *(tried by two different order of addition methods)*
5) 30% Fibre (1/3 CNF + 2/3 unrefined pulp) + 70% Perlite + 5 mg PAE & 25 mg CPAM-5min at 150 °C
6) 30% Fibre (1/3 CNF + 2/3 unrefined pulp) + 70% Perlite + 5 mg PAE & 25 mg PEI-5min at 150 °C

Suspensions were mixed using the order of addition shown in Fig. 1a, except where the effect of mixing order on wet strength development was investigated, which also used the scheme in Fig. 1b. Only the sample with 5 mg PAE sample cured at 150 °C for 5 min was tested for the effect of mixing order.

In Fig. 1a, perlite is added to CNF suspension first and then the perlite and CNF mixture is added to unrefined cellulose pulp suspension. PAE or any other positively charged polymers used with PAE for charge modification were added at the end on top of the entire suspension. Combination of PAE with other positively charged polymers was used to investigate the charge modification of the composites along with adsorption and wet strength properties.

In Fig. 1b, PAE is added to CNF mixture first and then this mixture is added to unrefined pulp suspension. Perlite suspension was then added last.

After initial air-drying, all the filters were then heated in an oven and then stored in a humidity controlled room (23 °C and 50%

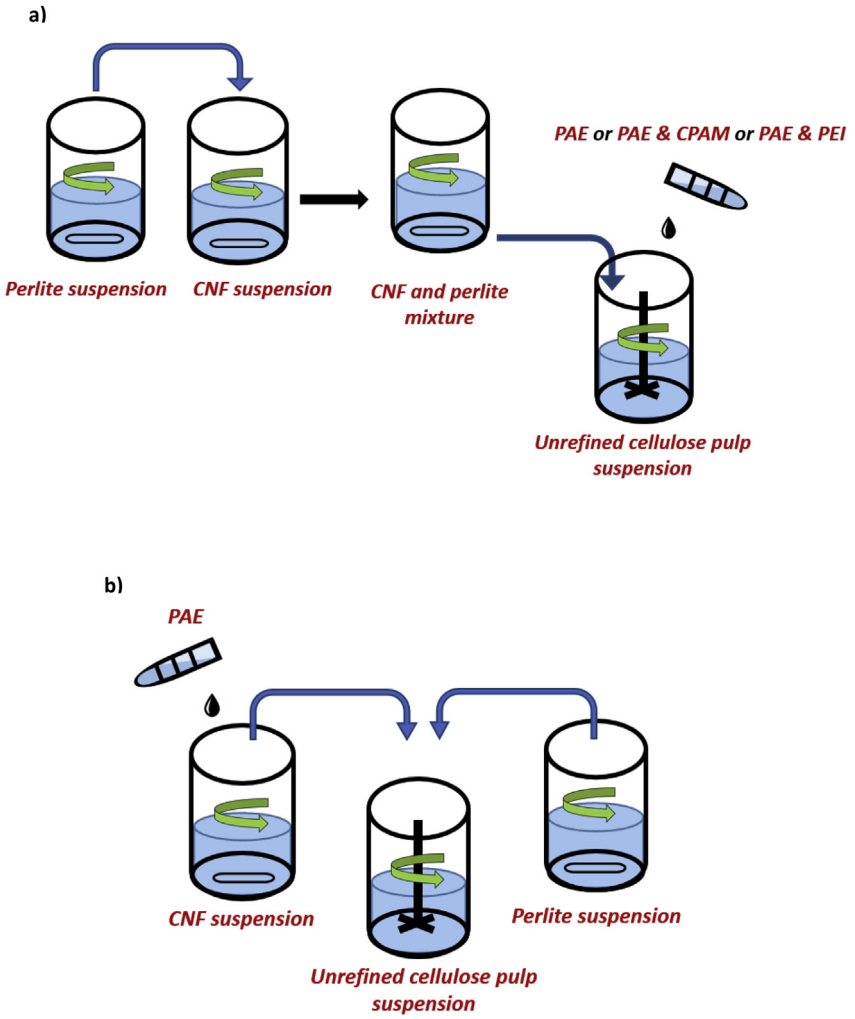

Fig. 1. Graphical representation of mixture preparation procedures.

relative humidity) for at least 24 h prior to any further use. The standard oven treatment was half an hour at 105 °C, except where otherwise noted.

2.2.2. Wet tensile strength measurements

Thickness of the composites was measured using L&W thickness tester after conditioning. An average of ten points was used to calculate the thickness of each sample. Following thickness measurements, each sample was cut into 15 mm wide strips using a sheet cutting machine. Wet strength measurements were conducted on an Instron model 5566 with a constant strain rate of 10 mm/min. At least 14 strips in total from two separately formed sheets for each sample was measured with a 100 mm test span. Sample strips were individually soaked in water for 1 min before measurement. Tensile index for each sample was calculated as tensile load per unit width divided by grammage.

2.2.3. Zeta potential

A Nanobrook Omni from Brookhaven Instruments was used to measure the zeta potential of each suspension used for making samples. A small quantity of each suspension was analysed in a cuvette cell at 25 °C before papermaking. The electrophoretic mobility was determined using laser Doppler velocimetry and zeta potential was calculated based on the Smoluchowski equation.

2.2.4. Adsorption properties

A dead-end stirred cell working with constant pressure was used to carry out adsorption experiments with 400 mL of either MY or MB dye solutions. The experimental procedure was explained comprehensively in our previous study (Onur et al., 2018). Effect of different compositions of charged polymers and CNF on charged dye molecule adsorption was investigated.

3. Results

In this section, wet tensile index of the composites was measured as a function of critical variables: PAE dosage, curing conditions and PAE adsorption methodology. Charge characteristics of the composites were investigated by zeta potential measurements. Contaminant adsorption properties were tested using an anionic (MY) and a cationic (MB) dye. Cationic polyelectrolyte addition was also examined in terms of charge modification, adsorption characteristics as well as wet strength improvement.

3.1. Wet tensile index

3.1.1. Effect of PAE dosage

Wet tensile strength properties of composites with varying PAE dosages and pulp content are presented in Fig. 2. The reference composite with refined pulp and 120 mg PAE has a wet tensile

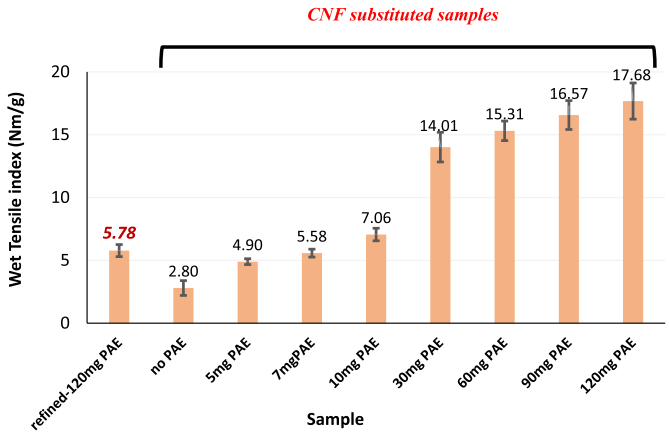

Fig. 2. Effect of PAE dosage on wet tensile index of the composites. (Curing at 105 °C for 30 min)

index of 5.78 Nm/g. Simultaneously substituting CNF for the refined pulp and eliminating PAE (Mixing procedure **(a)** in section 2.2.1 was used for sample preparation) reduced the wet tensile index to 2.80 Nm/g, showing that it is not possible to fully replace the PAE. The optimum PAE dosage with the CNF, which provides the reference wet strength, ranges between 5 mg and 7 mg under the usual curing condition and preparation technique.

3.1.2. Effect of curing conditions

The effect of curing condition was investigated with an addition level of 5 mg PAE. Samples were prepared with the procedure (Fig. 1a) given in section 2.2.1. The composites were treated at 105 °C for 1 h and 150 °C for 5 min, differing from the normal curing conditions (Fig. 3). One hour treatment at 105 °C and 5 min curing at 150 °C increased wet tensile index to 5.64 and 5.83 Nm/g, respectively. However, these differences are not statistically different from the reference material with 5.78 Nm/g. (T-test is given in supplementary material). It shows that either 1 h treatment at 105 °C or 5 min treatment at 150 °C can be selected with 5 mg PAE addition to achieve the same wet strength as the reference filter.

3.1.3. Effect of order of PAE addition

Here, PAE was added first to CNF and the mixture was then mixed with the unrefined fibres (see section 2.2.1, Fig. 1b); this differs from the previous method. Perlite suspension was added at the end and the resulting suspension was gently mixed before papermaking. Curing was set at 5 min, 150 °C. The results showed that the order of addition of resin to the fibres has no statistically significant effect (Fig. 4; with T-test analysis in supplementary material).

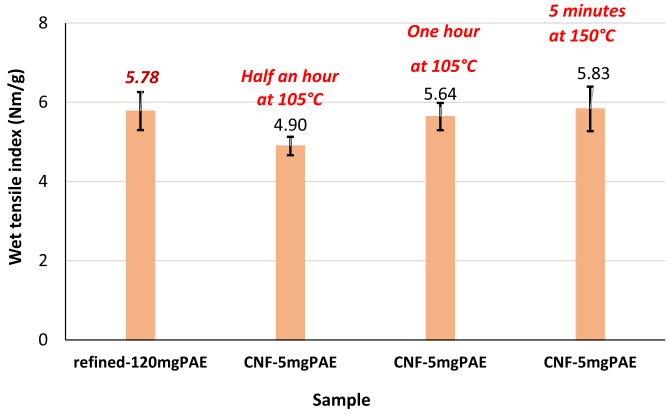

Fig. 3. Effect of curing on wet tensile index of the composites (with 5 mg PAE dosage).

3.2. Cationic polyelectrolyte addition: zeta potential and wet strength improvement

As the reduction in PAE amount also changes the charge of filter medium, charge modification was investigated with two cationic polyelectrolytes, CPAM and PEI, differing in morphology, to maintain the electrostatic adsorption properties. Sheets with CPAM and PEI were prepared by the method given in 2.1.1, Fig. 1a. Zeta potential measurements of the critical composites are given in Fig. 5. Results show that eliminating PAE dropped the electrical double layer net charge of the suspended particles from +30 mV to −37 mV, while charge is controlled from −27 mV to −15 mV by adding PAE up to 10 mg.

Substitution of 1/3 of the fibres by CNF decreased the zeta potential slightly, indicating an increase in negative charges on the surface of fibres upon homogenisation. Adding 25 mg of either CPAM or PEI with 5 mg PAE produced suspensions of zeta potential of +38 mV and +22 mV, respectively, which are similar to the reference sample.

Addition of PEI or CPAM in combination with PAE was tested to investigate the contribution of polyelectrolytes on wet strength development (Fig. 6). Adding 25 mg PEI with 5 mg PAE doubles composite wet strength. However, CPAM did not improve the wet strength significantly.

3.3. Adsorption properties

The effect of adsorbing 400 mL of anionic metanil yellow (MY) or cationic methylene blue (MB) solution was quantified on different composites. Fig. 7a and b shows the metanil yellow and methylene blue adsorption breakthrough curves, respectively. The refined-120 mg PAE composite (reference sample) has a higher adsorption capacity for MY molecules than the composite with CNF, 5 mg PAE & 25 mg CPAM (Fig. 7a). However, when CPAM is substituted for 25 mg PEI, the filter has a remarkable capacity for MY adsorption, which is even higher than that of the reference sample. Even though the zeta potential with combination of CPAM and PAE is similar to that of the reference sample, CPAM cannot

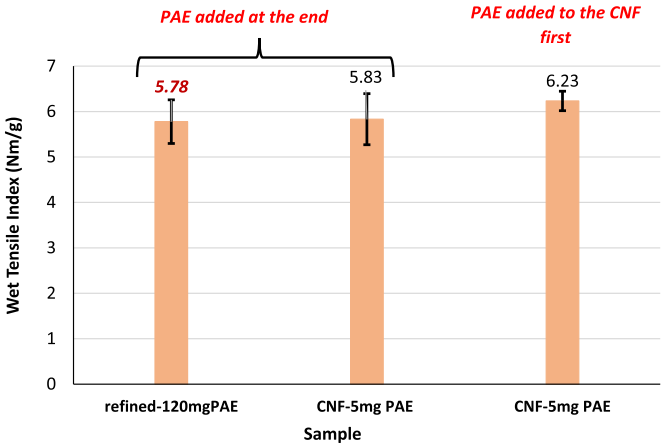

Fig. 4. Effect of order of PAE addition on wet tensile index of the composites (Curing at 5 min, 150 °C with 5 mg PAE).

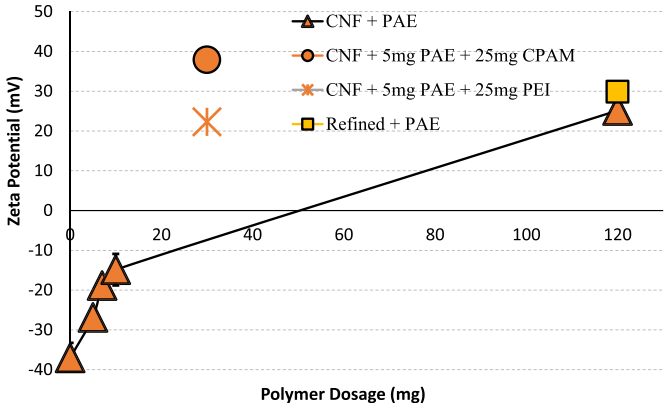

Fig. 5. Zeta potential values of composites.

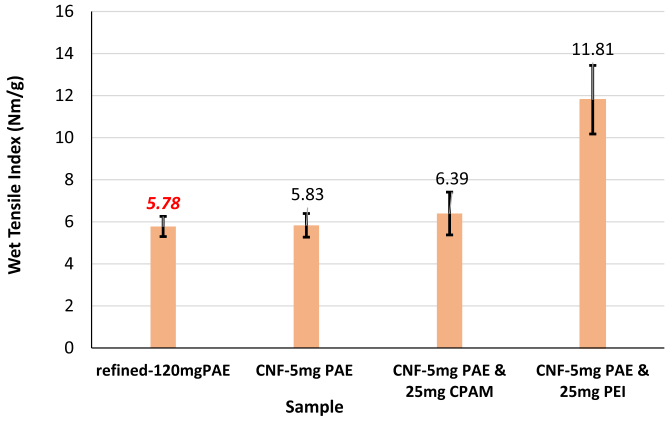

Fig. 6. Wet tensile strength properties of composites with PAE & PEI and PAE & CPAM polymer mixtures.

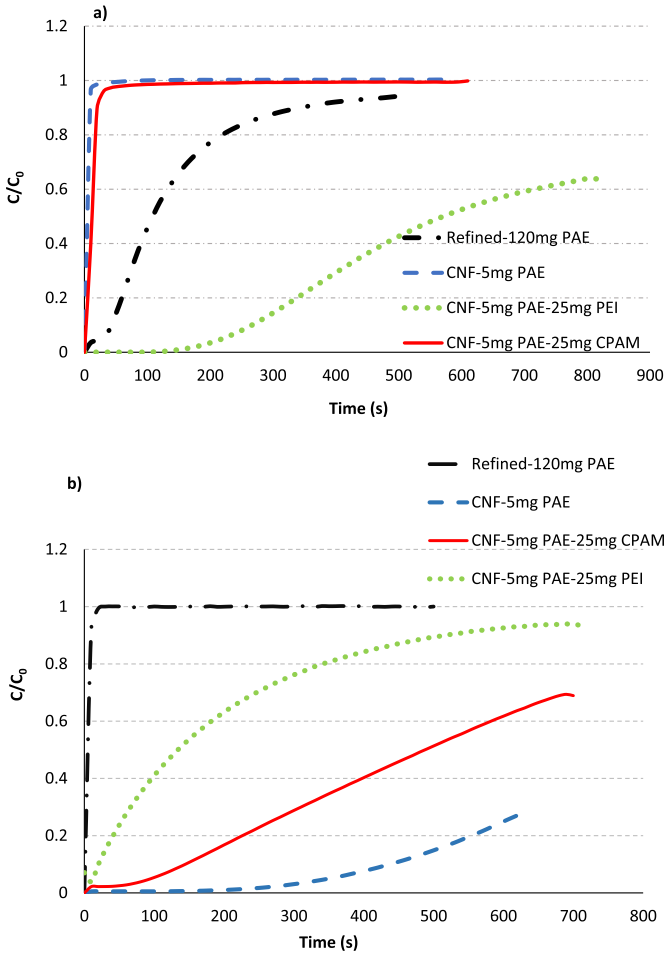

Fig. 7. Adsorption breakthrough curves of composites with (**a**) metanil yellow (**b**) methylene blue. (For interpretation of the references to colour in this figure legend, the reader is referred to the Web version of this article.)

provide the same adsorption characteristics with anionic MY. PEI addition (25 mg or less) combined with 5 mg PAE generates numerous positive charges, improving anionic contaminant adsorption onto the composites.

No additional polymer is needed for adsorbing the cationic methylene blue (Fig. 7b). The sample with 5 mg PAE and CNF provides an improved adsorption capacity shown by the breakthrough curve. Composites combining 5 mg PAE with CNF provide a remarkable separation of any cationic contaminant while retaining their original wet strength.

4. Discussion

Curing time and temperature are important variables affecting cellulosic composite wet strength at a given resin dosage. Optimising temperature and curing time can maximize the curing and crosslinking for the same amount of wet strength resin. The crosslinking of all PAE molecules on cellulose also minimizes their possible diffusion into the filtrate, an important requirement of filters in food or pharmaceutical applications. By efficient curing, either 5 min at 150 °C or 1 h at 105 °C, and substituting the refined fibre for CNF, the desired wet strength level was maintained while reducing the PAE usage by 95% (Figs. 2 and 3). This is a substantial contribution from a broad cleaner production perspective. As discussed in the introduction, CNF can be made from any cellulosic material including agricultural waste and degradation products from paper-mill processing. The straight-forward mechanical treatment we used here to produce CNF, with mechanical refining in a disk mill followed by homogenisation, does not require large factory floor area to implement and can be readily designed to any required capacity, thus allowing for on-site manufacture and use.

Adsorption in our filters is driven by electrostatic attraction between negatively and positively charged molecules. The original anionic charge of both cellulose and perlite favours the adsorption of cationic contaminants onto filters. On the other hand, cationic polymers can be adsorbed onto the fibres and perlite particles to promote anionic molecule adsorption onto filters. Charge modification is one of the reasons that PAE is used in filters in addition to the wet strength development. CPAM and PEI are the cationic polymers used in our study after PAE reduction to compensate for the loss of the positively charged PAE. Both polymers successfully restored the overall positive charge. However, there is a significant difference between the adsorption behaviour of negatively charged molecules onto samples prepared with either CPAM or PEI. CPAM is a linear and high molecular weight polymer forming flexible random coil configurations, whereas PEI is a highly branched polymer with a high charge density and much lower molecular weight. These two polymers have been previously studied and the effect of polyelectrolyte morphology on the adsorption and flocculation of microfibrillated cellulose (MFC) was analysed (Raj et al., 2016). Polyelectrolytes adsorb onto surfaces of opposite charges by electrostatic attraction. Equilibrium conformation of an adsorbed linear polymer chain is as a tails and loops configuration (Gregory and Barany, 2011). The size of the loops can be reduced if the

strength of the electrostatic interaction with the surface increases. CPAM bridges with a flattened conformation onto cellulose resulting in a smaller accessible area for negatively charged molecule adsorption. However, a branched polymer, such as PEI, adsorbs onto fibres as large rigid bridges by maintaining its shape without reconformation and flattening (Blanco et al., 2009) and leaving both the polymer and the surface more accessible to interact with the surrounding molecules. Anionic MY adsorbs onto PEI treated composites more efficiently than on CPAM treated composites; this is because most of the charges remain accessible in contrast to CPAM. PEI is a promising dendrimer to be used in conjunction with 5 mg PAE to retain adsorption characteristics. PEI also contributes to wet strength significantly (Fig. 6); a minute amount of PEI alone should be enough for both negatively charged molecule adsorption as well as wet strength development. While the contribution of cationic polymers to paper strength was already reported (Rahmaninia et al., 2018; Rice et al., 2018), the significant effect of PEI on wet strength was unexpected.

In the work here, we have shown that we can almost entirely replace PAE wet strength resin with CNF. That is, we are substituting a product with a long supply chain, a short shelf life and toxic by-products in manufacture and use with CNF, a biodegradable, renewable material which can be produced on-site from waste, thus promoting both industrial ecology and the circular economy.

This innovation also addresses the aspect of design for recycling. CNF, being composed only of cellulose is thus fully chemically compatible with micron-diameter cellulose fibres that are used to make paper. In fact, CNF has been widely investigated as a reinforcing fibre to improve the strength of conventional paper sheets (Taipale et al., 2010; Su et al., 2013), due to its outstanding web-like entangled structure, high aspect ratio and high strength (Li et al., 2016). The achievement of the required wet-strength, largely using only cellulose fibre-CNF hydrogen bonding and minimising cross-linking will allow re-dispersion in water. Thus filters wet-strengthened with CNF should be recyclable within a conventional paper recycling process, possibly with enhanced initial dispersion, because of the high wet strength.

5. Conclusions

This study investigated reducing the quantity of wet strength resin, PAE, used in cellulosic filter products by substituting a renewable, biodegradable material, cellulose nanofibres (CNF). Substituting CNF for refined fibre allowed us to reduce PAE content by 95% while retaining full wet strength. In addition, the use of PEI to substitute for the cationic charge lost upon removal of the PAE was found to allow for the adsorption of both negatively and positively charged contaminants, in comparison to filters prepared with PAE, which only adsorbed negatively charged contaminants. This substantial reduction in PAE usage is particularly interesting for cellulosic filters used in beverage filtration applications. PAE is used as an indirect food additive in these type of filter products and the allowed concentration is very limited. Therefore, CNF substitution is a promising strategy for high performance cellulose fibre based filters while reducing PAE usage by 95%, drastically reducing AOX generation in PAE production and application. CNF's biodegradable and renewable nature provides cleaner products by significantly reducing the chemical impact on the environment and should be further investigated for any paper product currently using PAE to develop the required wet-strength.

Acknowledgements

This work was supported by the Chemicals and Plastics Manufacturing Innovation Network and Training Program (C&P GRIP), Victorian Government, Monash University and 3M Australia.

Appendix A. Supplementary data

Supplementary data to this article can be found online at https://doi.org/10.1016/j.jclepro.2019.01.017.

References

Bajpai, P., 2018. Chapter 4 - additives for papermaking. In: Bajpai, P. (Ed.), Biermann's Handbook of Pulp and Paper, third ed. Elsevier, pp. 77–94.
Blanco, Á., Fuente, E., Monte, M.C., Cortés, N., Negro, C., 2009. Polymeric branched flocculant effect on the flocculation process of pulp suspensions in the papermaking industry. Ind. Eng. Chem. Res. 48 (10), 4826–4836.
Boufi, S., González, I., Delgado-Aguilar, M., Tarrès, Q., Pèlach, M.À., Mutjé, P., 2016. Nanofibrillated cellulose as an additive in papermaking process: a review. Carbohydr. Polym. 154, 151–166.
Deshmukh, N.S., Lapsiya, K.L., Savant, D.V., Chiplonkar, S.A., Yeole, T.Y., Dhakephalkar, P.K., Ranade, D.R., 2009. Upflow anaerobic filter for the degradation of adsorbable organic halides (AOX) from bleach composite wastewater of pulp and paper industry. Chemosphere 75 (9), 1179–1185.
Dufresne, A., 2013. Nanocellulose: a new ageless bionanomaterial. Mater. Today 16 (6), 220–227.
Gregory, J., Barany, S., 2011. Adsorption and flocculation by polymers and polymer mixtures. Adv. Colloid Interface Sci. 169 (1), 1–12.
Gunawardhana, T., Banham, P., Richardson, D.E., Patti, A.F., Batchelor, W., 2017. Upgrading waste whitewater fines from a pinus radiata thermomechanical pulping mill. Nord. Pulp Pap. Res. J. 32 (4), 656–665.
Hagiopol, C., Johnston, J.W., 2011. Chemistry of Modern Papermaking. CRC Press.
Lavoine, N., Desloges, I., Dufresne, A., Bras, J., 2012. Microfibrillated cellulose – its barrier properties and applications in cellulosic materials: a review. Carbohydr. Polym. 90 (2), 735–764.
Li, Q., Chen, W., Li, Y., Guo, X., Song, S., Wang, Q., Liu, Y., Li, J., Yu, H., Zeng, J., 2016. Comparative study of the structure, mechanical and thermomechanical properties of cellulose nanopapers with different thickness. Cellulose 23 (2), 1375–1382.
Min, Y., Huang, S., Wang, Y., Zhang, Z., Du, B., Zhang, X., Fan, Z., 2015. Sonochemical transformation of epoxy–amine thermoset into soluble and reusable polymers. Macromolecules 48 (2), 316–322.
Müller, G., 2003. Sense or no-sense of the sum parameter for water soluble "adsorbable organic halogens" (AOX) and "absorbed organic halogens" (AOX-S18) for the assessment of organohalogens in sludges and sediments. Chemosphere 52 (2), 371–379.
Obokata, T., Isogai, A., 2007. The mechanism of wet-strength development of cellulose sheets prepared with polyamideamine-epichlorohydrin (PAE) resin. Colloid. Surface. Physicochem. Eng. Aspect. 302 (1–3), 525–531.
Obokata, T., Yanagisawa, M., Isogai, A., 2005. Characterization of polyamideamine-epichlorohydrin (PAE) resin: roles of azetidinium groups and molecular mass of PAE in wet strength development of paper prepared with PAE. J. Appl. Polym. Sci. 97 (6), 2249–2255.
Onur, A., Ng, A., Garnier, G., Batchelor, W., 2018. Engineering cellulose fibre inorganic composites for depth filtration and adsorption. Separ. Purif. Technol. 203, 209–216.
Osman, W.H.W., Abdullah, S.R.S., Mohamad, A.B., Kadhum, A.A.H., Rahman, R.A., 2013. Simultaneous removal of AOX and COD from real recycled paper wastewater using GAC-SBBR. J. Environ. Manag. 121 (Suppl. C), 80–86.
Rahmaninia, M., Rohi, M., Hubbe, M.A., Zabihzadeh, S.M., Ramezani, O., 2018. The performance of chitosan with bentonite microparticles as wet-end additive system for paper reinforcement. Carbohydr. Polym. 179, 328–332.
Raj, P., Batchelor, W., Blanco, A., de la Fuente, E., Negro, C., Garnier, G., 2016. Effect of polyelectrolyte morphology and adsorption on the mechanism of nanocellulose flocculation. J. Colloid Interface Sci. 481, 158–167.
Rice, M.C., Pal, L., Gonzalez, R., Hubbe, M.A., 2018. Wet-end addition of nanofibrillated cellulose pretreated with cationic starch to achieve paper strength with less refining and higher bulk. Tappı Journal 17 (7), 395–403.
Sanjay, M.R., Madhu, P., Jawaid, M., Senthamaraikannan, P., Senthil, S., Pradeep, S., 2018. Characterization and properties of natural fiber polymer composites: a comprehensive review. J. Clean. Prod. 172, 566–581.
Savant, D.V., Abdul-Rahman, R., Ranade, D.R., 2006. Anaerobic degradation of adsorbable organic halides (AOX) from pulp and paper industry wastewater. Bioresour. Technol. 97 (9), 1092–1104.
Su, J., Mosse, W.K.J., Sharman, S., Batchelor, W.J., Garnier, G., 2013. Effect of tethered and free microfibrillated cellulose (MFC) on the properties of paper composites. Cellulose 20, 1925–1935.
Taipale, T., Österberg, M., Nykänen, A., Ruokolainen, J., Laine, J., 2010. Effect of microfibrillated cellulose and fines on the drainage of kraft pulp suspension and paper strength. Cellulose 17 (5), 1005–1020.
Varanasi, S., Henzel, L., Sharman, S., Batchelor, W., Garnier, G., 2018. Producing nanofibres from carrots with a chemical-free process. Carbohydr. Polym. 184, 307–314.
Zakaria, S., 2004. Development of wet-strength paper with dianhydride and diacid. Mater. Chem. Phys. 88 (2), 239–243.